Characterization of DnmA, the Dnmt2 homolog in *Dictyostelium discoideum*

Dissertation

submitted to the

Faculty of the Natural Sciences and Mathematics

of the University of Kassel, Germany

for the degree of

Doctor of Natural Sciences

presented by

Vladimir Maksimov

born in Saint-Petersburg

Kassel, July 2010

Cooperation and contributions

Some of the constructs used in this work were provided by B. Borisova-Todorova, S. Müller and A. Schöne, as indicated throughout the text.

AFM studies, Far-UV CD spectroscopy and mass spectrometry were done in collaboration with N. Anspach (Department of Genetics, Uni Kassel), Dr. T. Jurkowski (Jacobs University, Bremen) and O. Bertinetti (Department of Biochemistry, Uni Kassel), respectively.

The results of *in vitro* methylation assays were kindly provided by S. Müller on the basis of personal communication and were used for discussion in this work.

Supervision

First supervisor: Prof. Dr. Wolfgang Nellen
Department of Genetics, University of Kassel, Germany

Second supervisor: Prof. Dr. Friedrich W. Herberg
Department of Biochemistry, University of Kassel, Germany

Disputation: 18.08.2010

Acknowledgements

This PhD research was performed in the laboratory of Prof. Dr. Wolfgang Nellen in the Department of Genetics at the University of Kassel.

First, I would like to thank Wolfgang Nellen for giving me the opportunity to perform this PhD thesis under his supervision and for the great support, advices and guidance in both scientific and everyday life during all of the PhD time.

I would like to give my thanks to Prof. Dr. Friedrich W. Herberg for the opportunity to use mass spectrometry equipment and for accepting to be my second supervisor.

I would like to thank Prof. Dr. Markus Maniak for permission to use some equipment in the Department of Cell Biology and for some occasional discussions on the scientific topics.

I would also like to thank Prof. Dr. Mireille A. Schäfer for permission to use some of the equipment in the Radiolab.

Special thanks go to

Dr. Thomasz Jurkowski (Jacobs University, Bremen) for help with Far-UV CD spectroscopy and other collaboration.

Oliver Bertinetti (Department of Biochemistry) for performing MS experiments and analysis of my protein samples.

Nils Anspach for collaboration in AFM studies of DnmA-DNA interaction and fruitful discussions.

Sara Müller for valuable discussions and advices during the PhD research as well as for the permission to use some of her *in vitro* methylation data for discussion in this work.

And finally I would like to give my largest thanks to every person in the department, for collaborators which I did not mention here, for help, assistance, support, jokes, friendliness and concern.

Summary

Eukaryotic DNA m^5C methyltransferases (MTases) play a major role in many epigenetic regulatory processes like genomic imprinting, X-chromosome inactivation, silencing of transposons and gene expression. Members of the two DNA m^5C MTase families, Dnmt1 and Dnmt3, are relatively well studied and many details of their biological functions, biochemical properties as well as interaction partners are known. In contrast, the biological functions of the highly conserved Dnmt2 family, which appear to have non-canonical dual substrate specificity, remain enigmatic despite the efforts of many researchers.

The genome of the social amoeba *Dictyostelium* encodes Dnmt2-homolog, the DnmA, as the only DNA m^5C MTase which allowed us to study Dnmt2 function in this organism without interference by the other enzymes. The *dnmA* gene can be easily disrupted but the knock-out clones did not show obvious phenotypes under normal lab conditions, suggesting that the function of DnmA is not vital for the organism. It appears that the *dnmA* gene has a low expression profile during vegetative growth and is only 5-fold upregulated during development. Fluorescence microscopy indicated that DnmA-GFP fusions were distributed between both the nucleus and cytoplasm with some enrichment in nuclei. Interestingly, the experiments showed specific dynamics of DnmA-GFP distribution during the cell cycle. The proteins colocalized with DNA in the interphase and were mainly removed from nuclei during mitosis.

DnmA functions as an active DNA m^5C MTase *in vivo* and is responsible for weak but detectable DNA methylation of several regions in the *Dictyostelium* genome. Nevertheless, gel retardation assays showed only slightly higher affinity of the enzyme to dsDNA compared to ssDNA and no specificity towards various sequence contexts, although weak but detectable specificity towards AT-rich sequences was observed. This could be due to intrinsic curvature of such sequences. Furthermore, DnmA did not show denaturant-resistant covalent complexes with dsDNA *in vitro*, although it could form covalent adducts with ssDNA. Low binding and methyltransfer activity *in vitro* suggest the necessity of additional factor in DnmA function. Nevertheless, no candidates could be identified in affinity purification experiments with different tagged DnmA fusions. In this respect, it should be noted that tagged DnmA fusion preparations from *Dictyostelium* showed somewhat higher activity in both covalent adduct formation and methylation assays than DnmA expressed in *E.coli*. Thus, the presence of co-purified factors cannot be excluded. The low efficiency of complex formation by the recombinant enzyme and the failure to define interacting

proteins that could be required for DNA methylation *in vivo*, brought up the assumption that post-translational modifications could influence target recognition and enzymatic activity. Indeed, sites of phosphorylation, methylation and acetylation were identified within the target recognition domain (TRD) of DnmA by mass spectrometry. For phosphorylation, the combination of MS data and bioinformatic analysis revealed that some of the sites could well be targets for specific kinases *in vivo*. Preliminary 3D modeling of DnmA protein based on homology with hDNMT2 allowed us to show that several identified phosphorylation sites located on the surface of the molecule, where they would be available for kinases. The presence of modifications almost solely within the TRD domain of DnmA could potentially modulate the mode of its interaction with the target nucleic acids.

DnmA was able to form denaturant-resistant covalent intermediates with several *Dictyostelium* tRNAs, using as a target C38 in the anticodon loop. The formation of complexes not always correlated with the data from methylation assays, and seemed to be dependent on both sequence and structure of the tRNA substrate. The pattern, previously suggested by the Helm group for optimal methyltransferase activity of hDNMT2, appeared to contribute significantly in the formation of covalent adducts but was not the only feature of the substrate required for DnmA and hDNMT2 functions. Both enzymes required Mg^{2+} to form covalent complexes, which indicated that the specific structure of the target tRNA was indispensable. The dynamics of covalent adduct accumulation was different for DnmA and different tRNAs. Interestingly, the profiles of covalent adduct accumulation for different tRNAs were somewhat similar for DnmA and hDNMT2 enzymes. According to the proposed catalytic mechanism for DNA m^5C MTases, the observed denaturant-resistant complexes corresponded to covalent enamine intermediates. The apparent discrepancies in the data from covalent complex formation and methylation assays may be interpreted by the possibility of alternative pathways of the catalytic mechanism, leading not to methylation but to exchange or demethylation reactions. The reversibility of enamine intermediate formation should also be considered. Curiously, native gel retardation assays showed no or little difference in binding affinities of DnmA to different RNA substrates and thus the absence of specificity in the initial enzyme binding. The meaning of the tRNA methylation as well as identification of novel RNA substrates *in vivo* should be the aim of further experiments.

Charakterisierung von DnmA, dem Dnmt2-Homolog in *Dictyostelium discoideum*

Inaugural-Dissertation

zur

Erlangung des akademischen Grades eines

Doktors der Naturwissenschaften (Dr. rer. nat.)

im Fachbereich Naturwissenschaften und Mathematik

der Universität Kassel

vorgelegt von

Vladimir Maksimov

Kassel, July 2010

Erklärung

Hiermit versichere ich, dass ich die vorliegende Dissertation selbständig und ohne unerlaubte Hilfe angefertigt und andere als die in der Dissertation angegebenen Hilfsmittel nicht benutzt habe. Alle Stellen, die wörtlich oder sinngemäß aus veröffentlichten oder unveröffentlichten Schriften anderer Personen entnommen sind, habe ich als solche kenntlich gemacht.
Kein Teil dieser Arbeit ist in einem anderen Promotions- oder Habilitationsverfahren verwendet worden.

Kassel, den 07.2010

Zusammenfassung

Eukaryotische DNA m^5C Methyltransferasen (MTasen) spielen eine wesentliche Rolle bei vielen epigenetischen Prozessen wie Imprinting, X-Chromosom Inaktivierung, Stilllegung von Transposons und Genexpression. Die beiden DNA m^5C Methyltransferasefamilien Dnmt1 und Dnmt3 sind relativ gut untersucht und es sind viele Details bezüglich ihrer biochemischen Eigenschaften, der biologischen Funktion sowie Interaktionspartner bekannt. Trotz intensiver Bemühungen vieler Forscher bleibt im Gegensatz dazu die biologische Funktion der hoch konservierten Dnmt2 Familie, die nicht-kanonische Dualspezifizität zeigt, weiterhin sehr rätselhaft. Im Genom der sozialen Amöbe *Dictyostelium* ist ein Dnmt2-Homolog, DnmA, kodiert. Da DnmA die einzige Methyltransferase in diesem Organismus ist, erlaubt uns dies Dnmt2 Funktionen ohne den Einfluss anderer MTasen zu untersuchen. Ein Knockout des *dnmA* Gens zeigte unter normalen Laborbedingungen keinen offensichtlichen Phänotyp und scheint somit für den Organismus nicht essentiell zu sein. In vegetativen Zellen wird *dnmA* nur schwach exprimiert, in der Entwicklung ist die Expression jedoch um den Faktor fünf erhöht. Fluoreszenzmikroskopische Untersuchungen zeigten, dass DnmA-GFP Fusionsproteine im Zellkern angereichert sind, aber auch im Cytoplasma lokalisieren. DnmA-GFP zeigte eine interessante Verteilung während des Zellzyklus. Das Protein kolokalisierte mit DNA während der Interphase, war aber während der Mitose aus dem Zellkern ausgeschlossen.

DnmA ist eine aktive DNA m^5C MTase *in vivo* und ist für eine schwache aber detektierbare DNA Methylierung von einigen Regionen im Genom von *Dictyostelium* verantwortlich. Trotzdem zeigten Gelretardierungsexperimente nur eine leicht höhere Affinität des Enzyms gegenüber dsDNA im Vergleich zu ssDNA. Außerdem konnte bis auf eine leicht erhöhte Affinität zu AT- reichen Sequenzen keine Sequenzspezifität beobachtet werden. Dies kann möglicherweise auf eine intrinsische Krümmung der AT-reichen Sequenzen zurückzuführen sein.

Weiterhin zeigte DnmA keine kovalenten Komplexe mit dsDNA unter denaturierenden Bedingungen, obwohl diese mit ssDNA ausgebildet werden konnten. Die geringe Bindungs- und Methyltransferaseaktivität *in vitro* lässt vermuten, dass noch andere Faktoren für die Funktion der DnmA notwendig sind. Allerdings konnten keine Interaktionspartner durch Affinitätschromatographie mit verschiedenen DnmA Fusionsproteinen gefunden werden. In diesem Zusammenhang sollte erwähnt werden, dass DnmA Fusionsproteine, die direkt aus *Dictyostelium* isoliert wurden, *in vitro* eine höhere kovalente Komplexbildungs- und Methylierungsaktivität

zeigten als rekombinante DnmA aus *E. coli*. Es kann also nicht ausgeschlossen werden, dass doch weitere Proteine mit aufgereingt werden. Die geringere Fähigkeit der rekombinanten Proteine kovalente Komplexe zu bilden sowie die Tatsache, dass keine interagierenden Proteine gefunden werden konnten, führten zu der Annahme, dass möglicherweise posttranslationale Modifikationen Substraterkennung und Methylierungsaktivität beeinflussen könnten. Tatsächlich konnten einige Phosphorylierungs-, Methylierungs- und Acetylierungsstellen in der *target recognition domain* (TRD) von DnmA mittels Massenspektrometrie identifiziert werden. Die Kombination von MS und bioinformatischer Daten zeigte für die Phosphorylierungsstellen, dass diese durchaus Erkennungsstellen von spezifischen Kinasen *in vivo* entsprechen. Vorläufige Ergebnisse einer 3D Modellierung von DnmA anhand der Homologie zur hDNMT2 erlauben die Aussage, dass die Phosphorylierungsstellen auf der Außenseite des Moleküls zu finden sind, wo sie zugänglich für Kinasen wären. Das nahezu alleinige Vorkommen von Modifikationen in der TRD von DnmA kann möglicherweise die Interaktion des Proteins mit der Nukleinsäure modulieren.

DnmA konnte unter denaturierenden Bedingungen stabile kovalente Komplexe mit verschiedenen tRNAs aus *Dictyostelium* ausbilden, wobei die Position C38 im Anticodonloop als Zielnukleotid fingierte. Die Bildung von kovalenten Komplexen korrelierte nicht immer mit den Daten der *in vitro* Methylierungsassays, scheint aber sowohl sequenz- als auch strukturabhängig zu sein. Das von Mark Helm postulierte Sequenzmuster für optimale Methyltransferaseaktivität von hDNMT2 scheint einen signifikanten Beitrag für die kovalente Komplexbildung zu sein, ist aber nicht das einzige Merkmal, das für die Aktivität von DnmA und hDNMT2 wichtig ist. Beide Enzyme benötigen Magnesium für die Bildung kovalenter Komplexe, was einen Hinweis dafür gibt, dass die spezifische Struktur der tRNA für die Methylierungsreaktion unerlässlich ist. Die Dynamik der kovalenten Komplexbildung differiert für DnmA und verschiedene tRNAs, wobei interessanterweise die Profile für die Akkumulation von kovalenten Komplexen für DnmA und hDNMT2 sehr ähnlich sind. Ausgehend von dem vorgeschlagenen Mechanismus für DNA m^5C MTasen entsprechen die kovalenten Komplexe den kovalenten Enamin-Intermediaten. Die offensichtlichen Unterschiede zwischen den Daten von kovalenter Komplexbildung und Methylierung können möglicherweise durch unterschiedliche Wege des katalytischen Mechanismus erklärt werden, die entweder nicht zu Methylierung oder aber zu Demethylierung führen. Ebenfalls sollte die Reversibilität der Enamin-Intermediate in Betracht gezogen werden. Gelretardierungsexperimente zeigten keine oder nur geringe Unterschiede in der Affinität von DnmA zu verschiedenen tRNA Substraten, das gegen eine Spezifität des initialen Schrittes der

Enzymbindung spricht. Die Bedeutung der tRNA Methylierung sowie die Identifikation neuer RNA Substrate *in vivo* sollte das Ziel weiterer Experimente sein.

Table of Contents

1 List of Abbreviations

aa	amino acid
AFM	Atomic Force Microscopy
Amp	Ampicillin
AP	Alkaline Phosphatase
APS	Ammonium Persulphate
ATP	Adenosine-5'-triphosphate
as	antisense
5-azacytidine	5-aza-2'-deoxycytidine
BCIP	5-Bromo-4-Chloro-3-Indolyl Phosphate
bp	base pairs
BS	Blasticidin
BSR	Blasticidin Resistance cassette
BSA	Bovine Serum Albumin
cAMP	3'-5'-cyclic Adenosine monophosphate
cDNA	complementary DNA
DEPC	Diethylpirocarbonate
DAPI	4', 6-Diamidino-2-phenylindole
DNA	Deoxyribonucleic Acid
DMF	Dimethylformamide
DMSO	Dimethyl Sulfoxide
DTT	Dithiothreitol
dNTP	deoxyribonucleotide triphosphate
ds	double stranded
EDTA	Ethylenediaminetetraacetic Acid
EGTA	Ethyleneglycol-bis-(2-aminoethylether)-N,N'-
EMSA	Electrophoretic Mobility Shift Assay
Fig.	Figure
G418	Geneticin

GFP	Green Fluorescent Protein
hr(s)	hour(s)
HEPES	N-(2-Hydroxyethyl) Piperazine-N'-(2-Ethanesulfonic acid)
IPTG	Isopropyl-Beta-D-Thiogalactopyranoside
kb	kilobase pairs
kDa	kiloDalton
KO	Knock-Out
L	Liter
LC/MS	Liquid Chromatography/Mass Spectrometry
M	Molarity [mol/l]
mA	milliampere
MW	Molecular weight
NBT	Nitro Blue Tetrazolium chloride
NP40	Nonidet®P40 (also known as igepal)
NTP	ribonucleotide triphosphate
nt	nucleotide
OD_x	Optical density at wavelength x [nm]
PAGE	Polyacrylamide Gel Electrophoresis
PCR	Polymerase Chain Reaction
PEG	Polyethylene glycol
PMSF	Phenylmethylsulfonylfluorid
PNK	Polynucleotide Kinase
PTGS	Posttranscriptional Gene Silencing
RdRP	RNA-directed RNA Polymerase
tRNA	transfer-ribonucleic acid
RNAi	RNA interference
rcf	relative centrifugal force
rpm	revolutions per minute
RT	Room Temperature (usually 22°C)
SAM	S-Adenosyl-L-methionine

siRNA	small interfering ribonucleic acids
SDS	sodium dodecyl sulphate
ss	single stranded
TAE	Tris-Acetate-EDTA
TBE	Tris-Borate-EDTA
TAP	Tandem Affinity Purification
TBq	Terabecquerel
TEMED	N'N'N'N'-Tetramethylethylenediamine
Tris	Tris (hydroxymethyl) aminomethane
Triton-X-100	T-Octylphenoxypolyethoxethanol
U	Units
UTP	Uridine-5'-triphosphate
UV	Ultraviolet
V	Volt
v/v	Volume per volume
w/v	Weight per volume
W	Watt
wt	Wild-type

2 Introduction

2.1 Epigenetics

In Molecular biology, *epigenetics* refer to the study of inherited changes in gene expression patterns caused by mechanisms other than changes in the underlying DNA sequence, hence the name *epi-* (Greek: *επί-* over, above) *–genetics*. These changes are established during embryonic development and may be maintained through cell divisions for the rest of the cell's life. There are two main mechanisms involved in epigenetic processes. One represents regulation of gene expression patterns through various processes of chromatin remodeling, including histone modifications. The other one, which is tightly linked to chromatin remodeling, represents chemical modification of cytosine bases in DNA by converting cytosine to 5-methylcytosine, the process known as DNA methylation. In higher eukaryotes, the interplay between the m^5C methylation status of genomic DNA and specific combinations of histone modifications and/or histone variants leads to different states of chromatin, thereby creating transcriptionally competent euchromatin or silent heterochromatin. These regulatory layers result in epigenomic information that lies above the DNA sequence and is also inherited and susceptible to variation. Thus, the epigenome is the sum of both the chromatin structure and the DNA methylation patterns resulting from an interaction between the genome and the environment (Bronner et al, 2009). Genome and epigenome together, determine when genes are expressed, at which level and provide a cell memory for the maintenance of cellular functions.

2.1.1 DNA Methylation

Generally speaking, *in vivo* DNA methylation can occur at C5 and N4 of cytosine and N6 of adenine bases. Usually, N4-methylcytosine is restricted to bacteria, while N6-methyladenine can be found in bacteria, fungi, and lower eukaryotes such as green algae and ciliates. The only DNA methylation occurring among all domains of organisms is the C5-methylcytosine (m^5C) (Cheng, 1995); (Wion & Casadesus, 2006). In bacteria, DNA adenine and cytosine methylation play important roles as a protection against bacteriophage infection or maintenance of a species genome identity (Jeltsch, 2003). In this case, any unmethylated DNA will be recognized as foreign and be destroyed by endonuclease activity of restriction systems. Other functions of bacterial methylation

include methylation-guided mismatch-repair, chromosome replication and segregation (Wion & Casadesus, 2006).

The m^5C DNA methylation is the only DNA modification in genomic DNA of vertebrates, and it is conserved in most major eukaryotic groups, including plants, fungi, invertebrates and protists, although it has been lost from certain model organisms such as the budding yeast *Saccharomyces cerevisiae*, fission yeast *Schizosaccharomyces pombe* and nematode *Caenorhabditis elegans* (Bird, 2002); (Henderson & Jacobsen, 2007); (Goll & Bestor, 2005). The m^5C methylation of genomic DNA is an indispensible epigenetic mark throughout differentiation and development of most organisms and has a major role in many epigenetic regulatory processes, including genomic imprinting, X-chromosome inactivation, silencing of transposons and other repetitive DNA sequences, as well as expression of genes (Panning & Jaenisch, 1998); (Vaissière et al, 2008); (Feng et al, 2010). In higher eukaryotes, methylation occurs mainly in the context of CpG dinucleotides throughout the genome except for CpG islands (Feng et al, 2010). CpG islands (CGIs) are discrete CpG-rich regions, usually found to be unmethylated, which locate in the promoters and gene regulatory units of 50%–70% of genes (Blackledge et al, 2010). CGI methylation is involved physiologically in genomic imprinting and X-inactivation and pathologically in developmental diseases and cancer (Shen et al, 2007). Therefore, aberrant DNA methylation has an important impact on cancer development. In plants, DNA is highly methylated and m^5C is located mainly in symmetrical CpG and CpNpG sequences but it may occur also in other non-symmetrical contexts (Morales-Ruiz et al, 2006). Generally speaking, DNA methylation is thought to occur "globally" in vertebrates, with CpG sites being heavily methylated genome-wide except for those in CpG islands, whereas invertebrates, plants, and fungi have "mosaic" methylation, characterized by interspersed methylated and unmethylated domains (Suzuki & Bird, 2008). DNA methylation in coding regions (or gene body methylation) is conserved with clear preference for exons in most organisms, although it does not generally affect gene expression (Zhang et al, 2010).

Usually, DNA methylation is closely associated with histone modifications and it affects binding of specific proteins to DNA and formation of respective complexes in chromatin to control gene expression and genome stability (Feng et al, 2010). Similar to other biochemical modifications such as protein phosphorylation and acetylation, DNA methylation is also reversible (Niehrs, 2009). Demethylation may take place as a passive process because maintenance methylation can be inactivated during several cycles of DNA replication in preimplantation development (Reik et al, 2003); (Morgan et al, 2005). In addition to "global" demethylation during germ cell differentiation,

site-specific local demethylation also occurs throughout development and tissue differentiation (Zilberman, 2008); (Zhu, 2009).

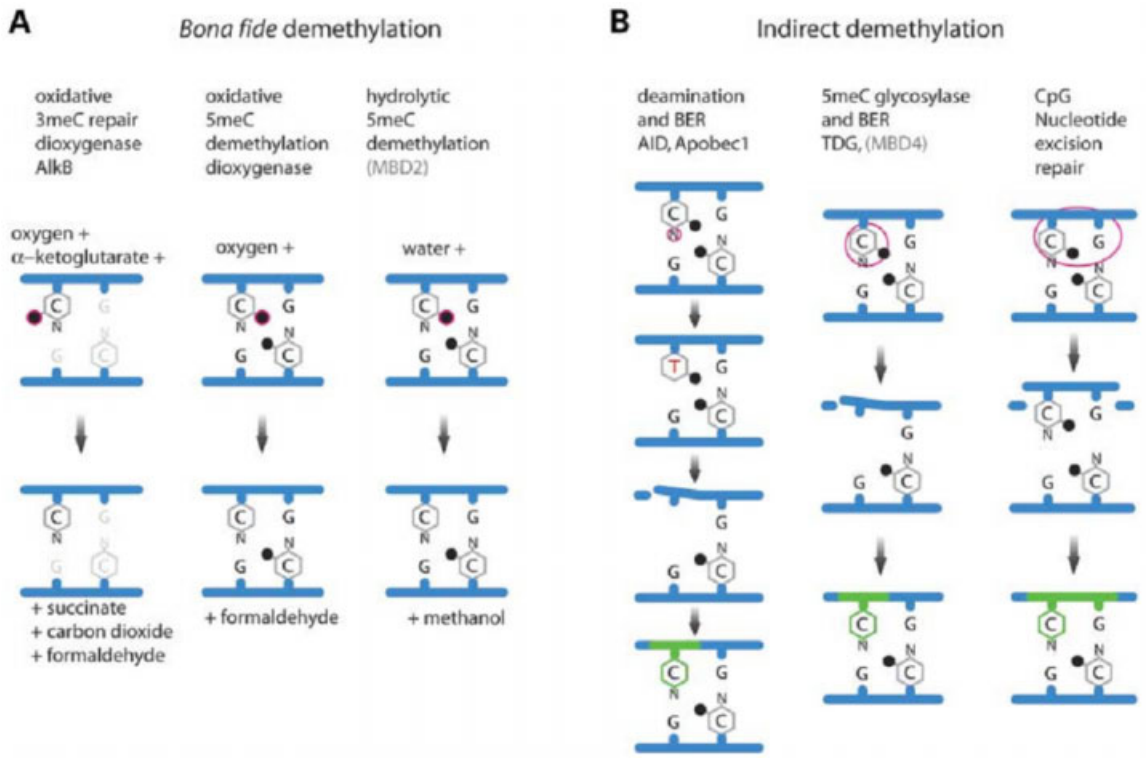

Figure 2.1.1 Mechanisms of DNA *bona fide* (**A**) and indirect (**B**) demethylation. Proposed pathways for DNA demethylation have different initial targets (purple rings). Methyl group is represented by black close cycles. *Bona fide* demethylation, i.e. direct removal of the methyl group, involves no DNA strand breaks. Oxidative demethylation of m^5C by a mechanism similar to m^3C repair by AlkB (Duncan et al, 2002), hydrolytic reduction (similar to that proposed for MBD2) (Bhattacharya et al, 1999); (Ng et al, 1999). Removal of a mismatched T following deamination of m^5C (Morgan et al, 2004) or removal of the m^5C by a glycosylase (Hardeland et al, 2003), would require replacement of the cytosine (green), by a base excision repair (BER). An activity has been described that exchanges the m^5CpG, through nucleotide excision repair (NER), perhaps by NER endonuclease XPG (Gehring et al, 2009). Adapted from Morgan et. al., 2005.

In plants, active demethylation (though it probably acts synergistically with passive loss of methylation) of promoters by the 5-methylcytosine DNA glycosylase or DEMETER (DME) is required for the expression of imprinted genes in endosperm, while the related Repressor of Silencing 1 (ROS1) is necessary for release of transcriptional silencing of a hypermethylated transgene (Morales-Ruiz et al, 2006). This subfamily of DNA glycosylases functions to promote DNA demethylation through a base excision-repair pathway. In animals, active DNA demethylation

also involves the base excision-repair pathway, where the AID/Apobec family of deaminases convert 5-methylcytosine to thymine followed by G/T mismatch repair by the thymine DNA glycosylases MBD4 or TDG (Chinnusamy & Zhu, 2009). The candidate mechanisms for DNA demethylation are schematically described on Figure 2.1.1.

2.1.2 Eukaryotic DNA Methyltransferases

In higher eukaryotes, DNA methylation occurs through DNA methyltransferases (Dnmts) that transfer the methyl group from S-Adenosyl-L-methionine (SAM or AdoMet) to cytosine bases to form 5-Methylcytosine (m^5C). In mammals, five distinct DNA m^5C methyltransferases (m^5C MTases) or MTase-like proteins have been found which share a high degree of homology mainly in their conserved catalytic domains (Tang et al, 2003); (Hermann et al, 2004). These proteins are divided into three families: Dnmt1 (maintenance MTase), two *de novo* enzymes Dnmt3a and 3b and the closely related but catalytically inactive Dnmt3L protein, and finally, Dnmt2 which contains all characteristic catalytic motifs of DNA MTases, has a residual DNA methylation activity but is also involved in methylation of at least some tRNAs (Figure 2.1.2) (Hermann et al, 2004); (Goll et al, 2006).

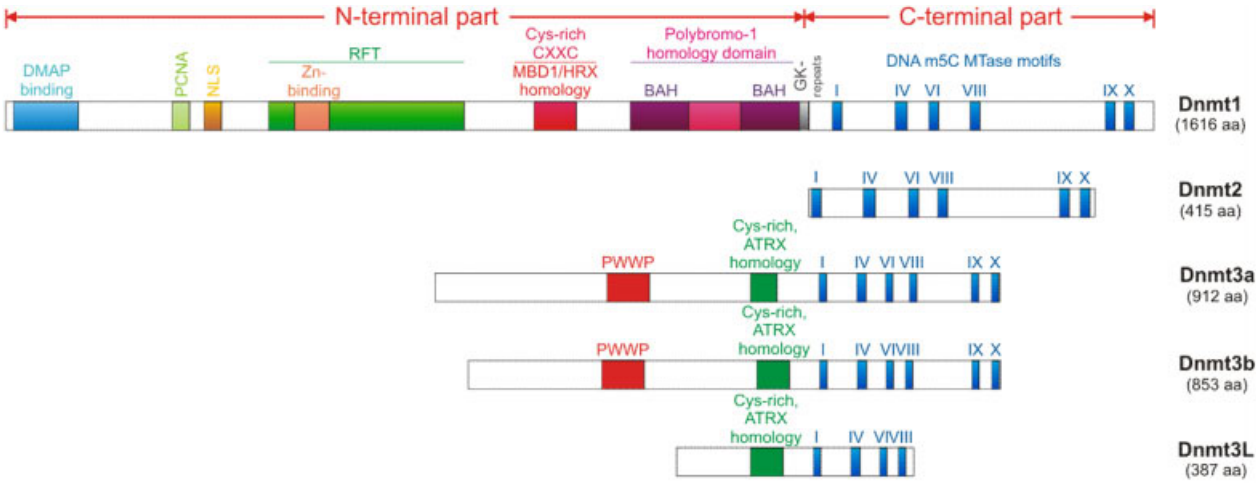

Figure 2.1.2 Schematic representation of murine Dnmt family. Roman numerals refer to conserved motifs of DNA MTases (Kumar et al, 1994); motif IV includes the Cys nucleophile that forms a transient covalent bond to C6 of the target cytosine. Other details are explained in the text or in work by Goll and Bestor, 2005. Adapted from Goll and Bestor, 2005, and Cheng and Blumenthal, 2008.

The C-terminal catalytic domains of all eukaryotic DNA m^5C MTases display high homology to

bacterial methyltransferases, which led to the conclusion that mammalian and prokaryotic enzymes share a common evolutionary origin (Bestor et al, 1988); (Goll & Bestor, 2005).

The Dnmt1 Family of DNA Methyltransferases

The first mammalian DNA MTase purified and cloned was later named Dnmt1 (Bestor et al, 1988). Mammalian Dnmt1 is a multidomain protein, which consist of a large N-terminal regulatory region and a C-terminal catalytic domain, which are separated by GK repeats (Jeltsch, 2006). The catalytic domain contains all the conserved amino acid motifs necessary for catalysis but by itself is catalytically inactive (Fatemi et al, 2001). The N-terminal tail contains several motifs of poorly understood functions, which serve to provide a platform for intracellular targeting and regulation of the Dnmt1 enzymatic activity (see Figure 2.1.2) (Cheng & Blumenthal, 2008). These include a nuclear localization signal (NLS), a domain which targets replication foci (RFT), a motif for interaction with PCNA (proliferating cell nuclear antigen binding domain), a zinc binding domain (Zn-domain), a cysteine-rich region (CXXC) and a polybromo-1 homology domain (PBHD) (Bestor, 2000); (Leonhardt et al, 1992); (Margot et al, 2003) and (Pradhan & Esteve, 2003). The N-terminal tail of Dnmt1 has been shown to interact with several other proteins like the transcriptional co-repressor DMAP1, the histone deacetylases HDAC1 and HDAC2, the transcription factor E2F1 and the Rb tumor suppressor protein (Masamitsu et al, 2009); (Myant & Stancheva, 2008); (Robertson et al, 2000). Dnmt1 shows a significant preference for hemimethylated CpG sites in DNA and it functions as a maintenance methyltransferase *in vivo* (Hermann et al, 2004). Consistently, Dnmt1 is highly expressed in proliferating cells and at low levels in differentiated cells (Jeltsch, 2006). Dnmt1 also seems to be involved in re-establishing of the original DNA methylation pattern upon DNA repair (Mortusewicz et al, 2005). However, there is also evidence that Dnmt1 is required for *de novo* methylation in a non-CpG context and even in CpG islands (Grandjean et al, 2007); (Jair et al, 2006).

The Dnmt3 Family of DNA Methyltransferases

The Dnmt3 family includes two active *de novo* Dnmts, Dnmt3a and Dnmt3b, and one regulatory protein, Dnmt3-Like protein (Dnmt3L) (Goll & Bestor, 2005). Dnmt3a and Dnmt3b have similar domain arrangements: both contain a variable region at the N terminus, followed by a PWWP domain that may be involved in non-specific DNA binding, a Cys-rich Zn-binding ATRX-DNMT3-DNMT3L homology domain (ADD domain, comprising six CXXC motifs) and a C-terminal

catalytic domain (see Figure 2.1.2) (Stephen et al, 2006); (Cheng & Blumenthal, 2008). The amino acid sequence of Dnmt3L is very similar to that of Dnmt3a and Dnmt3b in the ADD domain, but it lacks the conserved residues required for DNA MTase activity in the C-terminal domain (Jia et al, 2007). In mammals, Dnmt3a and Dnmt3b are expressed in a range of adult tissues but at lower levels than Dnmt1 (Goll & Bestor, 2005). *In vitro*, both recombinant Dnmt3a and Dnmt3b transfer methyl groups to hemimethylated and unmethylated substrates at equal rates and without evidence of intrinsic sequence specificity beyond the CpG dinucleotide (Okano et al, 1998a). However, later studies revealed that in addition to CpG, Dnmt3a methylated CpA but not CpT and CpC, and Dnmt3b methylated both CpA and CpT but scarcely CpC (Suetake et al, 2003). Interestingly, Dnmt3a showed higher DNA methylation activity than Dnmt3b towards naked DNA and the naked part of nucleosomal DNA, but scarcely methylated the DNA within the nucleosome core region, while Dnmt3b significantly did so, although with low activity (Takeshima et al, 2006). Furthermore, mouse Dnmt3a preferentially methylated the linker DNA and its activity was inhibited by the presence of histone H1 (Takeshima et al, 2008). These differences in enzymatic properties of Dnmt3a and Dnmt3b may contribute to the distinct functions of these enzymes *in vivo.* Indeed, Dnmt3a and Dnmt3b methylate different genomic DNA regions *in vivo*; while Dnmt3a is crucial for "global" methylation, including that of imprinted genes in germ cells and the short interspersed repeat SineB1, Dnmt3b is specifically required for methylation of pericentromeric minor satellite repeats during embryogenesis (Takeshima et al, 2006); (Rottach et al, 2009). Nevertheless, both Dnmt3a and Dnmt3b are involved in the methylation of some DMRs and long interspersed repeats IAP and Line1, which demonstrate overlapping function in some particular regions in genomic DNA (Kato et al, 2007). In contrast to the isolated catalytic domain of Dnmt1, C-terminal domains of Dnmt3a and Dnmt3b are catalytically active (Gowher & Jeltsch, 2002). Interestingly, the catalytic domain of Dnmt3a methylates DNA in a distributive manner, while Dnmt3b is a processive enzyme, which supported the suggestion that Dnm3b may be involved in methylation near methylated sites, acting in cooperation with Dnmt1 (Rottach et al, 2009). Dnmt3L colocalizes and coimmunoprecipitates with both Dnmt3a and Dnmt3b, and it enhances *de novo* methylation by both of these MTases (Hata et al, 2002); (Suetake et al, 2004); (Kareta et al, 2006). Moreover, recent studies have shown that Dnmt3L and Dnmt3a (or Dnmt3b) can form heterodimers and tetramers (3L-3a-3a-3L) via their C-terminal domains (Cheng & Blumenthal, 2008). Interestingly, Dnmt3a and Dnmt3b could also form homooligomers (or even 3a-3b heterooligomers) via alternative interfaces involving the DNA-binding domain. Nevertheless, the functions of Dnmt3a/b

oligomers and the reasons for lower activity in comparison to Dnmt3a-3L (or Dnmt3b-3L) heterotetramers remain unclear (Li et al, 2007).

The Dnmt2 Family of DNA Methyltransferases

Dnmt2 is the most widely distributed DNA MTase family and the members show a high level of conservation (35-50%) (Goll & Bestor, 2005). With the notable exception of *Caenorhabditis elegans* and *Saccharomyces cerevisiae*, this protein has been reported in many model organisms such as *Drosophila melanogaster*, *Arabidopsis thaliana*, *Xenopus laevis*, *Danio rerio*, *Mus musculus*, and *Homo sapiens*. It is also present in lower eukaryotes such as *Dictyostelium discoideum* and *Entamoeba histolytica*. Dnmt2 is relatively small protein of about 390 amino acids and contains only the catalytic domain, lacking any regulatory domains as in the Dnmt1 and Dnmt3 families (Bestor, 2000). Originally, this enzyme failed to show DNA methylation activity in the *in vitro* methylation assays, although denaturant-resistant complex formation of Dnmt2 to DNA was reported *in vitro*, which suggested that Dnmt2 can covalently bind to DNA (Okano et al, 1998b); (Dong et al., 2001). Later, residual methylation activity was shown *in vivo* and *in vitro*, however at a much lower level than for Dnmt1, Dnmt3a and 3b (Hermann et al, 2003); (Mund et al, 2004); (Kuhlmann et al, 2005). As a consequence, the DNA MTase activity of Dnmt2 has now been analyzed in various experimental settings and model organisms. Experiments in *Drosophila* suggested that Dnmt2 can methylate isolated cytosines without any recognizable target sequence specificity (Lyko et al, 2000). Similarly, purified recombinant human Dnmt2 methylated DNA substrates at about one out of 250 cytosine residues in a nonprocessive manner and with little or no sequence specificity (Hermann et al, 2003). The low DNA MTase activity and non-processivity can be explained by the requirement for a specific cofactor or by the presence of a sterically unfavorable tyrosine residue next to CFT tripeptide in the target recognition domain (TRD) of Dnmt2, which could impair the binding to dsDNA (Goll & Bestor, 2005). However, recent bisulfite sequencing analyses have suggested a significant locus-specific DNA methyltransferase activity of Dnmt2 on certain retroelements in *Dictyostelium* and *Drosophila* genomes (Kuhlmann et al, 2005); (Phalke et al, 2009). In general, model organisms, which carry a Dnmt2 homolog as the only DNA MTase gene, show very low levels of genomic DNA m^5C methylation (< 1%) mainly in non-CpG context (Lyko et al, 2000); (Kuhlmann et al, 2005); (Lavi et al, 2006).

In mammals, Dnmt2 is expressed in various splice forms in all tissues at low levels; with highest transcription rates in testis, ovary and thymus (Yoder & Bestor, 1998). However, Dnmt2 knock-out

mice and plants show no obvious phenotype and are viable and fertile (Okano et al, 1998b). In fact, knock-out mutants in almost all tested model organisms do not show strong phenotypes, if any (Wilkinson et al, 1995); (Kunert et al, 2003) and (Goll et al, 2006). The exceptions include *Dictyostelium* knock-out mutants, which showed minor developmental phenotypes (Katoh et al, 2006), and Dnmt2 knock-out of zebrafish, which uncovered lethal differentiation defects in the retina, liver and brain (Rai et al, 2007). Additionally, in *Entamoeba*, treatment with 5-Azacytidine (5-AzaC), an inhibitor of DNA MTase, was shown to cause a shift from a virulent to a non-virulent phenotype (Fisher et al, 2004); (Ali et al, 2007). The overexpression of Dnmt2 in *Drosophila* has been shown to extend the lifespan of flies, and the underlying mechanism has been linked to oxidative stress resistance (Lin et al, 2005). Similarly, the overexpression of Ehmeth (Dnmt2 homolog in *Entamoeba*) leads to a pleiotropic phenotype, with increased resistance to oxidative stress, upregulation of the heat shock protein HSP70 and the accumulation of multinucleated cells (Fisher et al, 2006).

The subcellular localization of an enzyme can be an important indicator for its biological function. Dnmt1 and Dnmt3a/3b/3L DNA MTases, for instance, are predominantly nuclear enzymes, consistent with their role in the modification of a DNA substrate (Bachman et al, 2001); (Spada et al, 2007). Remarkably, in all tested organisms Dnmt2 homologues showed some distribution between nuclear and cytoplasmic compartments. This notion was also confirmed by biochemical fractionation of protein extracts from *Drosophila* embryos (Schaefer et al, 2008), zebrafish (Rai et al, 2007) and *Entamoeba* (Banerjee et al, 2005), that revealed Dnmt2 protein both in nuclear and in cytoplasmic fractions. Moreover, the same studies also indicated that nuclear Dnmt2 is tightly associated with the nuclear matrix, and the *Entamoeba* Ehmeth has been found to associate with EhMRS2, a DNA that includes a scaffold/matrix attachment region (S/MAR) (Banerjee et al, 2005). The function of the nuclear matrix association is unknown yet, but might be an explanation for the difficulties during biochemical isolation of DNA substrates of Dnmt2, since matrix associated nucleic acids are commonly lost during standard nucleic acid purification procedures (Schaefer & Lyko, 2010).

2.1.3 Chromatin dynamics

In eukaryotic cells, DNA is tightly associated with histones and other proteins to form chromatin. The nucleosome is the basic building block of chromatin and consists of approximately 150 bp of DNA coiled around an octamer of core histones and linker histone H1. The histone octamer

contains two copies of each of the core histones, H2A, H2B, H3, and H4. The histone tails protrude from the globular center of the nucleosome where they may interact with various nuclear factors. The amino acid residues in histone tails as well as some residues within the histone fold are subject to a variety of post-translational modifications, including phosphorylation, acetylation, methylation, ubiquitylation and others (Ito, 2007). Combinations of modifications and specific distribution of various histone variants and non-histone proteins (e.g. HMG proteins, HP1 and various chromatin remodeling complexes) are involved in regulation of chromatin structure, thereby determining its different functional states and playing a role in all epigenetic events (Hon et al, 2009); (Ho & Crabtree, 2010).

Histone Post-Translational Modifications

Post-translational modifications affect the binding of effector proteins to the histones and, thus, regulate the nature of the protein complexes that will associate with a region of chromatin and function to activate or inhibit transcription or to maintain a specific chromatin structure. The ability of proteins to specifically associate with particular histone modifications is the basis of the histone code theory (Strahl & Allis, 2000); (Jenuwein & Allis, 2001).

Acetylation/Deacetylation

Histone acetylation occurs on Lys residues of histones H3 and H4, including H3K9, H3K14 and H4K12 and it is generally associated with regions of active transcription and chromatin decompaction. Many transcriptional coactivators contain histone acetyltransferase (HAT) activity (see Table 2.1.3), including CBP/p300, the p160/SRC family, and P/CAF (Bannister & Kouzarides, 1996); (Spencer et al, 1997); (Lau et al, 2000). In contrast, deacetylase activities have been detected in corepressor complexes, which are involved in transcriptional repression and chromatin compaction. Several HDAC containing complexes have been described thus far, which include Sin3, NuRD, Co-REST and BHC (de Ruijter et al, 2003); (Hakimi et al, 2003). Interestingly, the BHC complex contains either HDAC1 or HDAC2 and histone demethylase (LSD1) (Lee et al, 2006), and the arginine methyltransferase enzymes, like CARM1/PRMT4, have been found to interact with members of p160 family (An et al, 2004).

Methylation/Demethylation

Arginine methylation of histones H3 and H4 as well as lysine methylation may have positive or negative effects on transcription, depending on the methylation site(s) and methylation state (Wysocka et al, 2006); (Kouzarides, 2002). In mammals, PRMT1- and CARM1-catalyzed

asymmetric dimethyl-arginine is involved in gene activation while PRMT5-catalyzed histone symmetric dimethyl-arginine is associated with gene repression (Zhao et al, 2009). CARM1/PRMT4 and PRMT1, are transcriptional coactivators and exhibit different HMT specificities; CARM1 primarily methylates histone H3R2, 17 and 26, whereas PRMT1 methylates H4R3 (Kleinschmidt et al, 2008); (Fritsch et al, 2010); (An et al, 2004).

Table 2.1.3 Histone modifications and histone-modifying enzymes. Adapted from Kim et. al., 2009

Acetyltransferase	**Substrates**	**Deacetylases**	**Substrates**
HAT1	H4 (K5, K12)	SirT2–3	H4K16
GCN5, PCAF	H3 (K9, K14, K18)	**Lysine demethylases**	**Substrates**
CBP, P300	H3 (K14, K18), H4 (K5, K8), H2AK5, H2B (K12, K15)	LSD1/BHC110	H3 (K4, K9)
TIP60/PLIP	H4 (K5, K8, K12, K16), H3K14	JHDM1a-b	H3K36
HBO1	H4 (K5, K8, K12)	JHDM2a-b	H3K9
Lysine methyltransferases	**Substrates**	JMJD2A/JHDM3A, JMJD2B-C	H3 (K9, K36)
		JMJD2D	H3K9
SUV39H1–2	H3K9	JARID1A-D	H3K4
G9a	H3K9	UTX	H3K27
EuHMTase/GLP	H3K9	JMJD3	H3K27
ESET/SETDB1	H3K9	**Serine/threonine kinases**	**Substrates**
CLL8	H3K9	Haspin	H3T3
MLL1–5	H3K4	MSK1–2	H3S28
SET1A-B	H3K4	CKII	H4S1
ASH1	H3K4	Mst1	H2BS14
SET2	H3K36	Rsk2	H3S10
NSD1	H3K36	**Ubquitilases**	**Substrates**
SYMD2	H3K36	Bmi/Ring1a	H2AK119
DOT1	H3K79	RNF20/RNF40	H2BK120
Pr-SET7/8	H4K20	**Arginine methyltransferases**	**Substrates**
SUV4 20H1–2	H4K20	CARM1	H3 (R2, R17, R26)
EZH2	H3K27	PRMT4	H4R3
SET7/9	H3K4	PRMT5	H3R8, H4R3
R1Z1	H3K9		

Methylation of H3K9, H3-K27 and H4K20 is generally associated with heterochromatin and gene repression, whereas methylation of H3K4, H3K36, and H3K79 has been implicated in the transcriptional activation processes (Sims Iii et al, 2003). The H3K9 mono- and dimethylation are localized specifically to silent domains within euchromatin, whereas, H3K9me3 was enriched at pericentric heterochromatin (Rice et al, 2003). Nevertheless, di- and trimethylation of H3K9 can also occur in the transcribed region of active genes in mammalian chromatin (Vakoc et al, 2005). A large number of histone methyltransferases are responsible for methylation of different Lys residues

of H3 and H4 (see Table 2.1.3) (Fritsch et al, 2010).

Originally, methylated histone arginine and lysine residues have been considered static modifications. Nevertheless, the recent identification of enzymes that antagonize or remove histone methylation without the requirement for histone replacement has changed this view and now the dynamic nature of these modifications is being considered (Klose & Zhang, 2007). These novel enzymes include a deiminase that antagonizes histone arginine methylation, and demethylase (amine oxidase and hydroxylase) enzymes that directly remove histone lysine methylation (see Table 2.1.3) (Tsukada et al, 2006).

Phosphorylation/Dephosphorylation

H3, H4 and H2A have been shown to be phosphorylated *in vivo* (Peterson & Laniel, 2004). The best studied are the phosphorylation of histone H3. H3 phosphorylation is involved in a variety of cellular processes, such as chromosome condensation/segregation, transcriptional activation and repression, DNA repair and apoptosis (Kouzarides, 2007). Indeed, the H3S10 phosphorylation appears to have both positive and negative effects and only becomes important in combination with other histone marks within a specific chromatin context (Johansen & Johansen, 2006); (Houben et al, 2007).

Ubiquitylation and Sumoylation

Ubiquitylation is a very large modification, which has been originally found on H2A (K119) and H2B (K120 in human and K123 in yeast). Ubiquitylation of H2AK119 is mediated by the Bmi1/Ring1A protein found in the human Polycomb complex and is associated with transcriptional repression (Zhou et al, 2008). Like ubiquitylation, sumoylation is a very large modification and shows some similarity to ubiquitylation. This modification has been shown to take place on all four core histones, and specific sites have been identified on H4, H2A, and H2B (Nathan et al, 2006). Sumoylation antagonizes both acetylation and ubiquitylation, which occur on the same lysine residue, and consequently this modification is repressive for transcription in yeast (Garcia-Dominguez & Reyes, 2009).

Proline Isomerization

Prolines in proteins exist in either a *cis* or *trans* conformation. These conformational changes can severely distort the polypeptide backbone and are mediated by Peptidyl-prolyl *cis*/*trans* isomerases. Recently an enzyme, FPR4, has been identified in budding yeast that can isomerize prolines in the tail of H3 (Nelson et al, 2006). FPR4 isomerizes H3P38 and thereby regulates the levels of methylation at H3K36. The appropriate proline isomer is likely to be necessary for the recognition

and methylation of H3K36 by the Set2 methyltranferase. In addition, it is possible that demethylation of H3K36 is also affected by isomerization at H3P38 (Chen et al, 2006).

Histone variants

Whereas the core histones (H2A, H2B, H3 and H4) represent the majority of histones in all organisms, variant versions of these histones (with the exception of H4) exist in low steady-state levels, and they are thought to replace their core histone counterparts at strategic positions in the genome for specialized functions (Cheung & Lau, 2005). For example, the nucleosomes at the centromeres contain the H3 variant Cse4/CENP-A (in yeast/human), and they are thought to perform centromere-specific functions (Okamoto et al, 2007). The distribution of H3.3 variant suggests that it might play some role in the epigenetic marking of transcriptionally active genes, perhaps by mediating local alterations in chromatin structure (Jin & Felsenfeld, 2007). Like H3.3, H2A.Z is conserved from budding yeast to humans and is not distributed uniformly in the genome. The actual distribution and the proposed correlations with function differ among organisms. In *S. cerevisiae*, the H2A.Z homolog Htz1 is involved in the prevention of gene silencing caused by spreading of heterochromatin from neighboring telomeres or the HMR mating type locus (Meneghini et al, 2003). H2Av, the H2A.Z homolog of Drosophila, is involved in Polycomb-mediated silencing and establishment of centromeric heterochromatin (Swaminathan et al, 2005); (Zilberman et al, 2008). In chicken erythroid cells, H2A.Z appears to be concentrated at promoters of developmentally regulated and actively expressed genes (Bruce et al, 2005). At the human c-myc locus, H2A.Z is always enriched at the promoter, whether or not c-myc expression is induced, but is lost from the coding region after induction (Farris et al, 2005). Moreover, in human H2A.Z is excluded from the transcriptionally silent inactive X chromosome, while in early mouse embryos it localizes to the pericentric heterochromatin (Rangasamy et al, 2003). Interestingly, HP1α associates with H2A.Z- but not H2A-containing chromatin, which proposes that H2A.Z and HP1α could function together in compaction of chromatin at heterochromatic domains (Fan et al, 2004). Another histone variant, H2A.X in mammalian cells is rapidly phosphorylated in response to DNA damage and functions to mark the damaged area as well as to recruit DNA repair complexes (Thambirajah et al, 2009). MacroH2A has 3 isoforms: splice variants mH2A1.1 and mH2A1.2, and mH2A2, encoded by a separate gene (Costanzi & Pehrson, 2001). Early work implicated mH2A isoforms as having roles in the formation and maintenance of the inactive X chromosome and facultative heterochromatin. However, the activities of mH2A are not restricted to X chromosome inactivation

and recently new data became available suggested that this histone variant can participate in a broad range of chromatin structures (Abbott et al, 2005). mH2A can undergo several modifications, including methylation, ubiquitylation, poly (ADP)-ribosylation and phosphorylation and specifically recruit poly (ADP-ribose) polymerase 1 (PARP1) and *Xist* RNA. As with mono-ubiquitylation of canonical H2A and H2A.Z, mono-ubiquitylation of mH2A appears to have a role in the maintenance of the inactive X chromosome (Thambirajah et al, 2009). Histone H2A.Bbd (Barr body-deficient) is a novel histone variant which is largely excluded from the inactive X chromosome of mammals. Its distribution overlaps with regions of histone H4 acetylation in the nucleus suggesting its association with transcriptionally active euchromatic regions of the genome (Chadwick & Willard, 2001). Presence of H2A.Bbd within the NCP alter the conformation of the nucleosome in an acetylation-independent way, increasing the accessibility of protein complexes involved in activation of transcription to the DNA (González-Romero et al, 2008).

2.1.4 Interplay between DNA Methylation, Histone Modifications and Chromatin remodeling

One of the most fundamental questions in epigenetic research is how epigenetic modification patterns of DNA and histones are established, erased and translated. Here we summarize recent developments in characterizing the structural and functional linkage between the DNA methylation status, most important histone modifications and chromatin remodeling (Figure 2.1.4.1).

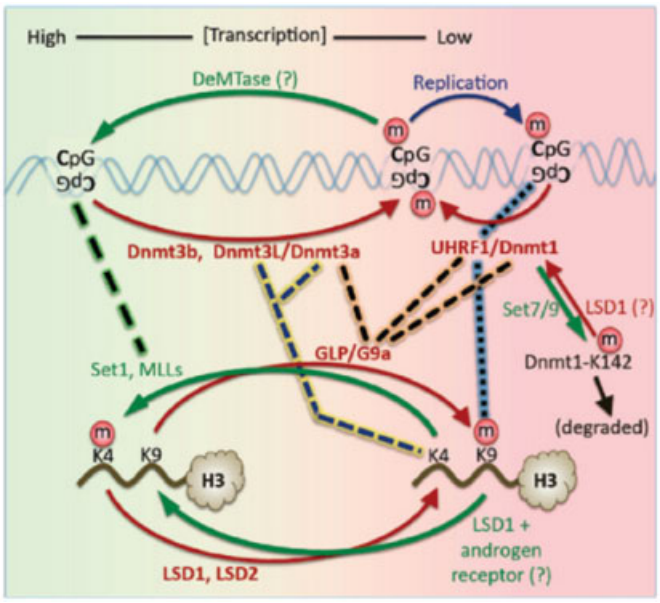

Figure 2.1.4.1 Diagram of interactions that regulate DNA methylation and associated histone H3 modifications. The actions of proteins and arrows are indicated by color: green for activities associated with an increased level of gene expression and red for those tending to decrease the level of expression. Binding interactions are indicated by dashed lines. The "m" in a red circle indicates one or more methyl groups in DNA (m5C) or hystone lysines (Kme). For details, see the text. Adapted from Cheng and Blumentahl, 2010.

DNA methylation has long been shown to have a transcriptional silencing function and is usually connected to the presence of unmodified H3K4 and methylated H3K9 and H3K27 residues (Cedar & Bergman, 2009). Moreover, methylation of H3K4 protects promoters from *de novo* DNA methylation in somatic cells (Weber et al, 2007); (Wen et al, 2008). In addition, tri-methylation of histone H3 lysine 27 (H3K27me3), has been shown to preferentially mark unmethylated DNA in early development and cause silencing by recruiting repressive Polycomb group complexes (Figure 2.1.4.2) (Schlesinger et al, 2007).

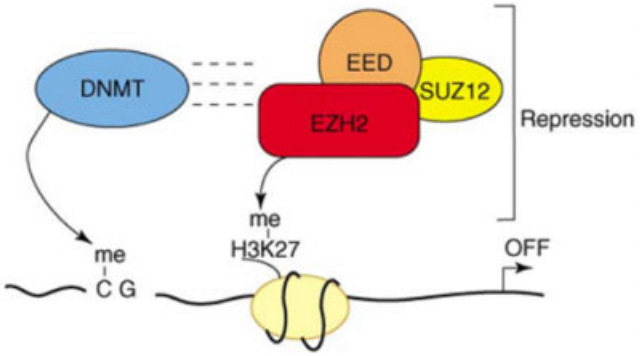

Figure 2.1.4.2 Mechanistic link between DNA methylation and PcG-mediated H3K27 methylation. PRC2/3 complexes comprise EZH2, EED and SUZ12 proteins. A DNA MTase (DNMT) might interact (dashed lines) with EZH2, EED and/or SUZ12. The interplay between these proteins would result in methylation of DNA and lysine 27 of histone H3, and consequent transcriptional repression. As in the case of the link between DNA and H3K9 methylation, the 'conversation' between methylated CpG and H3K27 methylation might be bidirectional. Adapted from Fuks, 2005.

In contrast to H3K4, methylation at H3K9 is positively correlated with DNA methylation (Nguyen et al, 2002). There is evidence that H3K9-CpG linked methylation represents an evolutionarily conserved silencing pathway. In the filamentous fungus *Neurospora* (Tamaru et al, 2003) and in the plant *Arabidopsis* (Jackson et al, 2002), the H3K9 methyltransferases DIM-5 and KRYPTONITE, respectively, are required for DNA methylation. In mammals, heterochromatin associated H3K9 methyltransferases Suv39h1 and Suv39h2 are required for Dnmt3b-dependent DNA methylation of satellite DNA at pericentromeric heterochromatin (Lehnertz et al, 2003). G9a and GLP (G9a-like protein), two related euchromatin-associated H3K9 methyltransferases, have also been implicated in DNA methylation at various loci, including imprinting centers (Tachibana et al, 2005), retrotransposons and satellite repeats (Dong et al, 2008), at G9a/GLP target promoters (Wagschal et al, 2008), and a set of embryonic genes (Tachibana et al, 2008); (Epsztejn-Litman et al, 2008). In these organisms, H3K9me3 can be a signal for DNA methylation, through links between HP1 homologues which bind to H3K9me3, and in turn recruit DNA MTases to the marked regions (Figure 2.1.4.3).

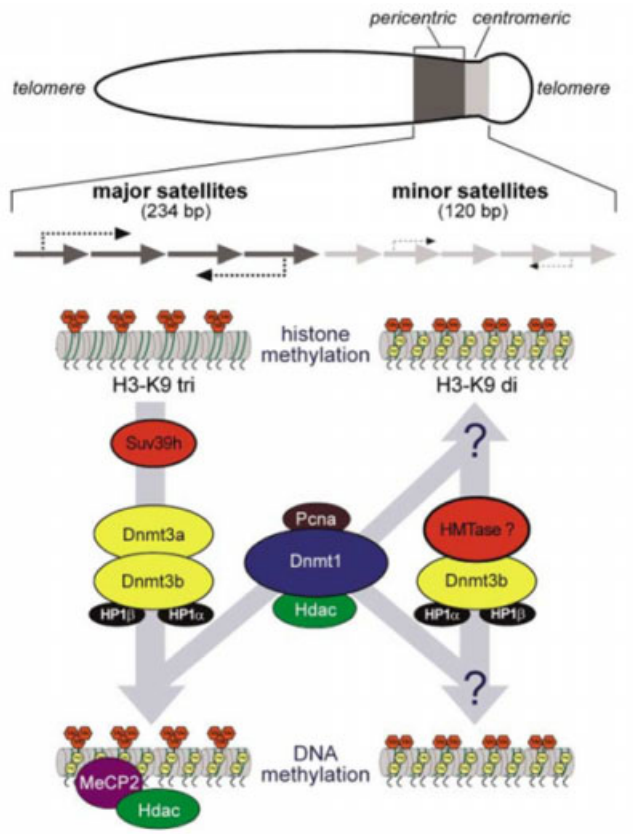

Figure 2.1.4.3 Histone and DNA Methylation Pathways at Mammalian Heterochromatin. The top diagram depicts the schematic localization of major and minor satellite repeats in pericentric and centromeric compartments on a mouse chromosome. Transcriptional activity across these repeats is indicated by dashed arrows. Suv39h-dependent H3K9me3 can direct DNA methylation at major satellites via targeting of a putative Dnmt3a/Dnmt3b-HP1α/HP1β complex. In addition, there is an Suv39h-independent pathway in which H3K9me2 is hypothesized to be mediated by an Suv39h-unrelated HMTase and which may interact with Dnmt3b to establish a silent chromatin domain at minor satellites. Dnmt1-mediated DNA methylation appears to be independent of H3K9 methylation, but is likely to participate in the above pathways in a manner that is currently undefined. Adapted from Lehnertz et.al., 2003

Conversely, in Arabidopsis, DNA methylation may also signal histone methylation (Gehring & Henikoff, 2007), and in cultured mammalian cells, the methyl-binding domain protein MeCP2 is associated with HMTase activity (Rottach et al, 2009). These suggest that DNA methylation can also signal histone methylation, although it may be limited to specific genomic regions or developmental stages (Lehnertz et al, 2003).

The dynamics of DNA methylation and histone modifications have raised several questions about additional mechanistic links. First, Dnmt1 alone is necessary but insufficient for proper maintenance methylation (Ooi & Bestor, 2008). Indeed, an accessory protein called UHRF1/Np95/ICBP90 (ubiquitin-like, containing PHD and RING finger domains 1 or nuclear protein of 95 kDa, or inverted CCAAT binding protein of 90 kDa) was discovered which can link Dnmt1 to hemimethylated CpGs and to H3K9me3. UHRF1 harbors five recognizable functional domains: a ubiquitin-like domain (UBL) at the N-terminus, followed by a tandem Tudor domain that binds H3K9me3, a plant homeodomain (PHD) that binds the histone H3 tail, a SET- and RING-associated (SRA) domain that binds hemimethylated CpG-containing DNA, and a really interesting new gene (RING) domain at the C-terminus that may provide UHRF1 with E3 ubiquitin

ligase activity for histones (Rottach et al, 2010); (Karagianni et al, 2007). UHRF1 binds both Dnmt1 and hemimethylated DNA, explaining its ability to target Dnmt1 to newly replicated DNA and that maintenance of DNA methylation is compromised in cells deficient for UHRF1 (Sharif et al, 2007); (Bostick et al, 2007). The fact that UHRF1 also binds methylated H3K9 indicates that UHRF1 is a key component in coupling maintenance methylation of DNA and histone modifications during DNA replication. Interestingly, the SRA domain of UHRF1 binds to hemimethylated DNA using the base flipping mechanism to flip 5-methylcytosine out of the DNA helix (Hashimoto et al, 2008); (Arita et al, 2008). Finally, UHRF1 also appears to interact with Dnmt3a and Dnmt3b, the two *de novo* DNA methyltransferases (Meilinger et al, 2009), which, therefore, might also contribute to the maintenance of DNA methylation on specific chromatin regions (Jones & Liang, 2009). Given its interaction with such a wide variety of chromatin regulators, including a histone acetyltransferase, and the H3K9 MTase G9a, it appears that UHRF1 serves as a focal point of epigenetic regulation mediated by chromatin modification enzymes (Achour et al, 2009); (Kim et al, 2008). Additionally, Dnmt1 performs its function in close cooperation with other proteins and complexes, including LSH (related to SNF2 family of chromatin-remodeling ATPases) (Myant & Stancheva, 2008), the developmental transcriptional repressor HESX1 (Sajedi et al, 2008), DMAP1 (Masamitsu et al, 2009) and Bmi1/Ring1A (member of the human PcG complex) (Negishi et al, 2007), although, the details of the mechanisms involved remain to be clarified.

Secondly, the ADD domain of Dnmt3L specifically interacts with the first six or seven residues of H3, only when H3K4 is not modified (H3K4me0) (Ooi et al, 2007). This suggests that Dnmt3L may function as a sensor for H3K4 methylation: when methylation is absent, Dnmt3L induces *de novo* DNA methylation by recruiting Dnmt3a to H3K4-hypomethylated regions of chromatin. Thus, the interaction of Dnmt3L with unmethylated H3K4 appears to be a central link between histone and *de novo* DNA methylation. However, there is evidence that Dnmt3a can independently recognize the H3K4me0 peptide by its ADD (Otani et al, 2009). Interestingly, this Dnmt3a ADD domain was reported to bind symmetrically dimethylated Arg3 in histone H4 (H4R3me2s), in addition to H3K4me0 (Zhao et al, 2009). Similar to Dnmt1, members of the Dnmt3 family exert their function *in vivo* cooperatively with other proteins and complexes, including Dnmt1 (Grandjean et al, 2007), histone methyltransferases (Suv39h, G9a and PRMT5) (Zhao et al, 2009), histone deacetylases (HDAC1) (Meilinger et al, 2009), methyl CpG binding protein (Mbd3) and components of the Brg1 complex (Datta et al, 2005).

Thirdly, members of MLL (mixed lineage leukemia) family of H3K4 MTases can directly or indirectly prevent DNA methylation or stabilize unmethylated DNA. Indeed, MLL proteins contain CXXC domains that can selectively bind unmethylated CpGs (Ayton et al, 2004); Cierpicki, 2010 #570}. In addition, another H3K4 methyltransferase, Set1, appears to interact with the DNA via an additional protein, the CXXC finger protein 1 (Cfp1/CGBP1) (Tate et al, 2009); (Courtney et al, 2009). Additionally, disruption of the genes for mammalian LSD1 and LSD2 revealed an essential role in maintaining "global" DNA methylation (Wang et al, 2009) and establishing maternal DNA genomic imprints (Ciccone et al, 2009), respectively. The possible explanation for LSD2-promoted DNA methylation is that demethylating of H3K4 makes imprinted loci more accessible to the Dnmt3a-Dnmt3L *de novo* DNA methylation machinery (Ciccone et al, 2009). As to LSD1, "global" DNA methylation may be also explained by generation of H3K4me0, which can be bound by UHRF1 or Dnmt3a, although an alternative mechanism is also possible. This alternative involves modulation of the stability of the maintenance DNA MTase Dnmt1, via methylation of that protein: Dnmt1 can be methylated at Lys142 by Set7/9 (a protein lysine methyltransferase), and this results in decreased stability (Esteve et al, 2009). In the absence of LSD1, Dnmt1 stability is reduced *in vivo*, which may be a reason for the progressive loss of DNA methylation (Wang et al, 2009).

Recently, a specific role of Dnmt2 in epigenetic silencing pathways has been found in *Drosophila* (Phalke et al, 2009). The authors have shown that Dnmt2 is required for epigenetic silencing of retrotransposons and subtelomeric repeats. The genetic data imply the Suv4-20/Hmt4-20 histone H4K20 methyltransferase (Sakaguchi et al. 2008) in the maintenance of retrotransposon silencing initiated by Dnmt2-dependent DNA methylation (Phalke et al, 2009). This is supported by the observation of strong reduction of histone H4K20 trimethylation in Dnmt2 mutants, suggesting that at least in *Drosophila*, the bulk of this histone modification depends on Dnmt2 function (Figure 2.1.4.4) (Phalke et al, 2009). Intriguingly, although *Dictyostelium* seems to lack canonical methyl-binding proteins, EhMLBP was identified in *Entamoeba*, which has no homologues in other organisms and preferentially binds to methylated interspersed nuclear elements, rDNA and DNA of some genes (Lavi et al, 2009). The EhMLBP protein could mediate the effects of DNA methylation by Ehmeth in this organism, though the detailed mechanism is not clear. Nevertheless, one broad theme that has become clear: a web of interactions tightly coordinates the modifications of DNA segments and its associated histone and non-histone proteins (Cheng & Blumenthal, 2010).

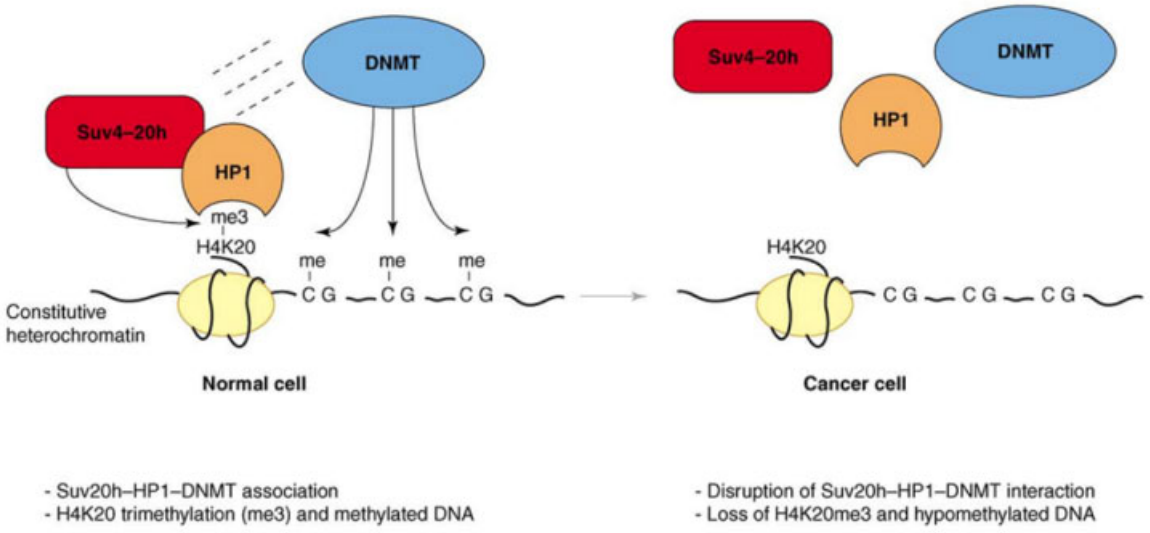

Figure 2.1.4.4 Putative link between DNA methylation and H4K20me3. In normal cells, DNA methyltransferase (DNMT) might interact with Suv4–20h enzyme. This interaction might be direct or through the HP1 protein (dashed lines), because this adaptor could bind to both DNMT and Suv4–20h. This would lead to concomitant H4K20me3 and methylation of DNA repeats. In cancer cells, the interaction of Suv4–20h, HP1 and DNMT could be disrupted, which would result in the DNA hypomethylation and decrease in H4K20me3. Adapted from Fuks, 2005.

2.2 Dnmt2 is a tRNA m^5C Methyltransferase

The presence of a Dnmt2 homologue does not necessarily predict the presence of DNA methylation. The genomes of nematodes, for instance, are generally considered to be unmethylated, and *Caenorhabditis elegans* belongs to the small group of organisms that does not contain any Dnmt-like gene. However, a Dnmt2 gene is present in the satellite nematode model *Pristionchus pacificus*, but there is no indication for DNA methylation (Gutierrez & Sommer, 2004). Moreover, for the pmt1 gene product, the Dnmt2 homolog in *Schizosaccharomyces pombe*, no catalytic DNA methyltransferase activity was detected (Wilkinson et al, 1995). This was attributed to the insertion of a Ser residue into a critical ProCys dipeptide that is essential for DNA methyltransferase activity in other enzymes. Interestingly, later study indicated that substantial DNA methyltransferase activity could be restored by removal of the inserted serine residue (Pinarbasi et al, 1996). Further inspection, however, revealed that this was most likely artificial: the inserted Ser did not disturb the structure of the catalytic domain and the enzyme displayed methylation activity on RNA *in vitro* (Becker, Müller, Nellen, Ehrenhofer-Murray, personal communication). *In vitro* experiments with other recombinant Dnmt2 proteins and RNA preparations from various model systems uncovered a prominent transfer RNA methyltransferase activity of the enzymes (Goll et al. 2006). Moreover,

this Dnmt2 activity was limited to the specific substrate, cytosine 38 in the anticodon loop of $tRNA^{Asp}$. These results suggested that Dnmt2 might have an additional function which is not related to DNA methylation. Interestingly, Dnmt2 displayed significant activity on *in vitro* transcribed $tRNA^{Asp}$, which suggests that the enzyme does not require other tRNA modifications (Jurkowski et al, 2008). Some other tRNAs are known to be methylated at C38 by unknown RNA m^5C methyltransferases (Sprinzl & Vassilenko, 2005), which open the possibility that Dnmt2 activity might not be limited to $tRNA^{Asp}$ (Jeltsch et al, 2006). Recent *in vitro* experiments have shown that hDNMT2 is also responsible for methylation of additional tRNAs at C38 (Helm, Lyko and Müller, personal communication). Moreover, 5-AzaC was shown to inhibit the RNA MTase activity of hDNMT2 at C38 of $tRNA^{Asp}$ and cause a substantial effect on the metabolic rate of human cancer cell lines, consistent with the hypothesis of Dnmt2 function in RNA metabolism (Schaefer et al, 2009). Remarkably, Dnmt2 utilizes a DNA MTase mechanism to perform tRNA methylation, although it does not share any significant sequence similarity with known RNA MTases (Jurkowski et al, 2008). Therefore, elucidating the catalytic mechanism used by Dnmt2 is critical for understanding the substrate specificity and the biological role of the enzyme. The tRNA methylation has been implied in the regulation of tRNA folding and stability (Alexandrov et al, 2006); (Helm, 2006). These properties of tRNA could in turn contribute to the rate and/or fidelity of protein synthesis, especially under specific conditions e.g. during aging, thus, changing metabolic pathways. Indeed, Dnmt2 knock-out phenotypes in zebrafish could be restored by cytoplasmic Dnmt2, but not nuclear, suggesting that the observed defects are the result of Dnmt2 function on cytoplasmic substrates (Rai et al, 2007). In this respect, an interesting finding was made in *Entamoeba*, where the glycolytic enzyme enolase was shown to act as a metabolic regulator of Ehmeth activity (Tovy et al, 2010).

2.2.1 Structural Motifs of DNA and RNA m^5C Methyltransferases

Catalytic domains of eukaryotic and prokaryotic DNA m^5C methyltransferases show extensive sequence homology and structural conservation and share ten characteristic conserved motifs (numbered I to X), which are usually arranged in a typical order (Goll & Bestor, 2005). Particularly, the structure of the catalytic domain of human DNMT2 remarkably resembles the structure of the bacterial DNA MTase M.*Hha*I (Dong et al, 2001). In addition to the 10 motifs, all Dnmt2 homologues share a distinct conserved stretch of 41 amino acids (266-306 of hDNMT2), including the nearly invariant CysPheThr tripeptide and an AspIle dipeptide between motifs VIII and IX, in a

region corresponding to the target recognition domain (TRD) of the bacterial MTases (Lauster et al, 1989); (Dong et al, 2001). Interestingly, the characteristic CysPheThr tripeptide is conserved in the Dnmt2 family but was not found in other eukaryotic (Dnmt1, Dnmt3a and Dnm3b) or in approximately 90 bacterial MTases (Vilkaitis et al, 2000). The high level of internal conservation in the TRD suggests that members of Dnmt2 family may recognize a specific kind of target, although the nature of the target is not yet clear. The general architecture of Dnmt2 homologues consists of a strongly conserved large subdomain and a poorly conserved small subdomain (Dong et al, 2001). The large subdomain consists of the motifs I to VIII and X, while the small one comprises motif IX and a variable region between VIII and IX with very low sequence conservation and variable length (except for the TRD). Motifs I-V and X organize the binding pocket for cofactor and methyl-group donor S-Adenosyl-L-methionine (SAM) and also play an important role in the formation of the active site. The catalytic site *per se* is formed from spatially arranged invariant PC dipeptide residues in motif IV, the ENV tripeptide in motif VI and the RXR tripeptide in motif VIII (Liu & Santi, 2000); (Jurkowski et al, 2008). These ten characteristic signature motifs are also present in RNA m^5C methyltransferases. However, the sequence context as well as the degree of conservation can vary, and sometimes the motifs can only be identified by structural homology. Usually, the order of the ten motifs is X-I-II-III-IV-V-VI-VII-VIII-IX, while in DNA m^5C MTases, motif X is C-terminal, although in case of some RNA m^5C MTases, the order of the motifs has been found rearranged (Liu & Santi, 2000). Despite the similar structural outline that is necessary for substrate recognition, SAM-binding and catalysis, profound differences regarding the residues involved in catalysis have been reported. Both DNA and RNA m^5C methyltransferases use highly conserved cysteines for the initial nucleophilic attack on the cytosine base, but the catalytic Cys of DNA MTases lies in motif IV (PC dipeptide), whereas RNA MTases use a conserved Cys in motif VI. Moreover, different invariant residues are used for binding the cytosine base in the active sites of the enzymes: DNA m^5C MTases use Glu in the ENV tripeptide (motif VI), while RNA m^5C MTases utilize Asp in the DAPC peptide (motif IV) (Bujnicki et al, 2004).

2.2.2 Catalytic mechanisms of DNA and RNA m^5C Methyltransferases

Dnmt2 has been shown to methylate both DNA and $tRNA^{Asp}$ at the cytosine-5 position (Goll et al, 2006). The methylation at the C5 is not a trivial reaction, because cytosine is an electron-poor heterocyclic aromatic ring system and the carbon 5 of cytosine is non-reactive. The reactions catalyzed by RNA and DNA m^5C MTases follow the reaction pathway of a Michael addition. The

catalytic mechanism of DNA m^5C MTases was first suggested and refined by Wu and Santi (Wu & Santi, 1987). Detailed kinetic analysis revealed a sequential order of DNA binding to the enzyme, followed by the binding of the cofactor SAM (Svedruzic & Reich, 2005). Methylation is initiated by a nucleophilic attack of an SH group from a catalytic Cys residue located in the conserved motif IV (GPPC) on the C6 position of the target cytosine, yielding a covalent intermediate between the base and the enzyme (Figure 2.2.2) (Kumar et al, 1994).

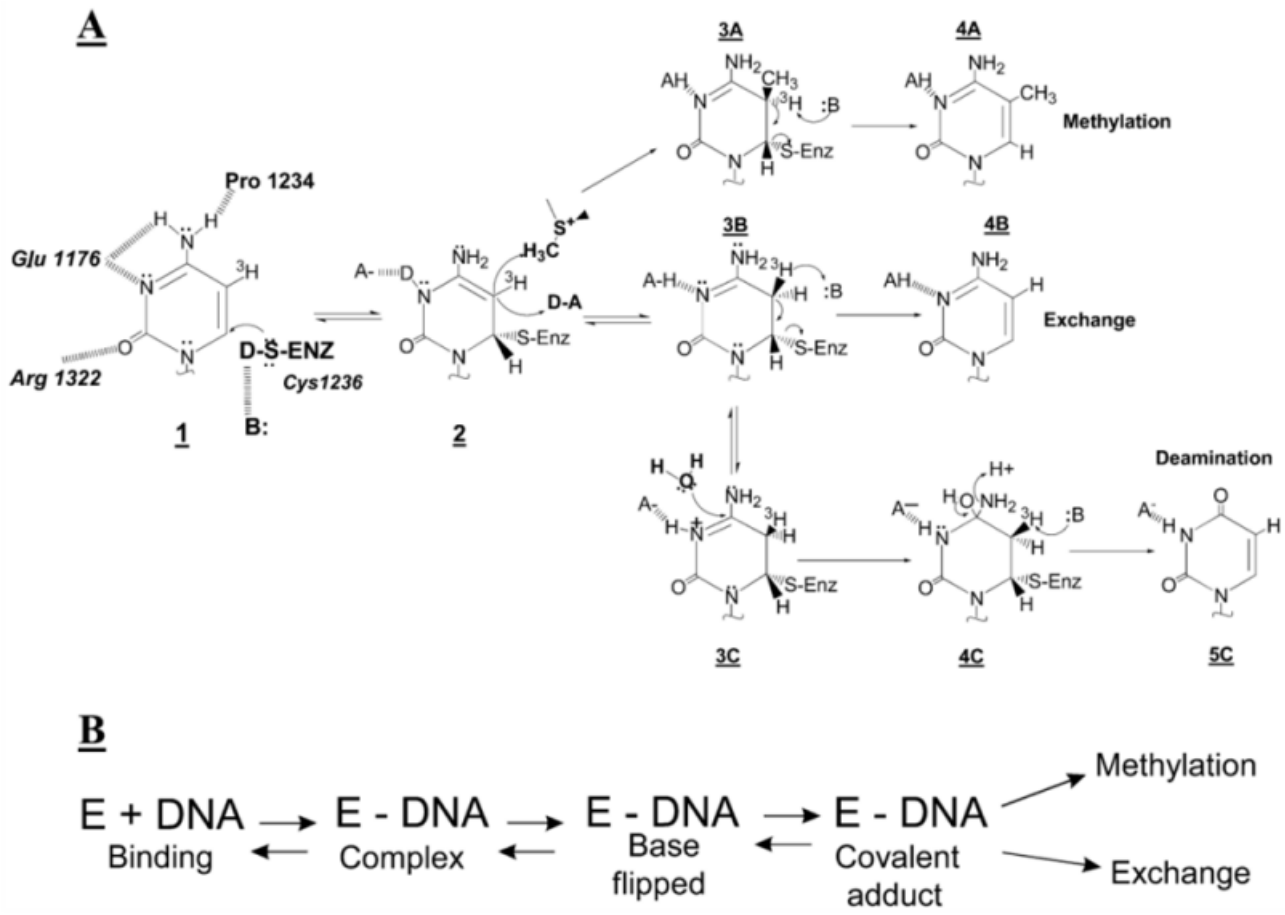

Figure 2.2.2 (**A**) Reactions catalyzed by cytosine C5 DNA methyltransferases: methylation (A) exchange (B) and deamination (C). (**B**) Four steps that control the target base attack by pyrimidine methyltransferases in a rapid equilibrium. Adapted from Svedruzic and Reich, 2005.

Thereby, the C5 position of the cytosine becomes activated and is capable of performing a nucleophilic attack on the methyl group bound to the cofactor SAM. The enzyme facilitates the nucleolphilic attack on the C6 atom by a transient protonation of the cytosine ring at the endocyclic nitrogen atom N3, which is stabilized by the Glu residue from a highly conserved motif VI (ENV)

(Jurkowski et al, 2008). The covalent complex between the methylated base and the DNA is resolved by deprotonation at the C5 position, which leads to the β-elimination of the cysteinyl group and the re-establishment of the aromatic ring (Motorin et al, 2009). Then, the methylated base together with the cofactor product, S-Adenosyl-L-homocysteine, is released. In addition to the residues already mentioned, the second Arg residue in motif VIII (RXR) plays an important role in the catalytic mechanism of DNA m^5C MTases (Gowher et al, 2006).

Interestingly, the core structure encompassing the SAM-binding pocket is similar for all methyltransferases, regardless of their targets (Cheng & Roberts, 2001). The question is how an enzyme can access the target cytosine base if it is embedded in a double helix. Based on crystal structure of the bacterial methyltransferase M.*Hha*I in complex with SAM and a duplex of DNA oligonucleotides, the base flipping hypothesis was suggested, where the target base is flipped out of the helix by a rotation on its flanking sugar-phosphate bonds by an angle of 180° (Klimasauskas et al, 1994). This enables the easy projection of the target base into the catalytic pocket of the methyltransferase without the cleavage of covalent bonds (Cheng & Roberts, 2001).

2.3 *Dictyostelium* as a model system to study Dnmt2 function

Different studies have suggested that Dnmt2 has a role in fundamentally different cellular pathways. The knock-out phenotypes in zebrafish demonstrate a tissue- or organ-specific role of cytoplasmic Dnmt2 during development (Rai et al, 2007), while other studies clearly show involvement of Dnmt2 in locus-specific DNA methylation and silencing of retrotransposones (Phalke et al, 2009); (Kuhlmann et al, 2005); (Harony et al, 2006). In addition, prominent enzymatic activities of Dnmt2 enzymes towards RNA substrates have been confirmed experimentally (Goll et al, 2006); (Jurkowski et al, 2008); (Müller, Nellen and Ehrenhofer-Murray, unpublished data). These findings opened interesting possibilities for Dnmt2 to have dual biological functions as DNA and RNA methyltransferase (Jeltsch et al, 2006). Nevertheless, recent studies focus mainly on RNA methylation activity of Dnmt2 homologues, since DNA methylation activity of the enzyme is relatively low. This even led to the conclusion that Dnmt2 is a highly specific RNA MTase rather than a DNA MTase (Goll et al, 2006); (Jurkowski et al, 2008). To resolve the question whether Dnmt2 methylates DNA, to clarify the meaning of tRNA methylation activity of the enzyme or to find other RNA targets *in vivo*, additional assays should be developed. Moreover, the experiments should be performed in the model systems, like *Dictyostelium* or *Drosophila*, where genomic DNA

is detectably methylated and Dnmt2 homologues are the only DNA MTase gene, and which have the advantage of powerful molecular tools and genetic tractability. In *Dictyostelium*, despite the very low genome-wide DNA methylation content of approximately 0.2 % of all cytosines, at least two specific regions were identified to be methylated (Kuhlmann et al, 2005). The retrotransposons DIRS-1 and Skipper carry mostly asymmetric m^5C methylation (in a non-CpG context), which is lost upon disruption of DnmA (Kuhlmann et al, 2005). A developmental role of DnmA has also been suggested (Katoh et al, 2006), but is discussed controversially. While Kuhlmann et al. reported a downregulation of DnmA throughout the development (Kuhlmann et al, 2005); Katoh et al. observed an increase of methylation during development and described morphological defects of DnmA mutants in late developmental stages (Katoh et al, 2006). Like in *Drosophila* and human, several tRNAs appear to be substrates for human DNMT2 in *Dictyostelium* (Maksimov, Müller and Nellen, unpublished data). In addition, both cytoplasmic and nuclear localization for DnmA was observed (Kuhlmann et al, 2005). The data suggest that *Dictyostelium* is a promising model organism to investigate Dnmt2 function, including the enigmatic tRNA methylation.

2.4 Aims of this work

Whereas the role of other Dnmt families has been extensively characterized, relatively poor and frequently controversial information is available on the biological functions and biochemical properties of Dnmt2. However, the extensive conservation of Dnmt2, a single copy gene in eukaryotes, with homologues in dozens of protist, plants, fungi, and animals is an indication of an important role for Dnmt2 proteins. In the present work we attempted to characterize DnmA, the Dnmt2 homolog in *Dictyostelium discoideum*. In order to gain a better understanding of the nuclear and cytoplasmic function of DnmA we performed a series of experiments to isolate and identify putative interaction partners by affinity purification of various epitope tagged fusions followed by mass-spectrometry. These data may provide the information on cellular processes in which this enzyme is involved.

Since DnmA, like other Dnmt2 homologues, lacks the regulatory N-terminal domain, it seems possible that post-translation modifications might regulate its function *in vivo*. Thus, we attempted to identify some of the common modifications, including phosphorylation, methylation and acetylation, on a tagged protein purified from different cell compartments and at different stages of the life cycle. This information could give us insight into potential modification enzymes and, thus,

the cell-signaling pathways, which modulate DnmA function.

Currenly, efforts are made to understand the biochemical properties of different Dnmt2 homologues. Although some generalized catalytic mechanism was proposed for human DNMT2 (Jurkowski et al, 2008), a number of details remain to be elucidated. Indeed, the extremely weak catalytic activity on DNA raises questions about target preference of Dnmt2 proteins. In this respect DnmA is an intriguing enzyme, because it has the Phe/Val substitution in the conserved CFT tripeptide within the TRD, which is thought to be involved in target recognition. Thus, we performed a series of comparative EMSAs to determine binding affinities of DnmA towards various DNA and RNA targets.

Interestingly, Goll and co-workers found that hDNMT2 is able to exclusively methylate position C38 in the $tRNA^{Asp}$ (Goll et al, 2006). Later it was found that some other tRNAs in the specific context of several invariant nucleotides (C32, A37 and C40; Helm, Lyko and Müller, personal communication) are also methylated in vitro. To estimate catalytic activity of DnmA towards different tRNA and DNA substrates, we experimentally assessed the first steps of the catalytic mechanism by trapping of covalent intermediates.

3 Materials

3.1 Chemicals and reagents

Acetic acid (100%)	Fluka, Deisenhofen
Acetone	Fluka, Deisenhofen
Acrylamide/bis-acrylamide (30% or 40%)	Roth, Karlsruhe
Agar-agar	Euler, Frankfurt am Main
Agarose	Sigma, Taufkirchen
Ammonium persulfate (APS)	Merck, Darmstadt
Ammonium sulphate	Roth, Karlsruhe
Bacto-peptone	Difco, Augsburg
Bacto-tryptone	Difco, Augsburg
ß-mercaptoethanol	Fluka, Deisenhofen
Boric acid	Roth, Karlsruhe
Bradford solution	Roth, Karlsruhe
Bromphenolblue	Fluka, Deisenhofen
Bovine serum albumin (BSA)	Roth, Karlsruhe
Calcium chloride ($CaCl_2$)	Roth, Karlsruhe
Calmodulin Affinity Resin (CAT#214303-52)	Stratagene, Santa Clara (USA)
Complete-mini (Protease Inhibitor Tablets)	Roche, Mannheim
Coomassie Brilliant Blue G-250	Serva, Heidelberg
dATP	MBI Fermentas, St. Leon-Rot
dCTP	MBI Fermentas, St. Leon-Rot
dGTP	MBI Fermentas, St. Leon-Rot
dTTP	MBI Fermentas, St. Leon-Rot
DAPI	Roth, Karlsruhe
DMSO	Sigma, Taufkirchen
DTT	Roth, Karlsruhe
EDTA	Roth, Karlsruhe
Ethanol (99.8%)	Roth, Karlsruhe

Ethidium bromide	Fluka, Deisenhofen
Formaldehyde (37%)	Roth, Karlsruhe
Formamide	Roth, Karlsruhe
Glycerol (86% or 99.8%)	Roth, Karlsruhe
Glycine	Roth, Karlsruhe
Guanidine thiocyanate	Roth, Karlsruhe
HEPES	Roth, Karlsruhe
IPTG	Roth, Karlsruhe
Imidazol	Roth, Karlsruhe
Avidin	Pierce, USA
Isopropanol	Roth, Karlsruhe
Liquid nitrogen	Messer Griesheim, Krefeld
Lithium chloride (LiCl)	Roth, Karlsruhe
Magnesium chloride ($MgCl_2$)	Roth, Karlsruhe
Magnesium sulphate (Mg_2SO_4)	Roth, Karlsruhe
Methanol	Roth, Karlsruhe
Methylene blue	Roth, Karlsruhe
Dry milk powder SUCOFIN	TSI, Zeven
MOPS (3-(N-morpholino) propanesulfonic acid)	Roth, Karlsruhe
NBT	BTS, St. Leon-Rot
N-lauroylsarcosine	Roth, Karlsruhe
Ni-Charged Resin Profinity^{TM} IMAC	BIO-RAD, München
Phenol/Chloroform/Isoamyl alcohol	Roth, Karlsruhe
PhosSTOP Phosphatase Inhibitor Cocktail Tablets	Roche, Mannheim
Protein A-Sepharose beads	Amersham, Freiburg
Polyethylene glycol (PEG) 6000	Roth, Karlsruhe
Potassium acetate (CH_3COOK)	Roth, Karlsruhe
Potassium chloride (KCl)	Roth, Karlsruhe
Potassium dihydrogenphosphate (KH_2PO_4)	Fluka, Deisenhofen
Potassium hydrogenphosphate (K_2HPO_4)	Fluka, Deisenhofen
PMSF (phenylmethylsulfonylfluoride)	Roth, Karlsruhe
rATP	MBI Fermentas, St. Leon-Rot

rCTP	MBI Fermentas, St. Leon-Rot
rGTP	MBI Fermentas, St. Leon-Rot
rUTP	MBI Fermentas, St. Leon-Rot
Sucrose	Roth, Karlsruhe
SDS -sodium dodecyl (lauryl) sulfate	Roth, Karlsruhe
Sephadex^{TM} G-50 Medium	GE Healthcare, Sweden
Sodium acetate (CH_3COONa)	Fluka, Deisenhofen
Sodium azide (NaN_3)	Merck, Darmstadt
Sodium carbonate (Na_2CO_3)	Roth, Karlsruhe
Sodium chloride (NaCl)	Fluka, Deisenhofen
Sodium citrate ($C_6H_5Na_3O_7$)	Roth, Karlsruhe
Sodium dihydrogenphosphate (NaH_2PO_4)	Fluka, Deisenhofen
Sodium hydrogenphosphate (Na_2HPO_4)	Fluka, Deisenhofen
Sodium hydrogensulfite ($NaHSO_3$)	Sigma-Aldrich, Germany
Sodium hydroxide (NaOH)	Roth, Karlsruhe
Strep Tactin® Superflow^{TM} Agarose	Novagen, USA
TEMED	Roth, Karlsruhe
Tris	Roth, Karlsruhe
Triton-X-100	Roth, Karlsruhe
Tween 20	Roth, Karlsruhe
Urea	Roth, Karlsruhe
Xylene cyanol FF	Fluka, Deisenhofen

3.2 Radioactive materials

[α-^{32}P] dATP (110 TBq/mmol)	Hartmann Analytic, Braunschweig
[γ-^{32}P] ATP (110 TBq/mmol)	Hartmann Analytic, Braunschweig
[α-^{32}P] UTP (110 TBq/mmol)	Hartmann Analytic, Braunschweig

3.3 Antibiotics

Ampicillin	Roth, Karlsruhe

Amphotericin B	PAA, Cölbe
Blasticidin S	MP Biomedicals, Eschwege
Geneticin (G418)	PAA, Cölbe
Penicillin/Streptomycin	PAA, Cölbe
Chloramphenicol	Sigma, Deisenhofen

3.4 Antibodies

Rat anti-alpha-Tubulin antibody (Y1/2; 1:5)	University of Kassel, DCB
Mouse anti-Myc antibody (9E10; 1:5)	University of Kassel
Mouse anti-His antibody (232-470-5; 1:5)	University of Kassel
Rabbit anti-GFP antibody (264-449-2; 1:5)	University of Kassel, DCB
Rabbit polyclonal anti-TAP antibody (#CAB1001; 1:5000)	OPEN BIOSYSTEMS, Huntsville
IgG, goat-anti-mouse, Alkaline phosphatase-coupled (1:10000)	Dianova, Hamburg
IgG, goat-anti-rabbit, Alkaline phosphatase-coupled (1:10000)	Dianova, Hamburg

3.5 Enzymes, kits and molecular weight markers

DNase I, RNase free	MBI Fermentas, St. Leon-Rot
Calf intestinal alkaline phosphatase (CIAP)	MBI Fermentas, St. Leon-Rot
Klenow DNA polymerase	MBI Fermentas, St. Leon-Rot
Proteinase K	Boehringer Mannheim, Mannheim
Pfu DNA polymerase	Dept. of Genetics, Uni-Kassel
Restriction endonucleases	MBI Fermentas, St. Leon-Rot, Gibco BRL, Eggenstein, New England Biolabs, Boehringer Mannheim, Mannheim
RNase A	Merck Biosciences, Bad Soden
RNase-inhibitor (RNasin®)	MBI Fermentas, St. Leon-Rot
Shrimp alkaline phosphatase (SAP)	MBI Fermentas, St. Leon-Rot

SP6 RNA polymerase	MBI Fermentas, St. Leon-Rot
T4 DNA-ligase	MBI Fermentas, St. Leon-Rot
T4- polynucleotide kinase	MBI Fermentas, St. Leon-Rot
T7 RNA polymerase	Dept. of Genetics, Uni-Kassel
Taq DNA-polymerase	Dept. of Genetics, Uni-Kassel
NucleoSpin® ExtractII	Macherey-Nagel, Düren
NucleoBond® PC 100	Macherey-Nagel, Düren
pGEM T-Easy cloning kit	Promega, USA
#SM0661 PageRuler™ unstained Protein Ladder	MBI Fermentas, St. Leon-Rot
#SM1811 PageRuler™ Plus Prestained Protein Ladder	MBI Fermentas, St. Leon-Rot
#SM0441 Prestained Protein Molecular Weight marker	MBI Fermentas, St. Leon-Rot
#SM1841 Spectra™ Multicolor Broad Range Protein Ladder	MBI Fermentas, St. Leon-Rot
#SM0311 GeneRuler™ 1 kb DNA Ladder	MBI Fermentas, St. Leon-Rot
#SM0324 GeneRuler™ 100 bp DNA Ladder Plus	MBI Fermentas, St. Leon-Rot
#SM0613 O'RangeRuler™ 50 bp DNA Ladder	MBI Fermentas, St. Leon-Rot

3.6 Primers and oligonucleotides

A list of all oligonucleotides used in this study is given below. All primer sequences are in 5′ to 3′ orientation. The single strand oligonucleotides were obtained from Invitrogen (Carlsbad, CA) or obtained from existing lab stocks.

DnmA_BamHI_for	GGGATCCGGAGAACAATTGAGAGTATTAG
DnmA_PstI_For	GATCCTGCAGAAAATGGAACAATTGAGAGT
DnmA_BamHI_Rev	GATCGGATCCTTTTTTTCCTTCTTTTTCCTT
DnmA_BglII_For	GATCAGATCTAAAATGGAACAATTGAGAGT
DnmA_forII	GTATAGAATCATATAGTGTTGAAG

DnmA_chk_rev	CAACCTTTTCATTATGTTTGTC
DnmA_chk_forII	TAGATCATATTCCAGGTTATG
rq_dnmA_for	GGAACAATTGAGAGTATTAG
rq_dnmA_rev	CCATGCATTCGCTTTAAATCCTTCTAACTCTTCAACACTATATG
rq_dnmA_revII	GCATGCATTCGCTTTAAATCCTTCTAACTCTTCAACACTATATG ATTC
DnmA_SII_for	GATCCGGAAGCGCATGGAGTCACCCACAATTCGAAAAATAAG
DnmA_SII_rev	AATTCTTATTTTTCGAATTGTGGGTGACTCCATGCGCTTCCG
CTAP_BamHI_For	GATCGGATCCATGGAAAAGAGAAGATGG
TAP_for	GGATCCGAAAAGAGAAGATGGAAAAAG
CTAP_MfeI_Rev	GATCCAATTGTCATTAGGTTGACTTCCCCG
CTAP_MluI_Rev	GATCACGCGTTCATTAGGTTGACTTCCCCG
GFP_BamHI_for	GGGATCCGGAAGTAAAGGAGAAGAACTTTTC
GFP_EcoRI_rev	CCAATTGTTATTTGTATAGTTCATCCATGC
GR6_HindIII_for	GAAGCTTAATGCCGAGGACACCATGC
GR6_HindIII_rev	GAAGCTTGAGACGAAGGATGAGTGCC
GR6_chk_for	CAAGAAGTTTGCAGAGCAG
DNMT1_oligo	GAAATACCAGGATATAACCAGGTTAGAC
DNMT2_oligo	GTCTAACCTGGTTATATCCTGGTATTTC
DNMT3_oligo	GGAAATACAGATATAACAGTTAGAGCCC
DNMT4_oligo	GGGCTCTAACTGTTATATCTGTATTTCC
DNMT5_oligo	GAAAATACCGGATATAACCGGATTAGAC
DNMT6_oligo	GTCTAATCCGGTTATATCCGGTATTTTC
DNMT7_oligo	CGGCCGCCTGCAGGTCGACCATATGGGAGAGCTCCCAACG
DNMT8_oligo	CGTTGGGAGCTCTCCCATATGGTCGACCTGCAGGCGGCCG
DNMT9_oligo	TGCATAGTGTCGTCGGTTCGGAATTTTTCAGTTTTTCGAC
DNMT10_oligo	GTCGAAAAACTGAAAAATTCCGAACCGACGACACTATGCA
DNMT11_oligo	GAAATATTCTATAGAGAACTAATTAGAC
DNMT12_oligo	GTCTAATTAGTTCTCTATAGAATATTTC
DNMT13_oligo	CAAATATTATTATATAATTATTATAGAC
DNMT14_oligo	GTCTATAATAATTATATAATAATATTTG
T7tr_Glu_for	GAATTGTAATACGACTCACTATAGGATCCTCATTGGTGTAGTCGG

T7tr_Glu_rev	GAATTGTAATACGACTCACTATAGGATCCTCCCCATTCGGGAATCG
T7tr	GAATTGTAATACGACTCACTATA
Glu_for	TCCTCATTGGTGTAGTCGG
Glu_rev	CTCCCCATTCGGGAATCG
tRNA-Phe-for	GAATTGTAATACGACTCACTATAGGGAGCCTTAGTAGCTCAGT TGG
tRNA-Phe-rev	CCTTAAGATCTTCAGTCTCACGCTCGTACCAACTGAGCTACTA AG
tRNA-Phe-revII	TGCCTCAGGCCGGGATCGAACCAGCGACCTTAAGATCTTCAG TC
Phe_XbaI	TCTAGATGCCTCAGGCCGGGA
LAspGUC	GGACAGTATTTTTCGCCTGTCACGCGAAAGGACAGAGG
LAspC38A	GGACAGTATTTTTCGCCTGTCAAGCGAAAGGACAGAGG
LGluUUC	GGACAGTATCACTAGTCTTTCACACTAGTAGACAGAGG
LGluUUC2	ATAATAATAGTCTTTCACACTATTATTAT
LGluC38T	ATAATAATAGTCTTTCATACTATTATTAT
BrgII	CCTCTGTCTAATACTGTCC
bi-DIRS-ltr-ufor	AGTTTTTAGTGTTATTATTTATATGT

3.7 Plasmids and standard vectors

DNA fragments amplified by PCR with *Taq* polymerase or *Taq*/*Pfu* mix were ligated into vector pGEM-T Easy (Promega, Madison, WI) or pJET1.1 (MBI Fermentas, Burlington, Canada) using T4 DNA ligase. *Dictyostelium* expression vectors were derived from the vector pDneo2 (Witke et.al., 1987)

pET15b-*dnmA*_wt: The plasmid pET15b-*dnmA* was originally created by B. Borisova-Todorova (PhD thesis) but the sequence contained two point mutations within cDNA of *dnmA* gene which caused the substitution of two amino acids in the protein sequence. The cDNA of *dnmA* gene was resqued with primers rq_dnmA_for and rq_dnmA_revII. The resulting pET15b-*dnmA*_wt contain one point mutation which do not change the protein sequence and therefore is a silent mutation.

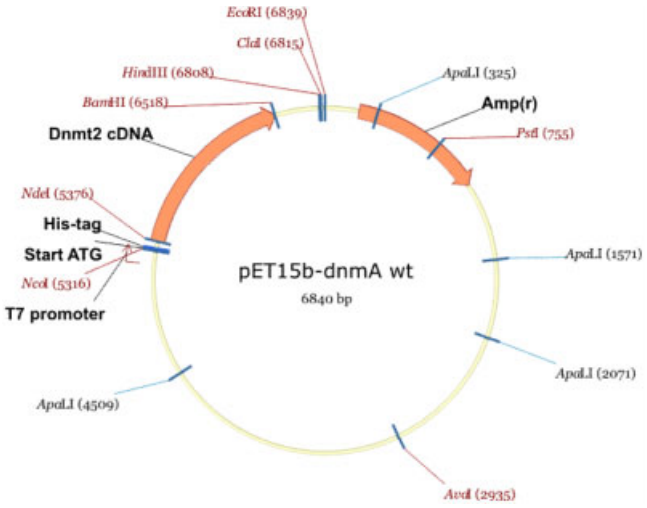

Figure 3.7.1 Map of *E.coli* expression vector pET15b-*dnmA*_wt. 6xHis-tag locates on the N-terminal tail of *dnmA* cDNA sequence.

pDneo2a-*dnmA-CTAP*/pDneo2a-*NTAP-dnmA*: For construction of N-terminal TAP-fusion, genomic DNA of *dnmA* gene was amplified by PCR with pair of primers: dnmA_BamHI_for and dnmA_BamHI_Rev. After cloning into pGEM T-Easy vector (Promega) and sequencing, correct *dnmA* DNA sequence was subcloned into pDneo2a-*NTAP* vector digested with BamHI. To construct pDneo2a-*dnmA-CTAP* plasmid, genomic DNA of *dnmA* gene was amplified by PCR using primers dnmA_PstI_For and dnmA_BamHI_Rev. PCR product was cloned into pGEM T-Easy vector (Promega), sequenced and correct sequence was excised using PstI and BamHI restriction enzymes and subcloned into pDneo2a-*CTAP* vector prepared by digestion of pDneo2a-*EriA-CTAP* plasmid with respective enzymes.

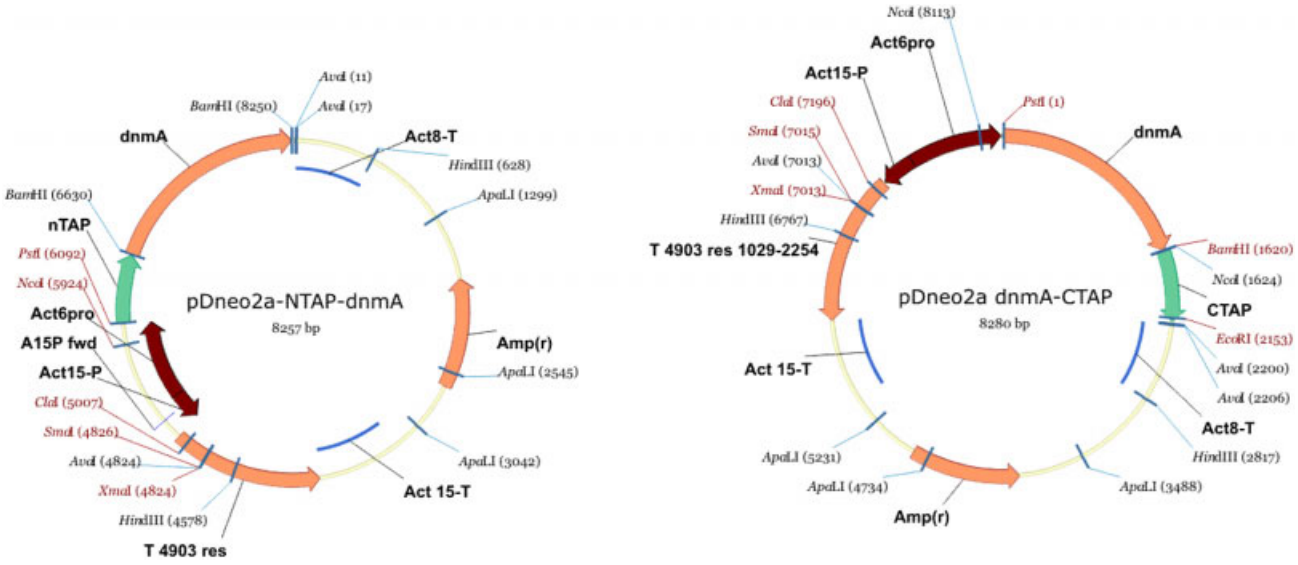

Figure 3.7.2 Maps of *Dictyostelium* expression vectors pDneo2a-*NTAP-dnmA* and pDneo2a-*dnmA-CTAP*. T 4903 res corresponds to geneticin resistance cassette.

pDneo2a-*dnmA-GFP*: Coding DNA sequence of GFP protein was amplified by PCR, using primers GFP_BamHI_for and GFP_EcoRI_rev. PCR product was cloned into pGEM T-Easy vector (Promega), sequenced and then correct sequence was excised by digestion with corresponding restriction enzymes and subcloned into pDneo2a-*dnmA* vector. pDneo2a-*dnmA* vector was prepared from pDneo2a-*dnmA-CTAP* plasmid by removing cDNA sequence of TAP, using BamHI and EcoRI restriction enzymes.

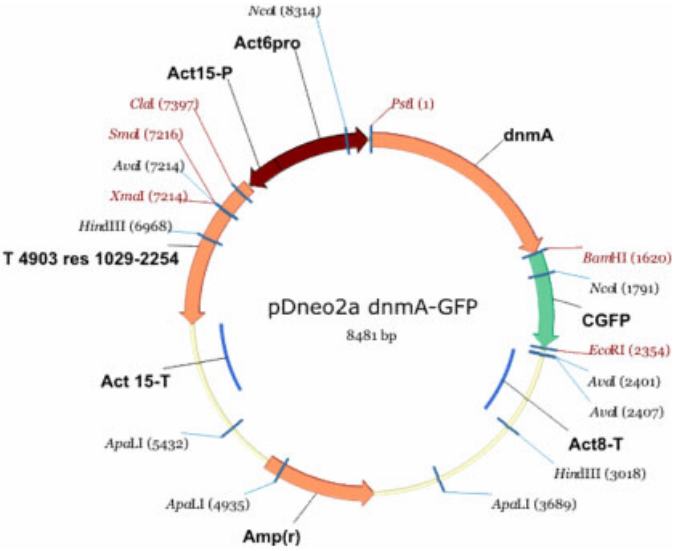

Figure 3.7.3 Map of *Dictyostelium* expression vector pDneo2a-*dnmA-GFP*. T 4903 res corresponds to geneticin resistance cassette.

pDneo2a-*dnmA-StrepII*: To construct plasmid pDneo2a-*dnmA-StrepII*, C-terminal TAP tag was removed from pDneo2a-*dnmA-CTAP* by digestion with BamHI and EcoRI restriction enzymes and substituted for StrepII tag cDNA sequence which was assembled from the two DNA oligonucleotides DnmA_SII_for and DnmA_SII_rev, carrying 5'-overhangs, mimicking digested BamHI and EcoRI sites for directional cloning.

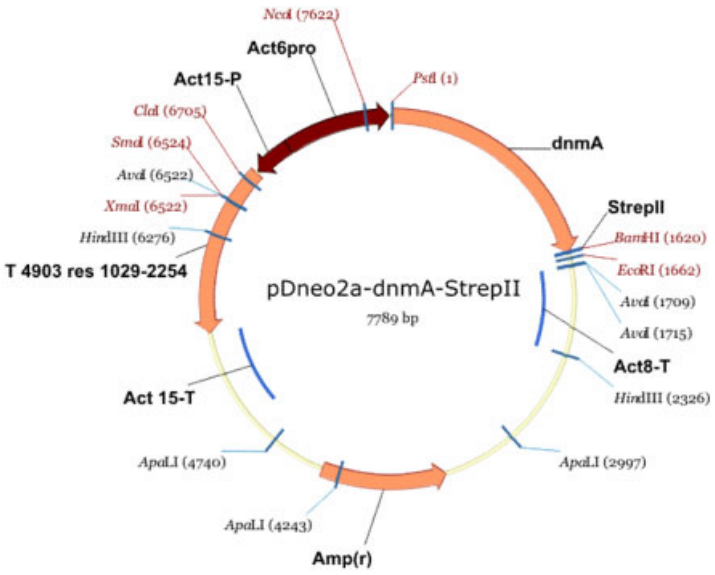

Figure 3.7.4 Map of *Dictyostelium* expression vector pDneo2a-*dnmA-StrepII*. T 4903 res corresponds to geneticin resistance cassette.

pJET1.1-Glu5/pJET1.1-Glu-SP/pJET1.1-Glu5R/pJET1.1-GluSPR: To construct these plasmids two pairs of primers: T7tr_Glu_for/Glu_rev and T7tr_Glu_rev/Glu_for were used to amplify cDNA of *Dictyostelium* $tRNA^{Glu(UUC-5)}$ and $tRNA^{Glu(CUA-5)}$ with attached T7 promoter DNA. The plasmids pGEM-Glu5#2 and pGEM-Glu_sup, kindly provided by Prof. Dr. Thomas Winckler (Friedrich-Schiller University, Jena), were used as a template for PCR amplification. The PCR products were subcloned into pJET1.1/blunt vector and the final constructs were used for *in vitro* transcription upon digestion with *Xba*I enzyme to produce $tRNA^{Glu(UUC-5)}$, $tRNA^{Glu(CUA-5)}$, $asRNA^{Glu(UUC-5)}$ and $asRNA^{Glu(CUA-5)}$, respectively (Figure 3.7.5).

pJET1.1-Phe2: The T7promoter was attached to cDNA of *Dictyostelium* $tRNA^{Phe(GAA-2)}$ using three overlapping oligos: tRNA-Phe-for, tRNA-Phe-rev and tRNA-Phe-revII. Oligos were annealed and filled in by one cycle of PCR with *Pfu* DNA polymerase and then full DNA sequence was amplified for 30 cycles with a 10:1 mix of *Taq*/*Pfu* DNA polymerases using primers: tRNA-Phe-for and Phe_XbaI to produce PCR fragment to ligate into pJET1.1/blunt vector. The final plasmid was used for in vitro transcription upon digestion with *Xba*I enzyme (Figure 3.7.6).

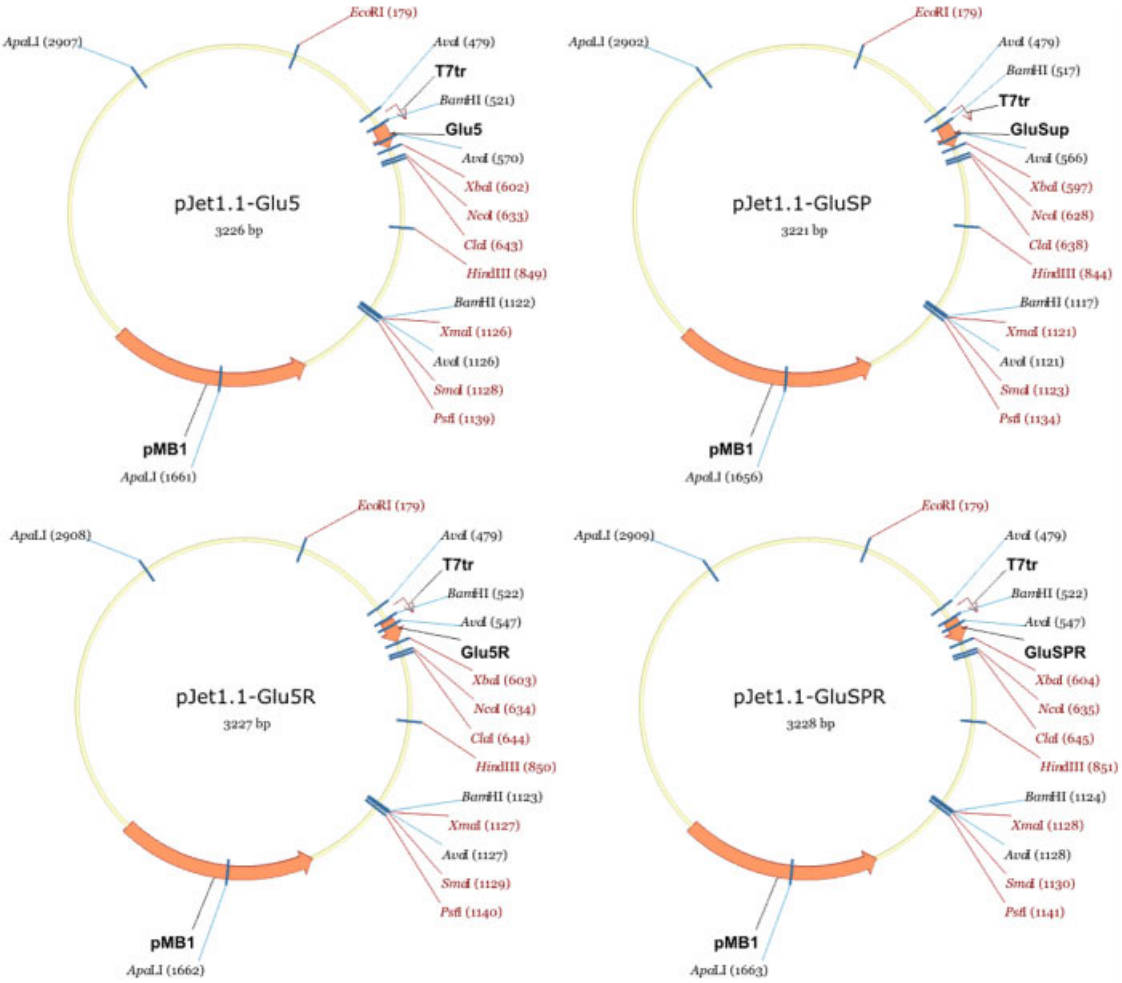

Figure 3.7.5 Maps of vectors for *in vitro* transcription.

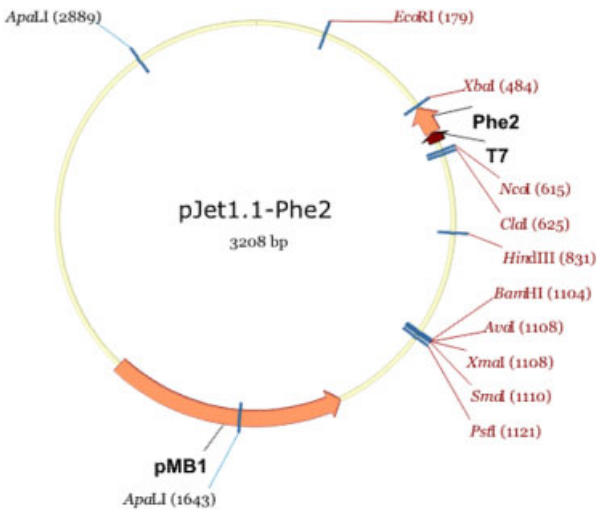

Figure 3.7.6 Maps of the pJET1.1-Phe2 vector for *in vitro* transcription.

3.8 Strains

Dictyostelium discoideum	Ax2-214 (*axeA2*, *axeB2*, *axeC2*; Watts and Ashworth, 1970)
Escherichia coli	DH5α™ (Invitrogen, Karlsruhe)
	BL21(DE3)pLysS (Promega, Mannheim)
Klebsiella aerogenes	(Williams & Newell, 1976)

3.9 Devices and other lab equipment

Autoclave	Zirbus, Bad Grund
Bio Imaging Analyzer	Raytest, Straubenhardt
BAS cassette 2025	Raytest, Straubenhardt
BioLogic Workstation (FPLC)	Bio-Rad, München
Cell counter (Coulter Counter ZM)	Coulter Electronics, Krefeld
Centrifuges:	
Avanti™ 30	Beckmann, München
Centrifuge 5417 C	Eppendorf, Hamburg
Rotina 48R	Hettich, Tuttlingen
Ultracentrifuge L3-50	Beckman, München
INTAS gel documenting system	INTAS, Göttingen
Electroporator (Gene PulserII®)	Bio-Rad, München
Electrophoresis chambers:	
Agarose gels	Mechanical workshop, Uni Kassel
Protein gels (SE 250)	Hoefer Pharmacia, SF, USA
PAGE gels	Mechanical workshop, Uni Kassel
Fluorescence microscope (Leica DM IRB)	Leica, Wetzlar
Geiger counter (Mini Monitor)	Mini Instruments, GB
Gel casting chambers	Mechanical workshop, Uni Kassel
Gel dryer	Bachofer, Reutlingen
Heating block	Electronic workshop, Uni Kassel
Hybridization oven	Bachofer, Reutlingen
Imager: Fujifilm FLA-7000	Raytest, Straubenhardt

Microflow hood	Nunc, Wiesbaden
Magnetic stirring plate	Bachofer, Reutlingen
Microscope	Zeiss, Jena
Microwave oven	Aldi, Essen
PCR-Mastercycler personal	Eppendorf, Hamburg
pH Meter Seven Easy	Mettler-Toledo, Giessen
Pipetboy (Accu Jet®)	Brand, Wertheim
Pipettes (20 µl, 200 µl, 1000 µl)	Gilson, Langenfeld
Spectrophotometer (Ultrospec® 2000)	Pharmacia Biotech, Freiburg
Power supplies:	
Power Pac 3000	Bio-Rad, Canada
EPS 600 and 3500	Pharmacia, Freiburg
Semidry blotting apparatus	Von Kreuz, Reiskirchen
Speed Vac® concentrator (SC 110)	Savant, USA
Ultra sonicator UP 200S	Dr. Hielscher GmbH, Stansdorf
UV table	Bachofer, Reutlingen
Vortex Genie	Bender Hohbein AG, Germany

3.10 Consumables

Whatman 3MM paper	Whatman, Göttingen
Becher glasses	Schott, Mainz
Costar plates	Schütt, Göttingen
Cryo tubes	Nunc, Wiesbaden
Disposable pipette tips	Sarstedt, Nürnbrecht
EP cuvettes (Gene Pulser® 0,4 cm)	Biorad, München
Falcon tubes (15 ml, 50 ml)	Sarstedt, Nürnbrecht
Glass pipettes	Hirschmann, Germany
Hybond nylon membranes (NX, N+)	Amersham, Freiburg
HisTrap®, Ni-NTA columns	Pharmacia, Freiburg
Injection needles	B.Braun, Melsungen
Injection syringes	B.Braun, Melsungen

Nitrocellulose membrane (porablot™ NCP)	Macherey Nagel, Düren
Parafilm	Schütt, Göttingen
Petri dishes	Sarstedt, Nümbrecht
PCR tubes	Sarstedt, Nürnbrecht
Sterile filter (0.22 µm, 0.45 µm pores)	Millipore, Eschborn
Scalpels	C.Bruno Bayha GmbH, Tuttlingen
Tubes (1,5 ml; 2 ml)	Sarstedt, Nürnbrecht

4 Methods

4.1 Manipulations with nucleic acids

4.1.1 Molecular cloning

Unless otherwise mentioned all methods used were according to Sambrook et. al.,1989, or if a commercial kit was used, according to the protocol supplied by the manufacturer. DNA fragments were amplified by PCR, using *Taq* DNA polymerase or a mixture of *Taq*/*Pfu* polymerases (10:1), from the Dictyostelium genomic DNA or from available plasmids. Amplified DNA fragments were ligated into the vector pJET1.1 (or when *Taq* polymerase was used into pGEM-T Easy vector) using T4 DNA ligase. The positive clones were sequenced to confirm the absence of mutations and correct sequences were excised from the cloning vector using appropriate restriction sites, located in the multicloning site of the vector or introduced during the PCR amplification. The resulting DNA fragments were subcloned into the desired vector digested at the complementary restriction sites.

4.1.2 Polymerase chain reaction (PCR)

Polymerase chain reaction was used to amplify DNA fragments *in vitro*. The following general protocol was used for amplification from plasmid and genomic DNA templates:

Reaction mixture:

1-5 µl	10 ng of plasmid or up to 1 µg of genomic DNA templates
1 µl	10 pmol of each primer (stock conc. 100 µM, working conc. 10 µM)
1 µl	dNTP mix (working conc. 10 mM of each)
5 µl	10xPCR buffer (100 mM Tris/HCl, pH 8.0, 0.1% Triton X-100, 50 mM KCl, 25 mM $MgCl_2$, Fermentas)
2 µl	*Taq* polymerase (or *Taq*/*Pfu* mixture (10:1) if necessary)

ad 50 µl total volume with H_2O^{mQ}

The following typical cycling protocol was used; however, modified in respect to the annealing temperatures (usually 1-2ºC less than lowest for used primers) and the elongation times (usually

2 min for 1 kb of an amplified DNA template).

1. step	2-5 min 95°C (initial denaturation)
2. step (30 cycles)	30-45 sec 95°C (denaturation)
	15-30 sec 45-55°C (annealing of primers)
	30 sec - 5 min 65-72°C (elongation)
3. step	5 min 65-72°C (final elongation)

4.1.3 Isolation of plasmid DNA from E.coli

Plasmid mini-preparation (by alkaline lysis)

1.5 ml of a bacterial culture, grown over night at 37°C was used to prepare plasmid DNA by the alkaline lysis method. *E.coli* DH5α™ cells were collected by centrifugation at 3500 rpm for 5 min and resuspended in 100 µl Solution I by strong vortexing. After adding 200 µl Solution II, the cells were lysed at RT for 5 min, and then neutralized with 150 ml Solution III. After 10 min incubation on ice, the samples were centrifuged at 14000 rpm for 15 min and the supernatant was collected and precipitated with 2.5V of pure (100%) ethanol. The pellet was washed with 70% ethanol, dried and dissolved in 20 µl UV-treated H_2O^{mQ}.

Plasmid midi-preparation using Macherey&Nagel kit

Kits and Nucleobond™ midi-columns Macherey&Nagel were used according to the manual of the manufacturer. All plasmids, used for transformation in *Dictyostelium* or for *in vitro* transcription, were prepared with the kit.

Plasmid maxi-preparation

For the preparation of large amounts of plasmid DNA 100-150 ml of *E. coli* cultures were used. The mini-preparation method was up-scaled respectively. Additionally, RNaseA, Proteinase K and phenol/chloroform extraction were used during preparations. In most cases additional step was applied for further purification of plasmid DNA. Briefly, after maxi-prep plasmid DNA was dissolved in the 490 µl of UV-treated H_2O^{mQ}, 10 µl of RNaseA (2mg/ml) was added, mixed and the DNA solution was incubated at 37ºC for 25 min followed by treatment with 5 µl of 25 mg/ml Proteinase K (in TE buffer) at 37ºC for 30 min. Equal volume (500 µl) of 8M LiCl was added to

the DNA solution and mixed by vortexing. After 30 min incubation on ice, the precipitate was discarded by centrifugation at 14000 rpm for 15 min at 4ºC and the plasmid DNA was precipitated from supernatant by equal volume (1000 µl) of pure (100%) ethanol. After incubation for 30 min on ice, DNA precipitate was collected by centrifugation at 14000 rpm for 15 min at 4ºC, washed 3 times with 70% ethanol and dissolved in the 300-400 µl of UV-treated H_2O^{mQ}.

TE buffer (pH 7.4 or 8.0):
10 mM Tris/HCl
1 mM EDTA

Solution I:
25 mM Tris/HCl, pH 7.4
10 mM EDTA
15% Sucrose

Solution II:
200 mM NaOH
1% SDS

Solution III:
3 M sodium acetate, pH 4.7

4.1.4 Restriction digestion

Digestion of genomic DNA or plasmid DNA was performed according to the manufacturer´s instructions. Most enzymes were purchased from Fermentas or New England Biolabs and were used with the supplied reaction buffers under appropriate reaction conditions.

4.1.5 Isolation of nucleic acids from *Dictyostelium discoideum*

Genomic DNA preparation from Dictyostelium discoideum - fast mini preparation (Barth et al, 1998)

Dictyostelium cells, grown on Costar 24-well plates (5 x 10^6 cells), were collected by centrifugation at 4000 rpm for 5 min. The cells were resuspended in 300 µl TES buffer (10 mM Tris/HCl, 1 mM EDTA, 0.7% SDS) and 30 µl of 25 mg/ml Proteinase K (in TE buffer) was added, followed by incubation at 45°C for 1 hour. The genomic DNA was extracted with phenol/chloroform and precipitated with ethanol. The genomic DNA, prepared by this method, was used for PCR.

Genomic DNA preparation from Dictyostelium discoideum - maxi preparation

1-2 x 10^8 cells were collected from axenic culture with high cell density (approximately 4-6 x 10^6) by centrifugation at 1700 rpm for 10 min at 4°C, washed once with ice-cold phosphate-buffered saline buffer (PBS, pH 6.7) and resuspended in 45 ml of nuclear lysis buffer. The cells were lysed by addition of NP40 to a final concentration of 0.5 % and incubation on ice for 10 min. The nuclear fraction was obtained by centrifugation at 4000 rpm for 15 min. The nuclear pellet was carefully resuspended in 5 ml SDS lysis buffer and incubated with 100 µl of 25 mg/ml Proteinase K solution (in H_2O^{mQ}) at 60°C for 2 hours. The genomic DNA was extracted twice with phenol/chloroform followed by centrifugation at 10000 rpm for 45 min and precipitated by adding 1/10V of 3M sodium acetate, pH 4.7 and 2V of pure (100%) ethanol. The DNA precipitate was washed with 70% ethanol, dried and carefully resuspended in 200-300 µl of UV-treated $H2O^{mQ}$.

Nucleus lysis buffer:
50 mM HEPES, pH 7.5
40 mM $MgCl_2$
20 mM KCl
5% Sucrose
0.5% NP 40

SDS lysis buffer:
TE buffer, pH 8.0
0.7% SDS

Isolation of total RNA from Dictyostelium discoideum (Maniak et al, 1989)

1–3 x 10^7 cells were pelleted by 1700 rpm for 10 min at 4ºC and lysed in 500 µl of Solution D. After addition of 50 µl 3 M sodium acetate (pH 4.7) and 500 µl phenol/chloroform the sample was vortexed and and incubated on ice for 20 min followed by centrifugation at 14000 rpm for 15 min. The upper phase, containing RNA was collected and precipitated by 1V of isopropanol. The RNA was pelleted by centrifugation at 14000 rpm for 15 min, washed twice with 70% ethanol, dried in the speed-vac and dissolved in 200 µl DEPC-treated H_2O^{mQ} or formamide.

Solution D (incomplete):
4 mM Guanidinium thiocyanate
25 mM Sodium citrate
0.5% Sarcosyl

To prepare a complete Solution D, immediately

DEPC-treated H_2O^{mQ}:
0.1% diethylpyrocarbonate
in $H2O^{mQ}$, incubate ON, autoclave

before use 360 µl β-mercaptoethanol was added
to 50 ml of solution (final conc. 0.1 M).

Extraction of small RNAs from total cellular RNA

To a total RNA, dissolved in 2 ml of DEPC-treated H_2O^{mQ}, PEG (MW=8000) was added to a final concentration of 5% and NaCl to a final concentration of 0.5 M. The sample was mixed, incubated on ice for 30 min and then high molecular weight nucleic acids were pelleted at 10000 rcf for 10 min. The resulting supernatant, containing tRNA, small rRNAs and siRNAs, was precipitated with 3V of ethanol after incubation at –20ºC for at least 2 hours. The RNA was washed twice with 70% ethanol, dried and dissolved in 200-300 µl of UV-treated $H2O^{mQ}$.

4.1.6 Standard gel electrophoresis of nucleic acid samples

Agarose gels

Generally, DNA or RNA preparations, digestion DNA fragments and PCR products were separated on 0.8 – 2% agarose gels. The corresponding amount of agarose was dissolved in 1xTBE buffer, melted in a microwave and after brief cooling period of time (10-15 min), ethidium bromide was added to a final concentration 0.5 µg/ml and the gel was poured into a horizontal gel-forming chamber. After polymerization, the samples mixed with 6x loading dye (60% Glycerol, 0.25 % w/v Bromophenol blue and 0.25 % w/v Xylene cyanol), were loaded and the gels were run using 1xTBE buffer at 4-5 V/cm for 30 – 60 min at RT. The results were documented using INTAS UV-systeme gel imager.

In some cases, the RNA was separated on 1.8 – 2 % denaturing GTC (20 mM) agarose gels. The agarose was melted in 100 ml 1xTBE buffer using a microwave and after cooling to 60ºC, 500 µl of 1 M guanidinium thiocyanate was added carefully. The samples of RNA to be run on the gel was mixed with 1V of denaturing RNA loading buffer (95% Formamide, 2 mM EDTA, 0.25 % w/v Bromophenol blue; 0.25 % w/v Xylene cyanol), heated for 5 min at 85ºC and cooled in ice before loading. The gels were run in the cold room at 4ºC at 4-5 V/cm for 30-60 min.

10xTBE buffer, pH 8.0:

1340 mM Tris base

450 mM Boric acid

25 mM EDTA
Autoclave for 20 min

Polyacrylamide gels

The DNA or RNA samples were separated on 6% polyacrylamide gels using 1xTBE buffer. Samples were prepared for loading as mentioned above for agarose gels. Gel 40 (Roth) was used for gel preparation. Gels were run at 3-4 V/cm for 20-30 min.

50 ml of PA gels:

7.5 ml Gel 40
10 ml 5xTBE, pH 8.0
50 µl TEMED
ad 50 ml with H_2O^{mQ}
250 µl APS (20%) – add before use.

4.1.7 Gel elution of DNA fragments from agarose gels

For elution of DNA fragment from the agarose gels, after gel electrophoresis the desired band was cut under UV light (366 nm). The DNA was purified using Nucleospin™ (Macherey & Nagel) purification kit according to the manual of the manufacturer.

Alternatively, another method was used. Gel was running in the 1xTBE buffer with ethidium bromide of a final concentration 1 µg/ml at 4-5 V/cm. After the desired DNA fragments reached approximately the middle of the gel, the run was stopped and some volume of the running 1xTBE buffer was removed from a chamber in a way that buffer contact only sides of the gel. The rest of the buffer was carefully removed from the top surface of a gel. A small piece of gel in front of the corresponding band was cut and the empty well was filled up with 3xTBE buffer, containing ethidium bromide of the same concentration as in a running buffer. The run was continued at 15-20 V/cm for 2-4 min until the DNA fragments migrated into the well. The buffer from the well containing DNA was collected and equal volume of H_2O^{mQ} was added to dilute the sample. After addition of 1/10V 3 M sodium acetate (pH 4.7) and equal volume of phenol/chloroform the sample was vortexed followed by centrifugation at 14000 rpm for 15 min. The upper phase was collected and DNA was precipitated by addition of 2.5V pure (100%) ethanol. The DNA pellet was washed twice with 70% ethanol and diluted in H_2O^{mQ}.

4.1.8 Digestion of plasmids for *in vitro* transcription

A set of plasmids, containing T7 promoter and cloned cDNA for different RNAs were used for *in vitro* transcription (see Materials). However, prior usage the plasmids had to be linearized with an appropriate restriction enzyme (*Xba*I, *Bam*HI or *Hin*dIII) right behind the RNA sequence to generate a stop signal for the T7 polymerase (run-off transcription). The linearized plasmids were separated from non-digested species by gel electrophoresis as described above. The DNA was purified via phenol/chloroform extraction, precipitated with 1/10V 3 M sodium acetate (pH 4.7) and 100% ethanol, washed twice with 70% ethanol and dissolved in 250-300 µl UV-treated H_2O^{mQ}.

4.1.9 *In vitro* transcription

In vitro transcription was used to generate radio-labeled or non-labeled RNA sequences that were used as substrates for studies of RNA-DnmA interactions. As templates different vectors were used (see Materials), which contain T7 promoter sequence for T7 RNA polymerase. Alternatively, PCR fragments, where T7 promoter sequence was included in the primers, were used as templates for *in vitro* transcription in some cases. Prior to transcription, a 5xNTPs mastermix was prepared, with 5 mM of each NTP. For radioactive *in vitro* transcription, the concentration of the cold nucleotide triphosphate which was also added in a radioactive form, e.g. [α-^{32}P]-UTP, was lowered to 2.5 mM, resulting in 0.5 mM final concentration of cold nucleotide triphosphate, while the other NTPs were kept constant at 1 mM final concentration in the transcription mixture. The transcription reaction was usually set up in a volume of 200 µl and incubated at 37ºC for 2-3 hours. After transcription was finished, samples were treated with DNaseI at 37ºC for 15 min and extracted with an equal volume of phenol/chloroform/isoamyl alcohol (Roth). Non-incorporated nucleotides were removed by a gel filtration through a Sephadex G-50 spin column. The concentration of *in vitro* transcribed RNA was measured by spectrophotometer.

Cold transcription mixture:

0.5-2 µg template DNA

40 µl 5x transcription buffer (Fermentas)

40 µl 5 mM NTP mix (ATP, CTP, GTP and UTP)

1 µl RNase inhibitor RNasin

2 µl T7 RNA polymerase

ad 200 µl with H_2O^{mQ}

Hot transcription mixture:

0.5-2 µg template DNA

40 µl 5x transcription buffer (Fermentas)

40 µl 5 mM NTP mix (ATP, CTP, GTP and 2.5 mM UTP)

2-4 µl [α-^{32}P]-UTP (10 µCi/µl, without stabilizing dye)

1 µl RNase inhibitor RNasin® (Fermentas)

2 µl T7 RNA polymerase

ad 200 µl with H_2O^{mQ}

4.1.10 Elution and precipitation of gel-purified tRNAs

For separation of *in vitro* transcripts and ^{32}P-labeled or non-labeled RNA, the samples were run on 6-8% denaturing polyacrylamide/urea gels, depending on the length of the RNA fragments. The gels were run in 1xTBE buffer by 15-20 V/cm for 3-4 hours.

Denaturing polyacrylamide/urea gel:

Urea	24 g (8 M)
5xTBE	10 ml
40% Polyacrylamide (Gel 40)	[x] ml

ad 50 ml H_2O^{mQ}

The polymerization of the gel was achieved by the addition of 50 µl TEMED and 250 µl 20% APS. The tRNA was eluted from the excised gel piece by incubation over night at RT in elution buffer (10 mM Tris/HCl. pH 7.5, 1 mM EDTA, 0.1% SDS, 80% Formamide). On the next day, the solution was cleared from residual gel by phenol/chloroform/isoamyl alcohol extraction and the upper phase was carefully collected, brought to 0.3 M NaCl and precipitated with 3V 100% ethanol by incubation at -20ºC for at least 2 hours. The tRNA was pelleted by centrifugation at 14000 rpm for at least 30 min at 4ºC. The ethanol was carefully removed, and the pellet was washed twice with 80 % EtOH. After a brief drying period in a speed-vac, the tRNA pellet was resuspended in UV-treated H_2O^{mQ} and stored at -20ºC.

4.1.11 Preparation of radioactively labeled DNA

Radioactive labeling of DNA by PCR

The method was used for labeling PCR fragments. PCR reaction was performed as usual in 50 µl of total volume and in the presence of dNTPs (final conc. 0.2 mM of dTTP, dCTP and dGTP), 0.1 mM dATP and 1 µl [α-^{32}P]-dATP (10µCi/µl) was added. For other details see in (4.1.2).

Klenow random labeling

The method was used for labeling PCR fragments. The DNA template together with the OLB-mix and the Klenow buffer was denatured by heating at 95ºC for 5 min followed by cooling step on ice for 5 min and the Klenow fragment^{exo-} and [α-^{32}P]-dATP (10µCi/µl) were added.

Reaction mixture:

5 µg	template DNA
3 µl	OLB-mix
2 µl	10x Klenow buffer (Fermentas)
2 µl	[α-^{32}P]-dATP
1 µl	Klenow fragment^{exo-}

ad 20 µl H_2O^{mQ}

The reaction was incubated at 37ºC for 1 hour. The free nucleotides were separated by centrifugation through a Sephadex G50 spinning column. The purified radioactive probe was then denatured by heating at 90ºC for 5 min, and used for hybridization.

OLB-mix:

200 mM Tris/HCl, pH 7.5

25 mM $MgCl_2$

10 mM ß-mercaptoethanol

1 M HEPES pH 6.6

13.5 U A_{260} oligos-hexamers (Fermentas)

0.25 mM dCTP, dGTP and dTTP

End-labeling with T4 Polynucleotide Kinase (PNK)

5´-End labeling was performed with T4 Polynucleotide Kinase (Fermentas) and [γ-^{32}P]-ATP. T4

PNK is a polynucleotide 5'-hydroxyl kinase that catalyzes the transfer of the γ-phosphate from ATP to the 5'-OH group of single and double stranded DNA and RNAs (forward reaction). The reaction is reversible and in the presence of ADP, T4 PNK exhibits 5'-phosphatase activity and catalyzes the exchange of terminal 5' phosphate group (exchange reaction).

Reaction mixture (forward reaction):

10-100 nmol	DNA oligo/RNA
2 µl	10x reaction buffer A (Fermentas)
2-5 µl	[γ-^{32}P]-ATP
10U	T4 PNK

ad 20 µl H_2O^{mQ}

The reaction was incubated at 37ºC for 1 hour, extracted with an equal volume of phenol/chloroform, and annealed to equimolar amount of non-labeled complementary oligo, by heating up to 90ºC and incubation at 37ºC for 25 min. Then the double stranded DNA was formed the solution was purified through a Sephadex G-50 spin column and precipitated with 100% ethanol. In case of labeled ssDNA/dsDNA/RNAs, purification and precipitation was performed directly after labeling. For labeling of 5'-protruding termini of DNA by exchange reaction the same protocol was applied. Instead of buffer A, the buffer B (Fermentas) was used and additionally 4 µl 24% PEG 8000 was added to the reaction mixture.

4.1.12 Elution and precipitation of gel-purified DNA oligonucleotides

For separation of ^{32}P-labeled DNA oligonucleotides, the samples were run on 8% denaturing polyacrylamide/urea gels (see 4.1.10 for details). The gels were run in 1xTBE buffer by 15-20 V/cm for 1-2 hours. The DNA was eluted from the excised gel piece by incubation over night at 60ºC in elution buffer (10 mM Tris/HCl. pH 8.0, 1 mM EDTA and 0.1% SDS). On the next day, the solution was cleared from residual gel by phenol/chloroform/isoamyl alcohol extraction and the upper phase was carefully collected, and DNA was precipitated with 1/10V 3 M Sodium acetate, pH 4.7, and 3V 100% ethanol followed by incubation at -20ºC for at least 2 hours. The DNA was pelleted by centrifugation at 14000 rpm for at least 30 min at 4ºC. The ethanol was carefully removed, and the pellet was washed twice with 70 % EtOH. After a brief drying period in a speed-vac, the DNA pellet was resuspended in UV-treated H_2O^{mQ} and stored at -20ºC.

4.2 Manipulations with proteins and protein extracts

4.2.1 Subcellular fractionation of *Dictyostelium* cells

The preparation of cellular and nuclear subfractions was performed as previously described with minor changes (Sherif Tawfic, 1997). 6 x 10^8 cells, grown to a density of 2-2.5 x 10^6 were collected, washed once with ice-cold PBS, pH 6.7 and suspended in 50 ml of CSK buffer (10 mM PIPES, pH 6.8, 100 mM NaCl, 0.3 M sucrose, 3 mM $MgCl_2$, 1 mM EGTA, 0.5% Triton X-100, 1 mM phenylmethylsulfonyl fluoride (PMSF) and 1x Complete protease inhibitor cocktail (Roche)) Cells were lysed for 20-30 min incubation on ice. The lysate was centrifuged at 4000 rpm for 15 min at 4ºC. Supernatant fluid was collected and centrifuged for 10000 rpm for 30 min at 4ºC. The pellet was discarded and the supernatant was collected as the cytosol fraction. The nuclear pellet from the first centrifugation step was used as the starting material for isolation of the various nuclear subfractions. To this end, the pellet was suspended in 2 ml of the digestion buffer (10 mM PIPES, pH 6.8, 50 mM NaCl, 0.3 M sucrose, 3 mM $MgCl_2$, 1 mM EGTA, 0.5% Triton X-100, 1 mM PMSF, 1x Complete protease inhibitor cocktail (Roche), RNase A 100 µg/ml and DNase I 100 µg/ml). This suspension was incubated for 30 min at RT followed by dropwise addition of 1 M $(NH_4)_2SO_4$ to a final concentration of 0.25 M. The material was centrifuged at 4000 rpm for 15 min at 4ºC and the supernatant fluid was collected as the chromatin fraction. The pellet was suspended in 2 ml of the CSK buffer containing 2 M NaCl and centrifuged at 4000 rpm for 15 min at 4ºC. The supernatant fluid was collected as the nuclear matrix fraction. The pellet from this step was suspended in TMED buffer (50 mM Tris/HCl, pH 7.9, 5 mM $MgCl_2$, 1 mM EGTA, 0.5 mM DTT, 200 mM NaCl, 0.5 mM PMSF and 1x Complete protease inhibitor cocktail (Roche)) and was designated as the core filament fraction.

4.2.2 Overexpression and purification of recombinant His-tagged DnmA from *E.coli*

The cDNA of *dnmA* was cloned with N-terminal His_6-tag in pET15b vector (Novagen) using the *Nde*I and *Bam*HI sites (see Materials). Recombinant proteins were expressed in *E.coli* (DE3) BL21 pLysS cells. Induction and protein purification were done as described previously with minor changes (Jurkowski et al, 2008). Briefly, the *E.coli* cells were induced at OD_{600}=0.6 with 1

mM IPTG and incubated for 3 hours at 22ºC. After harvesting by centrifugation at 4000 rpm for 10 min, the cells were resuspended in 40 ml of sonication buffer (30 mM KPi pH 7.0, 300 mM KCl, 10% (v/v) glycerol, 10 mM imidazole, 0.1 mM DTT) containing protease inhibitors (complete mini, Roche) and lysed by sonication with the Dr. Hielscher Ultraschallprozessor UP200S sonifier (5-10 times/15 sec, cycle 0.5/amplitude 50%). The crude cell lysate was pre-cleared by centrifugation at 10000 rpm for 15 min and the pellet and the supernatant were examined for the presence of the recombinant protein by Western blotting. The supernatant was processed further by incubation with Ni-Charged Resin (Profinity^{TM} IMAC, Bio-Rad) for 30 min at 4°C on rotating wheel. Usually 1 ml suspension of Ni-Charged Resin was used for cells collected from 500 ml of induced bacterial culture. After loading onto a polyprep column (Bio-Rad, Hercules, CA) and washing with 15 ml of sonication buffer, His_6- tagged DnmA was eluted with 1 ml of elution buffer (30 mM KPi pH 7.0, 300 mM KCl, 10% glycerol, 200 mM imidazole, 0.1 mM DTT). The eluate was dialysed in two steps: with dialysis buffer I (30 mM KPi pH 7.0, 200 mM KCl, 20% glycerol, 1 mM DTT) and dialysis buffer II (30 mM KPi pH 7.0, 100 mM KCl, 50% glycerol, 1 mM DTT).

4.2.3 Expression and purification of TAP-tagged DnmA from *Dictyostelium*

The TAP method requires fusion of the TAP tag, either N- or C-terminally, to the target protein of interest. Prior knowledge of complex composition or function is not required. Starting from a relatively small number of cells, potential interaction proteins or macromolecular complexes can be isolated and used for multiple applications (Puig et al, 2001). Its simplicity, high yield, and wide applicability make the TAP method a very useful procedure for protein purification and proteome exploration. The TAP tag consists of two IgG binding domains of *Staphylococcus aureus* protein A (ProtA) and a calmodulin binding peptide (CBP) separated by a TEV protease cleavage site (Figure 4.2.3A).

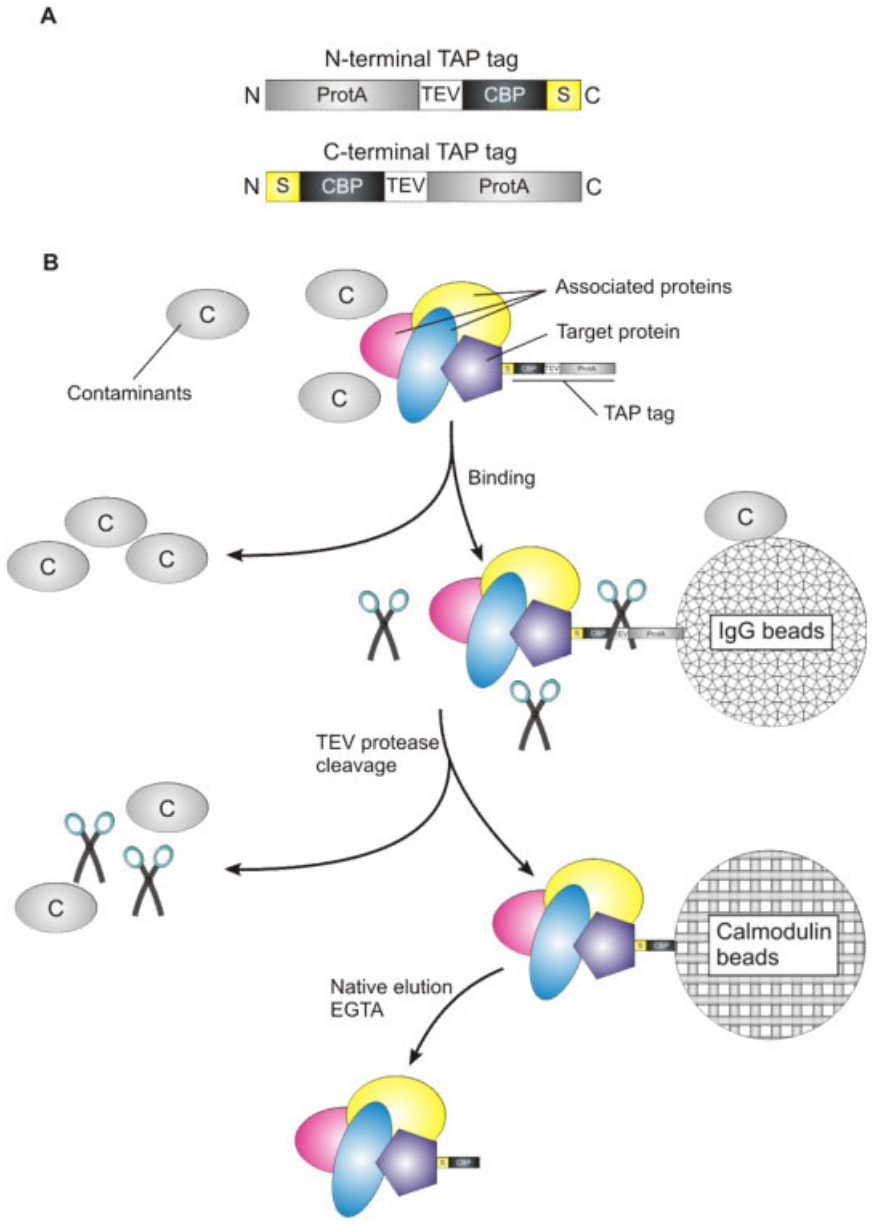

Figure 4.2.3 (**A**) Schematic representation of the C- and N-terminal TAP tags. Note that the relative order of the modules in the TAP tag is inversed in the two tags because the ProtA module needs to be located at the extreme N- or C-terminus of the fusion protein. (**B**) Overview of the TAP purification strategy.

ProtA binds tightly to an IgG matrix, requiring the use of the TEV protease to elute material under native conditions. The eluate of this first affinity purification step is then incubated with calmodulin-coated beads in the presence of calcium. After washing, which removes contaminants and the TEV protease remaining after the first affinity selection, the bound material is released under mild conditions with EGTA (Figure 4.2.3B).

To perform tandem affinity purification of TAP tagged DnmA and putative interaction partners, 2 x 10^9 cells were collected from 1 liter of shaking *Dictyostelium* culture, grown to a density of 2 x 10^6 cells/ml. All procedures after this point were carried out at 4ºC unless stated otherwise. The cells were centrifuged and resuspended in 40 ml of ice-cold IP150G buffer (10 mM Tris/HCl, pH 8.0, 150 mM NaCl, 300 mM Galactose, 0.1 mM PMSF, 1 mM β-mercaptoethanol and 1x protease inhibitor coctail (Roche)). Cells were lysed by addition of 10% NP40 (v/v) to a final concentration of 0.5% and incubation for 15-25 min on ice. The lysate was centrifuged for 15 min at 10000 rpm and the supernatant was collected and incubated with 250-300 µl of IgG-agarose for 1 hour at 4ºC with gentle rotation. The supernatant-agarose slurry was loaded onto a Poly-Prep® Chromatography column (0.8x4, Bio-Rad, Hercules, CA) and agarose beads were washed with 30 ml of IP150 buffer (10 mM Tris/HCl, pH 8.0, 150 mM NaCl, 0.1% NP40, 0.1 mM PMSF, 1 mM β-mercaptoethanol) then with 10 ml of TEV cleavage buffer (10 mM Tris/HCl, pH 8.0, 150 mM NaCl, 0.1% NP40, 0.5 mM EDTA, 1 mM DTT). The beads was transferred to a 2 ml eppendorf tube and supplied with 500 µl of TEV cleavage buffer with 100 U TEV protease (homemade, 20 µl, c.a. 0.5 µg/µl). The tube was rotated for 3.5 hours at 4ºC. The beads were pelleted by centrifugation at 600 rpm for 3 min and the supernatant was collected to 15 ml falcon tube. The beads were washed twice with 500 µl TEV cleavage buffer and supernatants combined with the first supernatant in the falcon tube to give a final volume of 1.5 ml. 3 ml of CaM binding buffer (10 mM Tris/HCl, pH 8.0, 150 mM NaCl, 0.1% NP40, 1 mM Mg acetate, 1 mM Imidazol, 2 mM $CaCl_2$ and 10 mM β-mercaptoethanol), 30 µl of 100 mM $CaCl_2$ and 250 µl of calmodulin-beads suspension were added to the falcon tube stepwise. The tube was rotated for 1-2 hours at at 4ºC. The slurry was transferred to a fresh polyprep column and washed with 10 ml of CaM binding buffer. The bound proteins were eluted stepwise by 500 µl of CaM elution buffer (10 mM Tris/HCl, pH 8.0, 150 mM NaCl, 0.1% NP40, 1 mM Mg acetate, 1 mM Imidazol, 2 mM EGTA and 10 mM β-mercaptoethanol). Elution fractions were run on a SDS-PAGE gel and analyzed by western blotting.

4.2.4 Expression and purification of StrepII-tagged DnmA from *Dictyostelium*

The *Strep*-tag®II (IBA) is an eight-residue peptide sequence (Trp-Ser-His-Pro-Gln-Phe-Glu-Lys) that exhibits strong intrinsic affinity towards streptavidin and can be fused to recombinant proteins in various fashions. To date, several established protocols are available, that allow quick

and mild purification of *Strep*-tag II fusion proteins, including their complexes with interacting partners, both from bacterial and eukaryotic cell lysates using affinity chromatography (Figure 4.2.4) on a matrix carrying an engineered streptavidin (*Strep*-Tactin®, IBA), which can be accomplished within 2hrs (Schmidt & Skerra, 2007). Selective and sensitive detection on western blots is achieved with *Strep*-Tactin/enzyme conjugates or another monoclonal antibody.

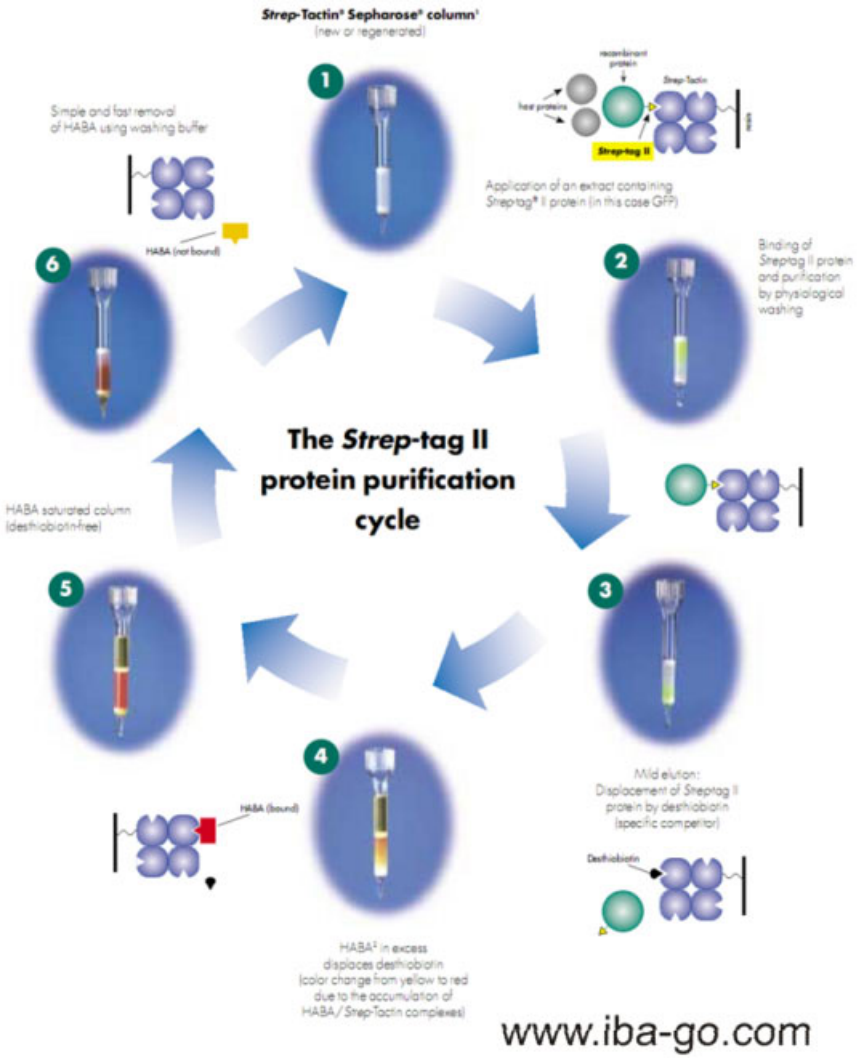

Figure 4.2.4 General scheme of Strep-tag technology. The Strep-tag II is a short peptide (8 amino acids, WSHPQFEK), which binds with high selectivity to Strep-Tactin, an engineered streptavidin. The binding affinity of the Strep-tag II to Strep-Tactin (Kd = 1 µM) is nearly 100 times higher than to streptavidin. After a short washing step, gentle elution of purified recombinant protein is performed by addition of low concentrations of biotin or desthiobiotin. Desthiobiotin is a stable, reversibly binding analog of biotin, the natural ligand of streptavidin.

Proteins containing the Strep-tag II epitope can be detected with high specificity and sensitivity using Strep-tag II antibodies. (Adapted from www.iba-go.com)

*Strep*II-tagged DnmA protein was isolated by affinity chromatography. Briefly, 6 x 10^8 of the *Dictyostelium* Ax2 *dnmA* KO/*dnmA_StrepII* cells were collected from 250 ml of shaking culture, grown to a density 2-2.5 x 10^6 cells/ml, washed twice with PBS, pH 6.7, and resuspended in 10 ml of ice-cold StrepII lysis buffer (30 mM KPi, pH 7.5, 150 mM KCl, 1 mM EDTA, 1 mM DTT, 5% glycerol and 1x Complete Mini Protease inhibitor cocktail (Roche)). To lyse the cells 10% (v/v) Triton X-100 was added to a final concentration of 0.75%. The lysate was incubated on ice for 15-20 min and pre-cleared by centrifugation at 10000 rpm for 30 min at 4°C. 250 µl of *Strep* Tactin® Superflow™ Agarose beads (Novagen) suspension was placed in a Poly-Prep® Chromatography column (0.8x4, Bio-Rad) and equilibrated with 5 ml of StrepII lysis buffer supplemented with 0.1% Triton X-100. The pre-cleared lysate was transferred onto the column and incubated for 30 min on a rotating wheel at 4°C. The flow-through was discarded and the beads were washed with 10 and then 5 ml of StrepII washing buffer (30 mM KPi, pH 7.5, 150 mM KCl, 1 mM EDTA, 0.1% Triton X-100, 1 mM DTT, 5% glycerol). *Strep*II-tagged DnmA was eluted 5 times with 250 µl of StrepII elution buffer (30 mM KPi, pH 7.5, 150 mM KCl, 1 mM EDTA, 0.1% Triton X-100, 1 mM DTT, 5% glycerol and 2.5 mM desthiobiotin). Elution fractions were separated by SDS-PAGE, combined, if necessary, and dialyzed overnight against dialysis buffer (30 mM KPi, pH 7.0, 100 mM KCl, 1 mM EDTA, 1 mM DTT, 50% glycerol). The samples were stored at -20°C before usage.

4.2.5 Protein quantification by Bradford assay

Protein concentration was determined by using the Bradford assay (Kruger, 1996). 1 to 10 µl of protein samples were diluted in 800 µl water and 200 µl Bradford solution (Bio-Rad) was added. The absorption of samples was measured by spectrophotometer at 595 nm. BSA solutions of known concentrations (0.1 - 20 µg/ml) was used to build a standard calibration curve.

4.2.6 Western blot

The protein samples were mixed with equal volume of 2x Laemmli buffer (125 mM Tris/HCl, pH 6.8, 10% Glycerol (v/v), 4% SDS (w/v), 2% β-mercaptoethanol (v/v) and 0.01%

Bromophenol blue (w/v)). The samples were placed on a heating block at 95ºC for 5 min, centrifuged at 14000 rpm for 2 min at RT and 10-15 µl of the SDS soluble supernatant was loaded onto a SDS-PAGE gel. SDS-PAGE gels were usually 8-12% depending on the size of separated proteins of interest.

For two SDS-PAGE gels:

Separating gel:

2.7-4 ml	Gel 30 (30% Acrylamide mix, Roth)
2.5 ml	1.5 M Tris, pH 8.8
0.1 ml	10% SDS
0.05 ml	20% APS
0.01 ml	TEMED

ad 10 ml with H_2O^{mQ}

Stacking gel:

0.83 ml	Gel 30 (30% Acrylamide mix, Roth)
0.63 ml	1 M Tris, pH 6.8
0.05 ml	10% SDS
0.025 ml	20% APS
0.005 ml	TEMED

ad 5 ml with H_2O^{mQ}

SDS-PAGE 5x Running buffer:

15.15 g Tris base

72 g Glycin

5 g SDS

ad 1000 ml with H_2O^{mQ} (The pH was adjusted to 8.3)

Up to 100 µg of proteins was run per mini-gel lane in a SDS-PAGE electrophoresis chamber (Bio-Rad) with 25 mA (constant) through the stacking gel and 35 mA (constant) through the separating gel. Proteins were transferred to PVDF membrane (45 µm pore size) by semi-dry transfer method (2 mA/cm^2 for 90 min at RT) using semi-dry blot buffer. Homogeneous loading and transfer of proteins was verified by staining the membrane with Ponceau-S dye (0.1% (w/v) in 5% acetic acid) for 5 min at RT followed by washing the excess of dye 2 times for 2 min with 1% acetic acid. After washing in PBS buffer to remove the Ponceau-S dye, the membrane was

blocked by incubation with 5% non-fat milk (w/v) or BSA in 1x PBST buffer (PBS supplemented with 0.1% Tween 20 (v/v)) for 2 hours at RT. After washing 3 x 5 min with 1x PBST buffer and 5% non-fat milk, the membrane was incubated with the primary antibody in the same buffer over night at 4ºC. After washing 3 x 15 min with 1x PBST buffer with 5% non-fat milk, the membrane was incubated with the appropriate secondary antibody conjugated to alkaline phosphatase (Dianova, Hamburg, Germany) at a dilution of 1:10000 in the same buffer for 2 hours at RT. After washing 3 x 15 min with 1x PBST buffer, the membrane was incubated in development buffer (0.2 mg/ml BCIP, 100 mM Tris/HCl, pH 9.5, 100 mM NaCl, 5 mM $MgCl_2$, 0.05% Tween 20) until blue staining was emerged, then the membranes were washed twice with water and photographed.

Semi-dry blot buffer:

5.82 g Tris base

2.93 g Glycin

0.38 g SDS

200 ml Methanol

ad 1000 ml with H_2O^{mQ}

BCIP solution:

50 mg/ml BCIP in DMF

4.3 Electrophoretic mobility shift assay

4.3.1 EMSA of DNA-DnmA interactions

To perform gel retardation assays [^{32}P]-labeled DNA oligonucleotides (ss or dsDNA) or non-labeled DNA were incubated in 20 µl of DNA binding buffer (10mM Tris HCl, pH 8.0, 50 mM NaCl, 1 mM $MgCl_2$, 5 % Glycerol (v/v), 0.2 mM PMSF and 1 mM DTT) for 15-30 min at RT with increasing amounts of His-DnmA (26-200 pmol). After indicated times samples were loaded on a native 8% PAGE gel and separated at 275 V (constant) at 4ºC for 2.5-3 hours. Gels were sealed in Saran Wrap and exposed to X-ray film (Contatyp CX-BL+ Medical X-ray film) for 2 to 7 days at -80°C. In case of DNA fragments larger than 200 bp, native agarose gels were used and electrophoresis was performed in 0.5x TAE buffer, pH 7.5.

50 ml of native 8% PA gels:

10 ml Gel 40 (40% aa, Roth)

10 ml 5xTBE, pH 8.0

50 µl TEMED

ad 50 ml with H_2O^{mQ}

250 µl APS (20%) – add before use.

4.3.2 Atomic force microscopy (AFM)

Mica surface preparation

After the exfoliation of the top layer, mica surface was exposed to the vapours of aminopropyltriethoxysilane (APTES) for at least 2 min. After successive washing with filtered $H2O^{mQ}$, the surface was dried with pressurized N.

Sample preparation

Samples was prepared as usually for EMSA assays, incubated for 5 min, diluted with 1:10 to 1:1000 with 10 mM Tris/HCl, pH 7.5, 5mM $MgCl_2$ and centrifuged for 2 min at 14000 rpm. The supernatant was used to drop on the mica surface and was removed immediately and the surface was washed with filtered $H2O^{mQ}$ and dried with pressurized N.

Imaging

Imaging was carried out with a Nanoscope® III Multimode™ Scanning Probe Microscope (Digital Instruments, Santa Barbara, CA) using silicon cantilevers NCH-Pointprobe Nanosensors (Neuchatel, Schweiz).

AFM technique

The scanning was performed in the Tapping mode, which is an intermittent-contact mode that allows medium resolution but very robust imaging conditions in most media of materials that are difficult to image by other AFM operation modes. TMAFM overcomes problems associated with friction and shear forces by alternative placing the tip in contact with the surface to increase the resolution, and then lifting it up to avoid damaging the sample surface. In a Tapping mode the cantilever oscillate near it resonance frequency and the tip strike the surface on each oscillation. The oscillation amplitude and, therefore, the associated energy is made to be sufficient to overcome the stickiness of the surface for a wide range of vertical positions of the cantilever.

4.3.3 EMSA of RNA-DnmA interactions

To perform gel retardation assays [^{32}P]-labeled RNAs were incubated in 20 µl of binding buffer (10 mM KPi, pH 7.0, 22.5 % glycerol (v/v), 25 mM KCl, 10 mM DTT and 2-10 mM $MgCl_2$ with or without SAM) for 15-30 min at RT with increasing amounts of His-DnmA (26-200 pmol). After indicated times samples were loaded on a native 6% PAGE gel and separated at 275 V (constant) at 4ºC for 2.5-3 hours. Gels were sealed in Saran Wrap and exposed to X-ray film (Contatyp CX-BL+ Medical X-ray film) for 2 to 7 days at -80°C.

50 ml of native 6% PA gels:

7.5 ml Gel 40 (40% aa, Roth)

10 ml 5xTBE, pH 8.0

50 µl TEMED

ad 50 ml with H_2O^{mQ}

250 µl APS (20%) – add before use.

4.4 Detection of denaturant-resistant covalent complexes

The samples were prepared mainly as described in (4.3.3). After incubation for 0.25-60 min, 10 µl of denaturing stop buffer (150 mM Tris/HCl, pH 8.0, 6% SDS (w/v), 30 mM EDTA 0.025% Bromophenol blue) was added and samples were incubated for 10 min at 65ºC. After cooling at RT, samples were loaded on a 9-10% SDS-PAGE gel and run at 20 V/cm (constant) at RT for 1.5-2 hours. Gels were sealed in Saran Wrap and exposed to X-ray film (Contatyp CX-BL+ Medical X-ray film) for 2 to 7 days at -80°C.

4.5 Cell biology methods

4.5.1 *Dictyostelium* axenic cell culture

Dictyostelium discoideum Ax2-214 strain and the derived transformants were grown axenically in shaking cultures using HL5 medium, supplemented with 50 µg/ml ampicillin, 10 U/ml penicillin, 10 µg/ml streptomycin and 0.25 µg/ml amphotericin. If necessary medium was supplied with selection antibiotics, geneticin and/or blasticidin S to final concentration 10 µg/ml. Cultures were grown shaking at 150 rpm from initial density 5 x 10^4 cells/ml at 22°C and

harvested at indicated cell densities.

HL5 medium, pH 6.7:

18 g Glucose

14.3 g Bacto-peptone

7.15 g Yeast extract

0.616 g $Na_2HPO_4x2H_2O$

0.486 g KH_2PO_4

ad 1000 ml H_2O

4.5.2 *Dictyostelium* transformation

Transformation of Dictyostelium using electroporation

Dictyostelium cells grown axenically in shaking culture were transformed by electroporation as previously described (Howard et al, 1988). 2 x 10^7 cells, grown to a density of 1-1.5 x 10^6 were collected, washed once with ice-cold PBS, pH 6.7, once with EP buffer and then resuspended in 800 µl EP buffer. 15–20 µg DNA was added and the cells were incubated on ice for 10 min. Electroporation was performed at 1 kV, 25 µF in a 0.4 cm electroporation cuvette the time constant between 3 and 4 ms). The cells were placed on a Petri dish, mixed with 2 drops (8 µl each) of 0.1 M $CaCl_2$ and 0.1 M $MgCl_2$ and incubated at RT for 15 min. Then 10 ml HL5 medium were added for incubation ON (12-16 hours). On the next day, the medium was replaced by the appropriate selection medium. The cells were cultured under selection until transformants were obtained. Every 72 hours the selective medium was aspirated and replaced with fresh selective medium.

1xPhosphate-buffered saline (PBS, pH 6.7):

16.012 g NaCl

1.53 g $Na_2HPO_4x2H_2O$

0.402 g KCl

38.2 g KH_2PO_4

ad 1000 ml H_2O^{mQ}, adjust to pH 6.7 with HCl, autoclave

EP buffer, pH 6.1:

10 mM Na_2HPO_4

50 mM Sucrose

Classical transformation of Dictyostelium discoideum

The transformation was performed as previously described (Nellen & Firtel, 1985); (Nellen & Saur, 1988). 15 ml of *Dictyostelium* cell culture, grown to a density of approximately 1 x 10^6 were poured in a Petri dish. After 30 min the cells have settled down on the bottom and the medium was changed with 10 ml MES-HL5. Simultaneously, the DNA sample was prepared: 20 µg DNA were diluted in 600 µl of 1 x HBS buffer and 38 µl 2 M $CaCl_2$ were added drop-wise to the solution under vigorous mixing. The DNA precipitated as micro-crystals during the following 25 min incubation at RT. The medium from the Petri dish was aspirated and the DNA solution was distributed drop-wise over the cells. After 20 min incubation, 10 ml MES-HL5 medium was added and the transformation reaction was incubated for 3 h at 22ºC. Then the medium was changed with 2 ml 18% glycerol in 1 x HBS. After 5 min, the Glycerol solution was removed carefully and 10 ml MES-HL5 medium was added. On the next day, the medium was changed with a selection medium, containing the appropriate antibiotic. For selection of resistant clones, the medium was changed every 72 hours.

MES-HL5, pH 7.1:

10 g Glucose
10 g Bacto-peptone
5 g Yeast extract
1.3 g MOPS
ad 1000 ml H_2O

2xHBS, pH 7.05:

4 g NaCl
0.18 g KCl
0.05 g NaH_2PO_4
2.5 g HEPES
0.5 g Glucose
ad 250 ml H_2O, sterilize by filtering

4.5.3 Subcloning of *Dictyostelium* on SM plates

Klebsiella aerogenes (KA) suspension was prepared by washing one KA plate with 5 ml PBS, pH 6.7. To obtain single clones of *Dictyostelium*, around 100-200 cells were resuspended in 100 µl freshly prepared KA suspension and plated on SM-agar plates. Plates were grown at 22°C for 72 hours until colony plaques emerged on the bacterial lawn. Individual clones were picked with tooth picks and placed in liquid culture on 24-well Costar plates. For each transformation 2-3 individual clones were assayed for expression of the transgene by western blot and/or fluorescence microscopy.

4.5.4 Development of *Dictyostelium* on nitrocellulose filters

Approximately 5 x 10^7 *Dictyostelium* cells were pelleted at 1700 rpm, washed once with PBS, pH 6.7, resuspended in 500 µl of PBS and plated on a black nitrocellulose filter (d=5 cm), which had been boiled beforehand for 5 min in water. The nitrocellulose filter had been placed over two layers of Whatman 3MM paper, soaked with phosphate buffer. The development was allowed to occur at 22°C in a closed chamber to prevent the drying of the filters. The development was checked optically every 2-3 hours. If necessary the aggregates were harvested by scratching the filters with a scalpel. The cells were disaggregated by vortexing in 10 ml PBS, pH 6.7, and the cells were processed further for isolation of total RNA or DNA according to the protocols.

4.5.5 Fluorescence microscopy

Cell fixation and immunofluorescence

Dictyostelium cells were grown over night on 18 mm coverslips (treated with HCl) to approximately 80% confluency and fixed by the Picric acid/Paraformaldehyde fixative. 0.2 g Paraformaldehyde was dissolved in 3.5 ml H_2O^{mQ}, at 40-50°C with 2-3 drops of 2 M NaOH, followed by addition of 5 ml 20 mM PIPES (pH 6.0) and 1.5 ml saturated Picric acid solution. Finally the pH of the fixative was set to 6.0. The fixative should be kept in the dark at RT. The medium from the top of coverslips was replaced for 200 µl fixative solution and incubated for 30 min in a dark moist chamber at RT. After fixation the coverslips were washed by immersion in 10 mM PIPES buffer (pH 6.0) and PBS/Glycine, placed back in the moist chamber and covered with 300 µl PBS/Glycine. After 2 x 5 min of washing step with 300 µl PBS/Glycine, the coverslips were incubated for 10 min with 250 µl 70% Ethanol to permeabilize the cell membranes. The cells were washed twice with 300 µl PBS/Glycine (by 5 min) and twice with 300 µl PBG (by 15 min) and incubated over night with 200 µl primary antibody solution (centrifuged at 14000 rpm for 3 min). On the next day, the primary antibody solution was discarded and the cells were washed 6 times with 300 µl PBG (by 5 min) and incubated with 200 µl secondary antibody (conjugated with a fluorescent dye and diluted 1:1000 in PBG) for 1 hour at 37°C. After incubation the cells were washed twice with 300 µl PBG (5 min) and 3 times with 300 µl PBS, pH 7.4 (5 min). Finally, the coverslips are immersed in H_2O^{mQ} and embedded with a drop of mounting media. The preparation was stored at 4°C in dark. In case of simple cell

fixation, the cells were washed 3 times with PBS, immersed in H_2O^{mQ} and embedded, directly after the PBS/Glycine wash step.

1 M Phosphate buffer, pH 6.7:

56.5 ml 1 M NaH_2PO_4

43.5 ml 1 M Na_2HPO_4

PBS/Glycine:

100 mM Glycine in 1 x PBS buffer, pH 7.4

PBG buffer:

0.5 % BSA (Sigma A9647)

0.045 % Fish gelatine (Sigma G7765 (45%))

ad 1000 ml with 1 x PBS, pH 7.4

Alternatively, cells were fixed in methanol for 10 min at -20ºC. Cells were blocked with 2% BSA (w/v) in PBS pH 7.4 for 30 min in dark at RT. The coverslips were incubated over night at 4ºC with the primary antibody, diluted in 1% BSA (w/v) in PBS pH 7.4. The coverslips were washed 3 x 5 min in PBS then incubated with the secondary antibody, diluted in 1% BSA (w/v) in PBS, pH 7.4 for 1 hour at RT. After 3 x 5 min washing with PBS buffer, the coverslips were mounted on a slide glass with a drop of mounting media. The slides were examined by fluorescence microscopy.

Mounting media preparation

10 ml 0.1 M KH_2PO_4 solution was mixed with 0.1 M Na_2HPO_4 solution until the pH equals 7.2. The resulting solution is diluted 1:10 in order to get a 0.01 M phosphate buffer. 20 g Polyvinylalcohol (Gelvatol, Sigma P-8136) was added to the solution and stirred over night. On the next day, 40 ml glycerol (Aldrich, 99.5%) was added and also stirred over night followed by 15 min centrifugation at 12000 rpm. The supernatant is collected and the pH of the supernatant was adjusted to 7, DABCO (1,4-diazabicyclo[2,2,2]octane) was added to a final concentration of 25 µg/ml). The embedding medium was filled in 10 ml syringes and stored at -20°C.

Microscopy

Images were acquired on a Leica DM IRB inverted fluorescence microscope equipped with a DC 350 camera and IM50 Acquisition software (Leica Microsystems, Wetzlar, Germany). Images were quantified and prepared for presentation using ImageJ program (http://rsbweb.nih.gov/ij/).

4.5.6 Preparation of competent *E.coli* cells

In order to transform bacterial cells it is necessary to render the bacteria partially permeable for nucleic acids, thus making them competent. The competence for transformation can be achieved by several methods, including electroporation and chemical transformation ($CaCl_2$-method), which is used to create the holes in the bacterial cell wall. Here the $CaCl_2$-method (Dagert & Ehrlich, 1979) was used. 5 ml of LB medium was inoculated with the appropriate bacterial strain and incubated overnight at 37ºC. 100 ml fresh LB medium was inoculated with 1 ml overnight culture. Cells were incubated at 37ºC by vigorous shaking until OD_{600}=0.4 was reached. Then, the cells were collected by centrifugation in a Falcon tube (4000 rpm, 10 min, 4ºC). The cell pellet was suspended very carefully in 50 ml of 50 mM $CaCl_2$ (sterile and ice-cold), and incubated for 30 min on ice. The cells were collected by centrifugation (4000 rpm, 10 min, 4ºC), and resuspended in 18 ml of 50 mM $CaCl_2$ (sterile and cold) plus 2.7 ml 100% Glycerol. Aliquots of 200 or 400 µl were prepared in pre-cooled Eppendorf tubes, and stored at -80ºC.

LB medium, pH 7.0:

10 g Bacto-tryptone

5 g Yeast extract

5 g NaCl

ad 1000 ml H_2O

4.5.7 Transformation of competent *E.coli* cells

One aliquot (200 µl) of competent *E.coli* was thawed on ice and a ligation mixture (20 µl) or 1 µl of plasmid DNA was added by gentle stirring the cells while pipetting. After 20 min incubation on ice, a heat shock was done for 90 sec at 42ºC and the cells were placed on ice for 10 min. Then 1 ml LB medium was added and the cells were incubated for 30 min at 37ºC. After 5 min centrifugation at 3500 rpm, the cell pellet was resuspended in 100 µl LB medium, plated on LB^{amp}-agar plate and incubated overnight at 37ºC.

LB-agar:	**LB^{amp} plates:**
LB medium	as LB-agar
13 g/l Agar-Agar	50 µg/ml ampicillin

5 Results

The Dnmt2 family of proteins consists of enzymes that display strong sequence similarities to DNA (cytosine-5)-methyltransferases (m^5C MTases) of both prokaryotes and eukaryotes. Human DNMT2 was the first MTase-like protein from higher eukaryotes the structure of which has been solved and some characteristic features were first examined *in vitro* (Dong et al, 2001). The experiments had shown that investigation of both *in vivo* and *in vitro* functions of Dnmt2-like proteins is quite a challenging task, requiring a careful choice of model organism to deal with as well as a reasonable attentiveness in experimental design. Since the slime mold *Dictyostelium discoideum* has the *DNMT2* homolog gene (*dnmA*) as the only member of the DNA methyltransferase family, shows some detectable level of genomic DNA methylation and provides easy and convenient gene manipulation techniques, it is perfectly suited for the investigation of Dnmt2 functions. Thus, let us start this work with the characterization of genomic locus of *dnmA* gene in *Dictyostelium discoideum*.

5.1 The Genomic Locus of the *dnmA* gene

Quite recently the genetic map of *Dictyostelium discoideum* was built based on results of *Dictyostelium* genome sequencing project (Eichinger et al, 2005). The analysis of the coding genomic sequences using the sequences of the human DNA methyltransferases by the BLASTP algorithm had revealed that a single gene encoding a putative DNMT2 homolog is present in the *Dictyostelium* genome (Kuhlmann et al, 2005). The gene was denominated as *dnmA*, and further sequence analysis showed that the DnmA protein has all characteristic DNA methyltransferase motifs (Dong et al, 2001). It is becoming clear that the distribution of genes in metazoan genomes is non-random ((Hurst et al, 2004), (Kosak & Groudine, 2004)). Functionally related genes are often located next to one another in the linear genome, and this proximity can be essential for their coordinated regulation during growth and development (Sproul et al, 2005). In addition, analysis of transcriptome datasets has shown that genes with a similar expression pattern are frequently located in clusters within the genome (de Wit et al, 2008). Analysis of genome-wide expression profiles during *Drosophila melanogaster* development has identified

many clusters of co-expressed neighboring genes, ranging from 10 to 30 genes in size (Spellman & Rubin, 2002). Furthermore, the human genome shows large regions in which most genes are expressed at high levels, alternating with regions that contain predominantly lowly expressed genes ((Caron et al, 2001), (Versteeg et al, 2003)). These observations strongly suggest that juxtaposition of genes in the linear genome can facilitate their coordinated regulation (Razin et al, 2007). Chromatin is a principal orchestrator of transcription. Neighboring genes can be packaged together into a single chromatin domain that may act as a regulatory unit ((Sproul et al, 2005), (Dillon, 2006) and (Talbert & Henikoff, 2006)). Therefore, on basis of the genetic map (Fey et al, 2009) and currently available *Dictyostelium discoideum* gene expression database (http://www.ailab.si/dictyExpress) which was constructed by Shaulsky and coworkers (Rot et al, 2009), we were able to make some suggestions on putative chromatin organization of the *dnmA* genomic locus and its possible connection with expression level of this gene.

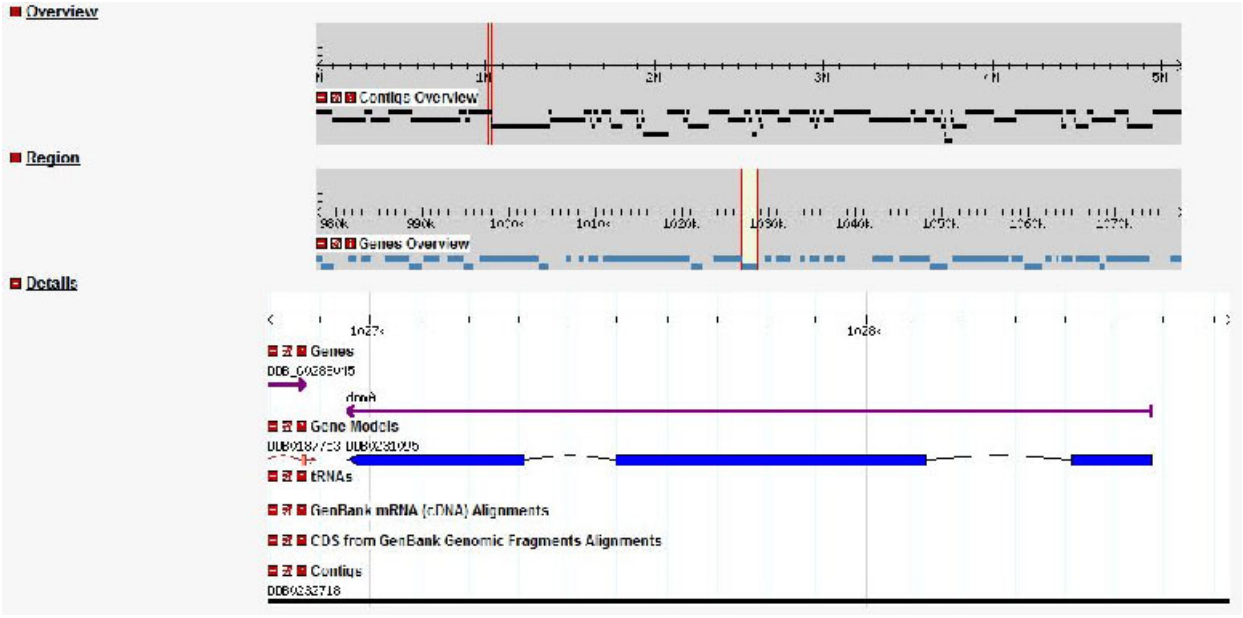

Figure 5.1.1 Scheme of the genomic locus of *dnmA* gene on chromosome 5 of the *Dictyostelium* genome.

Accordingly to the map of the *Dictyostelium* genome, the *dnmA* gene is located on chromosome 5 at the coordinates 1026957 to 1028573, Crick strand, based on Genome Browser (Figure 5.1.1, http://dictybase.org/gene/DDB_G0288047). We analyzed the neighbourhood of *dnmA* gene at this locus at the distances about 20 kbp left and right of *dnmA* and compared the expression

profiles available for this set of genes during development. The results of analysis are presented in the Figure 5.1.2 and Figure 5.1.3.

Figure 5.1.2 Scheme of the genomic region on left side of *dnmA* gene (upper panel). Lower panel represent developmental expression profiles for genes, adjacent to *dnmA*. The expression profiles of genes were high with comparison with *dnmA* profile.

The results appeared to be quite interesting as we can clearly see that adjacent genes indeed had a tendency to cluster into the groups. One of these groups consists of four genes (including *dnmA*), extend about 10 kbp and show similar low expression profiles (less than 10 times difference in expression level). This region is surrounded by sets of genes with relatively high levels of expression (more than 10 times difference in expression level).

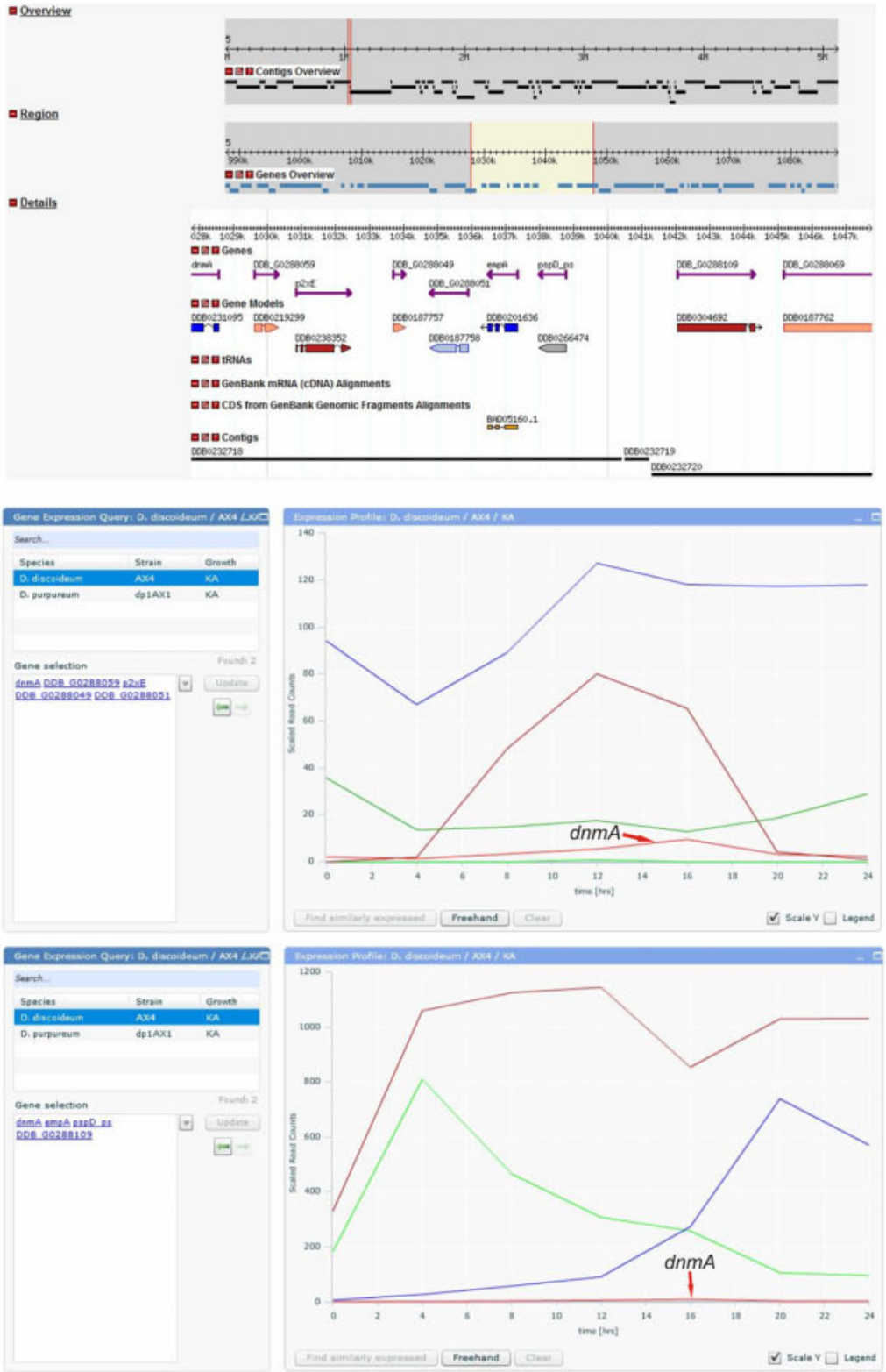

Figure 5.1.3 Scheme of the genomic region on right side of *dnmA* gene (upper panel). Lower panels represent developmental expression profiles for genes, adjacent to *dnmA*. The profiles of three genes closest to *dnmA* show

relatively low and comparable levels of expression. Genes, lying next to these demonstrate relatively high levels of expression.

Unfortunately, most of the tested genes are not annotated in the current version of *Dictyostelium* database and a function of their products is not known. Pfam search (http://pfam.sanger.ac.uk) also did not show any significant matches with the known conserved domains. Nevertheless, it is tempting to suggest that the group of genes, which include *dnmA* and share a low expression profile, may well be representing the functional chromatin domain, probably organized into facultative heterochromatin structures. Further experimental evidences must be gathered to come to a valid conclusion.

5.2 Intracellular localization of GFP-tagged DnmA

To study the nuclear localization of DnmA, the expression vector pDneo2a-*dnmA-GFP* was created and transformed into *Dictyostelium* cells to produce C-terminally GFP-tagged version of the protein (see Figure 3.7.3 in Materials/Plasmids). After fixation of cells using various protocols for immunofluorescence (see Methods), the cells were analyzed by fluorescence microscopy. The images revealed that GFP-tagged DnmA fusions can be found in interphase cells both in the cytoplasmic and nucleoplasmic compartments, although with some bias towards nuclei (Figure 5.2.1A). In some cells it appeared that DnmA-GFP partially co-localized with DAPI-stained DNA but this was not found for all cells and may depend on fixation procedures. Nevertheless, another explanation of this observation could be that DnmA protein is actually functional at certain stages of interphase, perhaps during S-phase of cell cycle. The distribution of proteins within the cytoplasm seems to be rather homogeneous with some slight tendency of accumulation near centrosomes (Figure 5.2.1B).

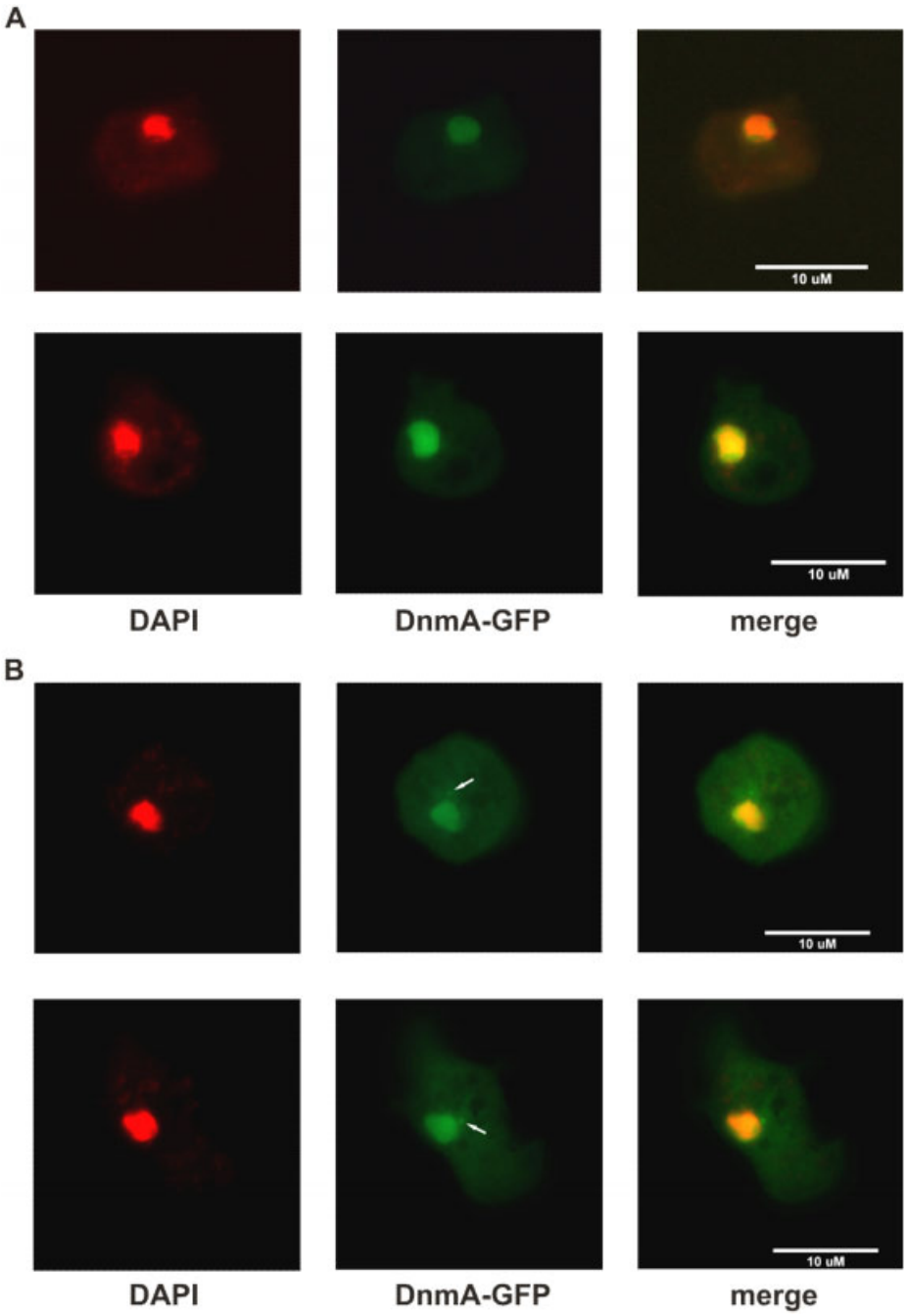

Figure 5.2.1 Localization of the DnmA-GFP fusion protein in fixed *Dictyostelium* DnmA KO cells. (**A**) Partial co-localization DnmA-GFP with DAPI stained DNA. (**B**) Slight enrichment of DnmA-GFP proteins in a regions marked by white arrows, presumably corresponding to centrosomes. White bars represent 10 micrometers.

It should be noted that the nucleoli which are usually more weakly stained by DAPI display a homogeneous distribution of DnmA during interphase in most cases. Nevertheless, some fixed cells in the interphase stage may show difference in protein distribution in the nucleoli and the

rest of the nuclei which could also represent the artifacts of fixation protocol (Figure 5.2.2A and B). This observation could demonstrate yet the redistribution of DnmA-GFP fusion during different stages of interphase. To further prove this assumption, additional experiments should be made with specific markers for G1, S and G2 stages of the cell cycle.

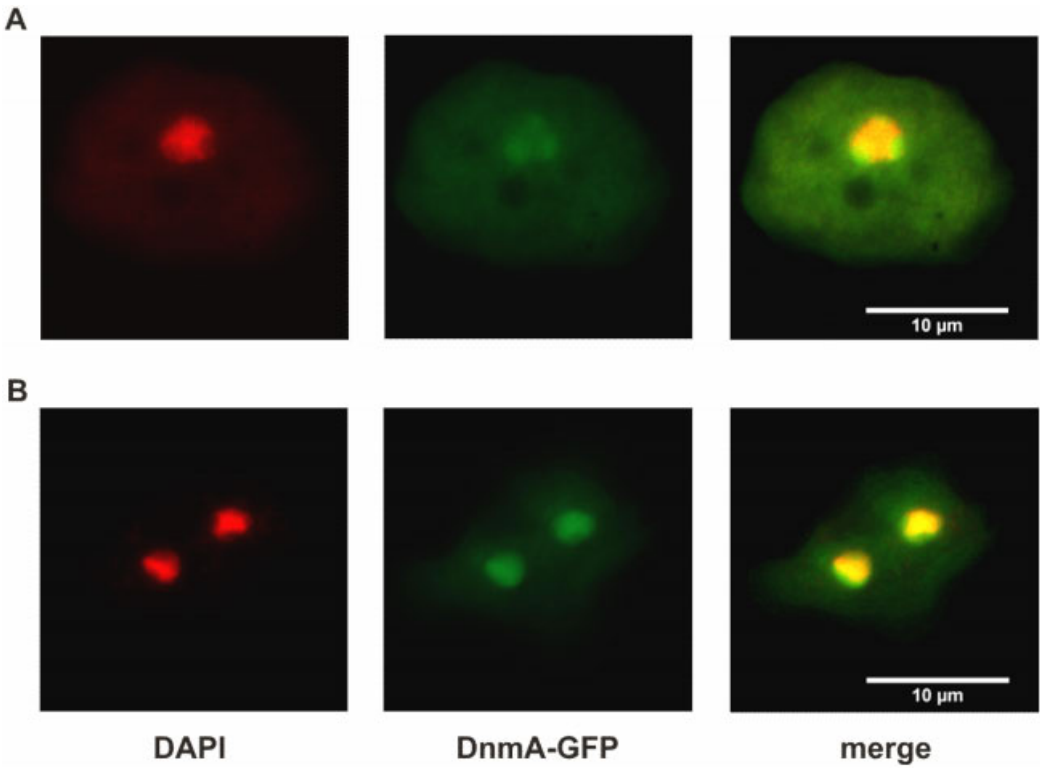

Figure 5.2.2 Localization of the DnmA-GFP fusion protein in nuclei of fixed *Dictyostelium* DnmA KO cells. (**A**) Local increase in green fluorescent signal in the regions of nuclei corresponding to nucleoli. In this case DAPI-staining may reflect the beginning of process of chromosome condensation and removal (active or passive) of DnmA-GFP fusion from nuclei. Such cells also demonstrate absence of the co-localization of DnmA-GFP and DAPI-Stained DNA. (**B**) Local decrease of DnmA-GFP signal in the nucleoli. This case represents the cells where partial co-localization of DnmA-GFP fusion with DAPI-stained DNA can still be observed and which stay likely in earlier phases of interphase, presumably S or early G2. White bars represent 10 micrometers.

The expression of full-sized GFP tagged DnmA could also be confirmed by western blotting with α-GFP antibodies. As expected the observed size of DnmA-GFP fusion is about 77 kDa which corresponds well to theoretical estimation of 72 kDa (Figure 5.2.3).

Additional evidences for the role of DnmA in the interphase of cell cycle rather than in the mitosis were gathered in the further examination of the DnmA-GFP localization during mitosis.

Cells at different mitotic stages in asynchronously grown *Dictyostelium* culture were found using DAPI staining as well as the antibodies directed against α-Tubulin, which stain the centrosomes and the mitotic spindle.

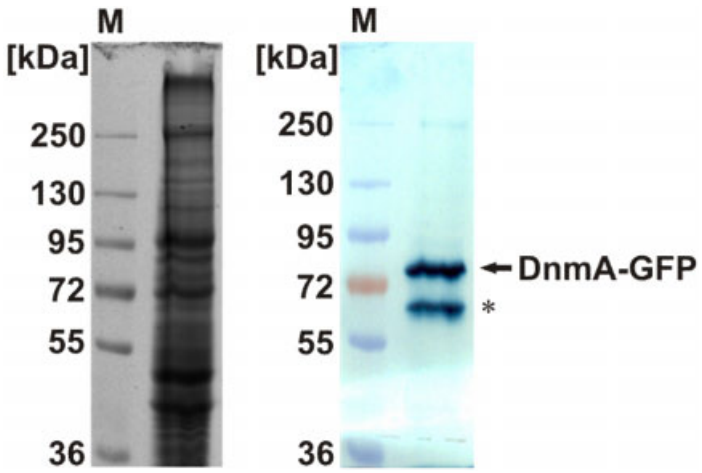

Figure 5.2.3 9% SDS-PAGE (left panel) and Western blot analysis (right panel) of cell extracts from DnmA-GFP expressing Dictyostelium DnmA KO cell line. Prestained protein marker (Fermentas, #SM1811) was used to determine the size of DnmA-GFP fusion protein. The theoretically calculated size for DnmA-GFP was 72 kDa. Additional minor band (*) below DnmA-GFP protein may correspond to a degradation product.

The mitotic cells show mainly homogeneous distribution of DnmA-GFP fusion within cells both in cytoplasmic and nucleoplasmic compartments. There appears to be no characteristic features but the observation that during the mitotic cycle the bulk of DnmA-GFP proteins had a tendency to leak out from nuclei into cytoplasm (Figure 5.2.4). This observation can be clearly seen from prophase till at least anaphase, and it is perhaps the result of partial distortion of the nuclear envelope during these phases of mitosis.

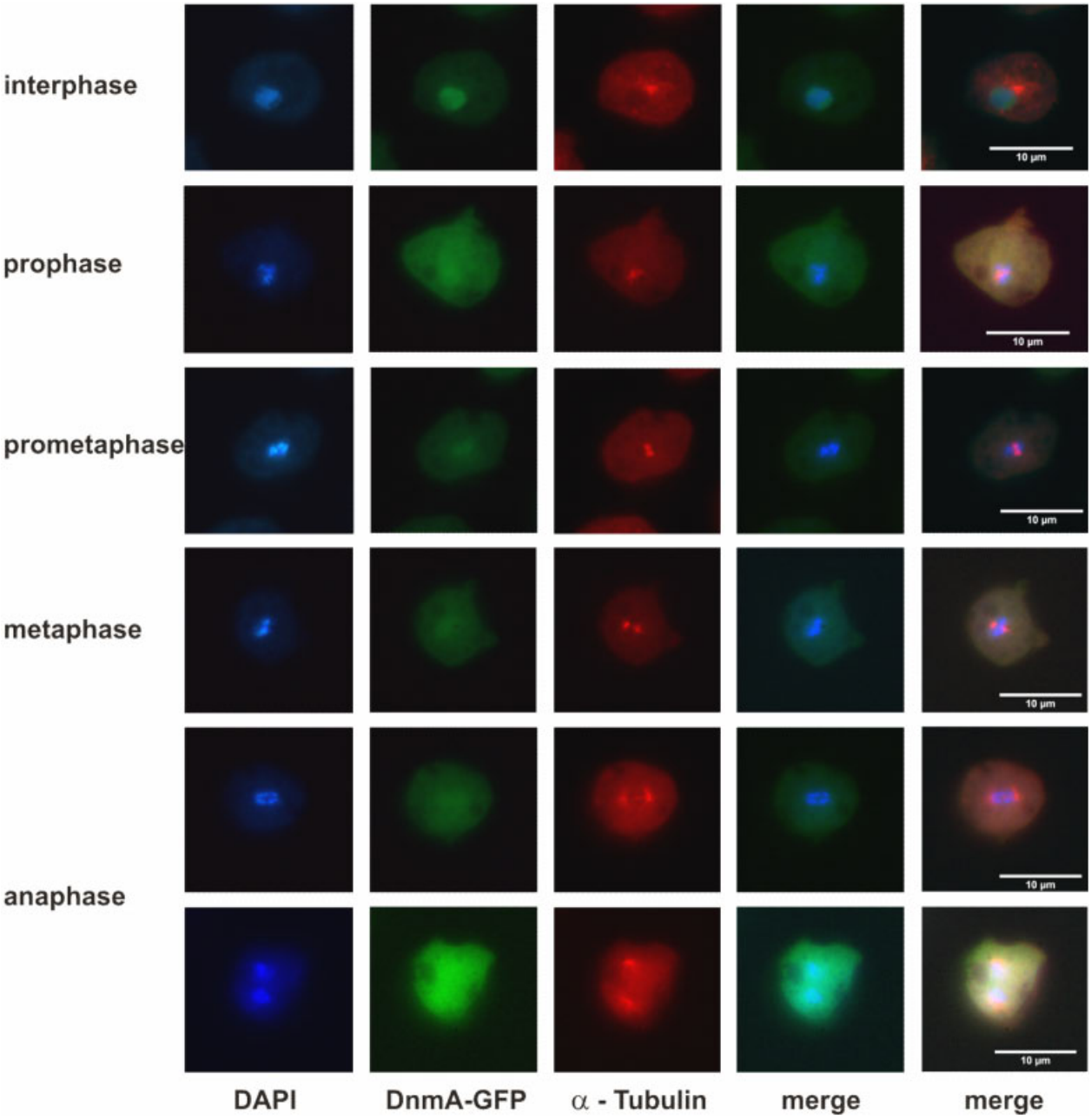

Figure 5.2.4 Localization of DnmA-GFP fusion proteins during mitotic cycle in fixed cells. Cells at different stages of mitosis were identified by DAPI staining and immunostaining with α-Tubulin antibodies. Most of mitotic phases were detected. White bars represent 10 micrometers.

We did not find clear telophase cells or cells undergo cytokinesis on our preparations, though we often observed cells with two nuclei. These represent the result of a failure in cytokinesis that is frequently found in axenically growing cell cultures. From the overall data we assume that

DnmA-GFP start accumulating in nuclei during telophase or shortly after this phase, most probably after reconstruction of intact nuclear envelopes (Figure 5.2.5).

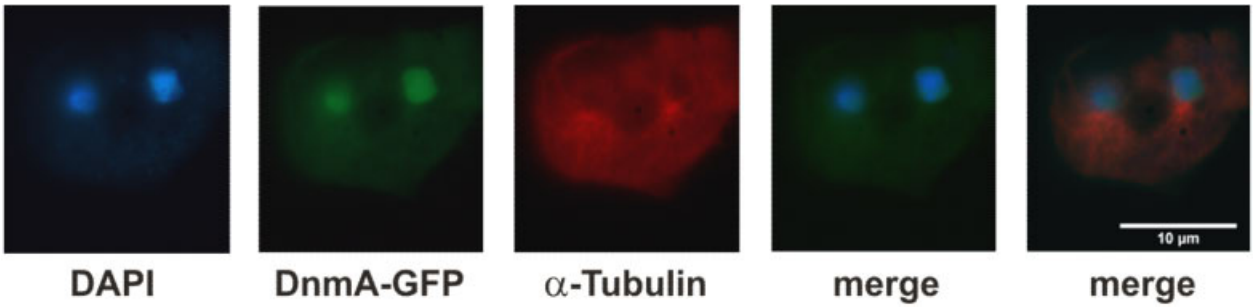

Figure 5.2.5 Localization of DnmA-GFP in the *Dictyostelium* cells carrying two nuclei due to cytokinesis error. DnmA-GFP fusion proteins accumulate within nuclei during or shortly after telophase. White bar represent 10 micrometers.

On the other hand, the dynamics of DnmA-GFP distribution during mitosis could indirectly support the suggestion that DnmA may be functional in the nuclei of interphase cells and has no specific function during mitosis. Diffusion of DnmA into the cytosol during mitotic phases may also provide means to allow for cytoplasmic functions of the protein, although additional experiments should be performed to support this hypothesis.

DNA methyltransferases, including Dnmt2-like proteins, are reported to be present in the nuclear matrix of almost all higher eukaryotes. Recently, it was shown that the Dnmt2 homolog Ehmeth in *Entamoeba histolyitica* is a nuclear matrix protein that binds EhMRS2, a DNA that includes a scaffold/matrix attachment region (Banerjee et al, 2005). Similar data was provided for Dnmt2-like m^5C methyltransferase in *Drosophila melanogaster*, where this protein was found to be associated with the nuclear matrix, mainly during mitosis (Schaefer et al, 2008). To test the possibility that DnmA protein in *Dictyostelium* is also involved in nuclear matrix structures, we performed subcellular fractionation to show the distribution of DnmA-GFP and DnmA-TAP fusion proteins within subcellular compartments. Figure 5.2.6 shows the principal of the experiment, resulting SDS-PAGE gels and western blots with antibodies against GFP and TAP to visualize DnmA-GFP and DnmA-TAP proteins in different subfractions. Indeed, significant amounts of DnmA proteins were found in the nuclear matrix and core filament fractions. This

bound DnmA was not removed by extensive washing steps and, therefore, represents a protein strongly embedded into corresponding structures.

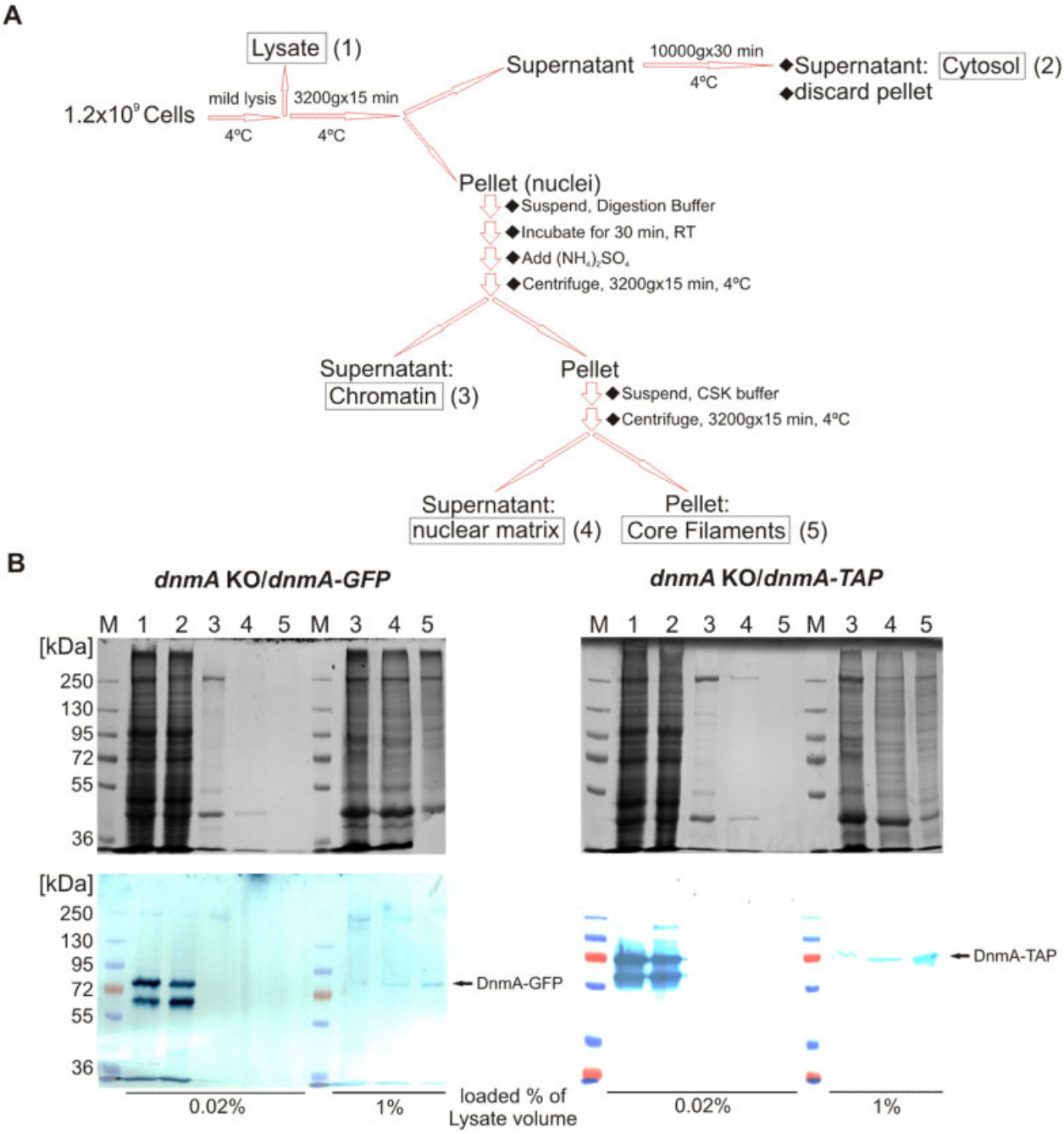

Figure 5.2.6 (**A**) Outline of the procedures employed for preparation of cellular and nuclear subfractions. The various cellular and nuclear subfractions isolated are shown in the boxes in the diagram. The details of the method are given in the Methods. Nuclear matrix represents a 2.0 M NaCl extract of NM plus intermediate filaments (NM-IF). Subfractions designated as 1, 2, 3, 4 and 5. (**B**) 8-9% SDS-PAGE gels of prepared fractions and corresponding

western blot analyses with antibodies against GFP and TAP. Loaded % of Lysate volume represent volume of loaded sample adjusted to total volume of cell lysate. Prestained protein marker (Fermentas, #SM1811) was used as the size reference.

5.3 Identification of putative interaction partners for DnmA *in vivo*

Affinity tags are highly efficient tools for purifying proteins and protein complexes from crude extracts. They can provide hundred- or even thousand-fold purification without prior steps to remove nucleic acid or other cellular material. In addition, the mild elution conditions employed make affinity tags useful for purifying individual proteins and especially protein complexes in their native state (Lichty et al, 2005). Importantly, affinity tags allow diverse proteins to be purified using generalized protocols in contrast to highly customized procedures associated with conventional chromatography, a compelling consideration for proteomics or structural genomics ventures. There are multiple choices of various affinity tags for protein purification that can make it difficult to decide on the most appropriate tag for a particular project. To identify potential protein partners of DnmA we have chosen two of the available tags, TAP and StrepII, based on several studies comparing affinity tags for protein purification (Arnau et al, 2006); (Lichty et al, 2005); (Schmidt & Skerra, 2007). These two affinity purification systems provide a reliable, relatively cheap and efficient ways to purify tagged proteins from a variety of eukaryotic cell extracts, including yeasts, *Drosophila* and mammalian cells.

5.3.1 Tandem affinity purification

Identification of components present in biological complexes requires their purification to near homogeneity. The tandem affinity purification (TAP) method as a tool was originally established in yeast to isolate highly purified native protein complexes in a very gentle and efficient way (Puig et al, 2001), but later was successfully adapted to various organisms, including mammalian cells and *Dictyostelium* (Koch et al, 2006). The details of purification protocol are represented in Methods.

For expression of N- and C-terminus TAP-tagged DnmA proteins in *Dictyostelium,* two expression vectors were created, pDneo2a-*dnmA-CTAP* and pDneo2a-*NTAP-dnmA* (see Figure 3.7.2 in Materials/Plasmids). These plasmids were used to transform *Dictyostelium dnmA* KO

strain and several positive clones that produced full-sized TAP-tagged DnmA were chosen for following experiments (Figure 5.3.1.1A, B).

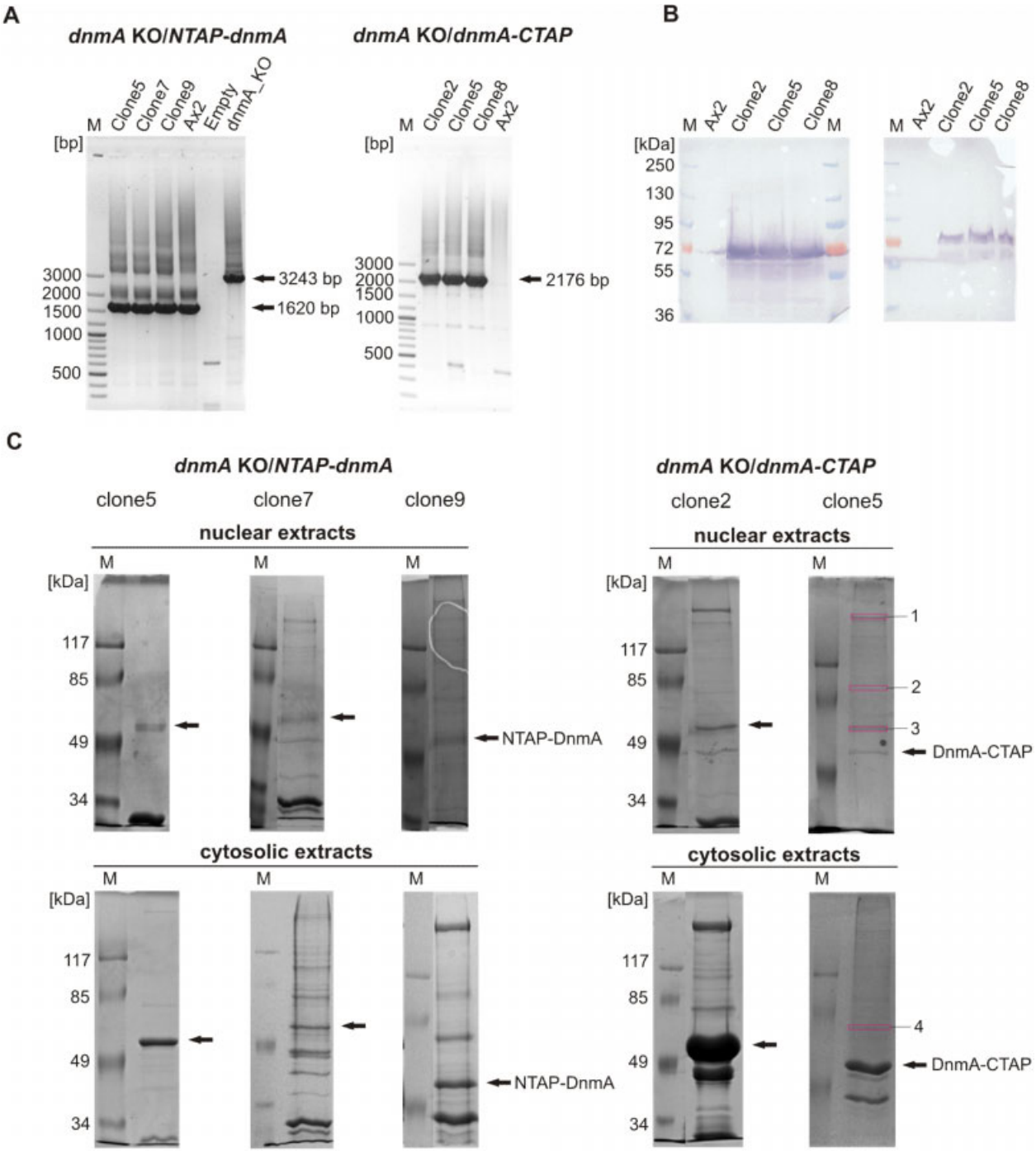

Figure 5.3.1.1 (**A**) 1% Agarose gel representing the results of genomic screening for *dnmA* KO *Dictyostelium* cells transformed with pDneo2a *NTAP-dnmA* and pDneo2a *dnmA-CTAP* vectors. The primers dnmA_BamHI_for and dnmA_BamHI_Rev were used to amplify DNA of *NTAP-dnmA* transgene in case of *Dictyostelium* clones,

transformed with pDneo2a-*NTAP-dnmA*. The expected PCR product for Ax2 strain and positive clones should correspond to full-sized genomic sequence of *dnmA*, namely 1620 bp. For *dnmA* KO strain, the expected size of PCR product is 3243 bp, since gene sequence were interrupted by bsR cassette of 1343 bp in length. In case of pDneo2a *dnmA-CTAP* vector, the primers dnmA_PstI_For and CTAP_MfeI_Rev were used to screen for positive clones. These pair of primers should amplify DNA of *dnmA-CTAP* transgene and give the PCR product of 2176 bp. In Ax2 wild-type strain no fragment is expected. GeneRuler™ 100 bp DNA ladder (Fermentas, #SM0324) was used as a size marker. (**B**) Western blotting with anti-TAP antibodies. Cytosolic and nuclear extracts, obtained from different dnmA KO/*dnmA-CTAP* clones, were tested for presence of TAP tagged protein of expected size about 65 kDa. Prestained protein marker (Fermentas, #SM1811) was used as the size reference. (**C**) 8-9% SDS-PAGE represents the results of tandem affinity purification of TAP tagged DnmA from different clones. Red squares demonstrate protein bands which were analyzed by mass spectrometry for putative interaction partners. Corresponding protein bands, were excised from PA gels, crashed and subjected to tryptic digestion followed by LC-MS/MS analysis (see Table 5.3.1.1). Prestained protein marker (Fermentas, #SM0441) was used as a size reference.

Dictyostelium dnmA KO mutant strain were used for transformation, based on general consideration that knock-out background would potentially favor of isolation of interacting proteins due to absence of competition binding with endogenous DnmA. Multiple experiments were done to isolate both N- and C-terminal TAP-tagged DnmA and associated partners by two specific affinity purification/elution steps. Figure 5.3.1.1C demonstrates SDS-PAGE gels of protein samples from several TAP purifications using different *Dictyostelium dnmA* KO clones, which express N- and C-terminus tagged DnmA. Though the overall quality of purifications was not good enough in terms of enrichment for co-purified proteins, a few protein bands finally were subjected to LC-MS/MS analysis (in collaboration with Bertinetti, Department of Biochemistry).

Table 5.3.1.1 represents the results of MS/MS analysis as a set of identified proteins, which could potentially be interaction partners for DnmA. Considering the score value as well as amounts of detected peptides for each protein, we assumed that only main components of protein bands could actually represent putative partners. Among these, we found that Cep192-like protein from band 1 deserved special attention. Indeed, it is a centrosomal protein and as we showed earlier, DnmA-GFP fusion can accumulate in the centrosomal region of *Dictyostelium* cells. We started to work with this candidate by generation of knock-out mutants for *cep192l* gene (cep192-like gene) to perform functional study, but we could not obtain any surviving clones. Taking into account the fact that human Cep192 protein is required for mitotic

centrosome and spindle assembly (Gomez-Ferreria et al, 2007), we assumed that the knock-out of the gene is lethal and cannot be achieved in haploid *Dictyostelium* cells (data not shown).

Table 5.3.1.1 The results of mass data analysis. MS analysis was performed on the hybrid quadruple linear ion trap instrument (Q TRAP 4000™ LC/MS/MS system). Data were analyzed using MASCOT® software (Matrix Science). Gene products with gene IDs marked in bold represent the main components of tested bands and putative partners for DnmA.

Band №	Gene database entries	Gene description	Total score
Band 1	**DDB_G0285313**	Similar to Centrosomal protein of 192 kDa (**Cep192**) and Spindle-defective protein 2 (**Spd-2**)	**1444**
	DDB_G0288259	***papA***, poly(A) polymerase	57
	DDB_G0278469	SMAD/FHA and bromodomain-containing protein	55
	DDB0220009	***irlB***, IRE family protein kinase	51
	DDB_G0269696	***pakD***, p21-activated protein kinase	50
	DDB_G0268778	***rbbB***, similar to H. sapiens Retinoblastoma binding proteins RBBP2	50
	DDB_G0270418	***top2***, DNA topoisomerase II	47
	DDB_G0288993	***smc6***, structural maintenance of chromosome protein	45
	DDB_G0270042	***ascc3l***, DEAD/DEAH box helicase U5 small nuclear ribonucleoprotein 200 kDa helicase	43
	DDB_G0288361	***kif13***, kinesin family member 13	43
Band 2	**DDB_G0279129**	***pan3***, ortholog of PAN3, a member of the Pan2p-Pan3p poly(A)-ribonuclease complex	**186**
	DDB_G0293252	putative RNA binding protein, contains 2 RRM1 domains, a SWAP/Surp and a C-terminal ENTH/VHS domain	61
	DDB_G0284103	***mybZ***, myb domain-containing protein	58
Band 3	**DDB_G0276109**	MPPN domain-containing protein, contains one MPPN (mitotic phosphoprotein N' end) domain	**555**
	DDB_G0283661	***ddx3***, conserved RNA helicase; very similar to mammalian DDX3X and DDX3Y, and yeast DBP1	45
Band 4	**DDB_G0273249**	***hspE***, heat shock protein, similar to *hsp 70*	**697**
	DDB_G0269144	***hspB***, heat shock protein, similar to *hsp 70*	**377**

Anyhow, despite all efforts on optimization of TAP procedure, we were unable to significantly improve the outcome of the proteins co-purified with DnmA in amounts that would be more

distinctive to represent potential partners. We proposed four main reasons for low effectiveness of the TAP method for purification of DnmA-associated proteins. First, for optimal results, it is preferable to maintain expression of the fusion protein at, or close to, its natural level. The overexpression of the DnmA could lead to competition between free proteins and proteins associated with interaction partners during purification procedure. Hence, the purified samples may well be overloaded with free unbound DnmA species. Second, the overexpression of protein can also induce its association with non-natural partners (heat shock proteins, components of proteasome) (Swaffield et al, 1995). Indeed, the presence of HspE and HspB as a major components of band number 4 (Figure 5.3.1.1C, and Table 5.3.1.1) may argue in favor of this assumption. Another problem consists of the difficulties in extraction of TAP tagged DnmA from the nuclear matrix and core filament structures as we have shown earlier for DnmA-GFP and DnmA-TAP fusions (see Figure 5.2.6). Finally, the TAP tag could interfere with binding of putative partners, perhaps due to steric hindrances.

To test whether the problem with a relatively large size of TAP tag is the issue in our case, we decided to develop another purification strategy, namely StrepII-tag affinity purification.

5.3.2 StrepII-tag affinity purification

The *Strep*-tag II, which is short, biologically inert, proteolytically stable and does not interfere with membrane translocation or protein folding, offers a versatile tool both for the rapid isolation of a functional gene product and molecular interaction analysis, including mass spectrometry (Vasilescu & Figeys, 2006).

To obtain a soluble full length Strep II tagged DnmA, another expression vector pDneo2a-*dnmA-StrepII* was constructed to use in *Dictyostelium* cells (see Figure 3.7.4 in Materials/Plasmids). After transformation of *dnmA* knock-out *Dictyostelium* strain with pDneo2a-*dnmA-StrepII* vector, several clones were obtained which were checked for presence of *dnmA-StrepII* sequence in genomic DNA by PCR screening (Figure 5.3.2.1). Two of these clones were used for following Strep II affinity purifications (see Methods for detailed protocol). Briefly, the fusion protein with putative interaction partners was purified with Strep-Tactin® Superflow™ agarose (Novagen) under native conditions.

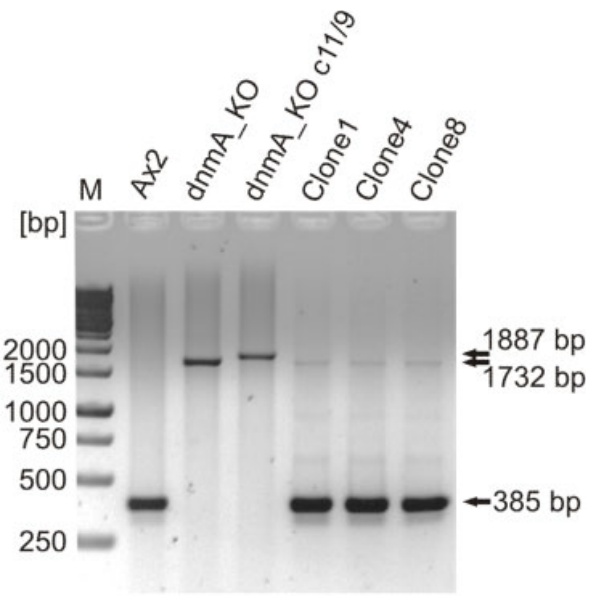

Figure 5.3.2.1 1% Agarose gel is representing the results of genomic screening for *dnmA* KO *Dictyostelium* cells transformed with pDneo2a *dnmA-StrepII* vector. The primers DnmA_forII and DnmA_chk_rev were used to amplify DNA region in *dnmA*, resulting in PCR product of 385 bp long for *Dictyostelium* wild type Ax2 strain. Two *dnmA* KO strains, containing two different bsR cassettes, should give PCR products of 1732 bp and 1887 bp, respectively. Finally, clones 1, 4 and 8 of *dnmA* KO strain, transformed with pDneo2a-*dnmA-StrepII* vector, represent PCR products of both 385 bp and 1732 bp, which is consistent with the presence of *dnmA-StrepII* transgene and *dnmA* KO. GeneRuler™ 1 kb DNA ladder (Fermentas, #SM0311) were used as a size marker.

Figure 5.3.2.2 demonstrates purified protein samples (elutions 1 to 5) from two independent purifications, fractionated by 9 % SDS-PAGE. The quality and purity of obtained samples was apparently very high in terms of both enrichment for DnmA-StrepII fusion and co-purified proteins. The marked bands were excised from the gels, subjected to tryptic digestion followed by LC-MS/MS analysis (in collaboration with Bertinetti, Department of Biochemistry).

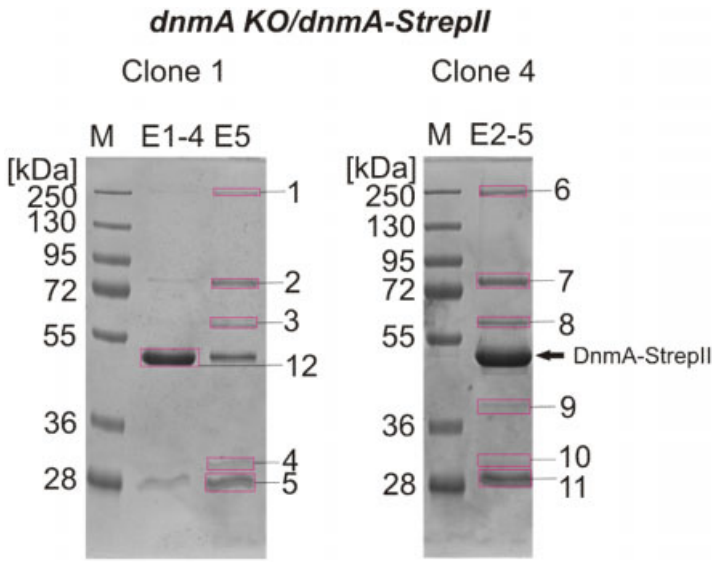

Figure 5.3.2.2 9% SDS-PAGE represent the results of affinity purification of StrepII-tagged DnmA from whole cell lysates of two different clones of *dnmA* KO/*dnmA-StrepII Dictyostelium* mutant. Red squares demonstrate protein

bands which were analyzed by mass spectrometry for putative interaction partners. Corresponding slices were excised from PA gels, crashed and subjected to tryptic digestion followed by LC-MS/MS analysis (see Table 5.3.2.1). Prestained protein marker (Fermentas, #SM1811) was used as a size reference.

Table 5.3.2.1 summarizes the results of MS analysis, obtained using MASCOT® software (Matrix Science). Most of the identified proteins belong to different types of biotin-dependent carboxylases, a group of enzymes that utilize a covalently bound prosthetic group, biotin, as a cofactor (Jitrapakdee & Wallace, 2003). These enzymes have been found in diverse biosynthetic pathways in a variety of prokaryotes and eukaryotes and function during fatty acid synthesis, gluconeogenesis and amino acid catabolism (Lydan & O'Day, 1991). The reactions catalyzed by most members of this group of enzymes share two common features: (1) carboxylation of biotin, via the formation of a carboxyphosphate intermediate, followed by (2) transcarboxylation of CO_2 from biotin to specific acceptor molecules to yield different products.

Table 5.3.2.1 The results of mass data analysis. MS analysis was performed on the hybrid quadruple linear ion trap instrument (Q TRAP 4000™ LC/MS/MS system). Data were analyzed by MASCOT® software (Matrix Science).

Band №	Gene database entries	Gene description	Total score
Band 1	DDB_G0288387	***accA***, acetyl-CoA carboxylase, biotin carboxylase	206
Band 2	DDB_G0275355	***pccA***, propionyl-CoA carboxylase, propanoyl-CoA:carbon dioxide ligase alpha subunit	1072
	DDB_G0287377	***mccA***, methylcrotonyl-CoA carboxylase, 3-methylcrotonyl-CoA:carbon dioxide ligase alpha subunit	974
Band 3	DDB_G0276341	***pccB***, propionyl-CoA carboxylase, propanoyl-CoA:carbon dioxide ligase beta subunit	798
	DDB_G0271960	***mccB***, methylcrotonyl-CoA carboxylase, 3-methylcrotonyl-CoA:carbon dioxide ligase beta subunit	340
Band 4	DDB_G0273065	***dscC-1***, discoidin I, gamma chain	297
	DDB_G0273063	***dscA-1***, discoidin I, alpha chain	237
Band 5	DDB_G0270214	***DD7-1***, galactose-binding domain-containing protein, similar to discoidin I, involved in O-glycosylation	750
	DDB_G0292552	***dscE***, discoidin II	631
Band 6	DDB_G0288387	***accA***, acetyl-CoA carboxylase, biotin carboxylase	1813
Band 7	DDB_G0275355	***pccA***, propionyl-CoA carboxylase, propanoyl-CoA:carbon	1183

		dioxide ligase alpha subunit	
	DDB_G0287377	***mccA***, methylcrotonyl-CoA carboxylase, 3-methylcrotonyl-CoA:carbon dioxide ligase alpha subunit	785
Band 8	DDB_G0276341	***pccB***, propionyl-CoA carboxylase, propanoyl-CoA:carbon dioxide ligase beta subunit	882
	DDB_G0271960	***mccB***, methylcrotonyl-CoA carboxylase, 3-methylcrotonyl-CoA:carbon dioxide ligase beta subunit	388
Band 9	DDB_G0288047	***dnmA***, DNA m^5C-methyltransferase, dnmt2 subfamily	449
Band 10	DDB_G0273067	***dscD-1***, discoidin I, D chain	330
	DDB_G0273065	***dscC-1***, discoidin I, gamma chain	328
	DDB_G0273063	***dscA-1***, discoidin I, alpha chain	322
	DDB_G0270214	***DD7-1***, galactose-binding domain-containing protein, similar to discoidin I, involved in O-glycosylation	314
Band 11	DDB_G0270214	***DD7-1***, galactose-binding domain-containing protein, similar to discoidin I, involved in O-glycosylation	1010
	DDB_G0292552	***dscE***, discoidin II	633
Band 12	DDB_G0288047	***dnmA***, DNA m^5C-methyltransferase, dnmt2 subfamily	1219

We conclude that the covalently bound biotin and its intermediates cause non-specific co-purification of these proteins with the DnmA-StrepII fusion. As to different discoidin proteins, these are usual non-specific contaminants, binding to sugars in the affinity matrix during affinity purifications in *Dictyostelium*. Indeed, mock Strep II purification from the cell extract of wild-type Ax2 *Dictyostelium* strain has shown the same pattern of co-purified proteins upon fractionation by SDS-PAGE, except for absence of protein band corresponding to DnmA-StrepII fusion (Figure 5.3.2.3).

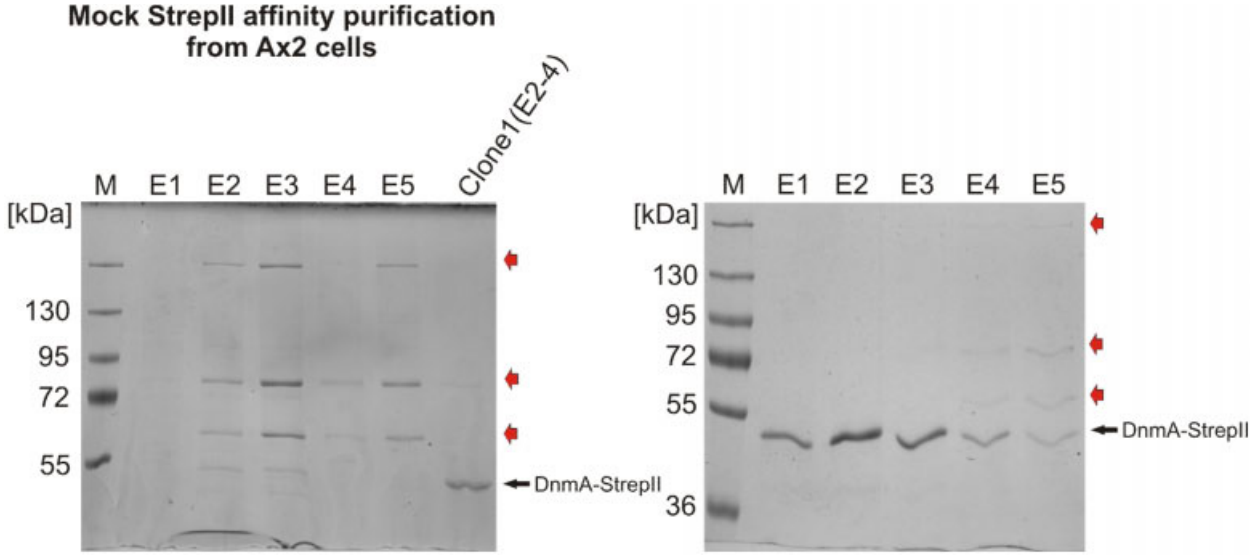

Figure 5.3.2.3 Left panel represents 9% SDS-PAGE of mock Strep II-tag affinity purification from whole cell lysate of *Dictyostelium* wild-type Ax2 strain (Elution steps 1-5). Last lane shows fractionation of DnmA-StrepII purification sample from clone1 of *dnmA* KO/*dnmA-StrepII* mutant as a control (combined elutions 2-4). Right panel represents 9% SDS-PAGE of affinity purification from clone 1 (Elution 1-5). Red arrows mark protein bands, equal for both mock and DnmA-StrepII purifications. Prestained protein marker (Fermentas, #SM1811) was used as a size reference.

Therefore, we have shown that except for these several expected proteins, co-purified with DnmA-StrepII due to presence of biotin intermediates, no potential interaction partners could be detected in our Strep II affinity purification experiments.

5.4 Expression and purification of recombinant His-DnmA from *E.coli*

For *in vitro* analysis of DnmA functions, recombinant protein was expressed in *E.coli* BL21 (DE3) pLys cells, using pET15b-*dnmA*_wt as an expression vector. This expression vector allowed us to produce preparative amounts of recombinant 6xHis-tagged DnmA protein using simple and powerful procedure of affinity chromatography (Kaller 2002).

E.coli cells were collected after different time of incubation at various IPTG concentrations and temperatures and samples were subsequently loaded on SDS-PAGE to determine optimal

conditions (Fig 5.4.1). Usually, *E.coli* cells were induced with 0.5 mM IPTG for 2 hrs at RT in 1L of shaking culture. Cells were harvested, lysed and His-DnmA was purified from a lysate.

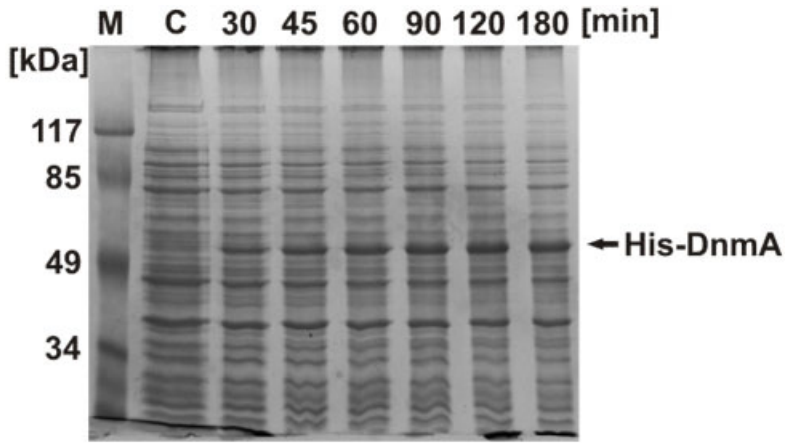

Figure 5.4.1 9% SDS-PAGE protein gel stained with Coomassie Blue showing overexpression of His-DnmA in *E.coli* BL21 (DE3) pLys strain as a function of induction by IPTG at different times. Cells were grown up to OD_{600} = 0.6 at 37 ºC, induced with 0.5 mM IPTG and incubated for 3 hrs at 22ºC. Aliquot of 50 µl was taken from cell culture prior induction followed by aliquots at each time points adjusted to increasing $OD_{600.}$ Corresponding volumes of 2xLaemmli buffer were added in each aliquots adjusted till 100 µl with TE buffer, pH 8.0, and all samples were boiled at 95ºC before 20 µl of each one was loaded into gel. Black arrow indicates accumulation of recombinant His-DnmA proteins during increasing incubation times. Prestained protein marker (Fermentas, #SM0441) was used to determine the size of His-DnmA. The obvious size is about 52 kDa which is in good agreement with theoretically calculated of 46.3 kDa.

As we expected, the overexpression resulted in a protein, which form the band of approximate molecular mass of 52 kDa, and this value is in a good agreement with the theoretically calculated mass of 46.3 kDa. The fusion protein was purified with Ni-charged resin (Bio-Rad) under native conditions and the purification process was monitored by loading samples from each step followed by SDS-PAGE and subsequent colloidal Coomassie Blue staining (Fig 5.4.2). Concentration of protein in most enrich fractions were measured and preparations were used directly for some of the following experiments. For the majority of *in vitro* experiments the elution fractions from separate purifications were pooled together and samples were then dialyzed against storage buffer containing 50% Glycerol (see Methods). The concentrations of resulting protein preparations were measured by Bradford assay and used for *in vitro* studies.

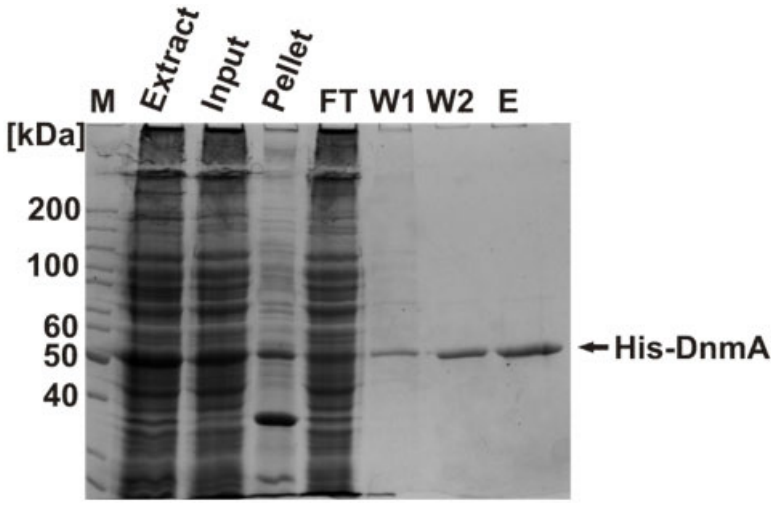

Figure 5.4.2 9% SDS-PAGE protein gel stained with Coomassie Blue to monitor purification of His-DnmA by Ni-NTA affinity chromatography from *E.coli* BL21 (DE3) pLys strain. Wash 1 (W1) and 2 (W2) were done in the presence of 10 and 15 mM Imidazole, accordingly. Aliquots of 50 µl from 10 ml of crude cell extract (Extract), pre-cleared extract (Input), Pellet, flow-through (FT) and wash step 1 (W1) were taken, mixed with 100 µl of TE buffer, pH 8.0, and 50 µl of 2xLaemmli buffer. Aliquot of 25 µl from 5ml of washing step 2 (W2) was taken, mixed with 125 µl of TE buffer, pH 8.0, and 50 µl of 2xLaemmli buffer. Elution (E) was performed routinely with 1 ml of elution buffer containing 250 mM Imidazole. Aliquot of 5 µl was taken and mixed with 10 µl of TE buffer, pH 8.0, and 5 µl of 2xLaemmli buffer. All samples were boiled at 95ºC before loading 20 µl of each into gel. Black arrow indicates position of recombinant His-DnmA protein. Unstained protein marker (Fermentas, #SM0661) was used to determine the size of His-DnmA.

To obtain highly purified His-DnmA preparations, gel filtration was applied as an addition step. The main application of gel filtration chromatography in molecular biology is the fractionation of globular proteins and other water-soluble polymers. This simple method allows separating molecules in solution based mainly on their size (more correctly, their hydrodynamic volume). To perform the method, several elution fractions were combined and concentrated, using Amicon® Ultra-4 Centrifugal Filter Devices (Millipore). Resulting samples were then loaded on HiLoad™ 16/60 Superdex™ 200 column (Amersham Biosciences). Appropriate fractions, containing His-DnmA protein, were collected, pooled and dialyzed against storage buffer with 50% Glycerol (Figure 5.4.2).

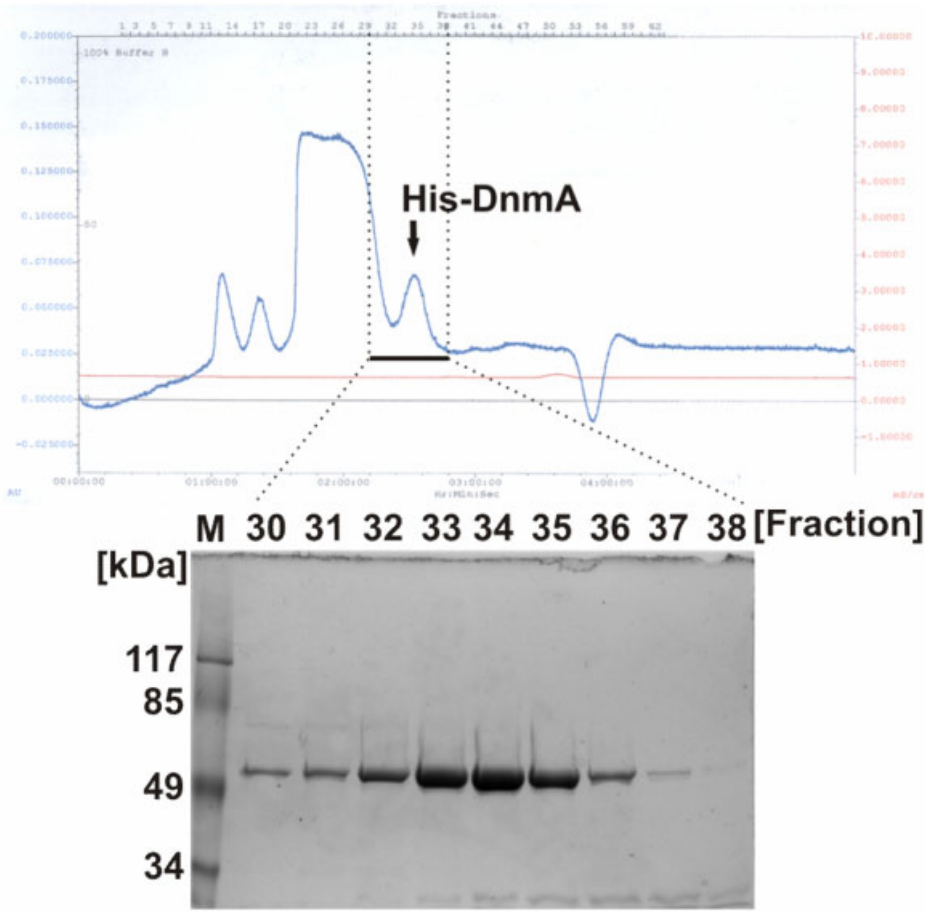

Figure 5.4.2 Gel filtration chromatography of recombinant His-DnmA protein. Upper panel show typical elution profile of His-DnmA protein preparations and lower panel represent 9% SDS-PAGE of fractions enriched in recombinant protein. Routinely, 10-15 ml of joined elution fractions from affinity purification step (from 1.5L of bacterial culture expressing His-DnmA) were concentrated by Amicon® Ultra-4 Centrifugal Filter Device (Millipore, 3K or 10K) and loaded on HiLoad™ 16/60 Superdex™ 200 (Amersham Biosciences, prep grade) column. Gel filtration was run at 0.5 ml/min flow rate using BIO-RAD Workstation. Peaks were analyzed by SDS-PAGE and fractions containing recombinant His-DnmA protein were pooled and dialyzed against storage buffer. Concentration of final protein preparations was measured by Bradford assay. Prestained protein marker (Fermentas, #SM0441) was used to determine the size of His-DnmA.

This purification step provided ultrapure His-DnmA preparations which were used for some binding assays as well as for Far-UV circular dichroism spectropolarimetry.

5.5 Expression and purification of StrepII-tagged DnmA from *Dictyostelium*

Recombinant 6xHis-tagged proteins have the advantage that they can be produced in relatively large amounts using simple well established procedure. On the other hand, expression of eukaryotic proteins in bacterial cells has some important disadvantages. The most critical is that such an expression can lead to production of mis-folded proteins as well as proteins lacking specific post-translational modifications. Those disadvantages may significantly reduce the yield of active recombinant protein in preparation or influence on its specific activity. Therefore we have chosen to use Strep-tag II affinity purification system described earlier for expression and purification of recombinant DnmA-StrepII from *Dictyostelium* cells.

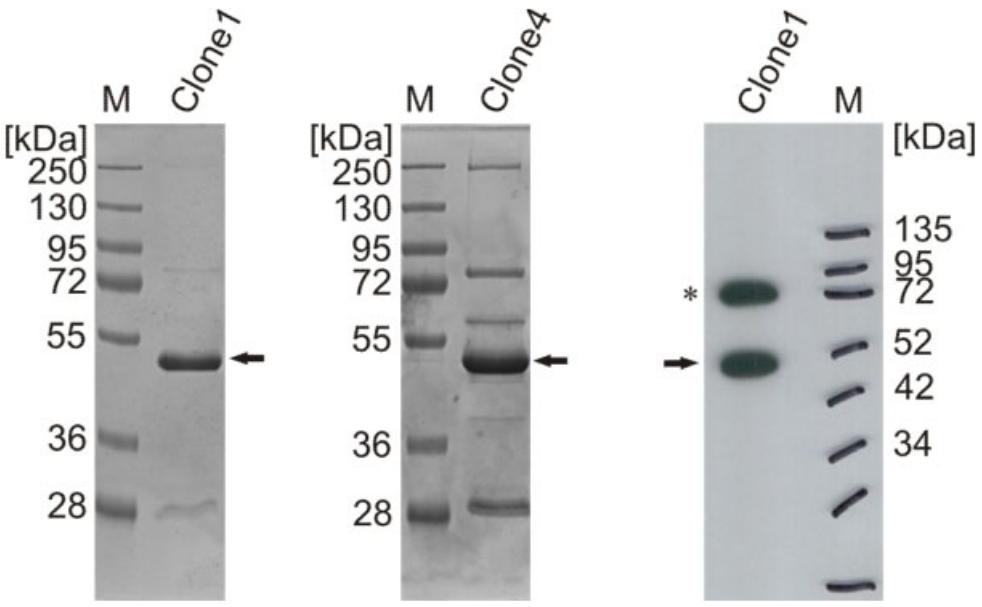

Figure 5.5.1 First two panels represent the 9% SDS-PAGEs of DnmA-StrepII protein purifications from cell extracts prepared from clones 1 and 4 of the *dnmA* KO/*dnmA-strepII Dictyostelium* strain. The third panel is a western blotting of DnmA-StrepII protein purified from clone1 of *dnmA* KO/*dnmA-strepII* strain with Strep-Tactin, conjugated with horse *radish* peroxidase (HRP) (kindly provided by Department of Biochemistry). Prestained protein markers (Fermentas, #SM1811 and #SM1841) was used to determine the size of the protein. Black arrows point out the bands, corresponding to DnmA-StrepII. Chemiluminescence at the position marked by the star (*) indicate the presence of an unknown, perhaps biotin-containing, protein.

The Strep II tag allows affinity chromatography on immobilized Strep-Tactin® (Novagen) under physiological conditions, enabling native, active StrepII-tagged proteins to be purified in a single step (see also chapter 5.3.2). Because it contains just 8 amino acids (WSHPQFEK) the Strep II tag could have a minimal effect on protein structure and function. The expression and purification of DnmA-StrepII protein from *Dictyostelium* cells usually leads to lower yields compared to production of His-DnmA in *E.coli*. However, there are great advantages since the protein is produced in its natural subcellular environment and, therefore, most likely correctly folded and modified. Figure 5.5.1 shows SDS-PAGE gels, representing the results of the purifications of soluble DnmA-StrepII fusion protein from the cell extracts of two independent overexpression clones and western blotting of purified protein with Strep-Tactin protein conjugated with horse *radish* peroxidase (HRP). The clone 1 of the *Dictyostelium dnmA* KO/*dnmA-StrepII* strain was chosen for maxi preparation of DnmA-StrepII protein to use in some following functional assays.

5.6 Circular dichroism spectropolarimetry of recombinant DnmA

To ensure that the recombinant His-tagged DnmA protein is properly folded, we analyzed several independent preparations by circular dichroism spectropolarimetry in collaboration with Tomasz Jurkowski from Jacobs University, Bremen. Far-UV circular dichroism (CD) spectropolarimetry of proteins can reveal important characteristics of their secondary structure (Greenfield, 2007). CD spectra can be readily used to estimate the fractions of a molecule that is in the α-helix conformation, the β-sheet conformation, the β-turn conformation or some other (e.g. random coil) conformation. These fractional assignments place important constraints on the possible secondary conformations that the protein can be in. CD spectra cannot, in general, say where the alpha helices that are detected are located within the molecule or even completely predict how many there are. Nevertheless, CD can be a valuable tool for verifying that the protein is in its native conformation, and if so, the type and amount of secondary structures can be estimated (Lee & Wallace, 2008).

The DnmA protein, as it can be expected due to high level of its conservation and homology among different species, contains coiled-coil regions, including different types of helices, portion of β-sheets, β-turns and non- or low-structured sequences. Indeed, analysis by various bioinformatics software, for example PHYRE - Protein Homology/analogY Recognition Engine

server (Kelley & Sternberg, 2009), based on available crystal structure of human Dnmt2, provided theoretical predictions on secondary structure components of DnmA. The results show that the estimated value for α-helical structures is about 31%, 12% for β-structures and 57% for other types of secondary structures, which cannot be identified by the software in detail (Figure 5.6.1).

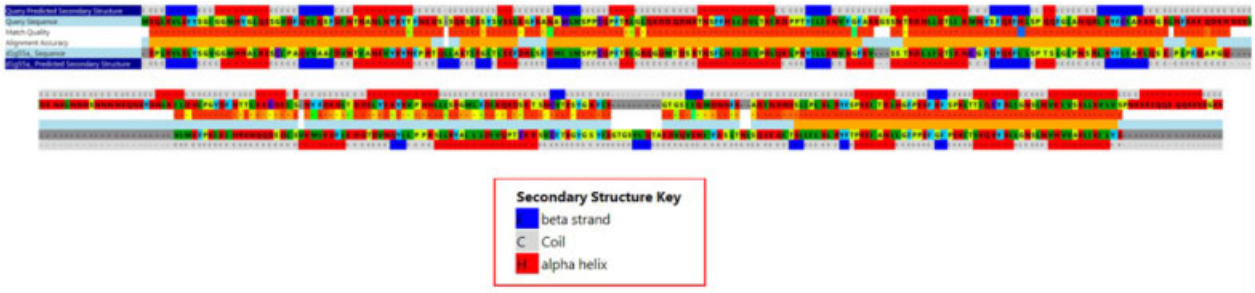

Figure 5.6.1 Bioinformatics analysis of DnmA amino acid sequence for secondary structures. Analysis was done using the PHYRE server (http://www.sbg.bio.ic.ac.uk/phyre/) and known crystallographic structure for human DNMT2 as a reference structure (http://www.pdb.org, entry 1G55). Default setup values were used for the analysis. Data show close similarity in amounts and distribution of secondary structure components between DnmA and hDNMT2.

We would therefore expect DnmA to exhibit spectra characteristics of α-helical proteins, which have to display a peak around 195-205 nm and minima at 208 and 222 nm (Figure 5.6.2). Unfortunately, in some cases the CD signal had low intensity and therefore the highest variability at the region from 190 to 200 nm, most likely due to the presence of some chemicals in the samples which may absorb the light at those wavelengths. Therefore the data (especially in wavelengths below 200 nm) have low accuracy and are not very reliable. Nevertheless, as shown on figure 5.6.2, all CD spectra of different recombinant DnmA preparations were superimposed and region from 205 till 250 nm was analyzed for presence of secondary structure components. CD spectra for 5 from 9 of checked protein preparations (S2, S3, V5, V6 and V7) were fitted and analysis has shown the presence of 30-35% α-helix, 13-15% β-strands and 46-56% of random coils. This result, indeed, is in good agreement with the secondary structure composition, theoretically calculated for the DnmA (31% α-helix, 12% β-structures and 57% of random coils).

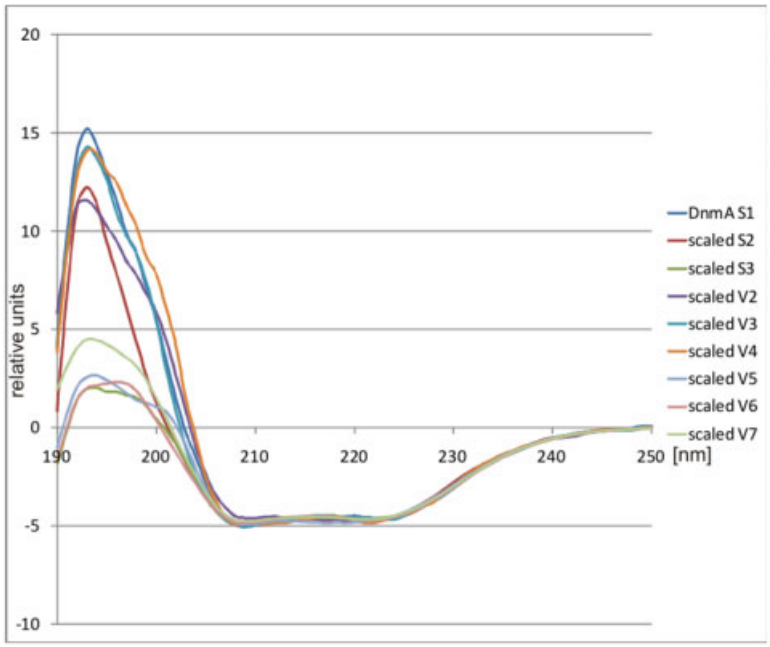

Figure 5.6.2 Alignment of the circular dichroism spectra of the different protein preparations (named S1-S3 and V2-V7). Data were fitted in the range of 250-205 nm. Secondary structure component analysis of the spectra was done in the range of 250-205). Far UV circular dichroism spectra were obtained with a Jasco J-815 circular dichroism spectrophotometer, using protein concentrations of 10 µM DnmA in PBS buffer. The spectra were recorded in a cell with a 0.1-mm path length in the wavelength window between 190 nm and 250 nm with a step size of 0.1 nm and bandwidth of 1 nm. For all spectra, 25 scans were performed and averaged. The buffer baseline was recorded and consequently subtracted from the protein spectra. All experiments were carried out at least twice.

Curiously, these DnmA preparations represented the recombinant protein purified in one step by Ni-NTA affinity chromatography followed by dialysis step against buffer containing 50% Glycerol and showed relatively better activity in binding or methylation assays (see below). On the other hand, protein preparations, which demonstrated different secondary structure compositions on CD spectra (52-72% α-helix, 1-19% β-strands and 24-33% of random coils), were additionally purified by gel filtration on HiLoad™ 16/60 Superdex™ 200 column (Amersham Biosciences) followed by concentration with Amicon® Ultra-4 Centrifugal Filter Devices (Millipore). Those preparations showed as well relatively low or even (in case of S1) no detectable activity on methylation assays (data not shown). It is rather unlikely that gel filtration itself may cause such negative effect on protein preparation, but concentration steps might lead to protein aggregation and therefore can be a reason of incorrect data upon circular dichroism

spectropolarimetry. Therefore, we can conclude that in case of some DnmA preparations, the majority of proteins were properly folded.

5.7 Electrophoretic Mobility Shift Assays

The DNA m^5C methyltransferases (m^5C MTases, EC2.1.1.73 for bacterial enzymes and EC 2.1.1.37 for animals and plants) share six strongly conserved and four weakly conserved sequence motifs that are diagnostic of this class of enzymes (Lauster et al, 1989),(Posfai et al, 1989). All members of the Dnmt2 family contain these 10 MTase motifs in the typical order (Bestor, 2000). In addition to the 10 motifs, all Dnmt2 homologues share a distinctive conserved stretch of 41 amino acids (247-287 of DnmA), including an invariant CysPheThr tripeptide and two dipeptides AspIle and GlySer between motifs VIII and IX. This region is frequently referred to as a target recognition domain (TRD) in bacterial DNA MTases (Lauster et al, 1989). The characteristic CysPheThr tripeptide is almost unique for the Dnmt2 family, excluding a few members like DnmA MTase from *Dictyostelium discoideum*, where this motif represented by CysValThr tripeptide. This high degree of internal conservation in the region of target recognition suggests that Dnmt2 homologues may recognize a specific kind of targets. Moreover, the presence of CysValThr but not CysPheThr tripeptide in the TRD of DnmA enzyme could also potentially influence the affinity and/or specificity of this member of Dnmt2 family towards the target.

One of the powerful methods to identify and potentially quantify nucleic acid binding activity and specificity of a protein is the gel retardation assay, commonly known as electrophoretic mobility shift assay (EMSA). This method can also provide information on the conditions that can alter the interaction, namely ionic strength, pH, temperature, presence and concentration of cofactors, etc. (Wang et al, 1977). Usually, radiolabeled DNA or RNA and protein are mixed together in buffered solution and after certain incubation times samples are subjected to native electrophoresis on a gel matrix (agarose or polyacrylamide). The protein-nucleic acid complexes migrate through the gel matrix slower than free nucleic acid, allowing both bound and free fractions to be observed as distinct bands upon visualization by autoradiography.

5.7.1 EMSA of DnmA binding with short single and double stranded DNA

To identify the binding capacity of DnmA and, potentially, the target motifs for DNA methylation in the *Dictyostelium* genome, electrophoretic mobility shift assays were performed using recombinant His-DnmA protein and different DNA substrates. For this purpose, DNA oligonucleotides were used for assays, which contained methylation sites determined earlier to be a target for the mammalian Dnmt1 and Dnmt3A/3B enzymes (Liu et al, 2003).

Table 5.7.1.1 The list of DNA oligonucleotides used for the EMSA assays. Different cytosine-containing motifs are underlined. The DNMT13_oligo does not carry any specific motifs but has a single cytosine residue only on each end. It, therefore, represents a control oligonucleotide.

DNMT1_oligo	GAAATACCAGGATATAACCAGGTTAGAC
DNMT3_oligo	GGAAATACAGATATAACAGTTAGAGCCC
DNMT5_oligo	GAAAATACCGGATATAACCGGATTAGAC
DNMT11_oligo	GAAATATTCTATAGAGAACTAATTAGAC
DNMT13_oligo	CAAATATTATTATATAATTATTATAGAC

As table 5.7.1.1 shows, the DNA oligonucleotides were 28 nucleotides in length. For experiments they were 5'-end labeled with T4 Polynucleotide Kinase (Fermentas) and [γ-^{32}P] ATP, and incubated with increasing amounts of His-DnmA protein for 30 min at RT followed by loading onto a 8% native PAGE gel (see Materials and Methods). Several experiments were done for the optimization of DnmA-DNA complex formation, including changes in buffer composition, pH and incubation times as well as the concentration of S-adenosyl-L-methyonine (SAM) or ATP as cofactors. Figure 5.7.1.1 shows that recombinant His-DnmA can bind single stranded DNA oligonucleotides. A set of experiments was performed to determine whether oligonucleotide sequence content (namely, the presence of deoxycytidine as the target nucleoside in different motifs) can influence the binding capacity of DnmA enzyme.

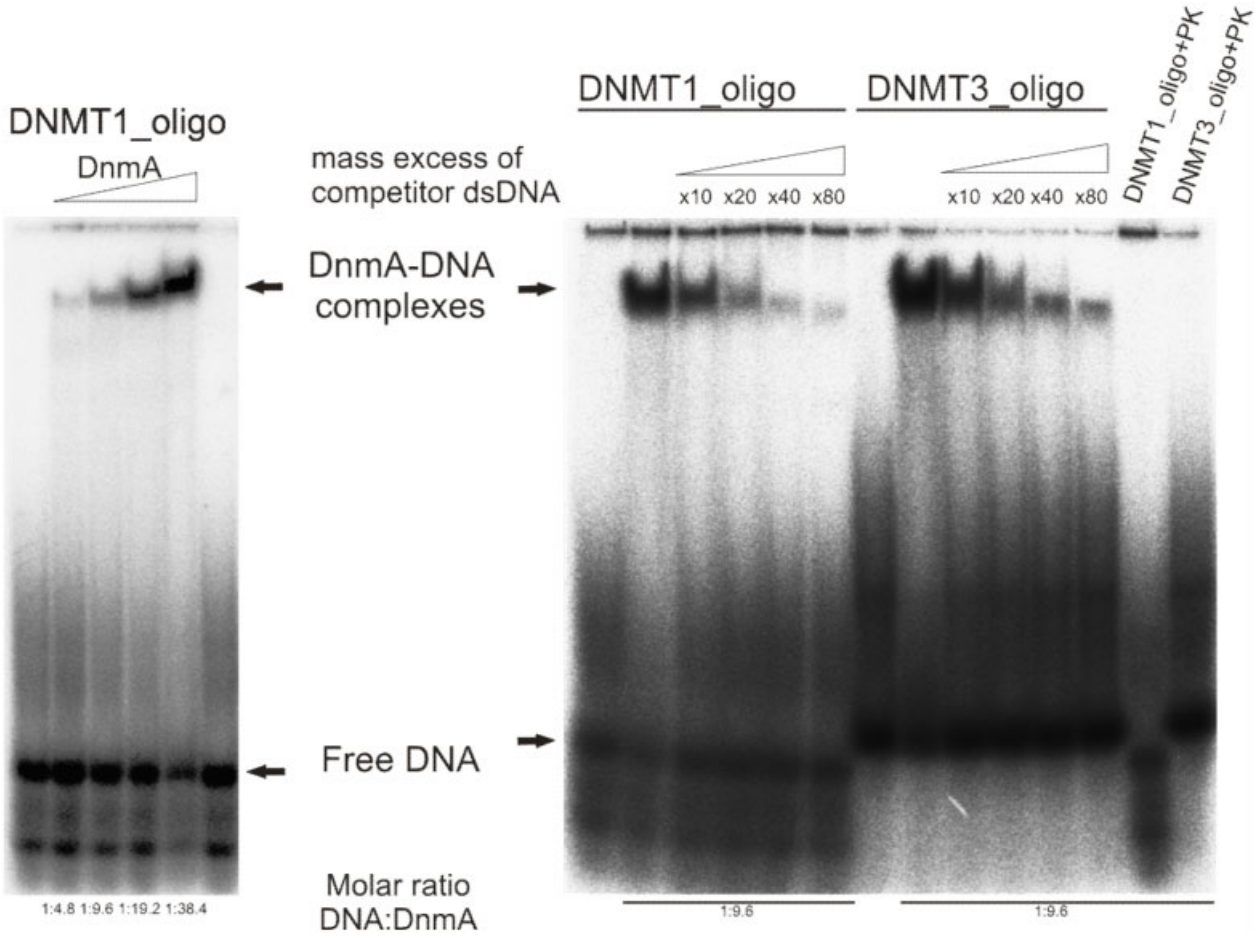

Figure 5.7.1.1 EMSA analysis of interaction between recombinant His-DnmA and short single stranded DNA. The left panel represents the formation of DNMT1_oligo-DnmA compexes. Shortly, equal amounts of [^{32}P]-labeled DNA oligonucleotides (50 ng or 5.5 pmol) were incubated in DNA binding buffer (10mM Tris HCl (pH 8.0), 50 mM NaCl, 1 mM $MgCl_2$, 5 % glycerol (v/v), 0.2 mM PMSF and 1 mM DTT) for 25 min at RT in the absence or presence of increasing amounts of His-DnmA (26-200 pmol per lane) and separated in a native PAGE. The right panel shows results of a binding assay in the presence of competitor DNA. Equal amounts of [^{32}P]-labeled DNA oligonucleotides (100 ng or 11 pmol) were incubated in DNA binding buffer for 25 min at RT in the presence of His-DnmA (100 pmol per lane) and increasing amounts of competitor dsDNA (linearized pGEM T-Easy plasmid). No obvious difference can be observed for interaction His-DnmA with both DNMT1_oligo and DNMT3_oligo. Similar results were obtained for other tested DNA oligonucleotides (data not shown). Although the composition stoichiometry of DnmA-DNA complexes is not clear, most likely these complexes represent non-specific binding of DnmA towards DNA. The last two lanes show binding experiment in presence of proteinase K. As expected, no complexes can be visualized in this case.

In some cases competition binding assays were done using competitor dsDNA. In these experiments we did not find any significant differences in binding affinities of the recombinant His-DnmA towards different DNA oligonucleotides. Thus, we conclude that DnmA does not

show any particular specificity to ssDNAs, carrying diverse motifs or only single C residues at the ends, and therefore, its interaction with ssDNA has non-specific nature.

Given that DnmA enzyme was originally discovered to be a DNA m^5C MTase and that it localizes preferentially in the cell nuclei, it was logical to conclude that it may require double stranded DNA as an appropriate substrate. In order to test this possibility, we used several pairs of the DNA oligonucleotides, containing the same motifs as described earlier, to create short double stranded DNAs and assess the binding capability of His-DnmA towards these targets (Table 5.7.1.2). Usually, 5' ends of one of the DNA oligonucleotides was radiolabeled with [^{32}P] and annealed with the complementary oligonucleotide to assemble short double stranded DNAs. The results demonstrated that recombinant His-DnmA can bind to short dsDNAs.

Table 5.7.1.2 Short dsDNAs used for the EMSA assays. Different cytosine-containing motifs are underlined. Notice, that DNMT13/14 dsDNA do not carry any specific motifs but have cytosine residues only on its ends and was used for as a control DNA.

DNMT1/2 dsDNA	DNMT1_oligo	GAAATACCAGGATATAACCAGGTTAGAC
	DNMT2_oligo	GTCTAACCTGGTTATATCCTGGTATTTC
DNMT3/4 dsDNA	DNMT3_oligo	GGAAATACAGATATAACAGTTAGAGCCC
	DNMT4_oligo	GGGCTCTAACTGTTATATCTGTATTTCC
DNMT5/6 dsDNA	DNMT5_oligo	GAAAATACCGGATATAACCGGATTAGAC
	DNMT6_oligo	GTCTAATCCGGTTATATCCGGTATTTTC
DNMT11/12 dsDNA	DNMT11_oligo	GAAATATTCTATAGAGAACTAATTAGAC
	DNMT12_oligo	GTCTAATTAGTTCTCTATAGAATATTTC
DNMT13/14 dsDNA	DNMT13_oligo	CAAATATTATTATATAATTATTATAGAC
	DNMT14_oligo	GTCTATAATAATTATATAATAATATTTG

Figure 5.7.1.2 shows as well some aspects of the DnmA-DNA interaction. First, DnmA forms complexes with all tested dsDNAs with seemingly the same efficiency. This indicates that DnmA forms a complex with dsDNA in a non-specific manner as it was concluded for DNA oligonucleotides. Second, as shown in panels (A) and (C), the formation of complexes by DnmA is inhibited in the presence of physiological concentration of ATP (1mM) (Eguchi et al, 1997). In the contrary, the presence of SAM (100 μM) increased the binding affinity of DnmA towards dsDNAs.

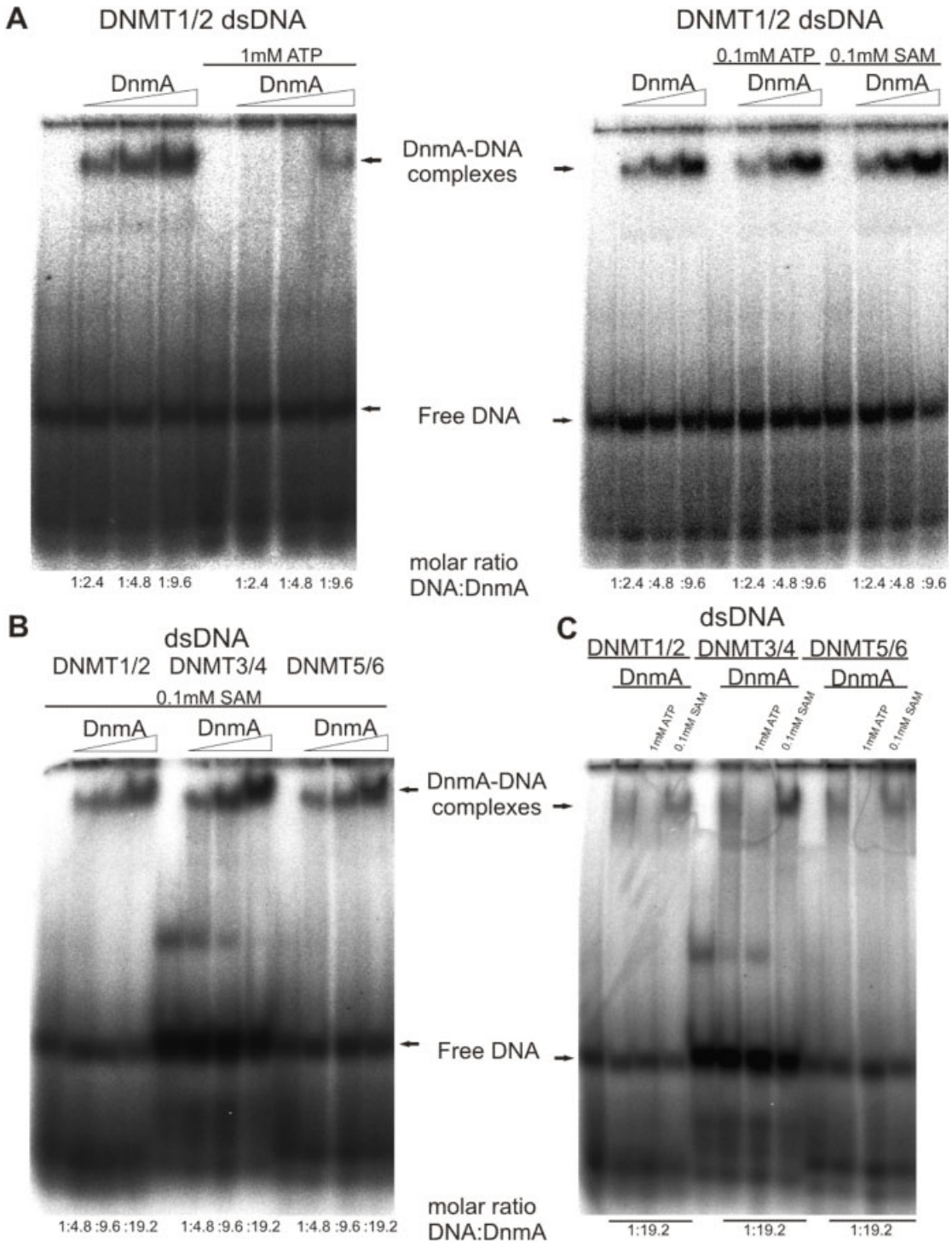

Figure 5.7.1.2 EMSA analysis of interaction between recombinant His-DnmA and short double stranded DNA. (**A**) Left and right panels show DnmA-dsDNA complex formation without and with ATP (100 µM and 1 mM) and SAM (100 µM). (**B**) Comparative analysis of DnmA binding to different dsDNAs in presence SAM (100 µM). (**C**) Comparative analysis of DnmA-DNA complex formation with different dsDNAs and with or without ATP (1 mM)

and SAM (100 µM). For all experiments, equal amounts of [^{32}P]-labeled DNA oligonucleotides (100 ng (5.5 pmol) or 200 ng, (11 pmol)) were incubated in DNA binding buffer (10mM Tris HCl (pH 8.0), 50 mM NaCl, 1 mM $MgCl_2$, 5 % glycerol (v/v), 0.2 mM PMSF and 1 mM DTT) for 25 min at RT in the absence or presence of increasing amounts of His-DnmA (26-100 pmol per lane) and separated in a native PAGE.

This observation was expected as the cofactor can influence the nucleic acid binding properties of the protein. The results also showed that no significant difference in binding affinity can be observed for all tested short dsDNA species.

At this point of our study we realized that the conditions which were used for assays was not quite optimal or, at least, can be somewhat improved. As one can see in figures 5.7.1.1 and 5.7.1.2, there were two major problems with current conditions. First, the quality of most of the commercial DNA oligonucleotides was not good enough to apply directly to an assay. Therefore, radiolabeled oligonucleotides did not give distinct sharp bands upon autoradiography. In this case, absence of visible differences in binding affinity of His-DnmA protein could be masked by binding to all kind of non-specific by-products of oligonucleotide synthesis. One can see on the autoradiographs that the amounts of these contaminants were reduced with increasing amounts of protein in binding reaction. Second, observed shifted bands may actually represent multiple DnmA-DNA complexes, with unclear stoichiometry. Indeed, one of the disadvantages of EMSA is that the oligomeric state of complexes cannot be directly determined or inferred from the position of migration in the gel. The situation becomes even more complicated due to absence of any reliable test to determine the fractional activity of recombinant DnmA in different preparations, which may be result of relatively weak capacity to bind nucleic acids. Nevertheless, the obtained experimental data allow us to conclude that recombinant His-DnmA can bind short single stranded and double stranded DNAs, complex formation has rather non-specific nature and that physiological concentrations of ATP and SAM can influence on DnmA-DNA complex formation.

To overcome the complications linked with quality of commercial DNA oligonucleotides, we performed additional experiments using gel purified oligonucleotides. Figure 5.7.1.3A and B show the results of DnmA binding experiments with purified short single stranded and double stranded DNAs. The conclusion we can make on the basis of these improved data is that recombinant His-DnmA binds to different species of short ssDNAs with similar and low affinities. No significant differences in binding affinities of DnmA were also detected among

different species of short dsDNAs. Nevertheless, the comparative analysis of binding with short ssDNA and dsDNA show that dsDNA is a better substrate for DnmA.

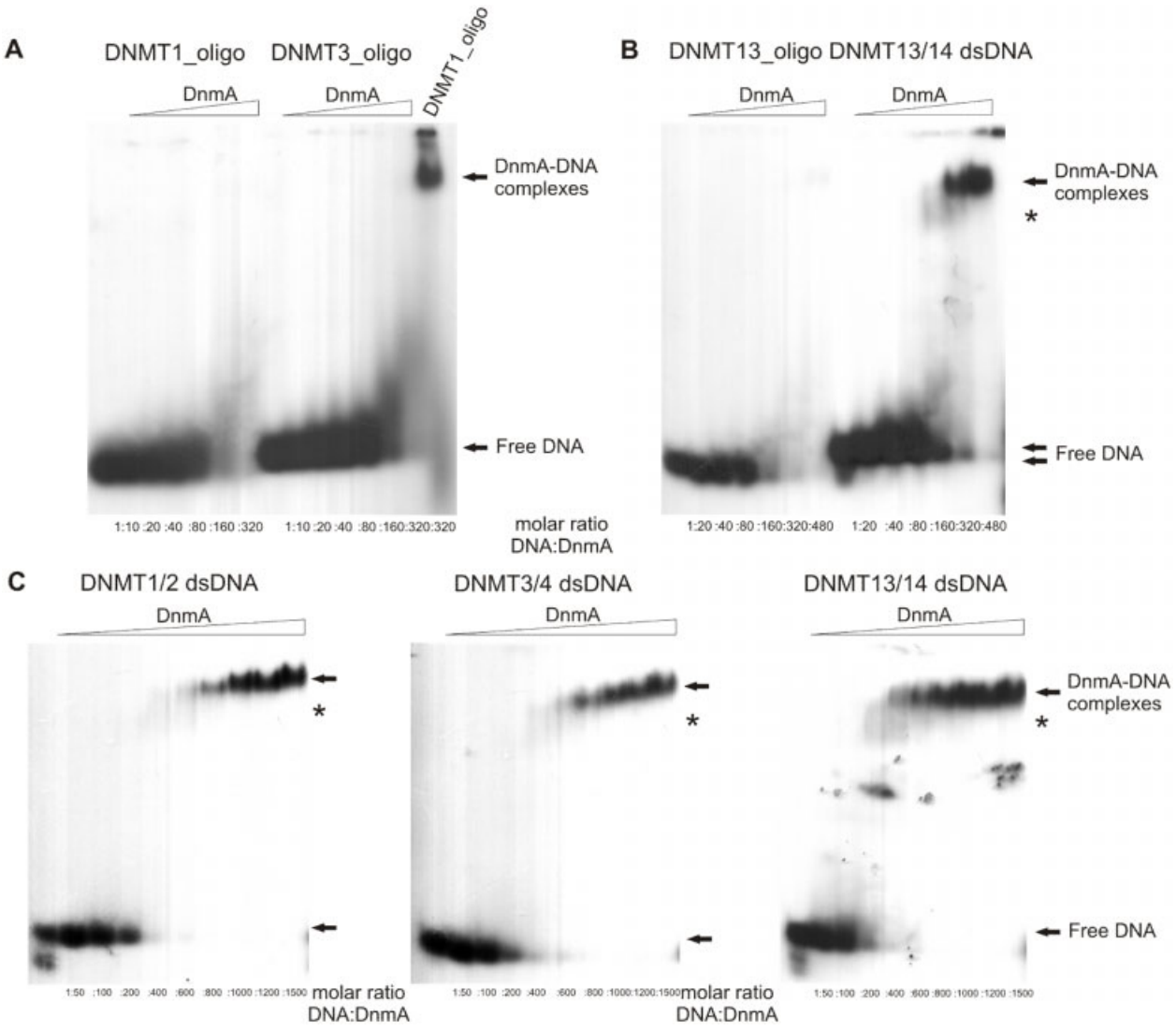

Figure 5.7.1.3 EMSA analysis of interaction between recombinant His-DnmA and DNA. (**A**) Comparative analysis of DnmA binding to purified DNA oligonucleotides. Last lane demonstrates complexes formed by DnmA with equal amount of non-purified DNMT1_oligo. This result additionally proves the non-specific manner of DnmA binding as well as complex nature of DnmA-DNA complexes. (**B**) Comparative analysis of DnmA binding to purified DNA oligonucleotide and dsDNA, formed by this oligonucleotide. These DNAs have no specific cytosine-containing motifs but only cytosines on the ends (see tables 5.7.1.1 and 5.7.1.2). (**C**) Comparative analysis of the three dsDNAs, containing different motifs. Black stars (*) demonstrate DnmA-DNA complexes with higher electrophoretic mobility. For all experiments, equal amounts of [^{32}P]-labeled DNA oligonucleotides (**A**: 18.2 ng or 2 pmol; **B**: 9.1 ng or 1 pmol) and dsDNAs (**B**: 18.2 ng or 1 pmol; **C**: 7.28 ng or 0.4 pmol) were incubated with 100

µM SAM in DNA binding buffer (10mM Tris HCl (pH 8.0), 50 mM NaCl, 1 mM $MgCl_2$, 5 % glycerol (v/v), 0.2 mM PMSF and 1 mM DTT) for 25 min at RT in the absence or presence of increasing amounts of His-DnmA (20-600 pmol per lane) and separated in a native PAGE.

In Figure 5.7.1.3B and C one may also see some weak indications on presence of DnmA-DNA complexes with higher mobility, which is marked by stars (*). Nevertheless, it seems that these complexes represent the tiny fraction of bound DNA species and can only be visualized after significant overexposure upon autoradiography. This observation leads us again to the conclusion about general low affinity of DnmA towards both short ssDNA and dsDNA and apparent absence of specificity in DnmA binding. Nevertheless, the detection of the slow migrating complexes in case of short dsDNAs may reflect some level of cooperativity in DnmA binding under the conditions used.

5.7.2 EMSA of DnmA binding with long double stranded DNA

In the nuclei of eukaryotic cells, most of genomic DNA is organized in chromatin structures of various levels of compaction, mainly due to interaction with histones (Margueron & Reinberg, 2010). Even actively transcribed genes are assembled in rows of nucleosomes (referred to as 'beads-on-a-string' or 10 nm structure) and, in fact, are not continuously held in an open configuration, but adopt a 30-nm-type structures most of the time (Sapojnikova et al, 2009). DNA in these structures is highly bended and supercoiled. There are plenty of factors other than histones known so far, which organize and change chromatin structures (El Hassan & Calladine, 1998). Most of these proteins can bind DNA and many of them bind preferentially to specific structures that DNA may adopt due to compaction and/or intrinsic properties of DNA sequence. These intrinsic characteristics of DNA sequences are determined by the physico-chemical properties of adjacent stacked bases, or base steps and by conformation of the sugar-phosphate backbone, and therefore together with the histones and non-histone proteins like HMGs, can influence the topology of the double helix (Packer & Hunter, 1998). These changes in DNA sequence (mostly DNA bending and kinking) in turn, may raise the accessibility of DNA for binding by other proteins (Fernandez & Anderson, 2007).

Due to the unexpected results of binding studies with short DNA oligonucleotides, we attempted to investigate whether intrinsic properties of longer stretches of DNA can influence binding

characteristics of DnmA. It was shown previously, that DnmA has weak but detectable DNA methyltransferase activity *in vivo* and bisulfite sequencing demonstrated enrichment of cytosine methylation in regions of, at least, two well known retrotransposones in *Dictyostelium* (Kuhlmann et al, 2005). We decided to amplify by PCR corresponding DNA regions as well as regions which did not show any methylation in bisulfite assays and test whether the intrinsic features of DNA sequences can favor the *in vitro* binding of DnmA.

To perform this task, we analyzed, at first, all chosen sequences for the presence of unusual topological features by using DNA tools software provided by ICGEB server (http://hydra.icgeb.trieste.it/dna/index.php). This server contains a collection of methods which graphically represent various DNA helix parameters including bendability and curvature propensity based on dinucleotide and trinucleotide models (Munteanu et al, 1998). Indeed, Figure 5.7.2.1 shows that DNA sequences which were tested have different topologies, although calculations can only be made for the preset conditions and no other parameters except for intrinsic properties of the DNA sequence can be applied. Several EMSA assays were done with these DNA sequences and recombinant His-DnmA. Usually, His-DnmA (6-120 pmol) was incubated for 25 min at 22ºC with purified DNA (2,75 pmol) in 20 µl of 10 mM PKi, pH7.5, 75 mM KCl, 1 mM $MgCl_2$, 0.2 mM PMSF, 1 mM DTT, 10% glycerol. The results demonstrate that there are some differences in overall dynamics of DnmA binding which is not extremely prominent but yet correlates with the predicted topological properties of DNA sequences. Figure 5.7.2.1 shows that the control sequences GR6_271 and GR6_342 (partial human *PLEC1* gene sequence) with a GC content of 65%, which represent no specific topological features, are occupied by DnmA in rather random manner. In the gels it leads to distribution of DNA almost along the whole lane with slow shifting towards complexes where presumably DNA is fully covered by DnmA following the increasing concentration of protein.

In contrast, sequences DIRS1_rLTR_280 (GC content of 31%), Skipper_LTR_389 (GC content of 21%) represent typical *Dictyostelium* AT-rich genomic DNA and they are highly bended according to the theoretical prediction. For these sequences the interaction with DnmA seems to be different: the gels show low amounts of complexes along the lanes and relatively strong accumulation of high molecular weight DnmA-DNA complexes at lower protein concentrations. These dynamics can be explained if DnmA proteins occupy the sites on DNA molecules in cooperative manner.

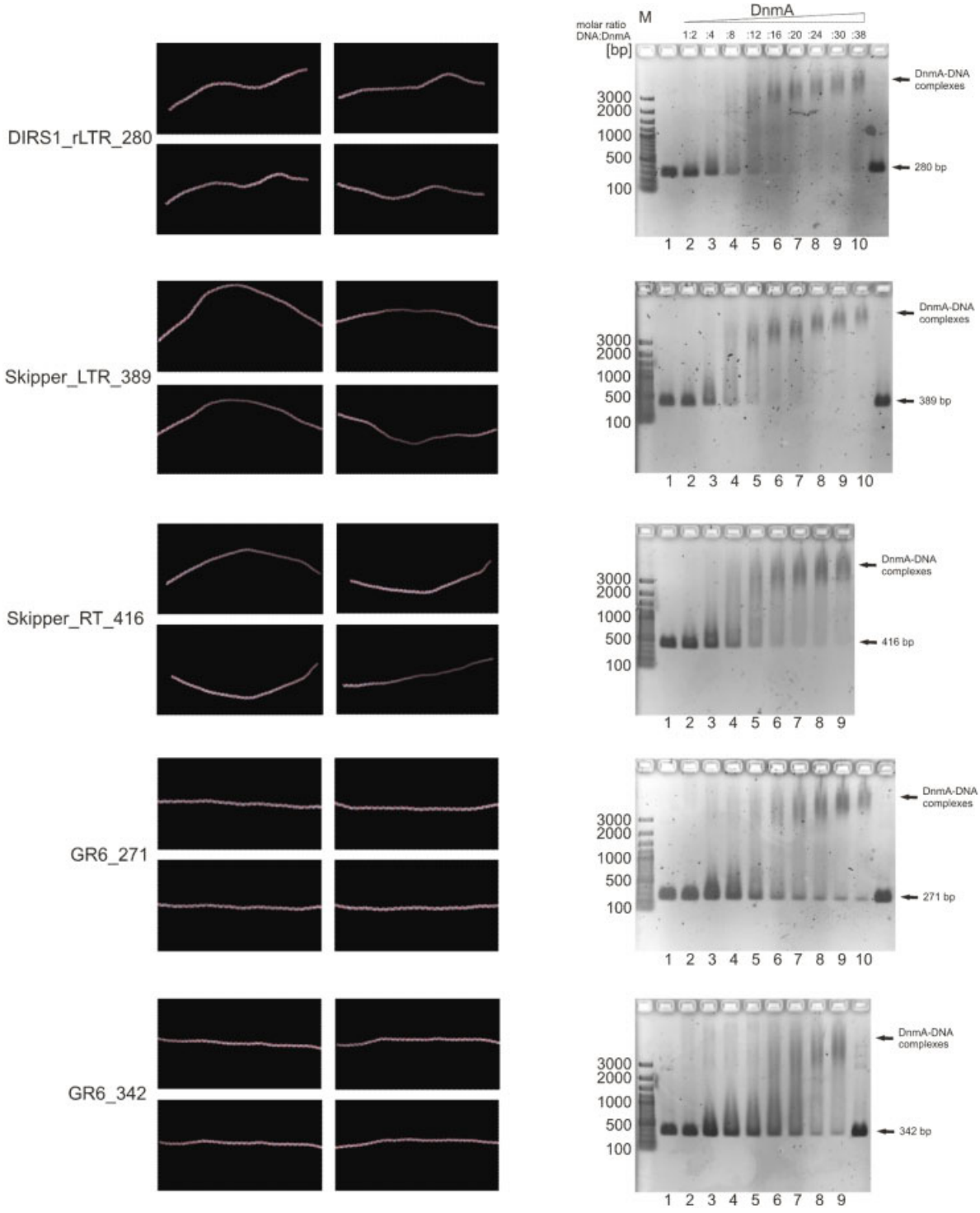

Figure 5.7.2.1 Left column of panels represent theoretical predictions of curvature for different dsDNA fragments. Right column of panels show the results of EMSA in native 1.2% agarose gels. Shortly, DNA fragments were amplified by PCR, purified and used for gel shift assays with increasing amounts of DnmA. Equal molar ratios of DNA/DnmA were used in each case. GeneRuler™ 100 bp DNA ladder (Fermentas, #SM0324) was used as a size marker.

The sequence of Skipper_RT_416 (GC content of 31.6%) can be placed somewhat between other species, probably due to less pronounced intrinsic DNA curvature.

To test that there are indeed difference in binding affinity of DnmA to different DNAs, a competitive EMSA experiment was done with DIRS1_rLTR_280 and GR6_342 DNAs.

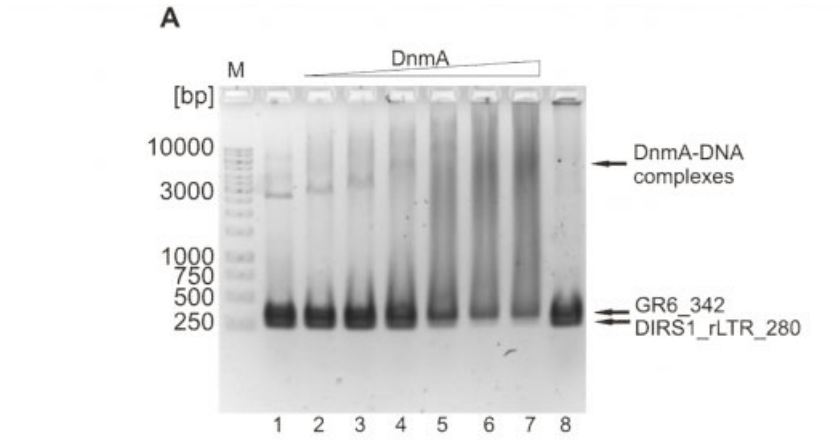

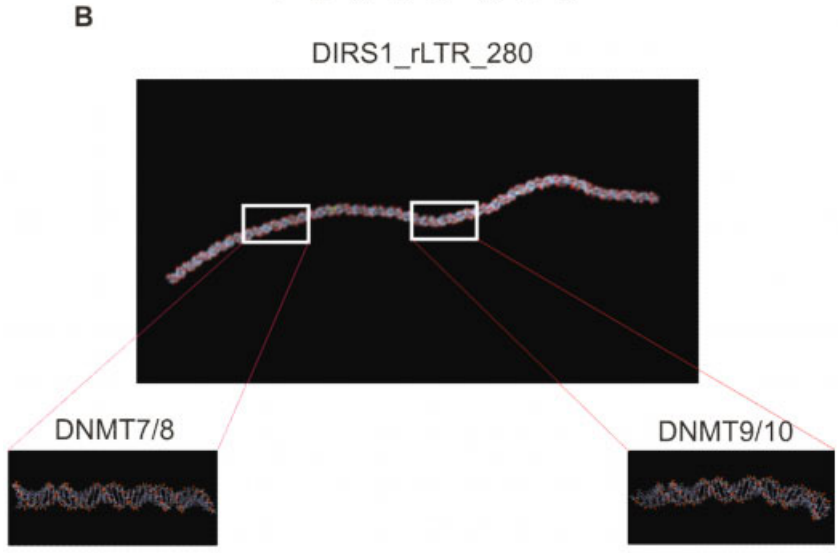

DNMT7/8	DNMT7_oligo	CGGCCGCCTGCAGGTCGACCATATGGGAGAGCTCCCAACG
dsDNA	DNMT8_oligo	CGTTGGGAGCTCTCCCATATGGTCGACCTGCAGGCGGCCG
DNMT9/10	DNMT9_oligo	TGCATAGTGTCGTCGGTTCGGAATTTTTCAGTTTTTCGAC
dsDNA	DNMT10_oligo	GTCGAAAAACTGAAAAATTCCGAACCGACGACACTATGCA

Figure 5.7.2.2 (**A**) Competition EMSA study of interaction DnmA with DIRS1_rLTR_280 and GR6_342 DNA sequences. Lower band, corresponding to DIRS1_rLTR_280 has a tendency to be shifted more effectively than the upper GR6_342 band. GeneRuler™ 1 kb DNA ladder (Fermentas, #SM0311) were used as a size marker. (**B**) Parts of DIRS1_rLTR_280 DNA sequence which were chosen to represent short dsDNA fragments of different curvature.

Figure 5.7.2.2A shows that material of the lower band on the gel, corresponding to DIRS1_rLTR_280 DNA shifts faster but some material of the upper band, containing GR6_342, remains yet at its original position. Hence we detected the small difference in DnmA binding affinities to different types of long dsDNAs.

To check whether the effects we observed for long dsDNAs are due to the presence of intrinsic DNA curvature, we designed oligonucleotides to mimic two sections of DIRS1_rLTR sequence in a way that DNMT7/8 represents no DNA bending upon theoretical prediction by bioinformatics software, but DNMT9/10 sequence has distinctive curvature (Figure 5.7.2.2B). The DNA oligonucleotides (each of 40 nucleotides in length) were [^{32}P]-radiolabeled, assembled into dsDNAs and used for gel shift assays with His-DnmA as described previously. However, the results did not show any detectable difference in affinity of DnmA to these short dsDNAs (data not shown).

5.7.3 AFM study of DnmA-DNA interaction

Since it was possible to show weak but detectable differences in affinity of DnmA towards long dsDNAs of various compositions, we decided to study the details of protein-DNA interaction by AFM (in collaboration with Anspach). For this study, we amplified the DNA region from plasmid pGEM T-Easy *DIRS1-rLTR* by PCR using commercially available primers M13 Seq and M13 rev. Purified PCR product of 571 bp, containing DIRS1_rLTR sequence (290 bp, GC content of 28.3%) flanked with 128 and 153 bp, corresponding to plasmid DNA sequences (Figure 5.7.3.1). These flanking sequences did not show any significant intrinsic DNA curvature as was tested by DNA tools software (ICGEB, http://hydra.icgeb.trieste.it/dna/index.php) and they had a usual GC content of 58.6% and 47.7%, respectively. Thus, the first question to be addressed by AFM studies was on the distribution of bound DnmA along the DIRS1_rLTR_571 fragment. This would indicate if naturally occurring *Dictyostelium* AT-rich sequences are preferential binding sites for DnmA. Second, the study could potentially show if there was any correlation between binding positions of the protein on DNA and theoretically predicted curvatures found within the DNA fragment. The third question would address the characteristics of DnmA binding, namely possible correlation between curvature implied by DnmA binding and naturally occurring curvatures within a tested DNA fragment.

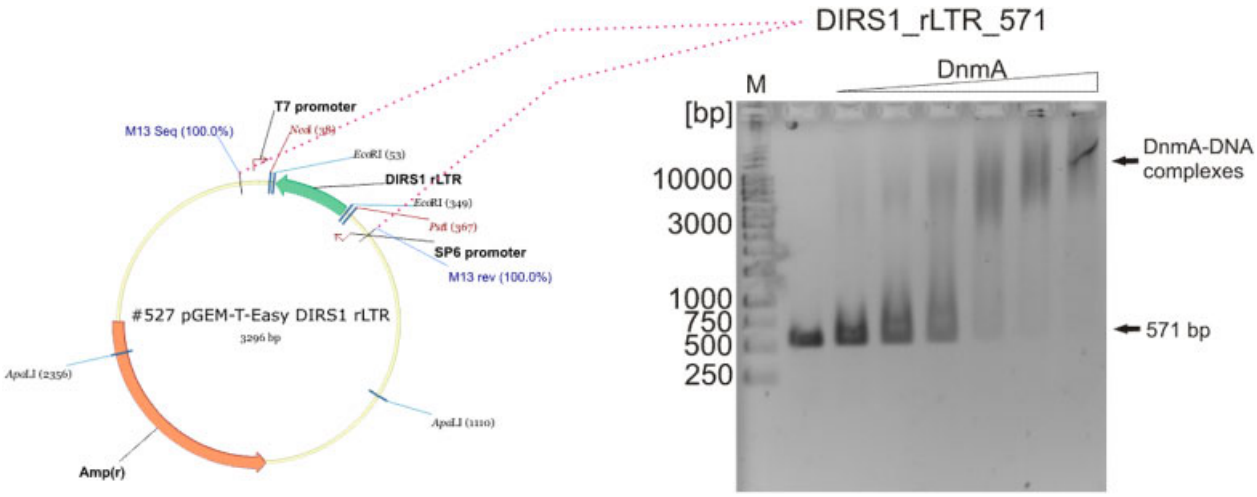

Figure 5.7.3.1 Schematic representation of plasmid pGEM T-Easy *DIRS1-rLTR* (left panel) that was used to amplify 571 bp DNA fragment, containing 290 bp of DIRS1_rLTR sequence. PCR was performed with primers M13 Seq and M13 rev. PCR product, named DIRS1_rLTR_571, was purified by agarose gel electrophoresis and used for AFM study. Right panel represent EMSA with DIRS_rLTR_571 fragment. Overall behavior of DnmA-DNA complexes is similar to behavior of DIRS1_rLTR_280 DNA fragment (see Figure 5.7.2.1) consistent with suggestion about presence of some level of cooperativity in DnmA binding. GeneRuler™ 1 kb DNA ladder (Fermentas, #SM0311) were used as a size marker.

Indeed, the preliminary results of AFM study performed by Nils Anspach, allowed us to demonstrate that complexes between the DIRS1_rLTR_571 DNA substrate molecule and a recombinant His-DnmA can be obtained, as it is shown in Figure 5.7.3.2. Bound DnmA proteins were detected along the entire DNA molecule with different frequencies. Figure 5.7.3.2B shows the distribution of bound DnmA on DNA substrate molecules. The ends of the DNA substrate cannot be distinguished one from another by AFM unless they are specifically marked. Therefore, the DNA molecule was folded in half and divided into 11 segments, each 10 nm long. Positions of the DNA molecule correspond to the segments on the *x*-axis in the distribution chart. The highest binding density with 38% of the total bound proteins appears to occur over the segments seven and eight. The segments nine, ten and eleven, which include methylated cytosines identified in earlier bisulfite studies, show together 25% binding rate. At last, the most remarkable finding is that the segments from six to eleven, containing DIRS-1_rLTR sequence, together represent 71% of all bound DnmA, while the segments one to five which contain

flanking DNA derived from plasmid sequence (pGEM T-Easy in this case), have only 29% of bound protein.

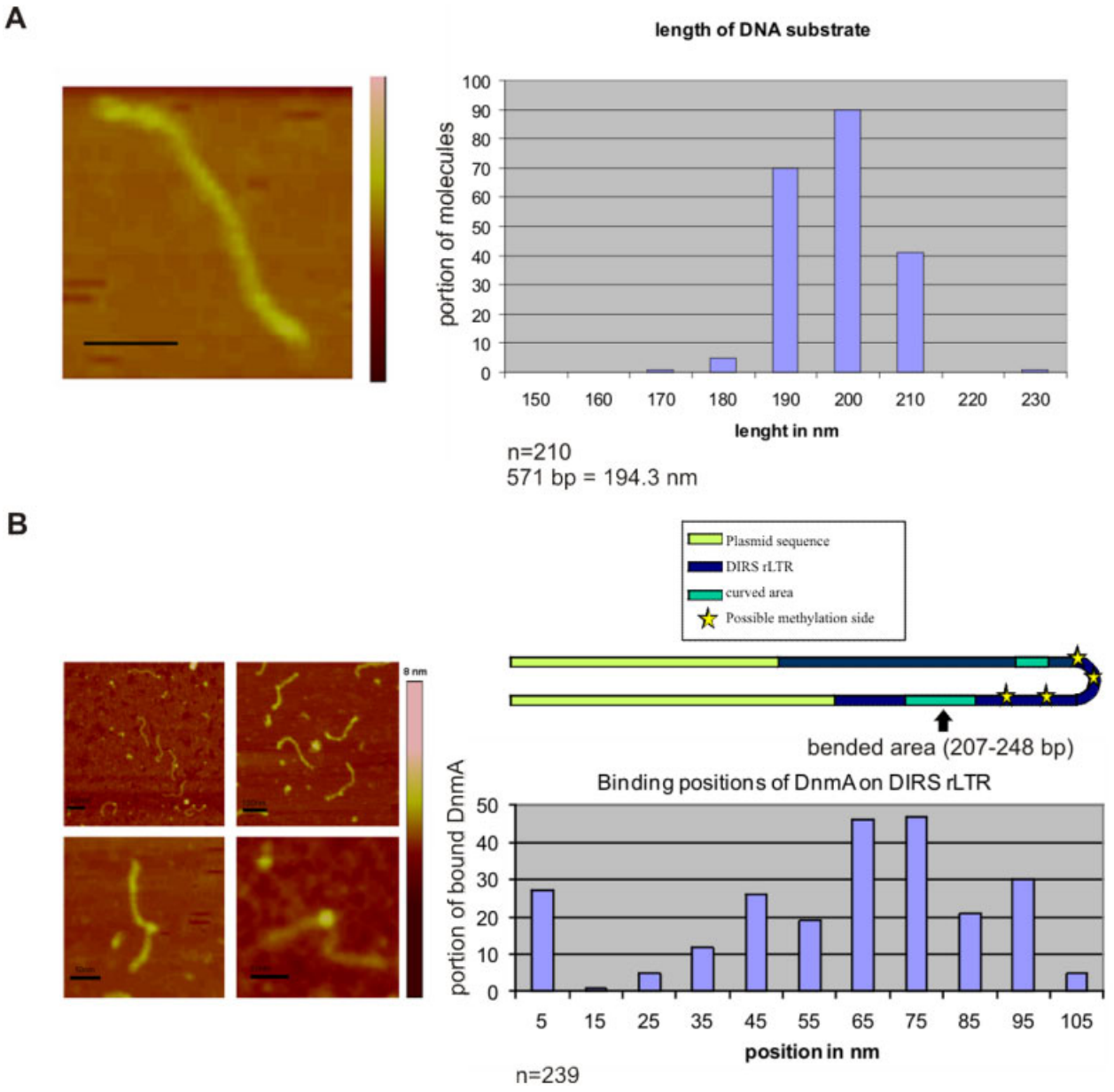

Figure 5.7.3.2 (**A**) The AFM topogram (left panel) shows a DIRS-1_rLTR_571 DNA substrate molecule (bar = 50 nm, height scale 5 nm). Right panel represent length distribution of 210 measured DNA molecules. The arithmetic mean corresponds to 194.3 nm. (**B**) Right panel: AFM images of individual DnmA/DNA-Complexes (5 nm height scale). Left panel: Distribution of bound DnmA molecules along the DIRS1_rLTR_571 DNA substrates (number of events, n = 244). A schematic representation of the folded DNA substrate is shown on the top of distribution graph (flanking plasmid sequences (pGEM T-Easy, green), DIRS-1 rLTR sequence (blue) and identified potentially

methylated cytosine bases (Kuhlmann et al., 2005) (yellow stars)). Segments on the x-axis of the graphic distribution in general outline are consistent with the regions on DNA sequence representation. Figure adapted from N. Anspach PhD thesis.

This finding allowed us to conclude that DnmA preferentially occupy the sites within DIRS1_rLTR DNA region and at some extent at the ends of DIRS1_rLTR_571 fragment. Moreover, the segments 7 and 8 show a possible intrinsic curvature of the DNA double helix. This DNA curvature can be calculated with the help of bend.it® server and visualized graphically using model.it® server (ICGEB, http://hydra.icgeb.trieste.it/dna/index.php, Figure 5.7.3.3). Calculation shows that at this region double helix (207 to 248 bp in terms of rLTR orientation) can take an angle of approximately 30 degrees.

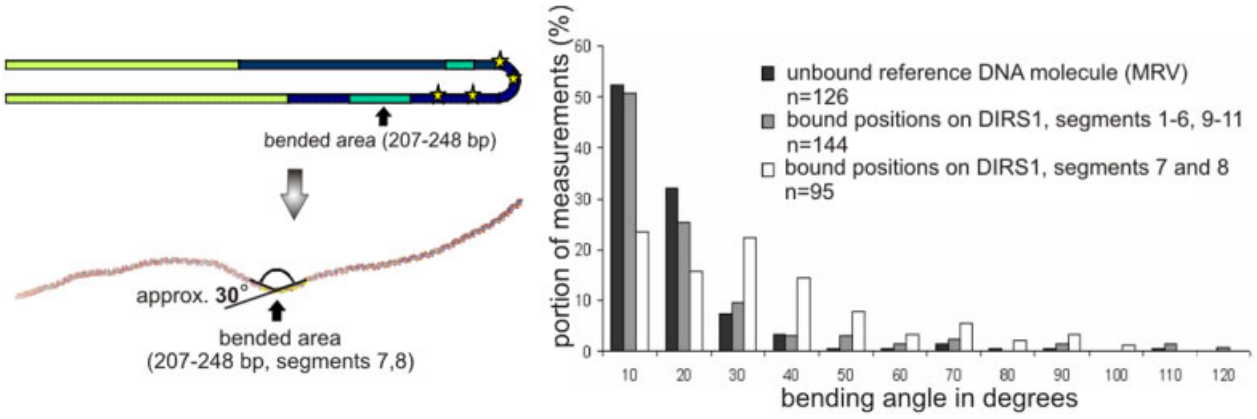

Figure 5.7.3.3 Left panel: Intrinsic curvature in the DNA substrate. Graphical representation of the binding substrate (Model it® Server). An angle of 30 degrees can be detected in the region of 207-248bp. Right panel: Distribution of DNA deflections on a protein binding sites. In regions where no intrinsic DNA bending (gray, n = 144) was predicted, no difference from a reference molecule (black, n = 126) are detected. In the region of predicted intrinsic DNA-bending (white, n = 95) portion of measurements corresponding to the angles of 0-20 degrees are reduced, but at the angle 30-50 are increased. Figure adapted from N. Anspach PhD thesis.

To determine whether the theoretically calculated intrinsic DNA curvature can be detected in the measured DnmA-DNA complexes, deflections of DNA paths for each of all protein binding sites was estimated (Figure 5.7.3.3, right panel). The distribution of the DNA deflections at the protein binding sites which is located within the segments 1-6 and 9-11 (no intrinsic DNA curvature) compared to those in segments 7 and 8 (intrinsic DNA curvature) is shown as a graphic representation. The reference data, representing an unbound DNA substrate were

obtained by measurement of randomly selected DNA sites. The graph shows that, in the case of the segments 1-6 and 9-11 the angular distribution corresponds to the reference molecule. This means in these regions there is no intrinsic curvature of DNA and that there are also no specific structural effects of bound protein on the DNA. Measurements of DnmA-DNA complexes in segments 7 and 8 show a reduced occurrence of small DNA deflections (within 0-20 degrees). However, DNA bending within the angles of 30-50 degrees occurs more frequently. This observation suggests that in the segments 7-8 intrinsic DNA curvature may play a role, though DNA bending as a result of specific DnmA binding cannot be entirely excluded.

5.7.4 EMSA of DnmA-RNA binding

Despite their amino acid sequences and structure closely resembling authentic DNA m^5C methyltransferases, some members of Dnmt2 family (human DNMT2) were recently shown to function as RNA methyltransferases transferring a methyl group specifically to the cytosine 38 in the anticodon loop of $tRNA^{Asp}$ (Goll et al, 2006). The function of Dnmt2 seems to be highly conserved and human protein restored methylation *in vitro* to RNA from Dnmt2-deficient strains of mouse and *Arabidopsis thaliana*, *Drosophila melanogaster* and *Dictyostelium discoideum* (Goll et al, 2006); (Jurkowski et al, 2008). Moreover, hDNMT2 was shown to methylate $tRNA^{Asp}$ in a manner that was dependent on preexisting patterns of modified nucleosides (Goll et al, 2006). Nevertheless, the binding characteristics of Dnmt2 proteins towards different RNA substrates were never examined. To address that issue, we performed EMSA analysis of DnmA-RNA binding. First of all we attempted to test the general ability of recombinant His-DnmA to bind to the fraction of an RNA preparation enriched for small RNAs (various tRNAs represent significant portion of such RNA preparations). The left panel in Figure 5.7.4.1A shows a 1.2% agarose gel where different dilutions of RNA preparation, enriched for small RNAs, from Ax2 *Dictyostelium* strain were fractionated for quality control. The right panel on the same figure shows the result of an EMSA in 1.2% agarose gel, so we concluded that DnmA does form complexes with RNA substrates.

To obtain a better resolution for different RNA species in RNA preparation we performed the EMSA using native PAGE. Figure 5.7.4.1B demonstrates unexpected characteristics of DnmA-RNA binding, namely the tendency of preferential binding of protein with long RNA species. Curiously, this result demonstrates that DnmA can bind to long RNA molecules with even higher

affinity than to tRNAs, some of which (for instance $tRNA^{Asp}$) represent target molecules for methylation *in vivo* and *in vitro*. Nevertheless, as we learned from DnmA-DNA binding studies, the interaction of protein with various RNA substrates may also be non-specific.

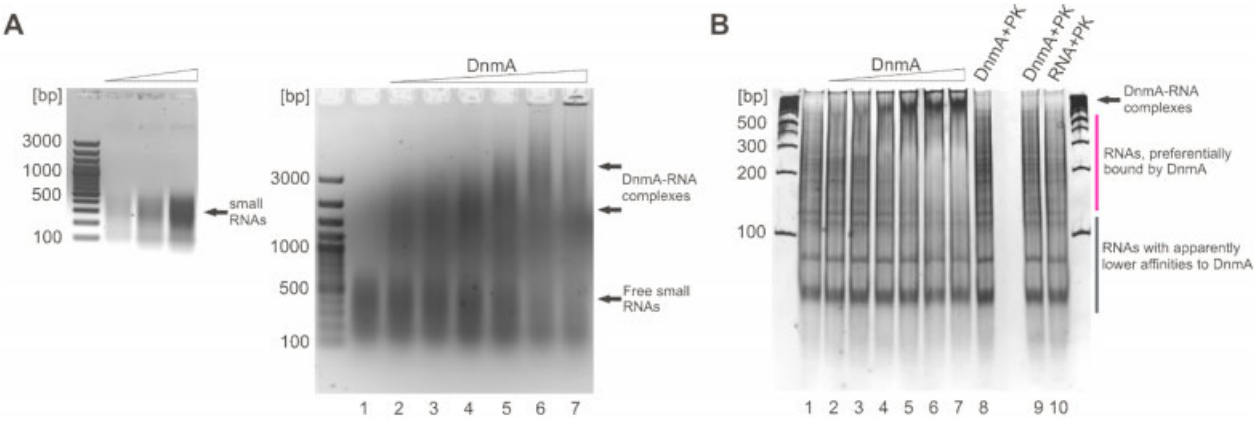

Figure 5.7.4.1 (**A**) 1.2% agarose gels represent quality control of RNA preparation enriched for small RNAs (left) and EMSA of DnmA binding (right). DnmA does form complexes with RNA. (**B**) EMSA in native 5% PA gel. The tendency of DnmA to bind different RNAs starting from longer species is clearly visible. Various tRNAs are fractionated somewhere between 100 and 200 bp of DNA reference marker. Appearance of complexes is the result of DnmA binding, since the presence of proteinase K (PK) in the reaction inhibits complex formation (lanes 8 and 9 is the same as lanes 4 and 5 except for presence of 2 µg of PK). GeneRuler™ 100 bp DNA ladder (Fermentas, #SM0324) was used as a size marker.

To test the ability of DnmA to bind various RNA substrates we prepared several constructs for *in vitro* transcription based on pJET1.1 vector (Fermentas). Final plasmids, named pJET1.1-Glu5, pJET1.1-Glu-SP, pJET1.1-Glu5R and pJET1.1-GluSPR, upon the linearization with *Xba*I enzyme allowed *in vitro* transcription to produce corresponding tRNAs and antisense RNAs (see Materials, Figure 3.7.5-6). Gel retardation assays were done using similar conditions as for studies of DnmA-DNA binding, except for some changes in concentration of salt, DTT and pH of incubation buffer. During these experiments, DnmA or hDNMT2 were added as a last component of binding reaction, so no pre-incubation of protein with SAM was allowed. Figure 5.7.4.2 shows the results of one such binding experiment. In absence of pre-incubation of DnmA with both RNA substrates, high levels of aggregation can be observed following an increasing concentration of protein in reaction. Another characteristic feature of DnmA binding is the presence of additional complexes (marked by red arrow) in case of $tRNA^{Glu(UUC-5)}$ substrate,

which is absent or at least do not form distinct band upon interaction of protein with asRNA$^{Glu(UUC-5)}$.

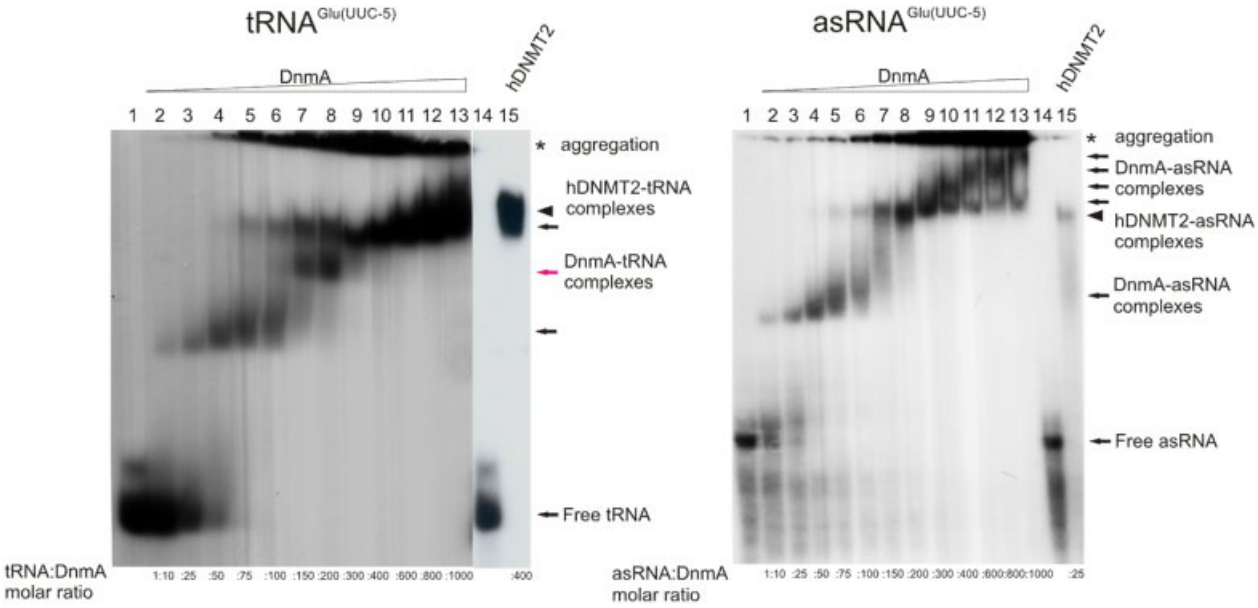

Figure 5.7.4.2 EMSA assays of DnmA binding with *Dictyostelium* tRNA$^{Glu(UUC-5)}$ (left) and antisence transcript of tRNA$^{Glu(UUC-5)}$ (termed asRNA$^{Glu(UUC-5)}$, right) in native 5% PAGE. Usually, His-DnmA (10-490 pmol) was incubated for 15 min at 22ºC with purified tRNA$^{Glu(UUC-5)}$ or antisense RNA$^{Glu(UUC-5)}$ (0,366 pmol) in 20 µl of 10 mM PKi, pH7.5, 75 mM KCl, 2 mM $MgCl_2$, 0.2 mM PMSF, 1 mM DTT, 10% glycerol and 100 µM SAM. Binding reactions with human DNMT2 (160 pmol in case of tRNA$^{Glu(UUC-5)}$ and 10 pmol in case of asRNA$^{Glu(UUC-5)}$) were performed at the same conditions except for incubation temperature of 37ºC. No pre-incubation of DnmA or hDNMT2 with SAM prior to addition of RNA substrate was allowed. EMSAs of hDNMT2 with corresponding RNA substrates is also shown (human DNMT2 enzyme was kindly provided by Tomasz Jurkowsky, Bremen). hDNMT2 preparations usually show better binding compared to DnmA (asRNA$^{Glu(UUC-5)}$, lanes 3 and 15).

Another profound difference between tRNA$^{Glu(UUC-5)}$ and asRNA$^{Glu(UUC-5)}$ is a formation of the additional DnmA-asRNA complexes up to aggregated material in the wells of the gel (Figure 5.7.4.2, right panel), though we cannot exclude that this complexes is a result of DnmA binding with shorter RNA products occurring due to incomplete *in vitro* transcription (radiolabeled RNA material below asRNA band on the gel). Indeed, for the tRNA$^{Glu(UUC-5)}$, no truncated RNA products were usually observed, therefore we cannot conclude at this point that the observed complexes are characteristic for asRNA$^{Glu(UUC-5)}$.

The gels in Figure 5.7.4.2 also provide some information on characteristics of human DNMT2 binding to RNA substrates. Indeed, binding of human protein with RNAs did not show significant aggregation (compare lanes 10 and 15 on the left gel) and demonstrated higher affinity towards RNA compared to DnmA (compare lanes 3 and 15 on the right gel). The difference in binding affinities could probably be the result of the earlier mentioned substitution Phe/Val in the conservative motif within TRD (CFT in hDNMT2 and other members of Dnmt2 family and CVT in DnmA), although we cannot exclude that it is a consequence of general lower activity of His-DnmA preparations. Indeed, recently cDNA of DnmA was subcloned from pET15b-*dnmA*_wt into pET28a(+) vector and new recombinant protein preparations produced in *E.coli* by using this expression vector had shown at least 5-fold increase in methyltransfer activity (Müller, personal communication).

We assumed that pre-incubation of DnmA with SAM could potentially help for DnmA-RNA complex formation due to an increased portion of active proteins preloaded with cofactor. Therefore, we included a 10 min pre-incubation step in the binding reactions prior to addition of the RNA substrates. Surprisingly, the pre-incubation step drastically changed the binding kinetics for DnmA in a way that neither aggregated material in the gel wells nor intermediate complexes could be detected, leaving only complexes of high molecular weight (Figure 5.7.4.3).

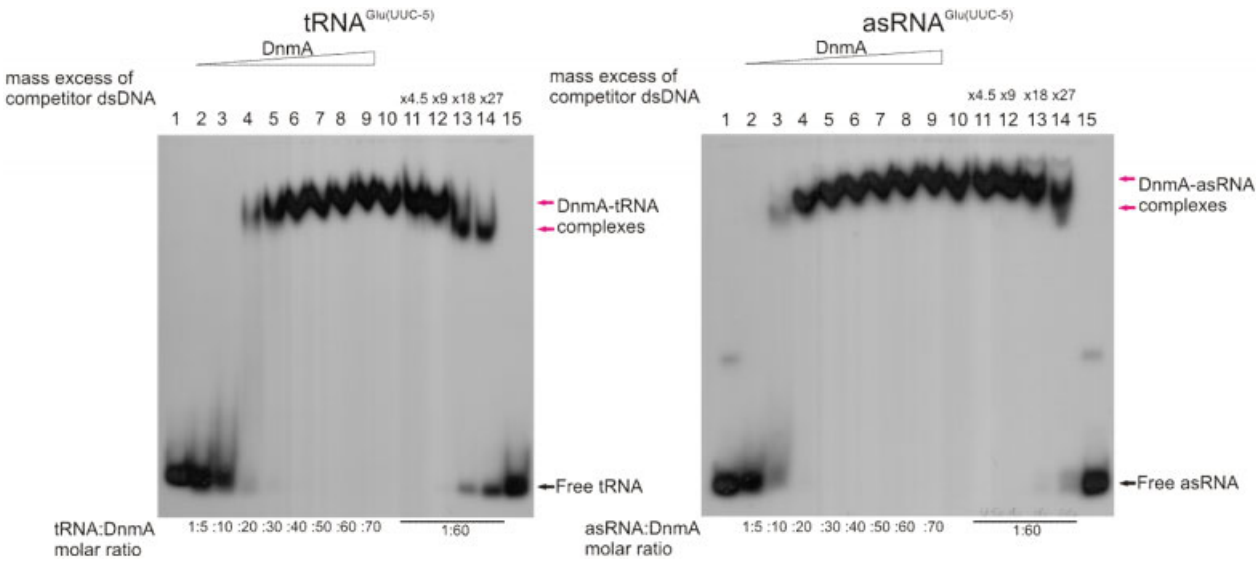

Figure 5.7.4.3 Lanes 1-9 represent EMSA assays of DnmA binding with *Dictyostelium* tRNA$^{Glu(UUC-5)}$ (left) and asRNA$^{Glu(UUC-5)}$ (right) in a native 5% PAGE. Lines 10-15 show competition assays with dsDNA (linearized pGEM T-Easy plasmid). These experiments were carried out using conditions which differ from the ones described in

Figure 5.7.4.2. Usually, His-DnmA (40-575 pmol) was incubated for 15 min at 22ºC with purified $tRNA^{Glu(UUC-5)}$ or antisense $RNA^{Glu(UUC-5)}$ (8 pmol) in 20 µl of 10 mM PKi, pH7.0, 35 mM KCl, 2 mM $MgCl_2$, 0.2 mM PMSF, 10 mM DTT, 22.5% glycerol and 100 µM SAM, and 10 min pre-incubation of DnmA with SAM prior to addition of RNA substrate were allowed.

These experiments had also shown that binding affinity of DnmA towards $tRNA^{Glu(UUC-5)}$ was approximately 1.5 times lower than for $asRNA^{Glu(UUC-5)}$ (Figure 5.7.4.3, compare lanes 4-5, 13 of left gel with lanes 3-4, 14 of right gel; compare molar ratios).

As it was demonstrated previously, hDNMT2 is able to transfer a methyl group to cytosine 38 of $tRNA^{Asp}$ from several species (Helm, Lyko and Müller, personal communication, (Jurkowski et al, 2008)). Thus, the gel retardation assays were performed with His-DnmA and *in vitro* transcribed $tRNA^{Asp(GUC-1)}$ (plasmid pJET1.1-Asp(GUC-1), containing cDNA for *Dictyostelium* $tRNA^{Asp}$ was kindly provided by S. Müller). The PA gel in the Figure 5.7.4.4 shows that binding affinity of DnmA to $tRNA^{Asp(GUC-1)}$ was similar to affinity of the protein to $asRNA^{Glu(UUC-5)}$ (compare lanes 3 and 4 of right gel in Figure 5.7.4.3 with lanes 5 and 7 in Figure 5.7.4.4).

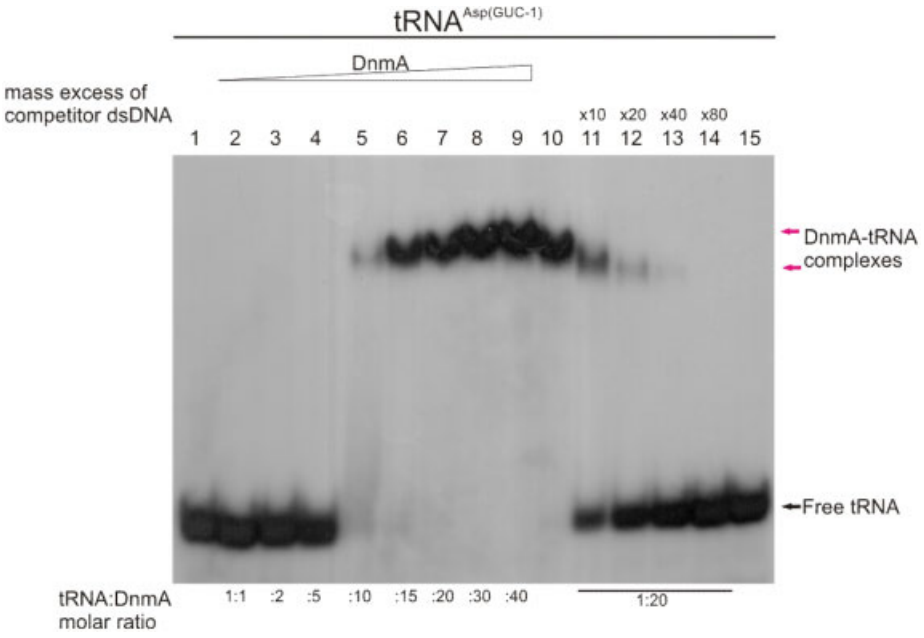

Figure 5.7.4.4 Lanes 1-9 represent EMSA assay of DnmA binding with *Dictyostelium* $tRNA^{Asp(GUC-1)}$ in native 5% PAGE. Lines 10-15 show competition assays with dsDNA (linearized pGEM T-Easy plasmid). These experiments were carried out using conditions described earlier with some minor changes (see Figure 5.7.4.3). His-DnmA (4-160 pmol) was incubated for 15 min at 22ºC with purified $tRNA^{Asp(GUC-1)}$ (4 pmol) in 20 µl of 10 mM PKi, pH7.0, 25

mM KCl, 2 mM $MgCl_2$, 0.2 mM PMSF, 10 mM DTT, 22.5% glycerol and 100 µM SAM (10 min pre-incubation of DnmA with SAM prior to addition of RNA substrate were allowed).

These experiments allowed us to conclude that there is weak but detectable difference in the binding affinity of the DnmA towards various RNA substrates of similar size but different composition.

To confirm that the reason of difference in the binding kinetics observed in the retardation assays (compare Figure 5.7.4.2 and 5.7.4.3-4) was only due to pre-incubation of DnmA with SAM, the assay was performed to test an influence of buffer components and pH on binding DnmA with $tRNA^{Glu(UUC-5)}$. As described earlier, in appropriate samples 10 min pre-incubation of DnmA with SAM prior to addition of RNA substrate were allowed. Figure 5.7.4.5 clearly demonstrates that increasing concentration of salt from 35 to 100 mM inhibits binding to some extent (compare lanes 2 and 3 or lanes 6 and 7, although the difference in the latter case was less pronounced). Indeed, the high ionic strength of a buffer can influence the electrostatic potentials of interacting surfaces of protein and DNA/RNA molecules (Norberg, 2003).

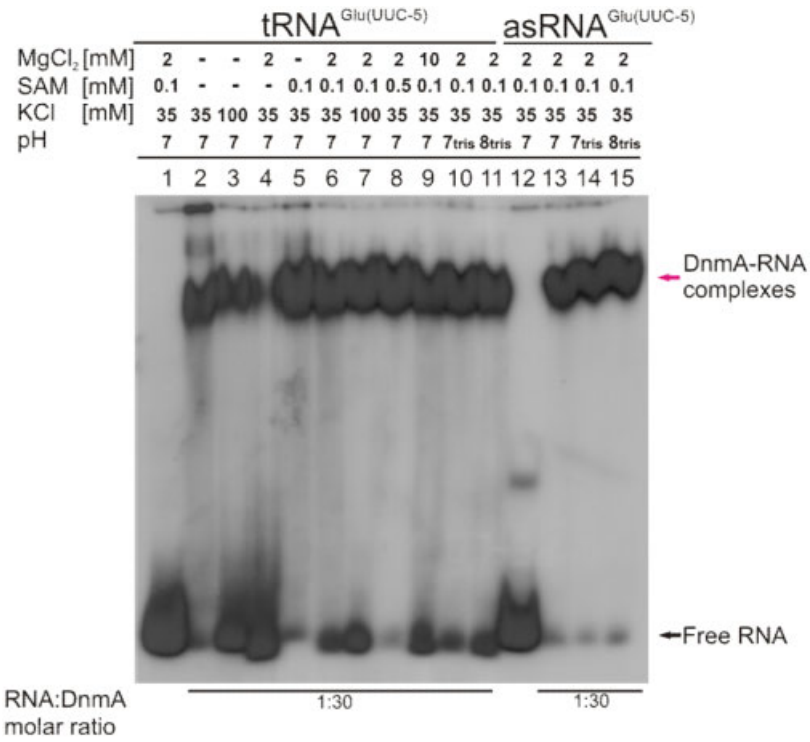

Figure 5.7.4.5 Influence of different components of incubation buffer on binding kinetics of DnmA. For this experiment His-DnmA (245 pmol) was incubated for 15 min at 22ºC with purified $tRNA^{Glu(UUC-5)}$ or antisense

$RNA^{Glu(UUC-5)}$ (8 pmol) in 20 µl of 10 mM PKi buffer, containing 0.2 mM PMSF, 10 mM DTT, 22.5% glycerol and different buffer composition and pH as well as with various concentrations of KCl, $MgCl_2$ or SAM (see the panel on top of the gel). In case of the samples where SAM was added, 10 min pre-incubation of DnmA with cofactor was allowed.

Lanes 2 and 4 as well as lanes 5 and 6 show that the presence of Mg^{2+} can also inhibit binding to tRNA, perhaps due to further compaction of RNA molecules, which leave less available surfaces for interaction with DnmA (free tRNA migrates faster in the gel in the presence of 2 mM $MgC1_2$).

Comparison of lanes 2 and 5 demonstrates that the presence of 100 µM SAM without Mg^{2+} ions does not influence on DnmA binding to tRNA. On the other hand, in the presence of 2 mM $MgC1_2$, the addition of 100 µM SAM improved the binding capacity of DnmA (compare lanes 4 and 6). Moreover, increasing concentration of SAM to 500 µM further improved DnmA binding (lanes 4, 6 and 8). Exchange of PKi buffer for Tris-HCl of the same pH 7.0 did not influence DnmA binding to RNA substrates (compare lanes 6 and 10 or lanes 13 an 14). Finally, incubation in Tris-HCl buffer, pH 8.0 inhibited DnmA binding to some extent (compare lanes 6, 10 and 11 or lanes 13, 14 and 15). Taken together these data demonstrate that pre-incubation of DnmA with SAM is likely the reason for different binding kinetics (Figure 5.7.4.2 and Figure 5.7.4.3). The observed small differences in binding affinities of DnmA towards tRNAs and antisence RNA substrates (Figure 5.7.4.3 and Figure 5.7.4.4) rather argue for a non-specific character of the interaction. Although, it is tempting to suggest that the presence of the specific DnmA-$tRNA^{Glu(UUC-5)}$ complexes (Figure 5.7.4.2, complexes marked by red arrow) may reflect the formation of productive complex between DnmA and the anticodon loop of $tRNA^{Glu(UUC-5)}$, which involve interaction with cytosine at the position 38 (Goll et al, 2006).

5.8 Denaturant-resistant DnmA-RNA complex formation

From the previous studies on binding capacity of DnmA towards DNA/RNA substrates, it seemed that the protein does not have any particular preference in binding to specific nucleotide contexts, except for relatively higher affinity to AT-rich DNA sequences (and/or intrinsic DNA curvature imposed by this type of sequences). On the other hand, the protein shows that its binding affinity increases in the row of ssDNA→dsDNA and it is almost the same for the tested

RNA substrates of the similar size. Thus, an important issue remained to be solved – what is the specific interaction of DnmA with the target nucleic acid? Since the molecular mechanism of cytosine methylation by members of Dnmt2 family enzymes is quite well studied we proposed that specific binding of protein with its target occurs when the protein enters the methylation reaction and forms a covalent intermediate which can potentially be arrested and detected. It has been well established that m^5C DNA MTases can form an irreversible covalent bond with 5-fluoro-2'-deoxycytosine (FdC) within an oligonucleotides. It was found also that hDNMT2 form denaturant-resistant (likely covalent) complexes with oligonucleotides independent of FdC (Dong et al, 2001). Since hDNMT2 shows a strong capacity for methylation of cytosine 38 in $tRNA^{Asp}$, it was suggested that other tRNAs, containing this particular target cytosine can be natural substrates for the members of Dnmt2 family (Jurkowski et al, 2008). If this was the case, it would be possible to trap covalent intermediates and potentially explore the characteristics of these complexes. To assess that question, the available data of genomic sequences of various tRNAs in *Dictyostelium* were analyzed for the presence of cytosine 38 in their anticodon loops (http://dictybase.org). Moverover, it was discovered by the group of Helm that the pattern of C32, A37 and C40, surrounding C38 was necessary for hDNMT2 to show optimal methyltransferase activity (Meusburger, PhD thesis, University of Heidelberg). As a result of search for C38 residues and this pattern in *Dictyostelium* tRNA gene sequences, a short list of different tRNAs was found (in collaboration with S. Müller, Table 5.8.1). Among all 22 genes encoding $tRNA^{Asp(GUC)}$, 3 genes of $tRNA^{Glu(CUC)}$ and 2-20 genes of $tRNA^{Glu(UUC)}$ were found carrying all four invariant residues C32, A37, C38 and C40.

Table 5.8.1 Genes encoding for tRNAs, containing the pattern of C32, A37 and C40 in *Dictyostelium*. The anticodons are marked by green. The nucleotide positions of 32, 37, 38 and 40 are marked by red. Match, partial match! and only C38! refer to the level of similarity to predicted full pattern (C32, A37, C38 and C40).

tRNA gene	Spliced transcript
DDB0234757	tRNA-Asp-GUC-1 on chromosome: 1; 1-22 genes TCCTTGTTGGTCTAGTGGTGAGGATTTTCGCCTGTCACGCGAAAGGCCCGGGTTCA ATTCCCGGACAGGGAG match
DDB0234935	tRNA-Glu-CUC-1 on chromosome: 3; 1, 3 genes TCCTCATTGGTGTAGTCGGTAACACTCTAGTCTCTCACACTGGTACCCCGGGTTCGA TTCCCGGATGGGGAG match
DDB0235073	tRNA-Glu-CUC-2 on chromosome: 6 TCCTCTTTGGTGTAGTCGGTAACACTCTAGTCTCTCACACTGGTACCCCGGGTTCGA TTCCCGGAAGGGGAG match

DDB0234758	tRNA-Glu-UUC-2 on chromosome: 1; 2-20 genes TCCTCATTGGTGTAGTCGGTAACACTCTAGTCTTTCACACTGGTACCTCGGGTTCGA TTCCCGAATGGGGAG match
DDB0234894	tRNA-Gly-GCC-1 on chromosome: 2; 1-18 genes GCGTATGTGGTCTAGTGGTATGATGCATCCCTGCCACGGATGCGAACTGGGTTCGA TTCCCAGCATACGCA partial match!
DDB0234732	tRNA-His-GUG-1 on chromosome: M GAGGGTATAGCTTAAGTGGTTAGAGTATTGGATTGTGACTTCAAAGATACCGGTTC GAGTCCGGTTACCTTCC only C38!
DDB0234854	tRNA-His-GUG-2 on chromosome: 2 ; 2-10 genes GCCGTGATAGTATAGTGGTAGTACATCAGATTGTGGCTCTGTTGACCCTGGTTCGA TTCCAGGTCGCGGCA partial match!
DDB0234860	tRNA-Leu-AAG-1 on chromosome: 2; 1-11 (-8) genes GTAAGCTTGCCCGAGCTGGTCTAAGGGGTTGCATTAAGGCTGCAATATCATTGATA CAAGGGTTCGAATCCCTTAGCTTACA only C38!
DDB0235066	tRNA-Leu-AAG-8 on chromosome: 6 GTAAGCTTGCCCGAGCTGGTTTAAGGGGTTGCATTAAGGCTGCAATATCATTGATA CAAGGGTTCGAATCCCTTAGCTTACA only C38!
DDB0234827	tRNA-Leu-UAG-1 on chromosome: 2; 1-2 genes GGGAGATTGGTCGAGTGGTTAAGACAATAGATTTAGGCTCTATCCTCCGGGGTCGC GGGTTCGAACCCCGCATCTCTCA partial match!
DDB0235138	tRNA-Leu-UAG-3 on chromosome: 6 GGAAGATTGGTCGAGATGGTTAAGACAATAGATTTAGGCTCTATCCTCCGGGGTCG TGGGTTCGAGTCCCTCATCTTCCA partial match!
DDB0234724	tRNA-Met-CAU-1 on chromosome: M GGTGAGATGGAATAATTGGTTAGTTCATTGGGTTCATGCCCCAAAGGTGTAGGTTC GAGTCCTACTCTTGCCA partial match!
DDB0234777	tRNA-Val-AAC-2 on chromosome: 1; 2-21 genes GTTCGGATGGTGTAGTCGGTTATCACGAATCCTTAACACGGATTAGGTCGTGGGTT CGATTCCCGCTCTGAATA only C38!
DDB0234789	tRNA-Val-CAC-1 on chromosome: 1 GGGAAAGTAGTGTAGTGGTTATCACGAGCCCTTCACACGGGTTAGGTCGTGGGTTC GATCCCCATCTATCTCA only C38!
DDB0234809	tRNA-Val-UAC-1 on chromosome: 1; 1, 4-7 genes GGTCGGATGGTGTAGTCGGTTATCACGGTTGCTTTACACGCAACAGGTCTCGAGTT CGATCCTCGGTCGGATCA partial match!
DDB0234912	tRNA-Val-UAC-2 on chromosome: 3 GGTTTGATGGTGTAGTTGGTTATCACGGTTGCTTTACACGCAACAGGTCTCGAGTTC GATCCTCGGTCGGATCA partial match!
DDB0235028	tRNA-Val-UAC-3 on chromosome: 5 GGTCAGATGGTGTAGTCGGTTATCACGGTTGCTTTACACGCAACAGGTCTCGAGTT CGATCCTCGGTCAGATCA partial match!
DDB0234735	tRNA-Phe-GAA-2 on chromosome: 2F ; 3-14, 16 genes GCCTTAGTAGCTCAGTTGGTACGAGCGTGAGACTGAAGATCTTAAGGTCGCTGGTT CGATCCCGGCCTGAGGCA partial context, no C38!

Several addition constructs were prepared to use for *in vitro* transcription, including $tRNA^{Glu(UUC-5)C38A}$, where cytosine 38 was substituted for adenine (kindly supplied by S. Müller) and $tRNA^{Phe(GAA-2)}$, where only C32 and C40 are presented (Table 5.8.1 and Figure 5.8.1A).

Figure 5.8.1B shows that DnmA indeed formed denaturant-resistant complexes with $tRNA^{Asp(GUC-1)}$, $tRNA^{Glu(UUC-5)}$ and $tRNA^{Glu(CUA-5)}$ while with other tRNAs (Phe(GAA-2) and Glu(UUC-5)C38A) and asRNAs no complexes was detected.

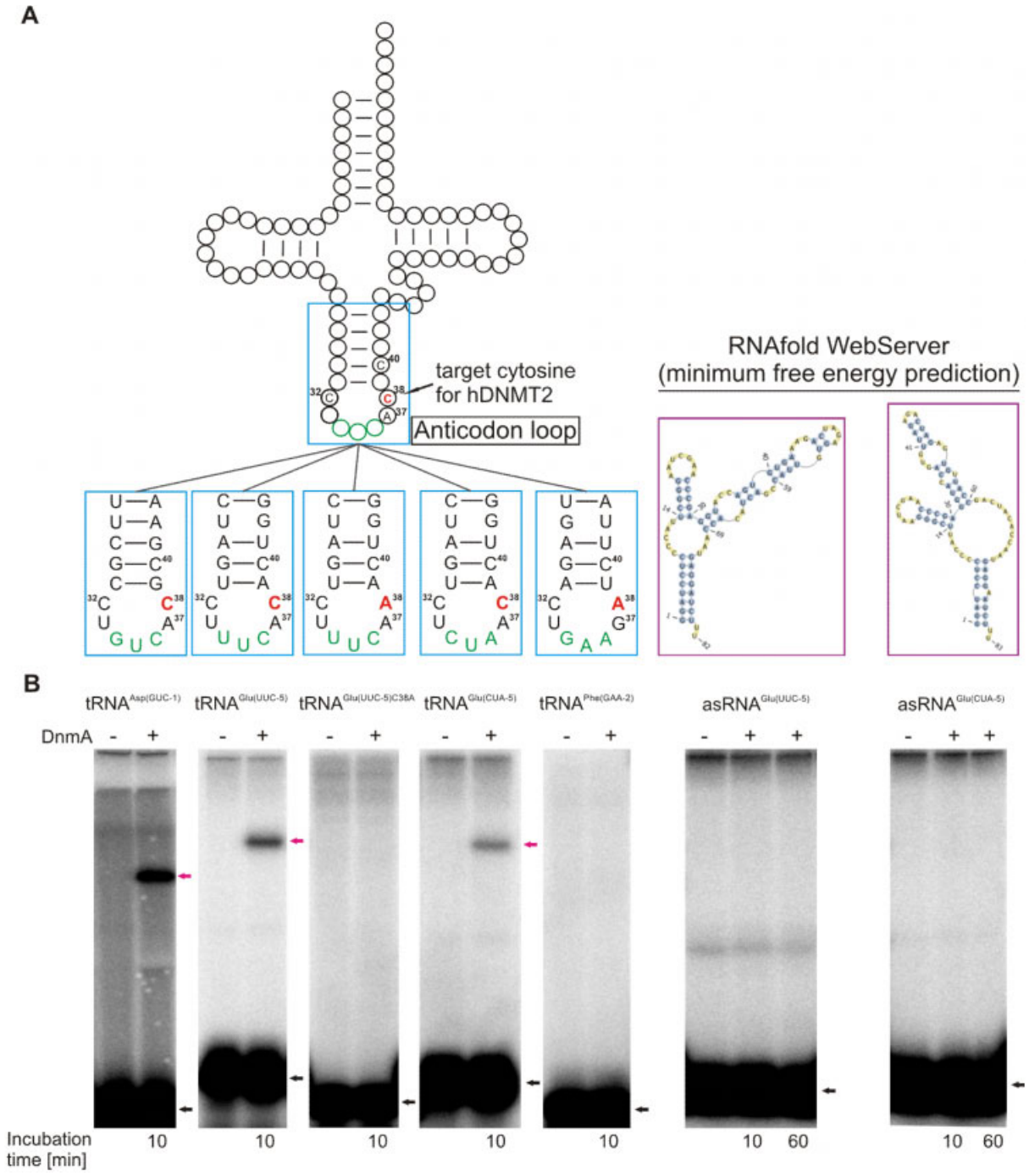

Figure 5.8.1 (**A**) Schematic representation of RNA substrates used for detection of denaturant-resistant DnmA-RNA complexes. Five different naturally occurring and modified tRNAs as well as two antisense RNA transcripts derived

from gene sequences of $tRNA^{Glu(UUC-5)}$ and $tRNA^{Glu(CUA-5)}$ were used for experiments. Positions of residues in the established pattern are shown by numbers. Target cytosine or other nucleosides at position 38 of anticodon loop is marked by red letter in bold. Anticodons of corresponding tRNAs is labeled by green letters. (**B**) Formation of denaturant-resistant DnmA-RNA complexes. Autoradiographs of gels correspond to upper schematic representations of RNA substrates. His-DnmA (190-200 pmol) was incubated with different RNA substrates (10 pmol) in 20 µl of 10 mM PKi buffer, pH7.0, 25 mM KCl, 2 mM $MgCl_2$, 10 mM DTT, 22.5% glycerol and 100 µM SAM, at 22ºC (10 min pre-incubation of protein with SAM was allowed). Reactions were terminated at the indicated times by addition of SDS to 2% and glycerol to 12% and heating at 65ºC for 10 min, subjected to 10% SDS-PAGE and autoradiographed. The synthesis, radioactive labeling and purification of RNA substrates have been described in Methods.

Formation of these complexes seemed to be very specific and could also be observed if appropriate tRNA substrates were embedded into larger RNA construct (Figure 5.8.2A), which did not interfere with folding of native tRNA structure. Figure 5.8.2B demonstrates that DnmA-RNA complexes appeared only in the case of gusPSTVd RNA transcripts, containing $tRNA^{Glu(UUC-5)}$ or $tRNA^{Glu(CUA-5)}$ sequences, while both empty gusPSTVd RNA transcript and gusPSTVd RNA, containing antisense $RNA^{Glu(CUA-5)}$ did not form such complexes with the protein.

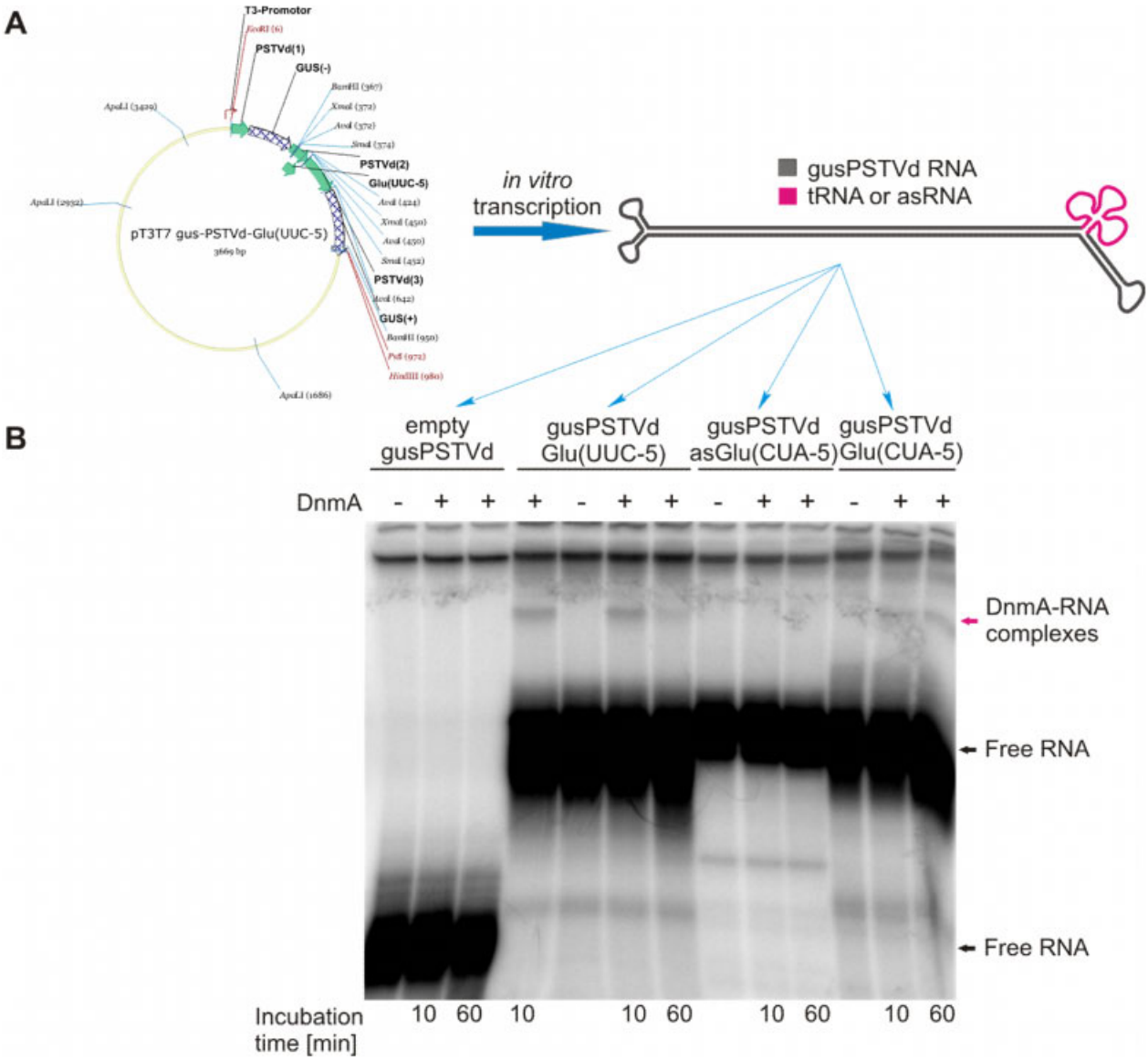

Figure 5.8.2 (**A**) Schematic representation of RNA substrates used for detection of denaturant-resistant DnmA-RNA complexes. Four different gusPSTVd constructs, containing naturally occurring and modified tRNAs as well as antisense RNA transcripts derived from gene sequence of $tRNA^{Glu(CUA-5)}$ were used for experiments (corresponding plasmids for *in vitro* transcription were kindly provided by A. Schöne). (**B**) Formation of denaturant-resistant DnmA-RNA complexes. His-DnmA (200 pmol) was incubated with different RNA substrates (1.95 pmol) in 20 µl of 10 mM PKi buffer, pH7.0, 25 mM KCl, 2 mM $MgCl_2$, 10 mM DTT, 22.5% glycerol and 100 µM SAM, at 22ºC (10 min pre-incubation of protein with SAM was allowed). Reactions were terminated at the indicated times by addition of SDS to 2% and glycerol to 12% and heating at 65ºC for 10 min, subjected to 7% SDS-PAGE and autoradiographed. The synthesis, radioactive labeling and purification of RNA substrates have been described in Methods.

To test the influence of different buffer components and pH on denaturant-resistant DnmA-RNA complex formation, an assay with $tRNA^{Glu(UUC-5)}$ as a substrate was performed (Figure 5.8.3). As described before in the indicated samples (5-11, the top panel in Figure 5.8.3) 10 min pre-incubation of DnmA with SAM prior to addition of the RNA substrate was allowed. The results clearly demonstrate that denaturant-resistant DnmA-RNA complexes could be formed only in the presence of both 2 mM $MgCl_2$ and 100 µM SAM (compare lanes 4, 5 and 6). Moreover, moderate levels of salt concentration (35 mM KCl) was required since increasing the concentration of KCl up to 100 mM decreased significantly the manifestation of DnmA-RNA complexes (compare lanes 6 and 7).

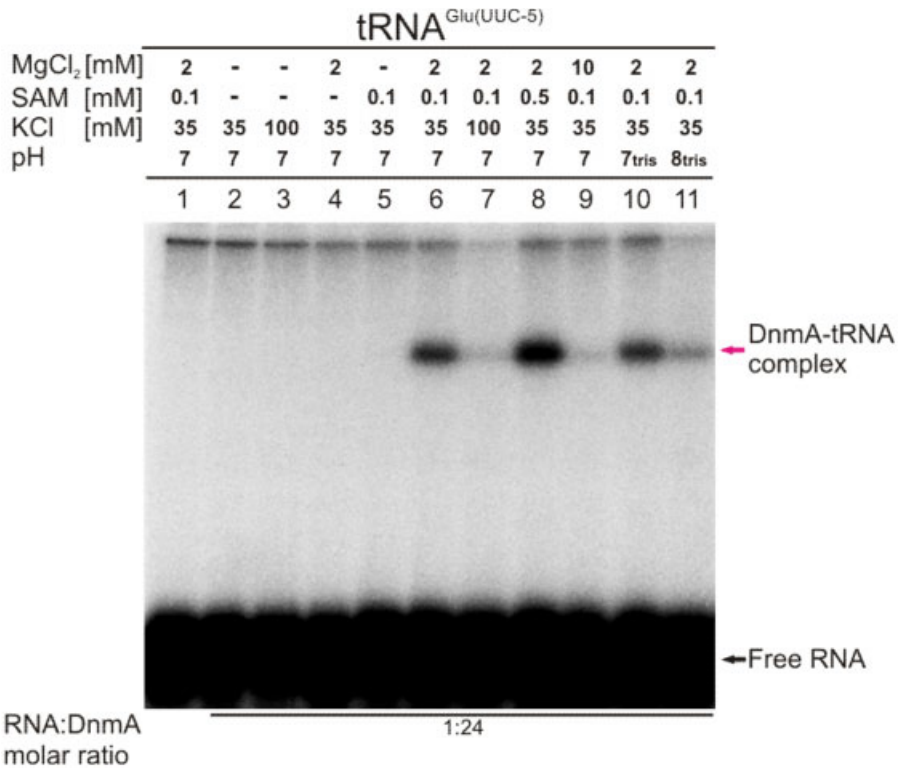

Figure 5.8.3 Influence of different components of incubation buffer on formation of denaturant-resistant DnmA-RNA complex. For this experiment His-DnmA (240 pmol) was incubated for 5 min at 22ºC with purified $tRNA^{Glu(UUC-5)}$ or antisense $RNA^{Glu(UUC-5)}$ (10 pmol) in 20 µl of 10 mM PKi buffer, pH 7.0, containing 0.2 mM PMSF, 10 mM DTT, 22.5% glycerol and different buffer composition and pH with various concentrations of KCl, $MgCl_2$ or SAM. In case of the samples where SAM was added, 10 min pre-incubation of DnmA with cofactor was allowed.

Moreover, higher concentration of SAM in solution (500 μM) seemed to improve catalytic activity of DnmA towards tRNA substrates, at least for $tRNA^{Glu(UUC-5)}$ (compare lanes 6 and 8). On the contrary, the presence of 10 mM $MgCl_2$ significantly decreased denaturant-resistant DnmA-RNA complex formation, perhaps due to further compaction of tRNA molecules which would potentially make C38 unavailable for protein (lanes 6 and 9). Changing the buffer from PKi to Tris-HCl of the same pH 7.0 did not influence the specific complex formation (similar to observation from gel retardation assays in native gels), while an increase of pH up to 8.0 reduced profoundly the amount of such complexes (which was less obvious for native complex formation in gel retardation assays) (compare lane 6 with lanes 10 and 11). More detailed studies of how various components of the incubation buffer and their concentrations influence DnmA-tRNA complex formation allowed us to formulate some generalized buffer, which provided optimal conditions to trap and visualize denaturant-resistant complexes. These conditions include low salt concentration 25 mM KCl, pH 6.5-7, 2 mM $MgCl_2$, 10 mM DTT, 22.5% glycerol and 100-500 μM of SAM. Pre-incubation of protein with SAM prior incubation with RNA substrate seemed to favor complex formation.

The presence of SAM, at least at the concentration of 100 μM, without $MgCl_2$ did not influence the binding of tRNA (Figure 5.7.4.5, compare lanes 2 and 5) but in the presence of 2 mM $MgCl_2$ could activate such binding (Figure 5.7.4.5, compare lanes 4, 6 and 8). It was also clear that SAM was a necessary cofactor to form specific denaturant-resistant DnmA-tRNA complexes (Figure 5.8.3, lanes 4 and 6). Taken together, these data suggest that in the presence of Mg^{2+} SAM could play both the role of a relatively weak allosteric effector which would reinforce the affinity of the enzyme for at least appropriate tRNA substrates and as a donor of methyl groups.

In the presence of 1 mM $MgCl_2$, SAM (100 μM) and the competitive inhibitor of SAM, sinefungin (100-1000 μM), could not inhibit or activate the binding activity of DnmA towards DNA of DIRS1_rLTR retrotransposon (data not shown). Nevertheless, sinefungin by its own prevented formation of denaturant-resistant protein-tRNA complexes and could inhibit its formation to some extent while present together with SAM in an equimolar amount (Figure 5.8.4B). This demonstrates that SAM can be relatively easy exchanged by sinefungin which was supported by observation that DnmA binds SAM with much lower affinity when compared to hDNMT2. Figure 5.8.5A demonstrates that at least the portion of recombinant hDNMT2 purified from *E.coli* (under the same conditions as used for recombinant DnmA), remains loaded with

endogenous SAM, which can be explained by stronger binding between hDNMT2 and cofactor, while DnmA might lose it during the purification procedure.

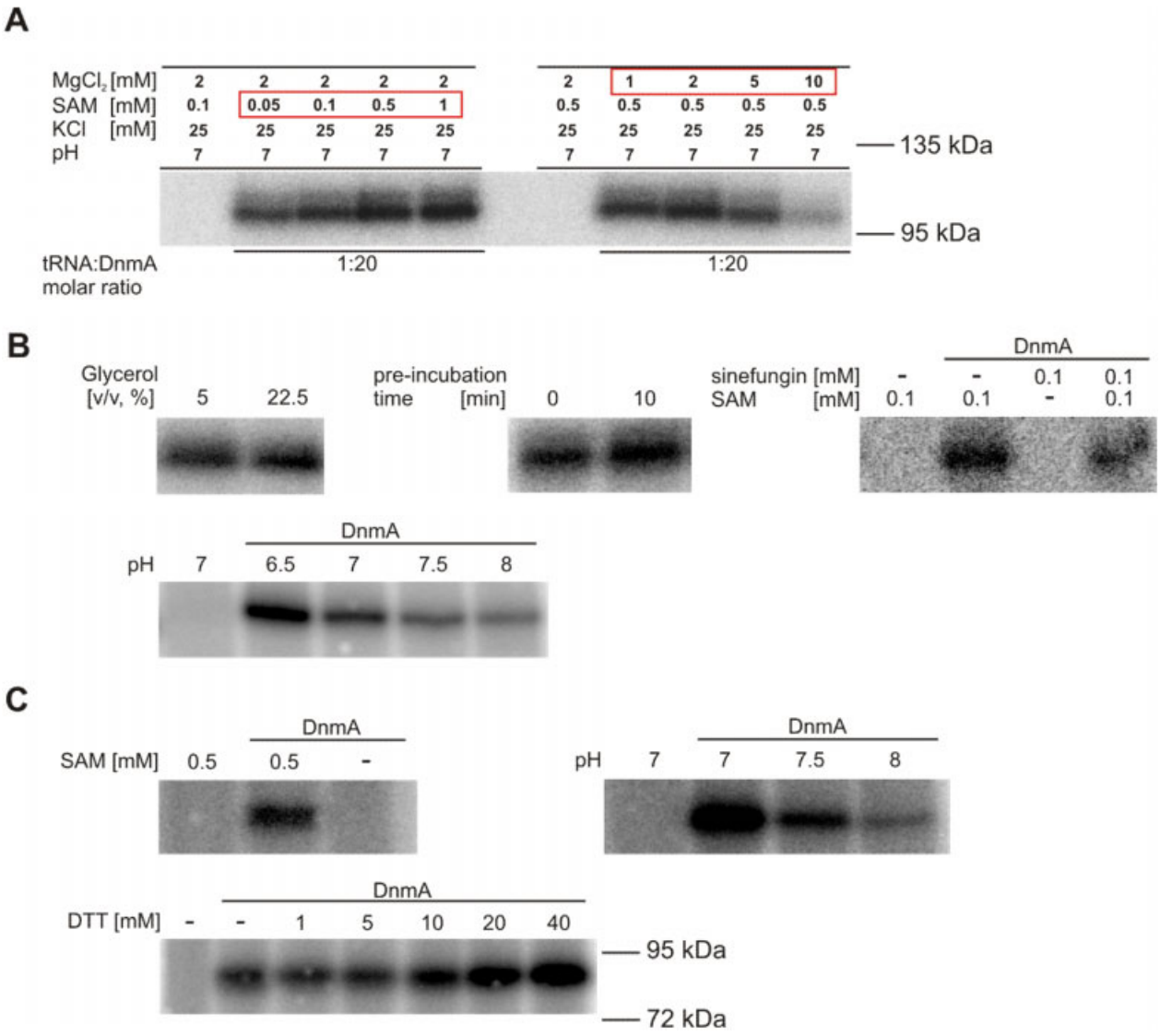

Figure 5.8.4 Detailed examination of buffer conditions for formation denaturant-resistant DnmA-tRNA complexes. All experiments were carried out at similar conditions except for pointed changes. His-DnmA (160-200 pmol) was incubated for 5 min at 22ºC with purified $tRNA^{Glu(UUC-5)}$ or $tRNA^{Asp(GUC-1)}$ (10-24 pmol) in 20 µl of 10 mM PKi buffer, pH 7.0, containing 25 mM KCl, 2 mM $MgCl_2$, 0.2 mM PMSF, 10 mM DTT, 22.5% glycerol and 500 µM SAM. As described before in appropriate samples 10 min pre-incubation of DnmA with SAM prior to addition of RNA substrate were allowed. (**A**) Influence of different concentrations of SAM and $MgCl_2$ on formation of DnmA-$tRNA^{Glu(UUC-5)}$ complexes. (**B**) Influence of glycerol concentration, presence of 10 min pre-incubation step, presence of sinefungin (competitive inhibitor analog of SAM) and pH in a range from 6.5 to 8. (**C**) Influence of presence of

SAM and different pH on DnmA-tRNA$^{Asp(GUC-1)}$ complex formation, including dependence on different concentrations of DTT.

As to other properties of hDNMT2 interaction with tRNA substrates, they are similar to those of DnmA. The presence of sinefungin or absence of Mg^{2+} ions prevents formation of denaturant-resistant hDNMT2-tRNA complexes (Figure 5.8.5B).

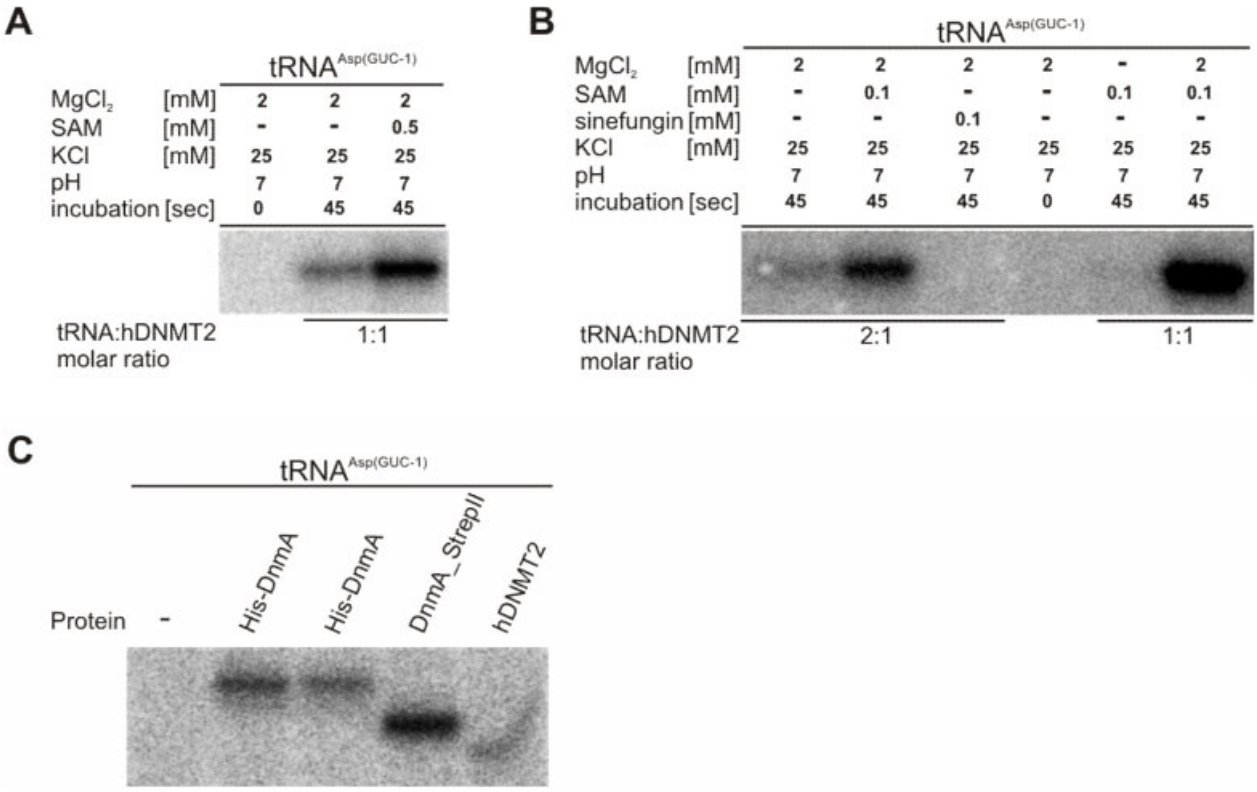

Figure 5.8.5 Formation of denaturant-resistant enzyme-tRNA complexes. All experiments were carried out at similar conditions except for pointed changes. hDNMT2 (65 pmol) was incubated for 45 sec at 37ºC with purified tRNA$^{Asp(GUC-1)}$ (20-40 pmol) in 20 µl of 10 mM PKi buffer, pH 7.0, containing 25 mM KCl, 2 mM $MgCl_2$, 0.2 mM PMSF, 10 mM DTT, 22.5% glycerol and 500 µM SAM. As described before in appropriate samples 10 min pre-incubation of enzymes with SAM prior to addition of RNA substrate were allowed. (**A**) Formation of denaturant-resistant hDNMT2-tRNA complexes. Human DNMT2 is characterized by stronger binding with SAM, since portion of protein purified from *E.coli* seems to be loaded with endogenous cofactor and remains in this bound form during purification. (**B**) Formation of hDNMT2-tRNA complexes in presence of sinefungin (competitive inhibitor of MTases) or absence of $MgCl_2$. (**C**) Formation of denaturant-resistant complexes with tRNA$^{Asp(GUC-1)}$ by different enzyme preparations, including DnmA-StrepII.

Figure 5.8.5C shows that the DnmA-StrepII fusion purified from *Dictyostelium* cells could also form complexes with appropriate tRNA substrates. Moreover, relatively low amounts of DnmA-StrepII protein appeared to be more efficient in complex formation compared to the His-DnmA protein, which can be either explained by more accurate folding of DnmA-StrepII in *Dictyostelium* or by the presence of appropriate post-translational modifications.

Denaturant-resistant complexes formed by recombinant DnmA (as well as hDNMT2) disappeared after a certain time of incubation. The half-time was characteristic for different tRNA substrates (Figure 5.8.6). Moreover, the kinetics of denaturant-resistant enzyme-tRNA complex formation was unlike the kinetics observed earlier for hDNMT2 and DNA oligonucleotides, where the time course of product accumulation was linear for more than 2 hrs (Dong et al, 2001).

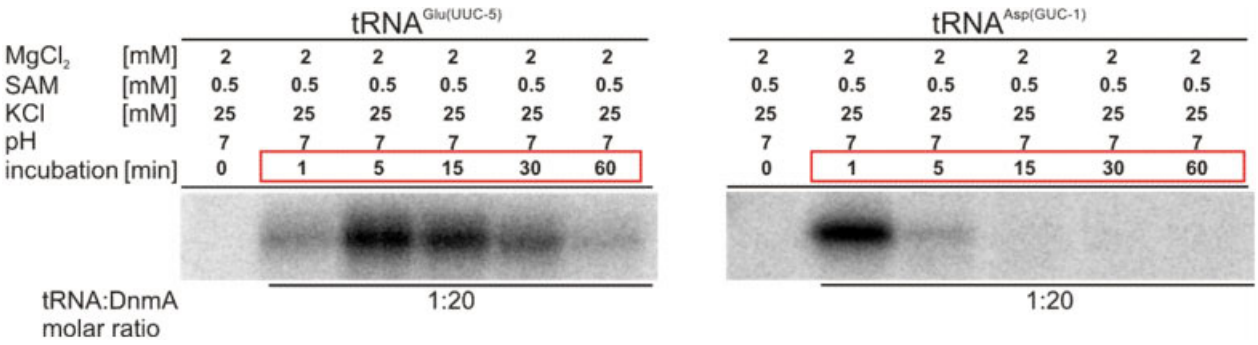

Figure 5.8.6 The time course of denaturant-resistant complex accumulation for DnmA and $tRNA^{Glu(UUC-5)}$ (left) or $tRNA^{Asp(GUC-1)}$ (right). All experiments were carried out at similar conditions. His-DnmA (200 pmol) was incubated for 5 min at 22ºC with purified $tRNA^{Glu(UUC-5)}$ or $tRNA^{Asp(GUC-1)}$ (10 pmol) in 20 µl of 10 mM PKi buffer, pH 7.0, containing 25 mM KCl, 2 mM $MgCl_2$, 0.2 mM PMSF, 10 mM DTT, 22.5% glycerol and 500 µM SAM. As described before in appropriate samples 10 min pre-incubation of DnmA with SAM prior to addition of RNA substrate were allowed.

More detailed time course assays, monitoring enzyme-tRNA complexes formation as a function of time revealed differences in catalytic activity of DnmA towards various tRNA substrates. Figure 5.8.7A shows the dynamics of DnmA-tRNA complex formation under different Mg^{2+} ion concentrations. The peaks, reflecting maximal amount of the observed complexes, appeared at the specific incubation times for different tRNA substrates.

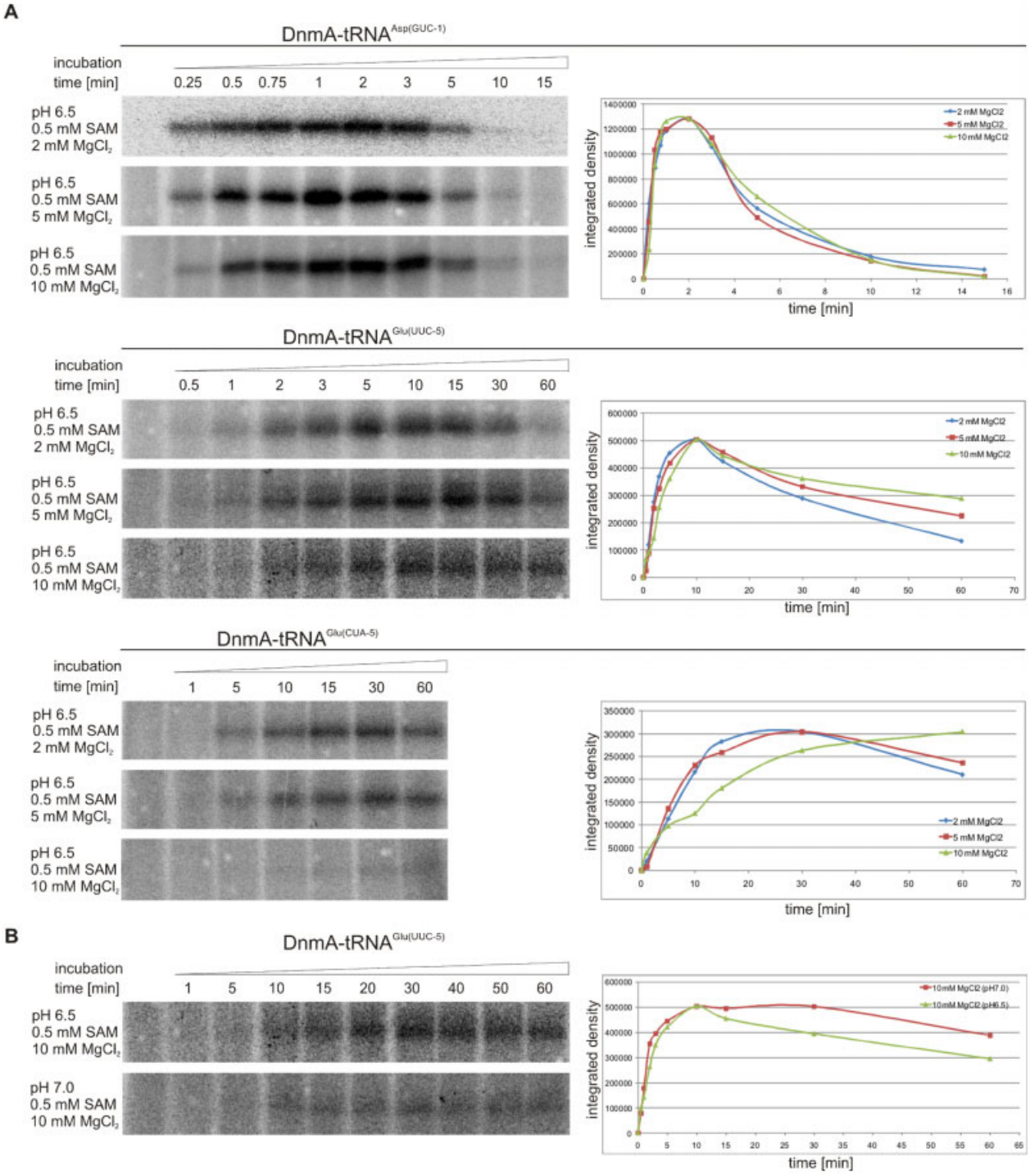

Figure 5.8.7 The time course of denaturant-resistant covalent intermediate accumulation for DnmA and various tRNA substrates. (**A**) Influence of different concentrations of Mg^{2+}. (**B**) Influence of different pH. All experiments were carried out at similar conditions. His-DnmA (120-160 pmol) was incubated for indicated times at 22ºC with purified tRNA substrates (10-24 pmol) in 20 µl of 10 mM PKi buffer, pH 6.5, containing 25 mM KCl, 0.2 mM

PMSF, 10 mM DTT, 22.5% glycerol and 500 µM SAM. 10 min pre-incubation of DnmA with SAM prior to addition of RNA substrates were allowed. Data were adjusted to the maximal observed value of integrated density.

In the presence of 2 mM $MgCl_2$ (Figure 5.8.7A, blue curves on the graphs), the peak of DnmA-tRNA$^{Asp(GUC-1)}$ complex accumulation appeared at approximately 2 min and complexes resolved mainly within 15 min. The accumulation kinetics for DnmA-tRNA$^{Glu(UUC-5)}$ and DnmA-tRNA$^{Glu(CUA-5)}$ was substantially different, with the observed peaks at approximately 10 and 25-30 min, respectively. In these two cases, the complexes also disappeared after much longer incubation times.

These experiments also provided information on the influence of Mg^{2+} concentration on kinetics of denaturant-resistant complex formation with different tRNA targets. Figure 5.8.7A shows that a change in concentration of Mg^{2+} from 2 to 10 mM seemed to have no effect on denaturant-resistant DnmA-tRNA$^{Asp(GUC-1)}$ complex formation. In contrast, increasing concentration of Mg^{2+} ions apparently influenced the dynamics of the DnmA-tRNA$^{Glu(UUC-5)}$ and DnmA-tRNA$^{Glu(CUA-5)}$ complex formation. These resulted in a shallower slope of the curves or even in a significant time shift of the observed maximal accumulation of denaturant-resistant products (Figure 5.8.7A, red and green curves). One possible explanation could be the three dimensional conformation of tRNA$^{Glu(UUC-5)}$ and tRNA$^{Glu(CUA-5)}$ which may be more sensitive for different concentrations of Mg^{2+} and in turn may inhibit some of the steps in the catalytic mechanism of the enzyme. The influence of changes in three dimensional conformation of either the tRNA substrate or both tRNA and enzyme on the catalytic activity may be also concluded from the proposed catalytic mechanism for DNA m^5C MTases (Svedruzic & Reich, 2005), where at least three amino acid residues of the enzyme are required for a specific fixation of the target cytosine base within the catalytic center of DnmA (Figure 5.8.8).

Taking into consideration the proposed catalytic mechanism, we concluded that observed denaturant-resistant DnmA-tRNA complexes most likely correspond to covalent enamine intermediate on a way of the catalytic mechanism of DnmA (Figure 5.8.8A). The formation of the covalent DnmA-tRNA$^{Asp(GUC-1)}$ intermediate appeared to be efficient and this complex was relatively easy resolved (Figure 5.8.7A). Moreover, multiple methylation assays demonstrated that tRNA$^{Asp(GUC-1)}$ is a good substrate for methylation, though increasing concentration of Mg^{2+} significantly inhibited the methyltransfer reaction (Müller, personal communication).

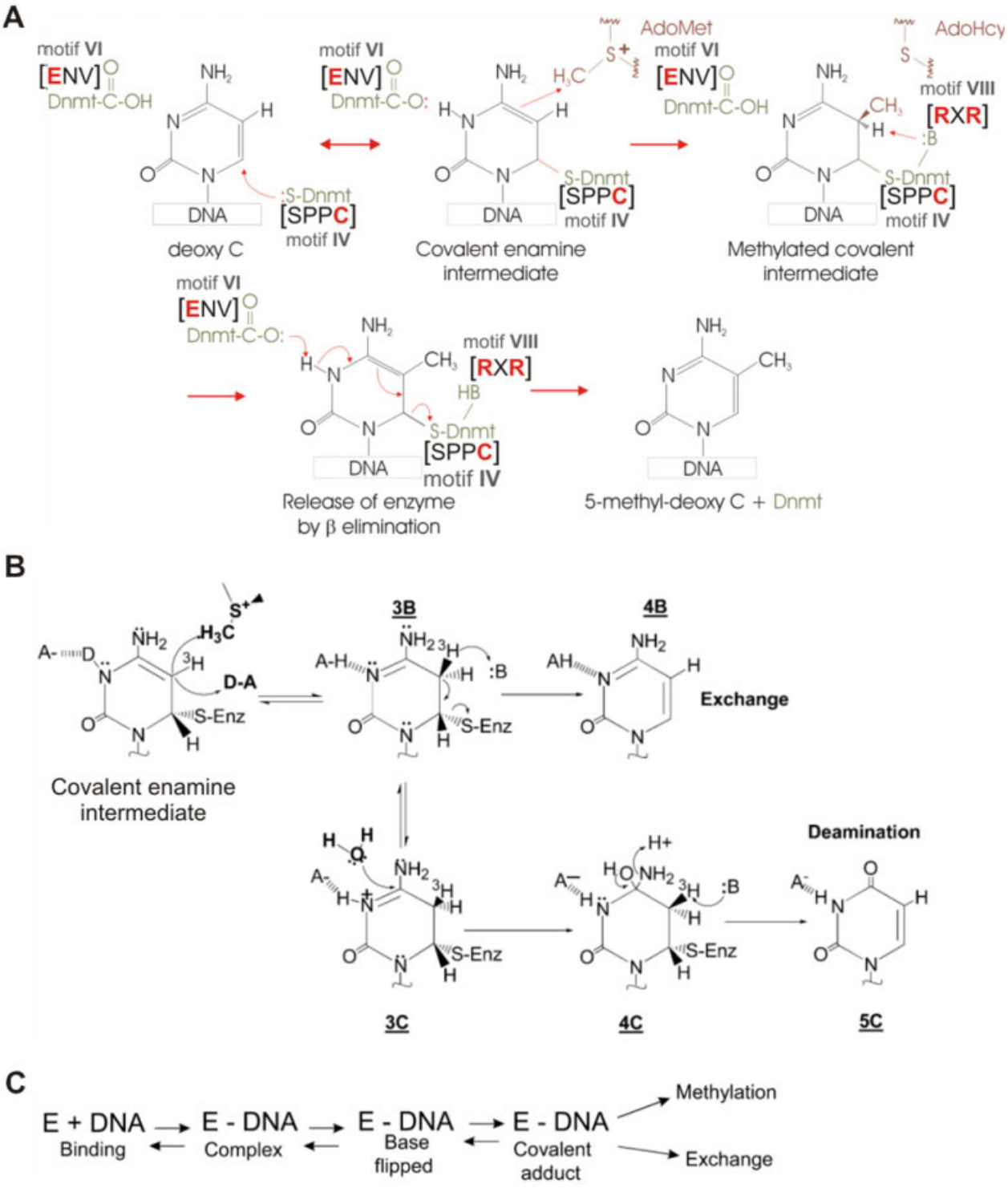

Figure 5.8.8 (**A**) Schematic representation of the main direction (methylation) in the catalytic mechanism proposed for DNA m^5C MTases. Conservative motifs, including invariant amino acid residues of DnmA enzyme are presented. Adapted from Goll et. al., 2006. The target cytosine interacts with active site residues to facilitate cysteine nucleophilic attack at the C6 position. Nucleophilic attack disrupts the pyrimidine's aromaticity, generating

the reactive covalent adduct (covalent enamine intermediate). Covalent enamine intermediate can readily undergo electrophilic addition, either through methylation (A) or protonation (3B). (**B**) Schematic representation of the side directions (exchange and deamination) in the catalytic mechanism, proposed for DNA m^5C MTases. 3B can lead to the exchange reaction (4B) or to mutagenic deamination (3B > 4C > 5C). Acidic groups are labeled as HA and basic groups are labeled as :B. All exchangeable protons are shown as D in intermediates. Conserved active site residues are indicated. Adapted from Svedruzic and Reich, 2005. (**C**) Four steps that control the target base attack by methyltransferases in a rapid equilibrium.

The increasing Mg^{2+} concentration, however, did not influence covalent DnmA-$tRNA^{Asp(GUC-1)}$ complex formation, and this apparent discrepancy may be explained by the existence of alternative way for electrophilic addition: not through methylation but through protonation, which leads to either exchange reaction or to mutagenic deamination (Figure 5.8.8B). The presence of alternative way in the catalytic mechanism of DnmA may also be a reason for low levels of $tRNA^{Glu(UUC-5)}$ methylation (Müller, personal communication) while the covalent DnmA-$tRNA^{Glu(UUC-5)}$ intermediate can still be observed (Figure 5.8.7A). On the other hand, it seems that formation of the enamine intermediate is a reversible reaction and the changes in an equilibrium state could also contribute to the low yield of methylated products. Intriguingly, the relatively high degree of methylation was observed for $tRNA^{Glu(CUA-5)}$ (Müller, personal communication), although there are apparent difficulties in DnmA-$tRNA^{Glu(CUA-5)}$ complex formation and resolving (Figure 5.8.7A). To provide more precise description of observed dynamics, additional data on the comparative contribution of alternative ways into catalytic mechanism and the equilibrium parameters of the reaction of the enamine intermediate formation are required. We cannot exclude as well the influence of differences in tertiary structure of tRNAs on observed dynamics, thus the control of RNA folding seems to be indispensable for proper analysis.

We found that increasing pH inhibited the methyltransfer reaction by DnmA (Sara Müller, personal communication), but has a less pronounced influence on covalent complex formation (Figure 5.8.7B). This may be explained by changes in the charge potential of the enzyme, leading to conformational changes or by influence of pH on local charges in the catalytic center, which could possibly influence the reaction on the way to enamine intermediate.

Additionally, Figure 5.8.9A clearly shows differences in the covalent intermediate formation between $tRNA^{Glu(UUC-5)}$ and $tRNA^{Glu(CUA-5)}$ which have the same sequence except for 2 bases

exchanged in the anticodon. This observation together with detected differences in methylation assays (Müller, personal communication) demonstrated that not only a certain pattern of invariant nucleotides found previously (C32, A37 and C40; Helm, personal communication) was important for successful activity of both DnmA and hDNMT2 enzymes but other features of the substrate molecules, perhaps specific folding which may favor better access of the protein to the target cytosine base.

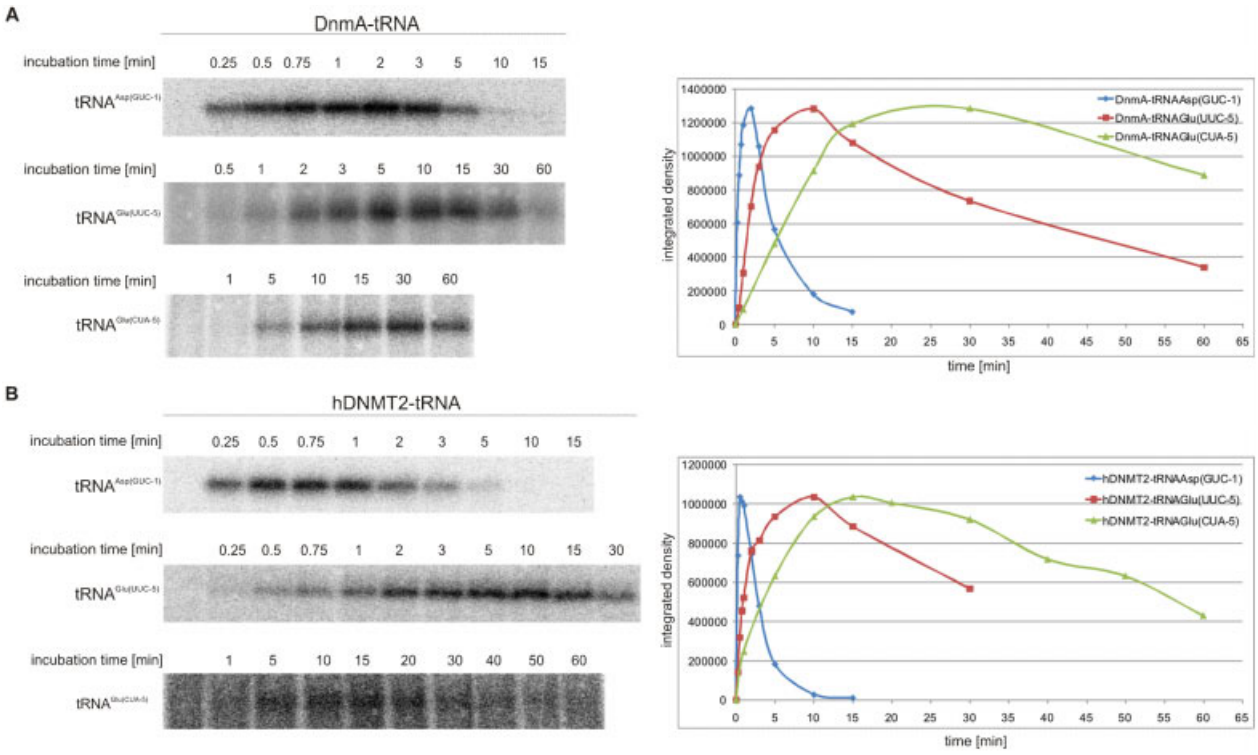

Figure 5.8.9 (**A**) The time course of covalent intermediate accumulation for DnmA and various tRNA substrates. All experiments were carried out at similar conditions. His-DnmA (120-160 pmol) was incubated for indicated times at 22ºC with purified tRNA substrates (10-24 pmol) in 20 µl of 10 mM PKi buffer, pH 6.5, containing 25 mM KCl, 2 mM $MgCl_2$, 0.2 mM PMSF, 10 mM DTT, 22.5% glycerol and 500 µM SAM. 10 min pre-incubation of DnmA with SAM prior to addition of RNA substrates were allowed. (**B**) The time course of covalent intermediate accumulation for hDNMT2 and various tRNA substrates. His-hDNMT2 (50-120 pmol) was incubated for indicated times at 37ºC with purified tRNA substrates (10-24 pmol) in 20 µl of 10 mM PKi buffer, pH 6.5, containing 25 mM KCl, 2 mM $MgCl_2$, 0.2 mM PMSF, 10 mM DTT, 22.5% glycerol and 500 µM SAM. 10 min pre-incubation of hDNMT2 with SAM prior to addition of RNA substrates were allowed. Data were adjusted to the maximal observed value of integrated density.

Figure 5.8.9 also shows that the dynamics of covalent complex accumulation for corresponding tRNAs was similar for DnmA and hDNMT2, with the observed peaks for hDNMT2-$tRNA^{Asp(GUC-1)}$ complex at approximately 1-2 min of incubation, hDNMT2-$tRNA^{Glu(UUC-5)}$ at 5-10 min and for hDNMT2-$tRNA^{Glu(CUA-5)}$ at 15 min (compare panels **A** and **B**). In this respect, it is interesting to notice that the experiments were conducted under the temperatures 22ºC for DnmA and 37ºC for human DNMT2, which are natural for respective organisms.

5.9 Denaturant-resistant DnmA-DNA complex formation

Considering the fact what members of Dnmt2 family were originally discovered as DNA m^5C MTase enzymes bearing all the features and motifs characteristic for those proteins, it was interesting if DnmA could also accept DNA sequences as a substrate *in vitro* and form corresponding covalent adducts. It was possible to show the formation of denaturant-resistant DnmA-DNA complexes with DNA of DIRS1-rLTR sequence which we used previously for an EMSA and AFM experiments. Figure 5.9.1 shows the result of one such assay and it is clear that DnmA can indeed form a small but detectable amount of covalent complexes, although with less efficiency compared to hDNMT2. Furthermore, these complexes can be trapped exclusively on DNA samples which were boiled and quenched on ice to provide single stranded DNA species. Another interesting observation from those experiments was the apparent independence of covalent intermediate formation from the presence or absence of Mg^{2+} ions. This suggested that dsDNA may not be an appropriate natural substrate for the enzyme unless some additional factors are involved in the methylation process which could assist to unwind the double helix and make the target cytosine base DNA more accessible for the protein. Indeed, it was not possible to detect any traces of methylated material in methylation assays for dsDNA of DIRS1_rLTR_280 *in vitro* (Müller, personal communication). Taking in account the proposed mechanism of m^5C methylation these results show that in case of dsDNA, the rate determining step in catalysis most likely could be the limited ability (if any) of enzyme alone to conduct a base flipping.

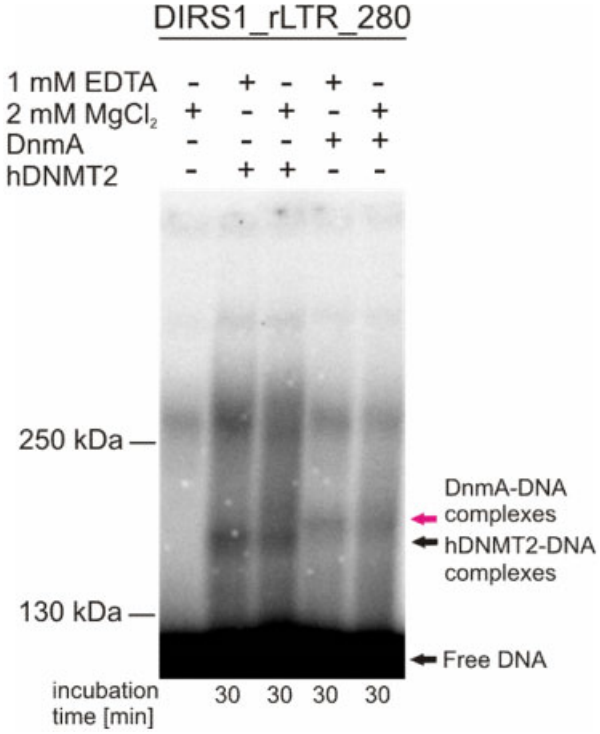

Figure 5.9.1 Trapped covalent DnmA-DNA and hDNMT2-DNA adducts using DNA sequence of DIRS1 (right LTR) retrotransposon. His-DnmA or His-hDNMT2 (120-200 pmol) was incubated for the indicated times at 22ºC (or 37ºC for human enzyme) with labeled DNA of *Dictyostelium* DIRS1_rLTR (200-300 pmol) in 20 µl of 10 mM PKi buffer, pH 7.0, containing 25 mM KCl, 2 mM $MgCl_2$ (or 1 mM EDTA), 0.2 mM PMSF, 10 mM DTT, 22.5% glycerol and 100 µM SAM. 10 min pre-incubation of enzymes with SAM prior to addition of RNA substrates were allowed.

From previous experiments with tRNAs, we hypothesized that certain structures of the substrate could be required for successful enzyme activity. To this end we designed several DNA oligonucleotides to mimic the structure of the anticodon loops of known tRNA targets to trap covalent intermediates (Figure 5.9.2A). Figure 5.9.2B shows the results of covalent complex formation between DnmA and DNA oligonucleotides of different sequence and structure. Surprisingly, all of the tested oligonucleotides gave a denaturant-resistant adducts, including the LAspC38A and LGluC38T (loop of Asp or Glu), which have the target C38 exchanged. Moreover in most cases the complexes were not forming discrete bands but rather gave a broader distribution, suggesting the presence of different types of the complexes.

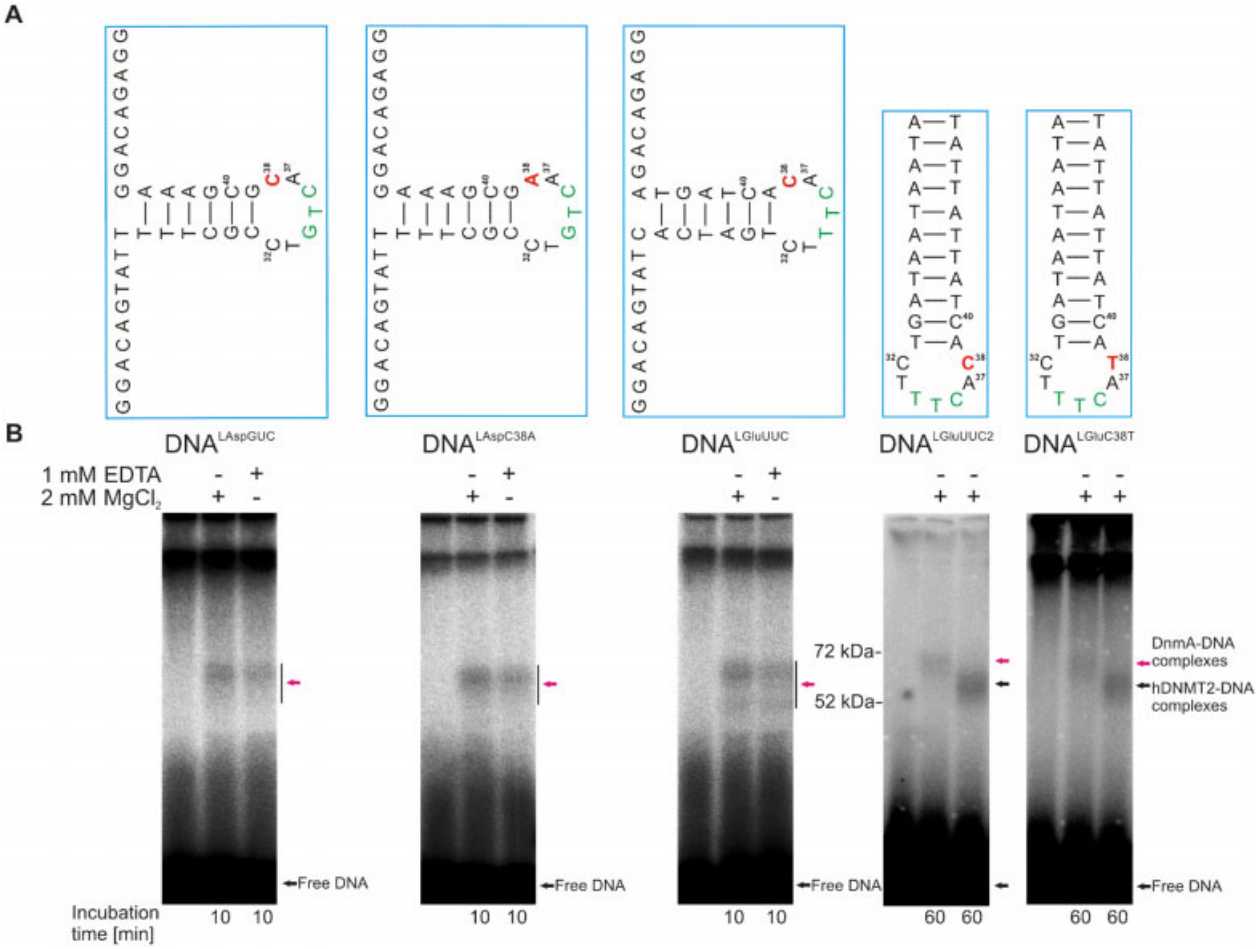

Figure 5.9.2 (**A**) Schematic representation of secondary structure for different DNA oligonucleotides. (**B**) Covalent intermediates formed by DnmA or hDNMT2 with different DNA oligonucleotides depicted above. His-DnmA or His-hDNMT2 (120-200 pmol) was incubated for the indicated times at 22ºC (or 37ºC for human enzyme) with labeled DNA oligonucleotides (200-300 pmol) in 20 µl of 10 mM PKi buffer, pH 7.0, containing 25 mM KCl, 2 mM $MgCl_2$ (or 1 mM EDTA), 0.2 mM PMSF, 10 mM DTT, 22.5% glycerol and 100 µM SAM. 10 min pre-incubation of enzymes with SAM prior to addition of RNA substrates were allowed. DnmA-DNA and hDNMT2-DNA complexes are indicated by red or black arrows, respectively.

Nevertheless, this observation may also be explained by some heterogeneity or impurity of the commercial DNA oligonucleotides, which as we noticed earlier may contain significant portion of byproducts from the synthesis reaction. At this point we have to assume that cytosines other than C38 can serve as targets for covalent linkage of the enzymes.

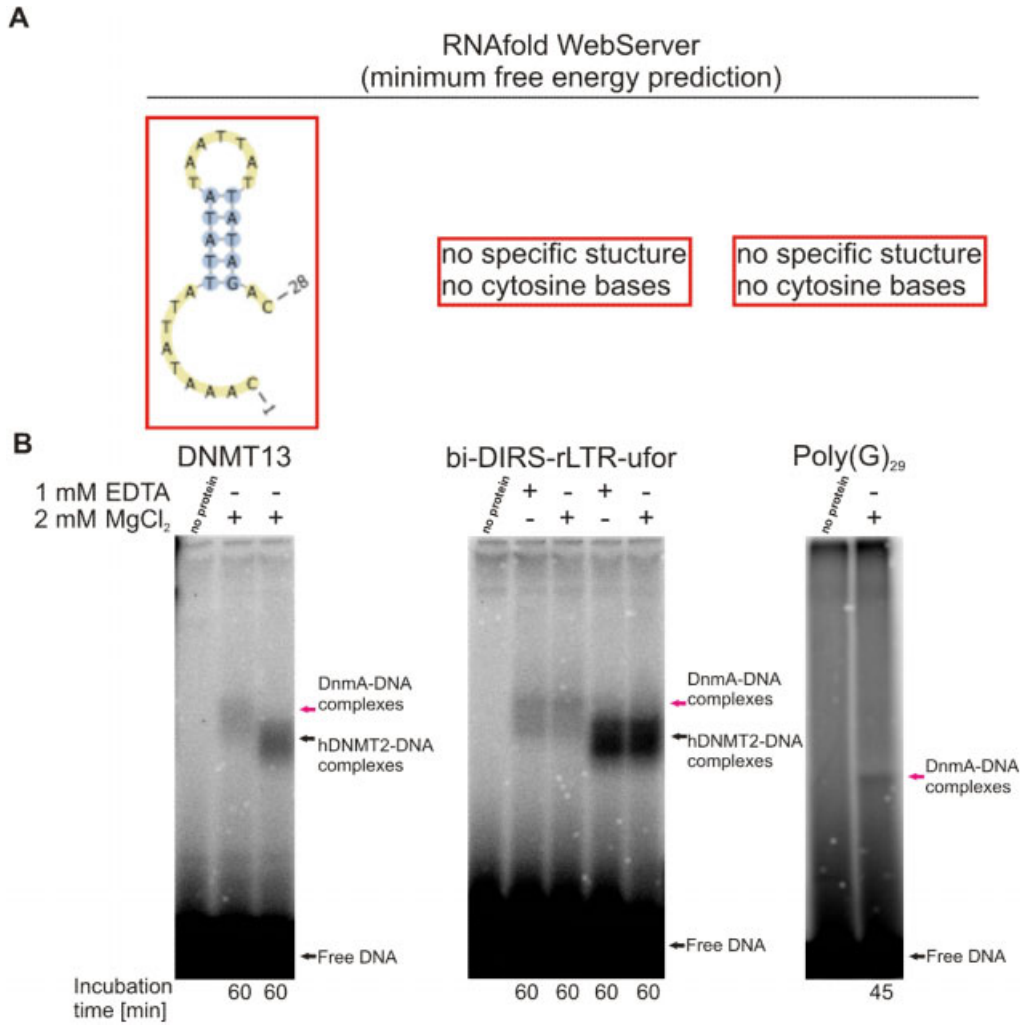

Figure 5.9.3 (**A**) Schematic representation of secondary structure for different DNA oligonucleotides. The bi-DIRS-rLTR-ufor represents the DNA oligonucleotide containing only G, T and A deoxynucleotides. (**B**) Covalent intermediates formed by DnmA or hDNMT2 with different DNA oligonucleotides depicted above. His-DnmA or His-hDNMT2 (120-200 pmol) was incubated for the indicated times at 22ºC (or 37ºC for human enzyme) with labeled DNA oligonucleotides (200-300 pmol) in 20 µl of 10 mM PKi buffer, pH 7.0, containing 25 mM KCl, 2 mM $MgCl_2$ (or 1 mM EDTA), 0.2 mM PMSF, 10 mM DTT, 22.5% glycerol and 100 µM SAM. 10 min pre-incubation of enzymes with SAM prior to addition of RNA substrates were allowed. DnmA-DNA and hDNMT2-DNA complexes are indicated by red or black arrows, respectively.

To test this possibility we used for the following experiments DNA oligonucleotides with and without cytosines and with no specific structures as predicted by RNAfold WebServer (http://rna.tbi.univie.ac.at/cgi-bin/RNAfold.cgi, Figure 5.9.3A). Surprisingly, denaturant-resistant intermediates were detected with both DnmA and hDNMT2 (Figure 5.9.3B). In these

experiments it is rather impossible to explain the appearance of covalent adducts by byproducts of the DNA oligonucleotide synthesis, so we can only suggest that somehow other bases can be involved in the first steps of the catalytic mechanism. Nevertheless, additional experiments are required to draw solid conclusions.

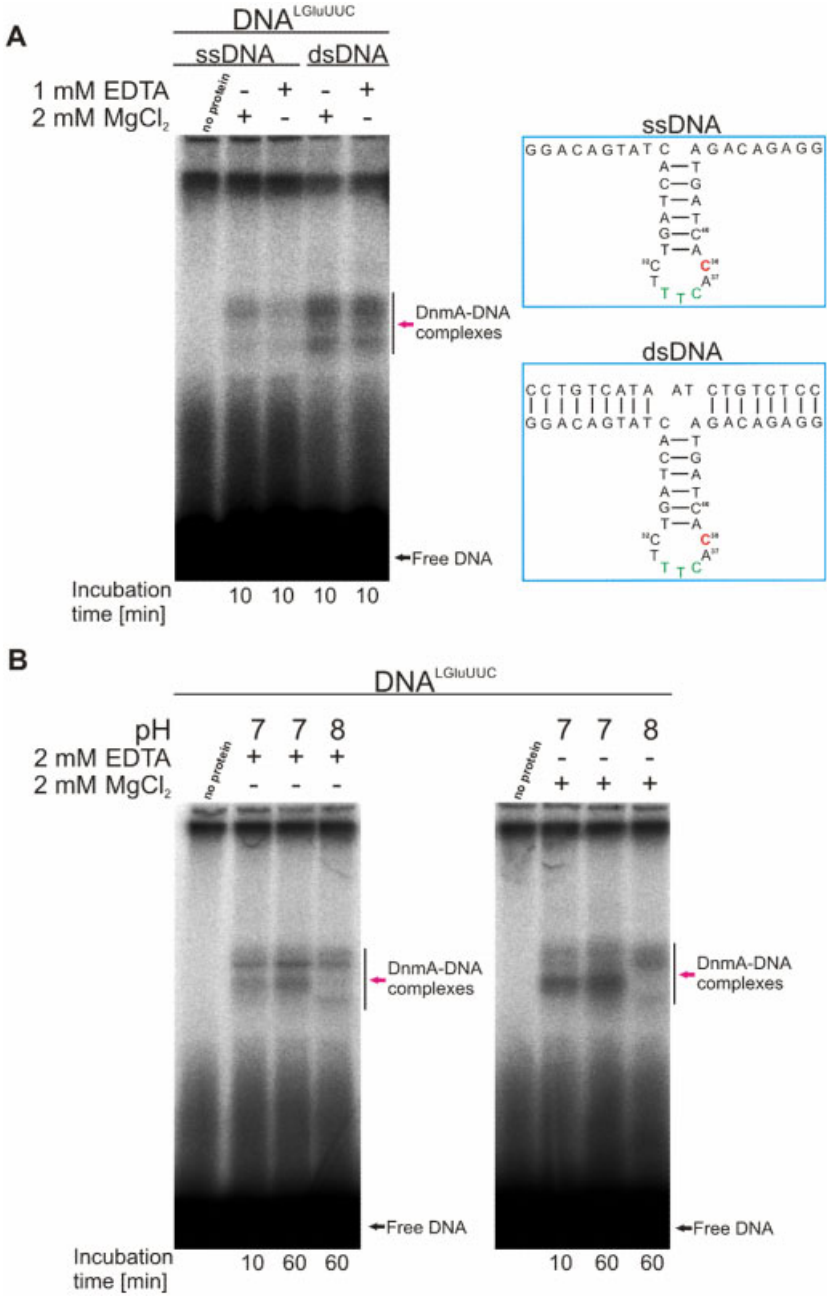

Figure 5.9.4 (**A**) Stabilization of secondary structure by additional DNA oligonucleotide. (**B**) Covalent intermediates formed by DnmA or hDNMT2 with different DNA oligonucleotides at different conditions. All

experiments were conducted as pointed out. Usually, His-DnmA or His-hDNMT2 (120-200 pmol) was incubated for indicated times at 22ºC (or 37ºC for human enzyme) with labeled DNA oligonucleotides (200-300 pmol) in 20 µl of 10 mM PKi buffer, pH 7.0, containing 25 mM KCl, 2 mM $MgCl_2$ (or 1 mM EDTA), 0.2 mM PMSF, 10 mM DTT, 22.5% glycerol and 100 µM SAM. 10 min pre-incubation of enzymes with SAM prior to addition of RNA substrates were allowed. DnmA-DNA complexes are indicated by red arrows.

From additional experiments on DNA oligonucleotides, we observed that stabilization of the tRNA-like DNA loop structure by another oligonucleotide, sealing the protruding non-paired ends of the target sequence increased to some extent the amount of trapped covalent intermediates (Figure 5.9.4A). Furthermore, Figure 5.9.4 shows that in some cases difference in the presence or absence of Mg^{2+} as well as in the pH of buffer influenced the way the covalent complexes are represented in a gel and that there is a slow accumulation of these complexes at least within 1 hr of incubation (Figure 5.9.4B).

5.10 Putative post-translational modifications on DnmA

The low efficiency of complex formation by the recombinant enzyme, the complete failure to achieve DNA methylation *in vitro* (Müller, personal communication) and the failure to define interacting proteins that could be required for DNA methylation *in vivo*, brought up the assumption that post-translational modifications, which would not be present on the E. coli expressed proteins, could influence target recognition and enzymatic activity. This could explain the observed relatively high activity of DnmA-StrepII protein preparations, purified from *Dictyostelium* cell extracts. To assess whether post-translational modifications played a role in the regulation of DnmA function, the mass spectrometry analysis was performed (collaboration with Bertinetti, Department of Biochemistry, Uni Kassel). Several DnmA-StrepII, DnmA-CTAP and His-DnmA protein preparations were analyzed, including the ones which were obtained in the experiments for detection of putative interaction partners, to identify the most common modifications known for eukaryotic proteins, namely phosphorylation (Kameshita et al, 2008), methylation (Esteve et al, 2009) and acetylation (Yang & Seto, 2008). Bands which represented DnmA-StrepII or DnmA-CTAP fusion proteins were distinct in the SDS-PAGE gels and correspond to the predicted size, indicating that no variable large post-translational modifications like glycosylation or ubiquitylation were present. All purifications were done in the presence of a Protease inhibitor cocktail (Roche). In some cases, Phosphatase inhibitor cocktail (PhoSTOP,

Roche) was used to exclude the non-specific dephosphorylation of the samples during the purification process. Figure 5.10.1 represents several SDS-PAGE gels, DnmA proteins from which were used for PTM analysis by mass-spectrometry (LC-MS/MS).

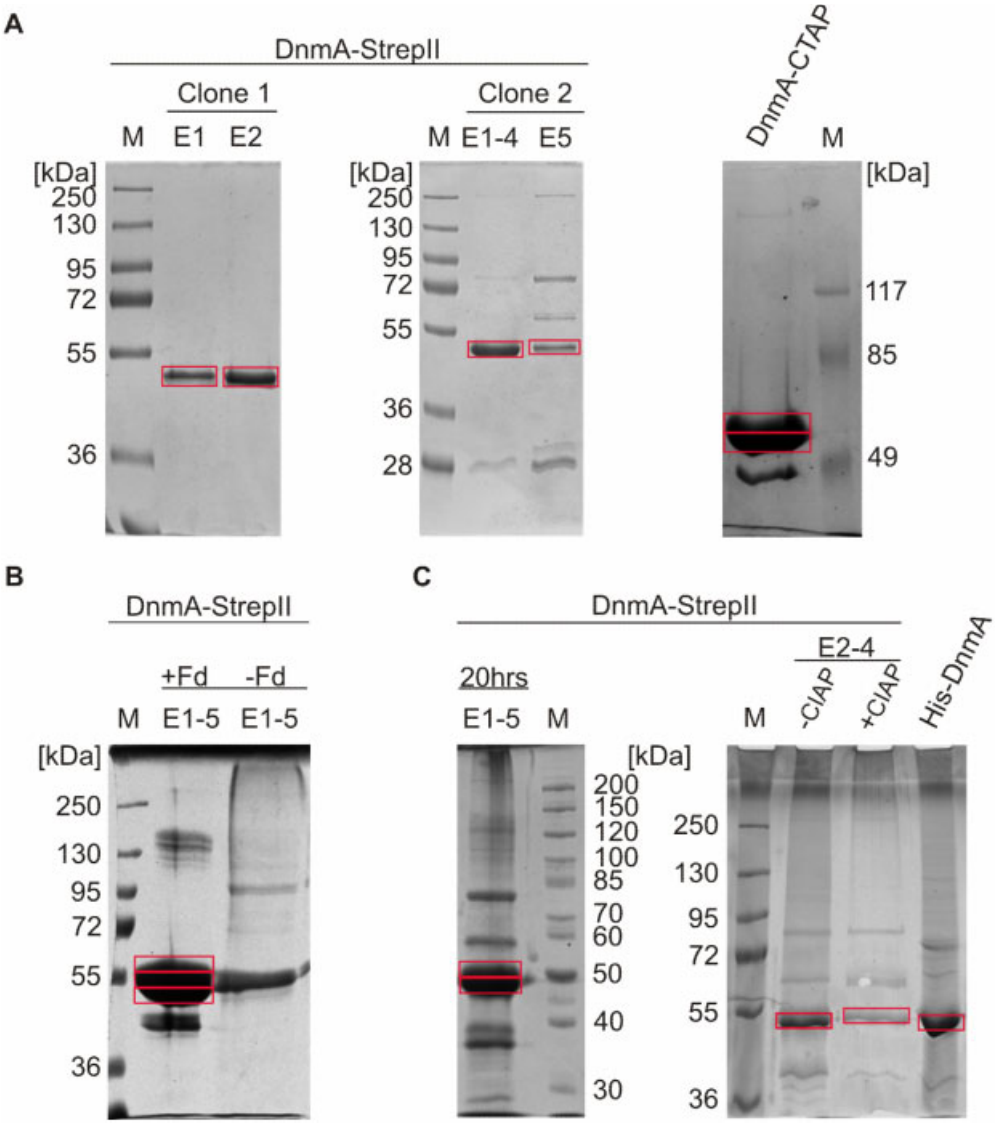

Figure 5.10.1 8-9% SDS-PAGE of different recombinant DnmA preparations. Red rectangles indicates the sections of the DnmA bands which were excised and digested with trypsin followed by subsequent liquid chromatography/mass spectrometry (LC-MS/MS) analysis. (**A**) First two panels (right) represent SDS gels of DnmA-StrepII protein, purified from cell extracts of *dnmA_KO*/*dnmA-strepII* (clone1 and 4) *Dictyostelium* strain, collected during vegetative growth in axenic culture. Proteins from separate elution steps (E1 and E2) were analyzed as well as from joined elutions, which were combined due to presence of significant portion of DnmA. Experiment was performed in absence of Phosphatase inhibitors. Last panel (left) represent SDS gel of DnmA-CTAP protein

preparation obtained from cell extract of clone5 of *dnmA_KO*/*dnmA-CTAP* by tandem affinity purification. Prestained protein markers (Fermentas, #SM1811 and #SM0441) was used as a size reference. (**B**) DnmA-StrepII protein purified from nuclei of *dnmA_KO*/*dnmA-strepII* strain after treatment of shaking culture with 0.1% Formaldehyde for 10 min. Experiment were done in presence of Phosphatase inhibitors. Prestained protein marker (Fermentas, #SM1811) was used as a reference. (**C**) Left panel show DnmA-StrepII preparation from *Dictyostelium* cell extract after 20 hours of development on PBS agar plates. Right panel represent DnmA-StrepII protein purified from *Dictyostelium* cells, collected during vegetative growth. Purified proten was divided into two aliquots and one of them treated with calf intestinal alkaline phosphatase (CIAP) for 30 min at RT before loading on the gel. His-DnmA protein preparation was also analyzed for PTM and results were used as the negative control. Prestained protein markers (Fermentas, #SM1811 and #SM0661) were used as a size references.

DnmA seems to be a mainly nuclear protein, though significant amounts can be also detected in cytoplasm. Therefore, in one experiment, the DnmA-StrepII protein was separately isolated from cytoplasm and nuclei of *Dictyostelium* cells in order to see potential differences in the PTM patterns of samples from different cell compartments. Most experiments were done using shaking axenic *Dictyostelium* cultures with cell densities of 2-3 x 10^6 cells/ml. Given the observations that Dnmt2 can be functionally involved in regulation of retrotransposon mobility during developmental stages in *Drosophila melanogaster* and *Dictyostelium discoideum*, one experiment was performed on the protein purified from *Dictyostelium* cells after 20 hours of development on PBS agar plates (Phalke et al, 2009), (Katoh et al, 2006). As a control recombinant His-DnmA protein purified from bacterial cells was used.

The mass spectrometry data showed several amino acids within DnmA-StrepII fusion protein which can undergo phosphorylation, methylation or acetylation, though the score values for peptides, carrying these modifications was not very high (Figure 5.10.2). Due to limitations of trypsin proteolysis (trypsin cleaves polypeptide chains mainly at the carboxyl side of the amino acids lysine or arginine, except when either is followed by proline), it was impossible to distinguish between some of these modifications or identify the exact location. Unfortunately an attempt to extract more precise data by using another type of digestions (for instance chymotrypsin, which preferentially cleaves peptide amide bonds where the carboxyl side of amide bond is a tyrosine, tryptophan, or phenylalanine) was not successful. Nevertheless, the results were repeatable and indicated that phosphorylation, methylation and acetylation occured mainly within the target recognition domain (TRD) of DnmA-StrepII and DnmA-TAP fusions purified from *Dictyostelium*. No modifications were found on recombinant His-DnmA protein

from *E.coli*. Interestingly, no obvious differences in the amount or location of the modifications in the TRD were detected in proteins purified either from cytoplasmic or nucleoplasmic compartments, although cytosolic DnmA-StrepII fusion showed additional phosphorylation and methylation/acetylation in a variable region between motifs VI and VII (Figure 5.10.2). Relatively lower amounts of these modifications in the TRD were detected on DnmA-StrepII fusions purified from *Dictyostelium* cell extract, obtained after 20 hrs of development, though these are preliminary data based on only one experiment (data not shown).

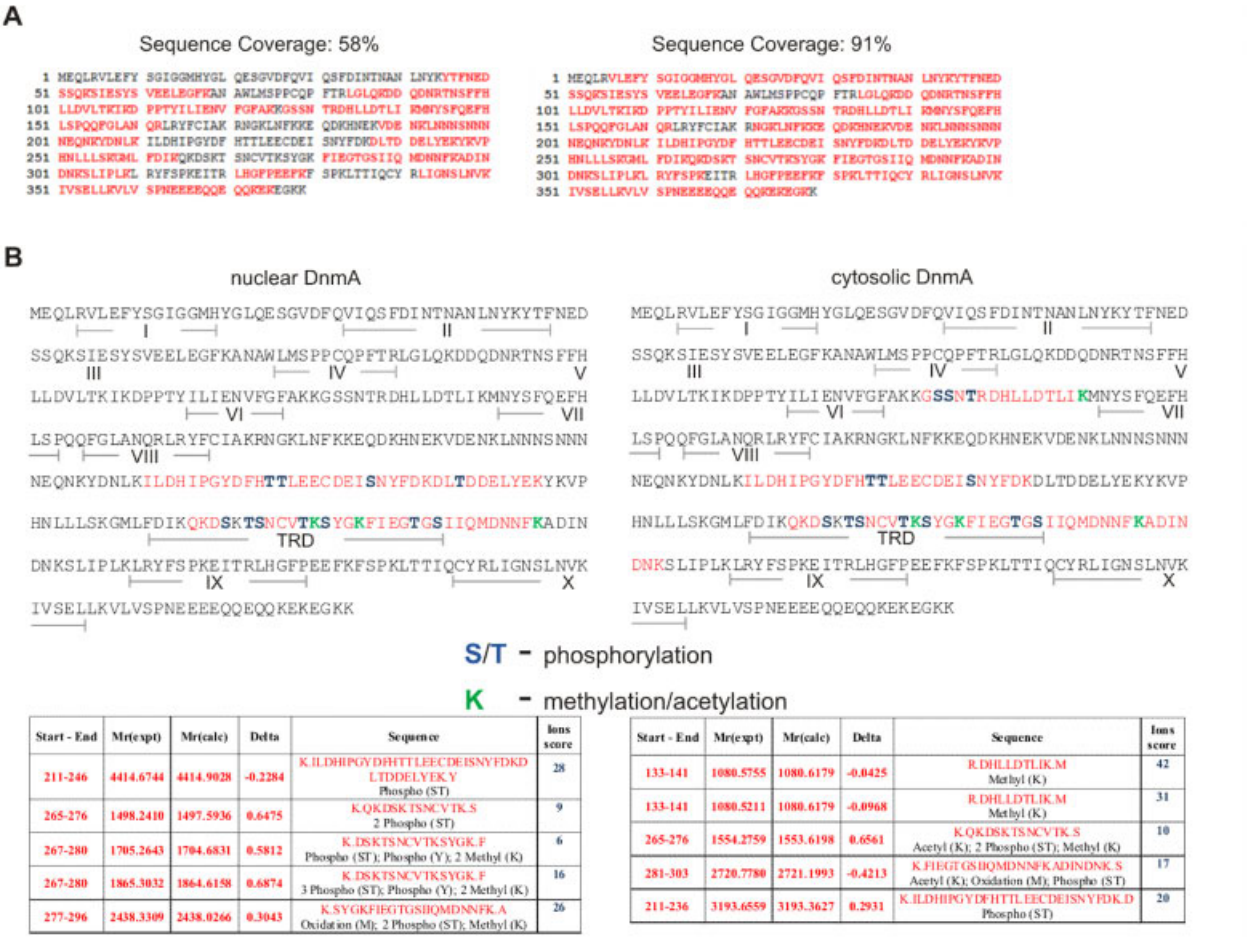

Start - End	Mr(expt)	Mr(calc)	Delta	Sequence	Ions score
211-246	4414.6744	4414.9028	-0.2284	K.ILDHIPGYDFHTTLEECDEISNYFDKDLTDDELYEK.Y Phospho (ST)	28
265-276	1498.2410	1497.5936	0.6475	K.QKDSKTSNCVTK.S 2 Phospho (ST)	9
267-280	1705.2643	1704.6831	0.5812	K.DSKTSNCVTKSYGK.F Phospho (ST); Phospho (Y); 2 Methyl (K)	6
267-280	1865.3032	1864.6158	0.6874	K.DSKTSNCVTKSYGK.F 3 Phospho (ST); Phospho (Y); 2 Methyl (K)	16
277-296	2438.3309	2438.0266	0.3043	K.SYGKFIEGTGSIIQMDNNFK.A Oxidation (M); 2 Phospho (ST); Methyl (K)	26

Start - End	Mr(expt)	Mr(calc)	Delta	Sequence	Ions score
133-141	1080.5755	1080.6179	-0.0425	R.DHLLDTLIK.M Methyl (K)	42
133-141	1080.5211	1080.6179	-0.0968	R.DHLLDTLIK.M Methyl (K)	31
265-276	1554.2759	1553.6198	0.6561	K.QKDSKTSNCVTK.S Acetyl (K); 2 Phospho (ST); Methyl (K)	10
281-303	2720.7780	2721.1993	-0.4213	K.FIEGTGSIIQMDNNFKADINDNK.S Acetyl (K); Oxidation (M); Phospho (ST)	17
211-236	3193.6559	3193.3627	0.2931	K.ILDHIPGYDFHTTLEECDEISNYFDK.D Phospho (ST)	20

Figure 5.10.2 (**A**) Sequence coverage in LC-MS/MS experiments varied from 58 to 91% of the entire DnmA sequence. (**B**) Localization of peptides (red) carried identified modifications (blue/green) over the DnmA sequence. Grey bars below amino acid sequence mark conservative catalytic motifs, including TRD. Identified modification sites are shown for proteins purified from nuclei and cytosol. Tables below protein sequences represent identified peptides carried relevant modifications for samples from corresponding cell compartments.

We assumed that the modifications in the conservative target recognition domain of DnmA could play a role in modulation of interaction with DNA or RNA substrates. This is circumstantially supported by observation that DnmA-CTAP and DnmA-StrepII fusions purified from *Dictyostelium* cells usually showed higher methyltransferase activity then recombinant His-DnmA preparations expressed in *E.coli* (Müller, personal communication).

Using commonly available bioinformatics tools like NetPhos 2.0 server (neural network predictions for serine, threonine and tyrosine phosphorylation sites in eukaryotic proteins) and NetPhosK 1.0 server (predictions of kinase specific eukaryotic protein phosphoylation sites) an attempt to analyze at least the phosphorylation data on DnmA was performed. Figure 5.10.3A shows the result of the theoretical predictions on serine and threonine phosphorylation sites in the DnmA sequence (http://www.cbs.dtu.dk/services/NetPhos/). Figure 5.10.3B represents the result of kinase specific phosphorylation predictions performed by NetPhosK 1.0 server (http://www.cbs.dtu.dk/services/NetPhosK/). Since we obtained data on phosphorylation within only two regions of DnmA, the predicted sites in these locations were relevant for the analysis. Indeed, the serine residues at the positions 129, 268, 271 and 287 as well as the threonine at the positions 223 and 239 had highest scores and were likely to be phosphorylated. Furthermore, the analysis showed that these and some other serine and threonine residues could be a target for several known kinases, including PKA, PKC, CKII and cdc2 (Figure 5.10.3B). CKII (casein kinase 2) and cdc2 (cell division control protein 2 homolog, also known as cyclin dependent kinase 1) is a highly conserved proteins and (together with PKA) function as key players in cell cycle regulation, specifically by controlling of G1/S and G2/M transitions (Hochegger et al, 2007) (Gao & Wang, 2006). Another important step in analysis of modifications involved determination of relevant amino acids within three dimensional structure of the protein. There are 3D modeling network tools available, for instance the SWISS-MODEL Workspace, which provides the possibility of protein structure homology modeling and quality assessment (http://swissmodel.expasy.org/). Methyltransferases of Dnm2 family are highly conserved and this conservation allowed to create a preliminary model of the DnmA protein, based on available crystallographic structure of human DNMT2 (hDNMT2Δ47-AdoHcy complex, PDB, entry 1G55). Figure 5.10.3C represents crystallographic structures of hDNMT2 and resulting 3D model of DnmA.

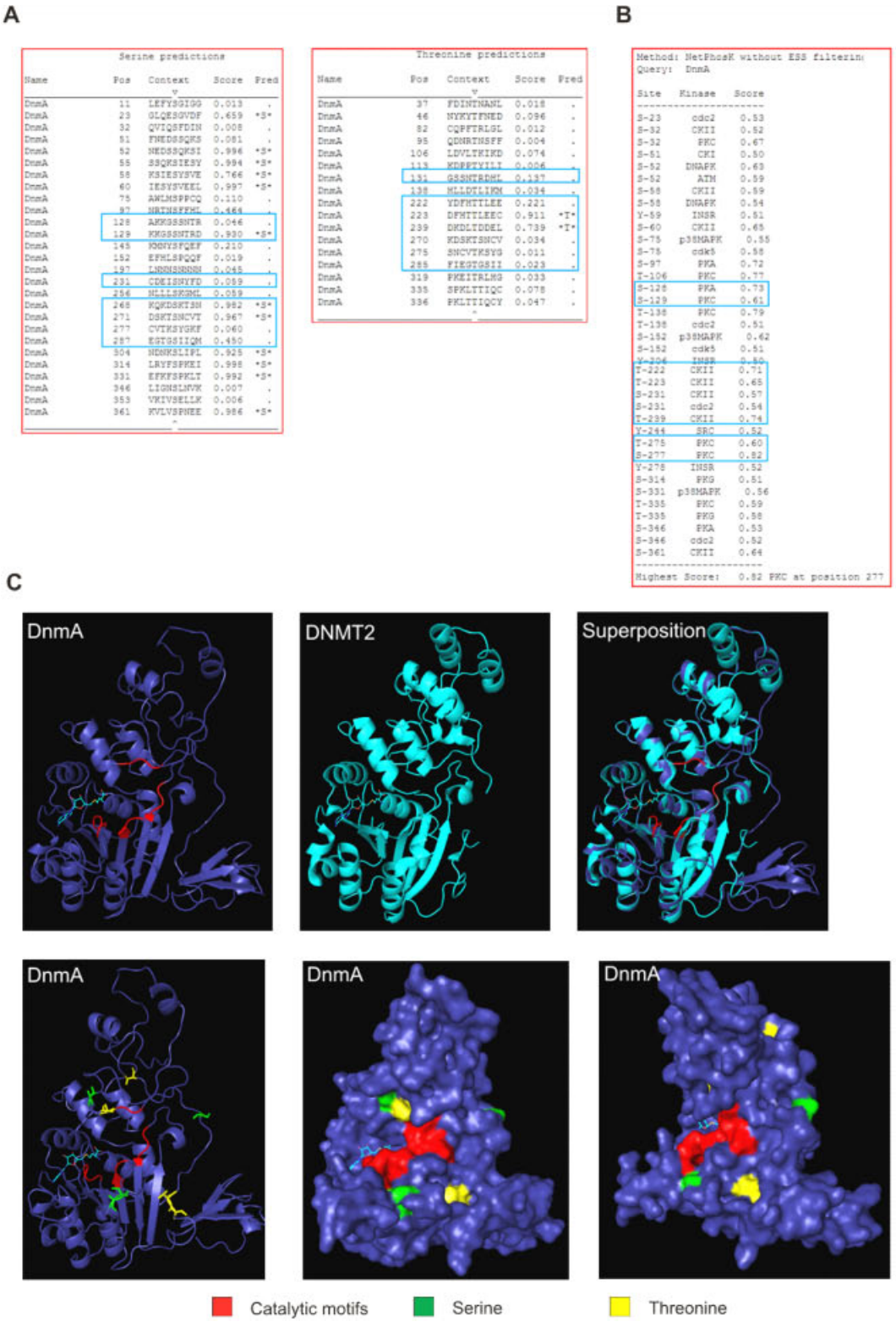

Figure 5.10.3 (**A**) Tables represent the results of serine and threonine phosphorylation sites prediction based on amino acid context (NetPhos 2.0 Server). Residues identified to be phosphorylated *in vivo* are marked by blue

rectangles. (**B**) Table represents the list of serine and threonine residues as putative targets for specific kinases (NetPhosK 1.0 Server, limited list of kinases are currently available for analysis). Residues identified to be phosphorylated *in vivo* and corresponding specific kinases are marked by blue rectangles. (**C**) Three upper pictures show PDB grade representation of tertiary structures of DnmA and hDNMT2 (DNMT2Δ47-AdoHcy complex, PDB: 1G55). Modeling was performed by SWISS-MODEL Server using crystallographic structure of hDNMT2 as a reference template and default setup (Arnold et al, 2006). Three lower pictures represent localization of serine/threonine residues selected in table B in the 3D model of DnmA. Surface-type representations demonstrate potential availability of marked amino acids to specific kinases.

The overall structures of both human and *Dictyostelium* enzymes are nearly superimposable, although protein structure refinement was not performed. The generated 3D model allowed us to localize the identified phosphorylation sites within the tertiary structure of DnmA (Figure 5.10.3C). The serine and threonine residues were found on the surface of the DnmA molecule and therefore could well be available for corresponding kinases. Thus, *in silico* prediction of potential serine and threonine phosphorylation sites and relevant putative kinases together with modeling of protein tertiary structure and data of *in vivo* occurring phosphorylation sites allowed to conclude that several specific kinases could potentially modulate DnmA function.

6 Discussion

6.1 *In vitro* characterization of DnmA function

The bisulfite sequencing analysis revealed several loci in the *Dictyostelium* (Kuhlmann et al, 2005) and *Drosophila* (Kunert et al, 2003) genomic DNA where cytosines appeared to be methylated mainly in an asymmetric manner. This raised the question about target specificity of Dnmt2 binding. To address this problem an EMSA assays were performed to define the binding affinity of DnmA to different DNA species. The obtained results showed that DnmA has in general low affinity to both single stranded and double stranded DNA and no specificity was detected for DNA oligonucleotides or short dsDNAs, despite different sequence contexts (see chapter 5.7.1). However, the comparative analysis showed that the affinity of the DnmA to dsDNA is higher than for ssDNA. These data suggest that DnmA has a broad specificity and may require additional factors to be targeted to specific locations in the genomic DNA. Additionally, the presence of SAM, the cofactor and donor of methyl group, significantly increased the binding of both ssDNA and dsDNA, whereas the presence of ATP inhibited such binding (Dong et al, 2001).

It was tempting to suggest that DnmA may recognize specific structures like bending or kinking within DNA sequences. Indeed, the genomic DNA of *Dictyostelium* is extremely AT-rich, and such DNA sequences are usually highly curved (Carrera & Azorin, 1994), which could influence the interaction with DNA binding proteins. To assess the possibility that AT-rich DNA sequence could be a better binding substrate for DnmA, a gel retardation assays with different types of relatively long dsDNAs were conducted. The results showed that DnmA preferentially bound to the AT-rich DNA sequences, which demonstrated strong intrinsic curvature. Moreover, the binding showed a weak but detectable cooperative character (see chapter 5.7.2). In this respect, it is interesting to note that human DNMT3A showed similar mode of binding to dsDNA in gel retardation assays (Kareta et al, 2006). For further analysis, AFM studies were performed in collaboration with N. Anspach, which revealed that DnmA did preferentially bind to the AT-rich segments of the designed dsDNA molecule and especially to the segments for which high levels of intrinsic curvature was theoretically predicted (see chapter 5.7.3). These experiments also

showed that binding of the protein contributed to further bending of corresponding DNA segments. These data suggest that DnmA might have been evolved to interact with AT-rich DNA sequences and its evolution could involve the substitution of V/F in the invariant CFT motif within the TRD of the Dnmt2 family. To support this idea the mutagenic analysis of the CVT motif of DnmA should be made followed by EMSA and AFM studies.

The first available data showed that Dnmt2 activity on a pre-modified $tRNA^{Asp}$ template was relatively strong (Goll et al, 2006), which might indicate that Dnmt2 participates in complex ribonucleic acid modification pathways *in vivo* (Jeltsch et al, 2006). Goll and co-authors suggested that Dnmt2 does not recognize *in vitro* transcribed, unmodified tRNA and concluded that correctly pre-modified substrates could be required for increased enzyme activity *in vitro* (Goll et al, 2006). Nevertheless, unmodified *in vitro* transcribed tRNAs were shown to be reproducibly modified by both the *Drosophila* and human Dnmt2 enzymes (Meusburger, PhD thesis). The observed difference might result from the design and conditions of the *in vitro* methylation assays and demonstrated the importance of appropriate pH, as well as DTT and Mg^{2+} concentrations. According to Goll et al., 2006, only the position C38 in the anticodon loop of $tRNA^{Asp}$ was methylated by Dnmt2. However, several other tRNAs were identified as a target, including $tRNA^{Val}$ (Helm, personal communication) and $tRNA^{Glu}$ (see chapter 5.8). Furthermore, C40 of $tRNA^{Phe}$ (*S. cerevisiae*) and C40/C42 of $tRNA^{Lys}$ (*D. melanogaster*) was shown to be methylated by Dnmt2 *in vitro* (Meusburger, PhD thesis). These data raised two major questions: what are the characteristics of the tRNA recognition by Dnmt2 proteins and what are the basics of the flexibility with respect to its substrate acceptance? To address the first of these questions, an EMSA was performed with DnmA and several *in vitro* transcribed *Dictyostelium* tRNAs ($tRNA^{Asp(GUC-1)}$, $tRNA^{Glu(UUC-5)}$ and $tRNA^{Glu(CUA-5)}$), as well as antisense $RNA^{Glu(UUC-5)}$ (see chapter 5.7.4). The results demonstrated that under similar conditions little if any difference is observed in binding affinities of DnmA towards tested RNA substrates. Interestingly, we also showed that despite similar binding affinities of DnmA to different RNA substrates, only $tRNA^{Asp(GUC-1)}$, $tRNA^{Glu(UUC-5)}$ and $tRNA^{Glu(CUA-5)}$ formed denaturant-resistant covalent adducts with the protein, while $tRNA^{Glu(UUC-5)C38A}$, $tRNA^{Phe(GAA-2)}$ and both antisense $RNA^{Glu(UUC-5)}$ and $RNA^{Glu(CUA-5)}$ did not form such complexes (see chapter 5.8). Additionally, the methylation was observed only for $tRNA^{Asp(GUC-1)}$, $tRNA^{Glu(UUC-5)}$ and $tRNA^{Glu(CUA-5)}$ (Müller, personal communication). The observation that only tRNA species which had C38 in the anticodon loop

formed covalent complexes with the DnmA and became methylated suggests that DnmA specifically recognize C38 position but not C40 or C42. This could be the result of the V/F substitution in the conserved CFT tripeptide within the TRD of DnmA. To further analyze this suggestion additional experiments are required with human or *Drosophila* Dnmt2.

In the literature there are examples of tRNA modification enzymes which target several positions within tRNAs in a sequence-independent but structurally-dependent manner (Hur & Stroud, 2007); (Motorin et al, 2009). The finding that the specific pattern containing invariant C32, A37 and C40 is required for methyltransfer activity of hDNMT2 (Helm, personal communication) suggested that the enzyme could target the C38 in both sequence-dependent and structurally-dependent ways. In contrast, $tRNA^{Asp(GUC-1)}$ and $tRNA^{Glu(UUC-5)}$ showed different dynamics in covalent complex accumulation with DnmA (see chapter 5.8) and significant difference in methylation (Müller, personal communication). The substantial difference was also observed for $tRNA^{Glu(UUC-5)}$ and $tRNA^{Glu(CUA-5)}$, which share the same sequence except for two nucleosides in their anticodons (UUC against CUA). Moreover, the concentration of Mg^{2+} ions influenced both covalent complex formation and methylation of tRNAs, which could be explained by conformational changes of tRNA molecules. Similar results were obtained in case of the hDNMT2. These data support the hypothesis that a specific structure of target sequence has a major contribution into the DnmA and hDNMT2 activity. To further address this question the comparative experiments on other tRNAs, containing C38 and the pattern of C32, A37 and C40, should be conducted. The preexisting modifications can significantly change the topology of tRNA molecules (Hur & Stroud, 2007). Therefore, it would also be interesting to investigate if pre-modified tRNAs are the better substrates for Dnmt2 enzymes compared to the corresponding *in vitro* transcribed variants. It is intriguing to speculate that Dnmt2 may also methylate other RNA species with stem-loop structures besides tRNAs. New methods should be developed to search for potential *in vivo* RNA targets for Dnmt2 proteins.

The available data suggested that Dnmt2 has a weak methyltransferase activity on unmodified DNA *in vitro* (Hermann et al, 2003). It was also shown that human Dnmt2 formed denaturant-resistant complexes with both DNA oligonucleotides and double stranded DNA (Dong et al, 2001). However, under conditions we used for experiments both the DnmA and hDNMT2 enzymes showed relatively weak covalent complex formation with only ssDNA species (see chapter 5.9), and no methylation was detected for double stranded DNA (Müller, personal

communication). The experiments also showed that DnmA-DNA covalent complexes had the tendency to accumulate at least within 1 hour of incubation, which was similar to the observation made for hDNMT2 (Dong et al, 2001). The accumulation of covalent adducts together with low methyltransfer activity may suggest that the rate determining step in the catalytic mechanism located after formation of covalent enamine intermediates. Usually, the Far-UV CD spectra showed that the majority of proteins in preparations were folded correctly (see chapter 5.7). In this respect, the absence of both methylation and covalent complex formation in case of dsDNA may additionally reflect the necessity for accessory factors which could be involved in the DNA methylation by DnmA *in vivo*.

Interestingly, the experiments with DNA oligonucleotides, mimicking the anticodon loop of several different tRNAs showed that DnmA as well as hDNMT2 could form covalent adducts (see chapter 5.9). Furthermore, the tRNA-like DNA oligonucleotides with the ends sealed by the complementary oligonucleotide (to stabilize the loop structure) showed more intensive formation of covalent complexes. Curiously, the covalent complex formation was independent on the presence or absence of the cytosine at the position corresponding to C38 in tRNAs. Moreover the character of obtained complexes reflected the situation as if other cytosines in the oligonucleotides were involved in covalent linkage with the enzymes. The complex formation was mainly independent from the presence of Mg^{2+} ions for both the DnmA and hDNMT2; however, in some cases the character of formed complexes was different. This suggests that the DNA oligonucleotides adopted different, perhaps more compact, conformations in the presence of Mg^{2+}. In this case some cytosines would become more available for the enzymes then others compared to situation without ions.

Unexpectedly, both the DnmA and hDNMT2 formed the denaturant-resistant covalent complexes with DNA oligonucleotides, containing no cytosines (see chapter 5.9). Moreover, such complexes were formed even with poly$(G)_{29}$, poly$(T)_{29}$ and poly$(A)_{29}$ DNA oligonucleotides, although they were relatively weaker than the ones with poly$(C)_{29}$ (Junk, diploma thesis). No evidences of such activity were shown for DNA m^5C methyltransferases so far. It is tempting to speculate that this may be the result of by-side activity of the enzymes, although the mechanism of such covalent linkages is not clear and should be further examined.

6.2 *In vivo* characterization of DnmA function

The expression levels of Dnmt2 family enzymes are usually relatively low in different species (Goll & Bestor, 2005); (Pradhan & Esteve, 2003). The *dnmA* gene also demonstrated the low level of expression with only 5 fold increase detected during development (see chapter 5.1). This low level of endogenous expression may reflect a highly specialized function of DnmA *in vivo*, possible in the silencing of certain type of retrotransposons, like Skipper (Kuhlmann et al, 2005) and in the maintenance of genome integrity (Phalke et al, 2009). The bisulfite sequencing of genomic DNA in the *Dictyostelium* revealed the methylated cytosines within the ORF of Skipper (Kuhlmann et al, 2005). This could lead to heterochromatization of corresponding DNA sequences and, thus, to the silencing of the retrotransposon. Interestingly, bioinformatics analysis of the *Dictyostelium* genome revealed absence of canonical methylbinding proteins (Borisova, PhD thesis), which could link the DNA methylation with a following processes. In contrast, the EhMLBP protein was isolated from *Entamoeba histolytica* that binds preferentially to the methylated long interspersed nuclear elements (LINE) and rDNA (Lavi et al, 2009). Additionally, the methylbinding protein MBD2/3 was identified in *Drosophila* that mediates interactions between the MI-2 chromatin complex and CpT/A-methylated DNA (Marhold et al, 2004). Recently, a specific role of Dnmt2 in epigenetic silencing of retrotransposons and subtelomeric repeats has been found in *Drosophila* (Phalke et al, 2009). The genetic data imply the Suv4-20/Hmt4-20 histone H4K20 methyltransferase (Sakaguchi et al. 2008) in the maintenance of retrotransposon silencing initiated by Dnmt2-dependent DNA methylation (Phalke et al, 2009). In this respect, it is interesting to note that *Dictyostelium* seems to be lacking the H4K20 methylation mark (Dubin, PhD thesis) and, therefore, other mechanisms could be involved in the regulation of Skipper retrotransposons. Anyway, the precise role of Dnmt2-mediated DNA methylation within an organism remains to be determined.

In vitro studies showed that the formation of covalent complexes between DnmA and double stranded DNA, derived from regions found to be methylated *in vivo*, was significantly suppressed. On the other hand, the presence of single stranded DNA substantially improved the formation of DnmA-DNA complexes (see chapter 5.9). These data in combination with the bisulfite sequencing results suggest that DnmA locally functions in the nucleus as a DNA m^5C methyltransferase but may require the ssDNA as an appropriate substrate. The observation that

the DnmA-GFP fusions colocalized with DNA in the interphase of cell cycle (most probably in the S phase) as well as the indication that the protein was tightly embedded into nuclear matrix, provided good circumstantial evidences for this hypothesis (see chapter 5.2).

Another possibility to control the activity of Skipper retrotransposon resulted from its unusual genomic organization. Skipper represents the retrotransposon with a *gag-pro-pol* ORF organization and the first example of a retrotransposon with a separate *pro* gene. The stop codon was found at a reading frame junction where a down-modulation of Skipper expression is expected and it appears to use stop codon suppression rather than frameshifting to modulate *pro* expression (Leng et al, 1998). It is tempting to speculate that the tRNA methyltransfer activity of DnmA may be involved somehow, since it was shown that some tRNA modifications could modulate both the codon suppression (Waas et al, 2007) and frameshifting (Beier & Grimm, 2001); (Hatfield, 1985). The presence of significant portion of DnmA-GFP fusions in the cytoplasmic compartment in *Dictyostelium* cells could indirectly favor the tRNA methyltransfer activity, although some tRNA modifications, including methylation, may occur in the nuclei of eukaryotes (Alfredo & Sylvia, 1980). The suggestion about a cytoplasmic function of DnmA also supported by experiments in zebrafish, where Dnmt2 knock-out phenotypes could be restored by cytoplasmic Dnmt2, but not nuclear (Rai et al, 2007), as well as by finding in *Entamoeba*, where the glycolytic enzyme enolase was shown to act as a metabolic regulator of the Dnmt2 homolog Ehmeth (Tovy et al, 2010). Additionally, it was shown that overexpression of the human DNMT2 in the transiently transfected NIH3T3 cells resulted in a predominantly cytoplasmic localization of the protein, which may also be consistent with its cytoplasmic function (Goll et al, 2006). However, other functions of DnmA, for instance, under environmental stress or aging should be also considered.

The observations that transgenically overexpressed DnmA-GFP was localized in both nucleus and cytoplasm and that it showed certain dynamics in distribution during the cell cycle (see chapter 5.2) may indicate that the localization of the protein is regulated. The overexpression of proteins can lead to an artificial distribution, but the experiments in *Drosophila* showed that the endogenous Dnmt2 has both cytoplasmic and nuclear localization (Kunert et al, 2003) as well as demonstrates specific dynamics (although opposite to DnmA-GFP in the *Dictyostelium* cells) throughout the cell cycle (Schaefer et al, 2008). Nevertheless, additional studies, perhaps

involving the regulated expression of transgenic DnmA or DnmA-specific antibodies, are required for more detailed picture of *in vivo* dynamics of the protein.

Unfortunately, the attempts to isolate interacting proteins that could be required for the DNA or tRNA methyltransfer activity of DnmA *in vivo* were unsuccessful and did not provide reliable candidates, although several different approaches were used (see chapter 5.3). Nevertheless, the protein related to the human Cep192, which is required for mitotic centrosome and spindle assembly in human cells (Gomez-Ferreria et al, 2007), was initially found as a potential interaction partner. In some *Dictyostelium* cells the overexpressed DnmA-GFP indeed showed the accumulation in a region, which we assumed corresponded to a centrosome. This could also be an artifact of DnmA-GFP overexpression or fixation procedure, since not all cells showed the accumulation (see chapter 5.2). Moreover, not all purifications showed the presence of Cep192-like protein (see chapter 5.3) and the protein was not identified as an interaction partner in the previously conducted yeast two-hybrid screenings (Borisova, PhD thesis). The attempts to generate the knock-out of the gene encoding Cep192-like protein in *Dictyostelium* were made, but did not give survivors (data not shown). This allowed us to conclude that the presence of the protein is vital which is consistent with its key role in centrosome function (Gomez-Ferreria et al, 2007). Despite the absence of reliable candidates for the interaction with DnmA in our purification experiments we cannot exclude the possibility that they exist in *Dictyostelium*, since at least one interaction partner was isolated for Ehmeth in *Entamoeba* (Tovy et al, 2010). The observed association of DnmA with the nuclear matrix seems to be a likely explanation for the difficulties during biochemical isolation of Dnmt2 interacting protein, since matrix associated proteins can be lost during purification. The overexpression of tagged DnmA may also contribute into low efficiency of purification procedures from both nuclear and cytoplasmic compartments. Thus, other purification methods or controllable transgenic expression of DnmA may be required to increase the yield of co-purified proteins.

The failure to define interacting proteins brought up the assumption that post-translational modifications could influence target recognition and enzymatic activity. MS data indicated that phosphorylation, methylation and acetylation occur within the target recognition domain (TRD) of DnmA purified from *Dictyostelium* (see chapter 5.9). Additionally, there was an indication that these modifications are less represented in the proteins isolated from *Dictyostelium* cells upon 20 hours of development. The proteins purified from cytoplasm also showed additional site

for phosphorylation/methylation between motifs VI and VII. Several putative target sites for phosphorylation as well as protein kinases were identified based on MS data and theoretical predictions. The preliminary 3D modeling of DnmA protein, based on homology with hDNMT2 allowed us to show that some of these phosphorylation sites are located on the surface of DnmA molecule and, thus, can be available for corresponding kinases *in vivo*. In this respect, it is interesting to note that some of the identified kinases including CKII (Faust & Montenarh, 2000), cdc2 (Terasaki et al, 2003) and PKC (Kenessey et al, 2006) are located in both nucleus and cytoplasm of eukaryotic cells, while PKA usually shows cytoplasmic localization (Tudisca et al, 2010).

The meaning of these modifications is not yet clear, however, the localization of modifications mainly within the TRD domain of DnmA may suggest their involvement in modulation of target recognition. To analyze this possibility, a protein sequence alignment for members of Dnmt2 family was performed, which showed the presence of conserved amino acid residues in their TRD domains. Some of these residues was found to be phosphorylated, methylated or acetylated in DnmA and could also be the targets for modifications in other Dnmt2 proteins (Fugure 6.2.1). Nevertheless, an additional data about modification status of Dnmt2 proteins in other organisms are required to make a solid conclusion.

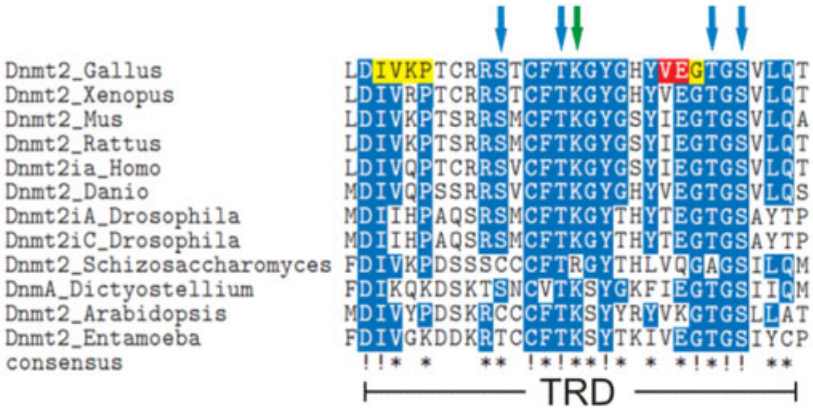

Figure 6.2.1 Alignment of TRD domains from the proteins of Dnmt2 family. Blue arrows point the position of conserved serines and threonines, which undergo phosphorylation in *Dictyostelium* DnmA. Green arrow represents the site of methylation/acetylation in DnmA. The pointed sites of modifications are conserved in Dnmt2 proteins.

7 Supplementary materials

Western-blots confirm that the denaturant- resistant complexes contain the His-tagged DnmA and hDNMT2 proteins (Mouse anti-His antibody). Corresponding covalent complexes marked by black arrows.

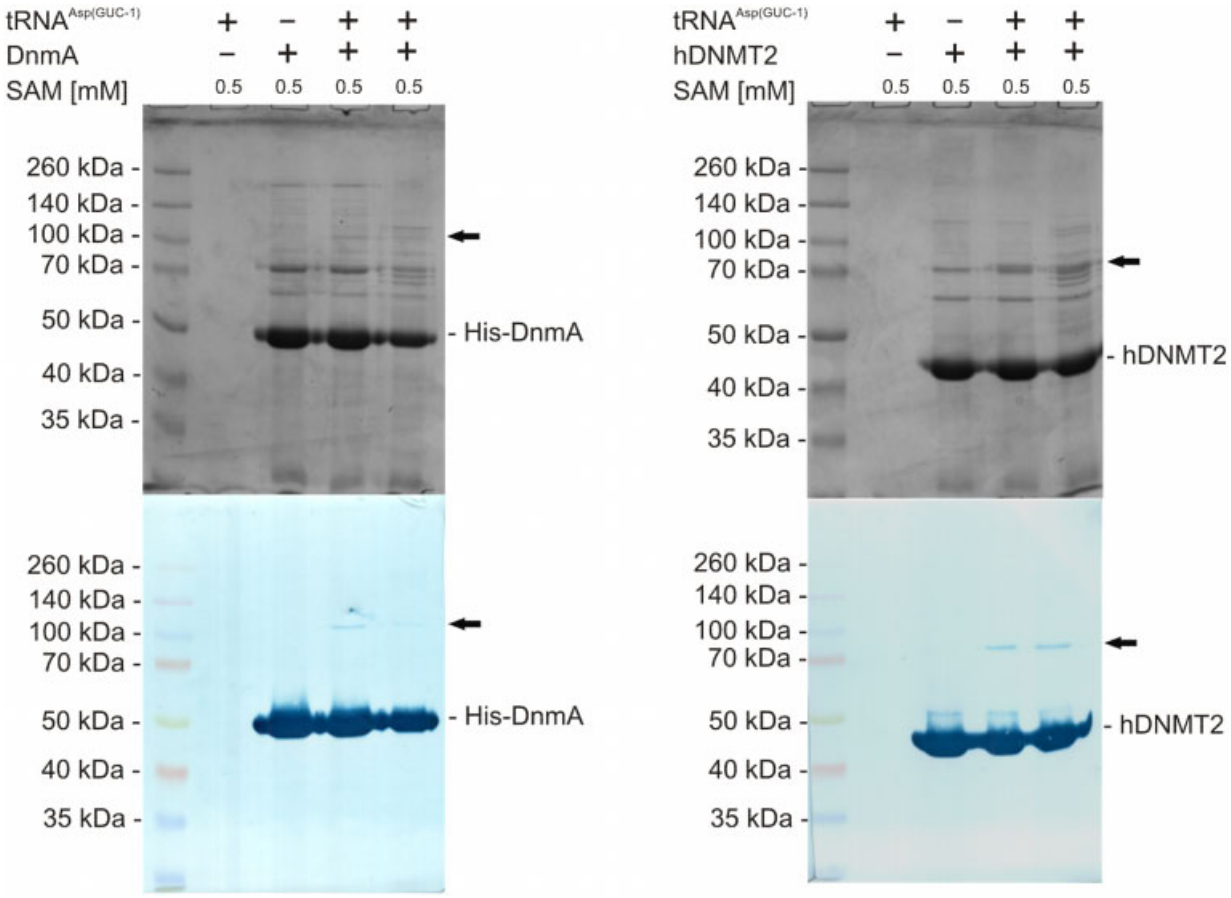

Both DnmA and hDNMT2 form covalent complexes with tRNA$^{Asp(GUC-1)}$. hDNMT2-tRNA complexes have higher mobility on SDS-PAGE, which correlate with higher mobility of human protein compared to DnmA.

Western-blot confirms that the denaturant- resistant DnmA-tRNA$^{Glu(UUC-5)}$ complex contain the His-tagged DnmA (Mouse anti-His antibody). Covalent complexes marked by black arrows.

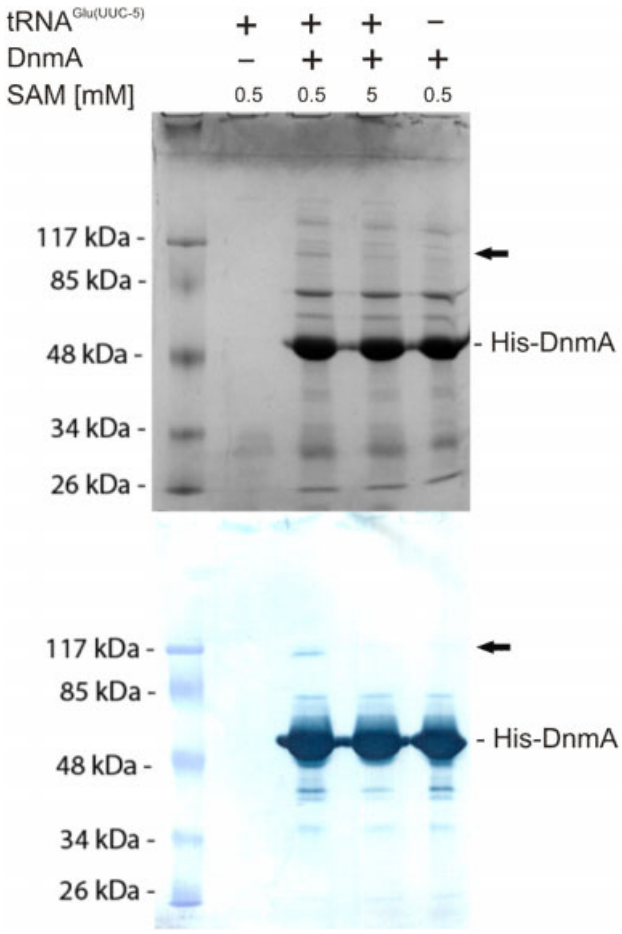

DnmA forms covalent complex with tRNA$^{Glu(UUC-5)}$.

8 References

Abbott DW, et al. (2005) Beyond the Xi. *Journal of Biological Chemistry* **280:** 16437-16445

Achour M, et al. (2009) UHRF1 recruits the histone acetyltransferase Tip60 and controls its expression and activity. *Biochemical and Biophysical Research Communications* **390:** 523-528

Alexandrov A, et al. (2006) Rapid tRNA Decay Can Result from Lack of Nonessential Modifications. **21:** 87-96

Alfredo C, and Sylvia JK (1980) The nucleus as the site of tRNA methylation. *Journal of Cellular Physiology* **103:** 29-33

Ali I, et al. (2007) Growth of the protozoan parasite Entamoeba histolytica in 5-azacytidine has limited effects on parasite gene expression. *BMC Genomics* **8:** 7

An W, Kim J, and Roeder RG (2004) Ordered Cooperative Functions of PRMT1, p300, and CARM1 in Transcriptional Activation by p53. *Cell* **117:** 735-748

Arita K, et al. (2008) Recognition of hemi-methylated DNA by the SRA protein UHRF1 by a base-flipping mechanism. *Nature* **455:** 818-821

Arnau J, et al. (2006) Current strategies for the use of affinity tags and tag removal for the purification of recombinant proteins. *Protein Expression and Purification* **48:** 1-13

Arnold K, et al. (2006) The SWISS-MODEL workspace: a web-based environment for protein structure homology modelling. *Bioinformatics* **22:** 195-201

Ayton PM, Chen EH, and Cleary ML (2004) Binding to Nonmethylated CpG DNA Is Essential for Target Recognition, Transactivation, and Myeloid Transformation by an MLL Oncoprotein. *Mol Cell Biol* **24:** 10470-10478

Bachman KE, Rountree MR, and Baylin SB (2001) Dnmt3a and Dnmt3b Are Transcriptional Repressors That Exhibit Unique Localization Properties to Heterochromatin. *Journal of Biological Chemistry* **276:** 32282-32287

Banerjee S, et al. (2005) Entamoeba histolytica DNA methyltransferase (Ehmeth) is a nuclear matrix protein that binds EhMRS2, a DNA that includes a scaffold/matrix attachment region (S/MAR). *Molecular and Biochemical Parasitology* **139:** 91-97

Bannister AJ, and Kouzarides T (1996) The CBP co-activator is a histone acetyltransferase. *Nature* **384:** 641-643

Barth C, Fraser DJ, and Fisher PR (1998) A rapid, small scale method for characterization of plasmid insertions in the Dictyostelium genome. *Nucl Acids Res* **26:** 3317-3318

Beier H, and Grimm M (2001) Misreading of termination codons in eukaryotes by natural nonsense suppressor tRNAs. *Nucl Acids Res* **29:** 4767-4782

Bestor T, et al. (1988) Cloning and sequencing of a cDNA encoding DNA methyltransferase of mouse cells : The carboxyl-terminal domain of the mammalian enzymes is related to bacterial restriction methyltransferases. *Journal of Molecular Biology* **203:** 971-983

Bestor TH (2000) The DNA methyltransferases of mammals. *Hum Mol Genet* **9:** 2395-2402

Bhattacharya SK, et al. (1999) A mammalian protein with specific demethylase activity for mCpG DNA. *Nature* **397:** 579-583

Bird A (2002) DNA methylation patterns and epigenetic memory. *Genes & Development* **16:** 6-21

Blackledge NP, et al. (2010) CpG Islands Recruit a Histone H3 Lysine 36 Demethylase. *Molecular Cell* **38:** 179-190

Bostick M, et al. (2007) UHRF1 Plays a Role in Maintaining DNA Methylation in Mammalian Cells. *Science***:** 1147939

Bronner C, et al. (2009) UHRF1 Links the Histone Code and DNA Methylation to Ensure Faithful Epigenetic Memory Inheritance. *Genetics & Epigenetics***:** 29

Bruce K, et al. (2005) The replacement histone H2A.Z in a hyperacetylated form is a feature of active genes in the chicken. *Nucl Acids Res* **33:** 5633-5639

Bujnicki JM, et al. (2004) Sequence-structure-function studies of tRNA:m5C methyltransferase Trm4p and its relationship to DNA:m5C and RNA:m5U methyltransferases. *Nucl Acids Res* **32:** 2453-2463

Caron H, et al. (2001) The Human Transcriptome Map: Clustering of Highly Expressed Genes in Chromosomal Domains. *Science* **291:** 1289-1292

Carrera P, and Azorin F (1994) Structural characterization of intrinsically curved AT-rich DNA sequences. *Nucl Acids Res* **22:** 3671-3680

Cedar H, and Bergman Y (2009) Linking DNA methylation and histone modification: patterns and paradigms. *Nat Rev Genet* **10:** 295-304

Chadwick BP, and Willard HF (2001) A Novel Chromatin Protein, Distantly Related to Histone H2a, Is Largely Excluded from the Inactive X Chromosome. *The Journal of cell biology* **152:** 375-384

Chen Z, et al. (2006) Structural Insights into Histone Demethylation by JMJD2 Family Members. **125:** 691-702

Cheng X. (1995) Structure and Function of DNA Methyltransferases. Vol. 24, pp. 293-318.

Cheng X, and Blumenthal RM (2008) Mammalian DNA Methyltransferases: A Structural Perspective. *Structure* **16:** 341-350

Cheng X, and Blumenthal RM (2010) Coordinated Chromatin Control: Structural and Functional Linkage of DNA and Histone Methylation. *Biochemistry* **49:** 2999-3008

Cheng X, and Roberts RJ (2001) AdoMet-dependent methylation, DNA methyltransferases and base flipping. *Nucl Acids Res* **29:** 3784-3795

Cheung P, and Lau P (2005) Epigenetic Regulation by Histone Methylation and Histone Variants. *Mol Endocrinol* **19:** 563-573

Chinnusamy V, and Zhu J-K (2009) RNA-directed DNA methylation and demethylation in plants. *Science in China Series C: Life Sciences* **52:** 331-343

Ciccone DN, et al. (2009) KDM1B is a histone H3K4 demethylase required to establish maternal genomic imprints. *Nature* **461:** 415-418

Costanzi C, and Pehrson JR (2001) MACROH2A2, a New Member of the MACROH2A Core Histone Family. *Journal of Biological Chemistry* **276:** 21776-21784

Courtney MT, Jeong-Heon L, and David GS (2009) CXXC finger protein 1 restricts the Setd1A histone H3K4 methyltransferase complex to euchromatin. *FEBS Journal* **277:** 210-223

Dagert M, and Ehrlich SD (1979) Prolonged incubation in calcium chloride improves the competence of Escherichia coli cells. *Gene* **6:** 23-38

Datta J, et al. (2005) Physical and Functional Interaction of DNA Methyltransferase 3A with Mbd3 and Brg1 in Mouse Lymphosarcoma Cells. *Cancer Res* **65:** 10891-10900

de Ruijter AJM, et al. (2003) Histone deacetylases (HDACs): characterization of the classical HDAC family. *Biochem J* **370:** 737-749

de Wit E, et al. (2008) Global Chromatin Domain Organization of the <italic>Drosophila</italic> Genome. *PLoS Genet* **4:** e1000045

Dillon N (2006) Gene regulation and large-scale chromatin organization in the nucleus. *Chromosome Research* **14:** 117-126

Dong A, et al. (2001) Structure of human DNMT2, an enigmatic DNA methyltransferase homolog that displays denaturant-resistant binding to DNA. *Nucl Acids Res* **29:** 439-448

Dong KB, et al. (2008) DNA methylation in ES cells requires the lysine methyltransferase G9a but not its catalytic activity. *EMBO J* **27:** 2691-2701

Duncan T, et al. (2002) Reversal of DNA alkylation damage by two human dioxygenases. *Proceedings of the National Academy of Sciences of the United States of America* **99:** 16660-16665

Eguchi Y, Shimizu S, and Tsujimoto Y (1997) Intracellular ATP Levels Determine Cell Death Fate by Apoptosis or Necrosis. *Cancer Res* **57:** 1835-1840

Eichinger L, et al. (2005) The genome of the social amoeba Dictyostelium discoideum. *Nature* **435:** 43-57

El Hassan MA, and Calladine CR (1998) Two distinct modes of protein-induced bending in DNA. *Journal of Molecular Biology* **282:** 331-343

Epsztejn-Litman S, et al. (2008) De novo DNA methylation promoted by G9a prevents reprogramming of embryonically silenced genes. *Nat Struct Mol Biol* **15:** 1176-1183

Esteve P-O, et al. (2009) Regulation of DNMT1 stability through SET7-mediated lysine methylation in mammalian cells. *Proceedings of the National Academy of Sciences* **106:** 5076-5081

Fan JY, et al. (2004) H2A.Z Alters the Nucleosome Surface to Promote HP1a-Mediated Chromatin Fiber Folding. **16:** 655-661

Farris SD, et al. (2005) Transcription-induced Chromatin Remodeling at the c-myc Gene Involves the Local Exchange of Histone H2A.Z. *Journal of Biological Chemistry* **280:** 25298-25303

Fatemi M, et al. (2001) The activity of the murine DNA methyltransferase Dnmt1 is controlled by interaction of the catalytic domain with the N-terminal part of the enzyme leading to an allosteric activation of the enzyme after binding to methylated DNA. *Journal of Molecular Biology* **309:** 1189-1199

Faust M, and Montenarh M (2000) Subcellular localization of protein kinase CK2. *Cell and Tissue Research* **301:** 329-340

Feng S, et al. (2010) Conservation and divergence of methylation patterning in plants and animals. *Proceedings of the National Academy of Sciences***:** -

Fernandez AG, and Anderson JN (2007) Nucleosome Positioning Determinants. *Journal of Molecular Biology* **371:** 649-668

Fey P, et al. (2009) dictyBase--a Dictyostelium bioinformatics resource update. *Nucl Acids Res* **37:** D515-519

Fisher O, Siman-Tov R, and Ankri S. (2004) Characterization of cytosine methylated regions and 5-cytosine DNA methyltransferase (Ehmeth) in the protozoan parasite Entamoeba histolytica. Vol. 32, pp. 287-297.

Fisher O, Siman-Tov R, and Ankri S (2006) Pleiotropic phenotype in Entamoeba histolytica overexpressing DNA methyltransferase (Ehmeth). *Molecular and Biochemical Parasitology* **147:** 48-54

Fritsch L, et al. (2010) A Subset of the Histone H3 Lysine 9 Methyltransferases Suv39h1, G9a, GLP, and SETDB1 Participate in a Multimeric Complex. **37:** 46-56

Gao Y, and Wang H-Y (2006) Casein Kinase 2 Is Activated and Essential for Wnt/Î²-Catenin Signaling. *Journal of Biological Chemistry* **281:** 18394-18400

Garcia-Dominguez M, and Reyes JC (2009) SUMO association with repressor complexes, emerging routes for transcriptional control. *Biochimica et Biophysica Acta (BBA) - Gene Regulatory Mechanisms* **1789:** 451-459

Gehring M, and Henikoff S (2007) DNA methylation dynamics in plant genomes. *Biochimica et Biophysica Acta (BBA) - Gene Structure and Expression* **1769:** 276-286

Gehring M, Reik W, and Henikoff S (2009) DNA demethylation by DNA repair. *Trends in Genetics* **25:** 82-90

Goll MG, and Bestor TH. (2005) EUKARYOTIC CYTOSINE METHYLTRANSFERASES. Vol. 74, pp. 481-514.

Goll MG, et al. (2006) Methylation of tRNAAsp by the DNA Methyltransferase Homolog Dnmt2. *Science* **311:** 395-398

Gomez-Ferreria MA, et al. (2007) Human Cep192 Is Required for Mitotic Centrosome and Spindle Assembly. **17:** 1960-1966

González-Romero R, et al. (2008) Quickly evolving histones, nucleosome stability and chromatin folding: All about histone H2A.Bbd. *Gene* **413:** 1-7

Gowher H, and Jeltsch A (2002) Molecular Enzymology of the Catalytic Domains of the Dnmt3a and Dnmt3b DNA Methyltransferases. *Journal of Biological Chemistry* **277:** 20409-20414

Gowher H, et al. (2006) Mutational Analysis of the Catalytic Domain of the Murine Dnmt3a DNA-(cytosine C5)-methyltransferase. *Journal of Molecular Biology* **357:** 928-941

Grandjean Vr, et al. (2007) Inheritance of an Epigenetic Mark: The CpG DNA Methyltransferase 1 Is Required for De Novo Establishment of a Complex Pattern of Non-CpG Methylation. *PLoS ONE* **2:** e1136

Greenfield NJ (2007) Using circular dichroism spectra to estimate protein secondary structure. *Nat Protocols* **1:** 2876-2890

Gutierrez A, and Sommer RJ (2004) Evolution of dnmt-2 and mbd-2-like genes in the free-living nematodes Pristionchus pacificus, Caenorhabditis elegans and Caenorhabditis briggsae. *Nucl Acids Res* **32:** 6388-6396

Hakimi M-A, et al. (2003) A Candidate X-linked Mental Retardation Gene Is a Component of a New Family of Histone Deacetylase-containing Complexes. *Journal of Biological Chemistry* **278:** 7234-7239

Hardeland U, et al. (2003) The versatile thymine DNA-glycosylase: a comparative characterization of the human, Drosophila and fission yeast orthologs. *Nucl Acids Res* **31:** 2261-2271

Harony H, et al. (2006) DNA methylation and targeting of LINE retrotransposons in Entamoeba histolytica and Entamoeba invadens. *Molecular and Biochemical Parasitology* **147:** 55-63

Hashimoto H, et al. (2008) The SRA domain of UHRF1 flips 5-methylcytosine out of the DNA helix. *Nature* **455:** 826-829

Hata K, et al. (2002) Dnmt3L cooperates with the Dnmt3 family of de novo DNA methyltransferases to establish maternal imprints in mice. *Development* **129:** 1983-1993

Hatfield D (1985) Suppression of termination codons in higher eukaryotes. *Trends in Biochemical Sciences* **10:** 201-204

Helm M (2006) Post-transcriptional nucleotide modification and alternative folding of RNA. *Nucl Acids Res* **34:** 721-733

Henderson IR, and Jacobsen SE (2007) Epigenetic inheritance in plants. *Nature* **447:** 418-424

Hermann A, Gowher H, and Jeltsch A (2004) Biochemistry and biology of mammalian DNA methyltransferases. *Cellular and Molecular Life Sciences (CMLS)* **61:** 2571-2587

Hermann A, Schmitt S, and Jeltsch A (2003) The Human Dnmt2 Has Residual DNA-(Cytosine-C5) Methyltransferase Activity. *Journal of Biological Chemistry* **278:** 31717-31721

Ho L, and Crabtree GR (2010) Chromatin remodelling during development. *Nature* **463:** 474-484

Hochegger H, et al. (2007) An essential role for Cdk1 in S phase control is revealed via chemical genetics in vertebrate cells. *The Journal of cell biology* **178:** 257-268

Hon GC, Hawkins RD, and Ren B (2009) Predictive chromatin signatures in the mammalian genome. *Hum Mol Genet* **18:** R195-201

Houben A, et al. (2007) Phosphorylation of histone H3 in plants--A dynamic affair. *Biochimica et Biophysica Acta (BBA) - Gene Structure and Expression* **1769:** 308-315

Howard PK, Ahern KG, and Firtel RA (1988) Establishment of a transient expression system for Dictyostelium discoideum. *Nucl Acids Res* **16:** 2613-2623

Hur S, and Stroud RM (2007) How U38, 39, and 40 of Many tRNAs Become the Targets for Pseudouridylation by TruA. **26:** 189-203

Hurst LD, Pal C, and Lercher MJ (2004) The evolutionary dynamics of eukaryotic gene order. *Nat Rev Genet* **5:** 299-310

Ito T (2007) Role of Histone Modification in Chromatin Dynamics. *J Biochem* **141:** 609-614

Jackson JP, et al. (2002) Control of CpNpG DNA methylation by the KRYPTONITE histone H3 methyltransferase. *Nature* **416:** 556-560

Jair K-W, et al. (2006) De novo CpG Island Methylation in Human Cancer Cells. *Cancer Res* **66:** 682-692

Jeltsch A (2003) Maintenance of species identity and controlling speciation of bacteria: a new function for restriction/modification systems? *Gene* **317:** 13-16

Jeltsch A (2006) On the enzymatic properties of Dnmt1: Specificity, processivity, mechanism of linear diffusion and allosteric regulation of the enzyme. *Epigenetics* **1:** 63–66

Jeltsch A, Nellen W, and Lyko F (2006) Two substrates are better than one: dual specificities for Dnmt2 methyltransferases. *Trends in Biochemical Sciences* **31:** 306-308

Jenuwein T, and Allis CD (2001) Translating the Histone Code. *Science* **293:** 1074-1080

Jia D, et al. (2007) Structure of Dnmt3a bound to Dnmt3L suggests a model for de novo DNA methylation. *Nature* **449:** 248-251

Jin C, and Felsenfeld G (2007) Nucleosome stability mediated by histone variants H3.3 and H2A.Z. *Genes & Development* **21:** 1519-1529

Jitrapakdee S, and Wallace JC (2003) The Biotin Enzyme Family: Conserved Structural Motifs and Domain Rearrangements. *Current Protein & Peptide Science* **4:** 217-229

Johansen K, and Johansen J (2006) Regulation of chromatin structure by histone H3S10 phosphorylation. *Chromosome Research* **14:** 393-404

Jones PA, and Liang G (2009) Rethinking how DNA methylation patterns are maintained. *Nat Rev Genet* **10:** 805-811

Jurkowski TP, et al. (2008) Human DNMT2 methylates tRNAAsp molecules using a DNA methyltransferase-like catalytic mechanism. Vol. 14, pp. 1663-1670.

Kameshita I, et al. (2008) Cyclin-dependent kinase-like 5 binds and phosphorylates DNA methyltransferase 1. *Biochemical and Biophysical Research Communications* **377:** 1162-1167

Karagianni P, et al. (2007) ICBP90, a novel methyl K9 H3 binding protein linking protein ubiquitination with heterochromatin formation. *Mol Cell Biol***:** MCB.01598-01507

Kareta MS, et al. (2006) Reconstitution and Mechanism of the Stimulation of de Novo Methylation by Human DNMT3L. *Journal of Biological Chemistry* **281:** 25893-25902

Kato Y, et al. (2007) Role of the Dnmt3 family in de novo methylation of imprinted and repetitive sequences during male germ cell development in the mouse. *Hum Mol Genet* **16:** 2272-2280

Katoh M, et al. (2006) Developmentally Regulated DNA Methylation in Dictyostelium discoideum. Vol. 5, pp. 18-25.

Kelley LA, and Sternberg MJE (2009) Protein structure prediction on the Web: a case study using the Phyre server. *Nat Protocols* **4:** 363-371

Kenessey A, Sullivan EA, and Ojamaa K (2006) Nuclear localization of protein kinase C-{alpha} induces thyroid hormone receptor-{alpha}1 expression in the cardiomyocyte. *Am J Physiol Heart Circ Physiol* **290:** H381-389

Kim JK, et al. (2008) UHRF1 binds G9a and participates in p21 transcriptional regulation in mammalian cells. *Nucl Acids Res***:** gkn961

Kleinschmidt MA, et al. (2008) The protein arginine methyltransferases CARM1 and PRMT1 cooperate in gene regulation. *Nucl Acids Res* **36:** 3202-3213

Klimasauskas S, et al. (1994) Hhal methyltransferase flips its target base out of the DNA helix. **76:** 357-369

Klose RJ, and Zhang Y (2007) Regulation of histone methylation by demethylimination and demethylation. *Nat Rev Mol Cell Biol* **8:** 307-318

Koch KV, et al. (2006) Identification and isolation of Dictyostelium microtubule-associated protein interactors by tandem affinity purification. *European Journal of Cell Biology* **85:** 1079-1090

Kosak ST, and Groudine M (2004) Gene Order and Dynamic Domains. *Science* **306:** 644-647

Kouzarides T (2002) Histone methylation in transcriptional control. *Current Opinion in Genetics & Development* **12:** 198-209

Kouzarides T (2007) Chromatin Modifications and Their Function. *Cell* **128:** 693-705

Kruger NJ (1996) The Bradford Method for Protein Quantitation. In *The Protein Protocols Handbook*, pp 15-20.

Kuhlmann M, et al. (2005) Silencing of retrotransposons in Dictyostelium by DNA methylation and RNAi. *Nucleic Acids Research* **33:** 6405-6417

Kumar S, et al. (1994) The DNA (cytosine-5) methyltransferases. *Nucl Acids Res* **22:** 1-10

Kunert N, et al. (2003) A Dnmt2-like protein mediates DNA methylation in Drosophila. Vol. 130, pp. 5083-5090.

Lau OD, et al. (2000) p300/CBP-associated Factor Histone Acetyltransferase Processing of a Peptide Substrate. *Journal of Biological Chemistry* **275:** 21953-21959

Lauster R, Trautner TA, and Noyer-Weidner M (1989) Cytosine-specific type II DNA methyltransferases : A conserved enzyme core with variable target-recognizing domains. *Journal of Molecular Biology* **206:** 305-312

Lavi T, et al. (2006) Sensing DNA methylation in the protozoan parasite Entamoeba histolytica. Vol. 62, pp. 1373-1386.

Lavi T, Siman-Tov R, and Ankri S (2009) Insights into the mechanism of DNA recognition by the methylated LINE binding protein EhMLBP of Entamoeba histolytica. *Molecular and Biochemical Parasitology* **166:** 117-125

Lee MG, et al. (2006) Functional Interplay between Histone Demethylase and Deacetylase Enzymes. *Mol Cell Biol* **26:** 6395-6402

Lee W, and Wallace BA (2008) Protein secondary structure analyses from circular dichroism spectroscopy: Methods and reference databases. *Biopolymers* **89:** 392-400

Lehnertz B, et al. (2003) Suv39h-Mediated Histone H3 Lysine 9 Methylation Directs DNA Methylation to Major Satellite Repeats at Pericentric Heterochromatin. **13:** 1192-1200

Leng P, et al. (1998) Skipper, an LTR retrotransposon of Dictyostelium. Vol. 26, pp. 2008-2015.

Leonhardt H, et al. (1992) A targeting sequence directs DNA methyltransferase to sites of DNA replication in mammalian nuclei. *Cell* **71:** 865-873

Li J-Y, et al. (2007) Synergistic Function of DNA Methyltransferases Dnmt3a and Dnmt3b in the Methylation of Oct4 and Nanog. *Mol Cell Biol* **27:** 8748-8759

Lichty JJ, et al. (2005) Comparison of affinity tags for protein purification. *Protein Expression and Purification* **41:** 98-105

Lin M-J, et al. (2005) DNA Methyltransferase Gene dDnmt2 and Longevity of Drosophila. *Journal of Biological Chemistry* **280:** 861-864

Liu K, et al. (2003) Endogenous Assays of DNA Methyltransferases: Evidence for Differential Activities of DNMT1, DNMT2, and DNMT3 in Mammalian Cells In Vivo. Vol. 23, pp. 2709-2719.

Liu Y, and Santi DV (2000) m5C RNA and m5C DNA methyl transferases use different cysteine residues as catalysts. *Proceedings of the National Academy of Sciences of the United States of America* **97:** 8263-8265

Lydan MA, and O'Day DH (1991) Endogenous biotinylated proteins in dictyostelium discoideum. *Biochemical and Biophysical Research Communications* **174:** 990-994

Lyko F, Ramsahoye BH, and Jaenisch R (2000) Development: DNA methylation in Drosophila melanogaster. *Nature* **408:** 538-540

Maniak M, Saur U, and Nellen W (1989) A colony-blot technique for the detection of specific transcripts in eukaryotes. *Analytical Biochemistry* **176:** 78-81

Margot J, Ehrenhofer-Murray A, and Leonhardt H (2003) Interactions within the mammalian DNA methyltransferase family. *BMC Molecular Biology* **4:** 7

Margueron R, and Reinberg D (2010) Chromatin structure and the inheritance of epigenetic information. *Nat Rev Genet* **11:** 285-296

Marhold J, et al. (2004) The Drosophila MBD2/3 protein mediates interactions between the MI-2 chromatin complex and CpT/A-methylated DNA. *Development* **131:** 6033-6039

Masamitsu N, et al. (2009) Dmap1 plays an essential role in the maintenance of genome integrity through the DNA repair process. *Genes to Cells* **14:** 1347-1357

Meilinger D, et al. (2009) Np95 interacts with de novo DNA methyltransferases, Dnmt3a and Dnmt3b, and mediates epigenetic silencing of the viral CMV promoter in embryonic stem cells. *EMBO Rep* **10:** 1259-1264

Meneghini MD, Wu M, and Madhani HD (2003) Conserved Histone Variant H2A.Z Protects Euchromatin from the Ectopic Spread of Silent Heterochromatin. **112:** 725-736

Morales-Ruiz T, et al. (2006) DEMETER and REPRESSOR OF SILENCING 1 encode 5-methylcytosine DNA glycosylases. **103:** 6853-6858

Morgan HD, et al. (2004) Activation-induced Cytidine Deaminase Deaminates 5-Methylcytosine in DNA and Is Expressed in Pluripotent Tissues. *Journal of Biological Chemistry* **279:** 52353-52360

Morgan HD, et al. (2005) Epigenetic reprogramming in mammals. *Hum Mol Genet* **14:** R47-58

Mortusewicz O, et al. (2005) Recruitment of DNA methyltransferase I to DNA repair sites. *Proceedings of the National Academy of Sciences of the United States of America* **102:** 8905-8909

Motorin Y, Lyko F, and Helm M (2009) 5-methylcytosine in RNA: detection, enzymatic formation and biological functions. *Nucl Acids Res* **38:** 1415-1430

Mund C, et al. (2004) Comparative analysis of DNA methylation patterns in transgenic Drosophila overexpressing mouse DNA methyltransferases. Vol. 378, pp. 763-768.

Munteanu MG, et al. (1998) Rod models of DNA: sequence-dependent anisotropic elastic modelling of local bending phenomena. *Trends in Biochemical Sciences* **23:** 341-347

Myant K, and Stancheva I (2008) LSH Cooperates with DNA Methyltransferases To Repress Transcription. *Mol Cell Biol* **28:** 215-226

Nathan D, et al. (2006) Histone sumoylation is a negative regulator in Saccharomyces cerevisiae and shows dynamic interplay with positive-acting histone modifications. *Genes & Development* **20:** 966-976

Negishi M, et al. (2007) Bmi1 cooperates with Dnmt1-associated protein 1 in gene silencing. *Biochemical and Biophysical Research Communications* **353:** 992-998

Nellen W, and Firtel RA (1985) High-copy-number transformants and co-transformation in Dictyostelium. *Gene* **39:** 155-163

Nellen W, and Saur U (1988) Cell-cycle dependent transformation competence in Dictyostelium discoideum. *Biochemical and Biophysical Research Communications* **154:** 54-59

Nelson CJ, Santos-Rosa H, and Kouzarides T (2006) Proline Isomerization of Histone H3 Regulates Lysine Methylation and Gene Expression. **126:** 905-916

Ng H-H, et al. (1999) MBD2 is a transcriptional repressor belonging to the MeCP1 histone deacetylase complex. *Nat Genet* **23:** 58-61

Nguyen CT, et al. (2002) Histone H3-Lysine 9 Methylation Is Associated with Aberrant Gene Silencing in Cancer Cells and Is Rapidly Reversed by 5-Aza-2'-deoxycytidine. *Cancer Res* **62:** 6456-6461

Niehrs C (2009) Active DNA demethylation and DNA repair. *Differentiation* **77:** 1-11

Norberg J (2003) Association of protein-DNA recognition complexes: electrostatic and nonelectrostatic effects. *Archives of Biochemistry and Biophysics* **410:** 48-68

Okamoto Y, et al. (2007) A minimal CENP-A core is required for nucleation and maintenance of a functional human centromere. *EMBO J* **26:** 1279-1291

Okano M, Xie S, and Li E (1998a) Cloning and characterization of a family of novel mammalian DNA (cytosine-5) methyltransferases. *Nat Genet* **19:** 219-220

Okano M, Xie S, and Li E. (1998b) Dnmt2 is not required for de novo and maintenance methylation of viral DNA in embryonic stem cells. Vol. 26, pp. 2536-2540.

Ooi SKT, and Bestor TH (2008) Cytosine Methylation: Remaining Faithful. **18:** R174-R176

Ooi SKT, et al. (2007) DNMT3L connects unmethylated lysine 4 of histone H3 to de novo methylation of DNA. *Nature* **448:** 714-717

Otani J, et al. (2009) Structural basis for recognition of H3K4 methylation status by the DNA methyltransferase 3A ATRX-DNMT3-DNMT3L domain. *EMBO Rep* **10:** 1235-1241

Packer MJ, and Hunter CA (1998) Sequence-dependent DNA structure: the role of the sugar-phosphate backbone. *Journal of Molecular Biology* **280:** 407-420

Panning B, and Jaenisch R (1998) RNA and the Epigenetic Regulation of X Chromosome Inactivation. *Cell* **93:** 305-308

Peterson CL, and Laniel M-A (2004) Histones and histone modifications. *Current Biology* **14:** R546-R551

Phalke S, et al. (2009) Retrotransposon silencing and telomere integrity in somatic cells of Drosophila depends on the cytosine-5 methyltransferase DNMT2. *Nat Genet* **41:** 696-702

Pinarbasi E, Elliott J, and Hornby DP (1996) Activation of a Yeast Pseudo DNA Methyltransferase by Deletion of a Single Amino Acid. *Journal of Molecular Biology* **257:** 804-813

Posfai J, et al. (1989) Predictive motifs derived from cytosine methyltransferases. *Nucl Acids Res* **17:** 2421-2435

Pradhan S, and Esteve P-O (2003) Mammalian DNA (cytosine-5) methyltransferases and their expression. *Clinical Immunology* **109:** 6-16

Puig O, et al. (2001) The Tandem Affinity Purification (TAP) Method: A General Procedure of Protein Complex Purification. *Methods* **24:** 218-229

Rai K, et al. (2007) Dnmt2 functions in the cytoplasm to promote liver, brain, and retina development in zebrafish. Vol. 21, pp. 261-266.

Rangasamy D, et al. (2003) Pericentric heterochromatin becomes enriched with H2A.Z during early mammalian development. *EMBO J* **22:** 1599-1607

Razin SV, et al. (2007) Chromatin Domains and Regulation of Transcription. *Journal of Molecular Biology* **369:** 597-607

Reik W, Santos F, and Dean W (2003) Mammalian epigenomics: reprogramming the genome for development and therapy. *Theriogenology* **59:** 21-32

Rice JC, et al. (2003) Histone Methyltransferases Direct Different Degrees of Methylation to Define Distinct Chromatin Domains. **12:** 1591-1598

Robertson KD, et al. (2000) DNMT1 forms a complex with Rb, E2F1 and HDAC1 and represses transcription from E2F-responsive promoters. *Nat Genet* **25:** 338-342

Rot G, et al. (2009) dictyExpress: a Dictyostelium discoideum gene expression database with an explorative data analysis web-based interface. *BMC Bioinformatics* **10:** 265

Rottach A, et al. (2010) The multi-domain protein Np95 connects DNA methylation and histone modification. *Nucl Acids Res* **38:** 1796-1804

Rottach A, Leonhardt H, and Spada F. (2009) DNA methylation-mediated epigenetic control. Vol. 108, pp. 43-51.

Sajedi E, et al. (2008) DNMT1 interacts with the developmental transcriptional repressor HESX1. *Biochimica et Biophysica Acta (BBA) - Molecular Cell Research* **1783:** 131-143

Sapojnikova N, et al. (2009) The Chromatin of Active Genes Is Not in a Permanently Open Conformation. *Journal of Molecular Biology* **386:** 290-299

Schaefer M, et al. (2009) Azacytidine Inhibits RNA Methylation at DNMT2 Target Sites in Human Cancer Cell Lines. *Cancer Res* **69:** 8127-8132

Schaefer M, and Lyko F (2010) Solving the Dnmt2 enigma. *Chromosoma* **119:** 35-40

Schaefer M, Steringer JP, and Lyko F (2008) The Drosophila Cytosine-5 Methyltransferase Dnmt2 Is Associated with the Nuclear Matrix and Can Access DNA during Mitosis. *PLoS ONE* **3:** e1414

Schlesinger Y, et al. (2007) Polycomb-mediated methylation on Lys27 of histone H3 pre-marks genes for de novo methylation in cancer. *Nat Genet* **39:** 232-236

Schmidt TGM, and Skerra A (2007) The Strep-tag system for one-step purification and high-affinity detection or capturing of proteins. *Nat Protocols* **2:** 1528-1535

Sharif J, et al. (2007) The SRA protein Np95 mediates epigenetic inheritance by recruiting Dnmt1 to methylated DNA. *Nature* **450:** 908-912

Shen L, et al. (2007) Genome-Wide Profiling of DNA Methylation Reveals a Class of Normally Methylated CpG Island Promoters. *PLoS Genet* **3:** e181

Sherif Tawfic (1997) Association of protein kinase CK2 with nuclear matrix: Influence of method of preparation of nuclear matrix. Vol. 64, pp. 499-504.

Sims Iii RJ, Nishioka K, and Reinberg D (2003) Histone lysine methylation: a signature for chromatin function. *Trends in Genetics* **19:** 629-639

Spada F, et al. (2007) DNMT1 but not its interaction with the replication machinery is required for maintenance of DNA methylation in human cells. *The Journal of cell biology* **176:** 565-571

Spellman P, and Rubin G (2002) Evidence for large domains of similarly expressed genes in the Drosophila genome. *Journal of Biology* **1:** 5

Spencer TE, et al. (1997) Steroid receptor coactivator-1 is a histone acetyltransferase. *Nature* **389:** 194-198

Sprinzl M, and Vassilenko KS (2005) Compilation of tRNA sequences and sequences of tRNA genes. *Nucl Acids Res* **33:** D139-140

Sproul D, Gilbert N, and Bickmore WA (2005) The role of chromatin structure in regulating the expression of clustered genes. *Nat Rev Genet* **6:** 775-781

Stephen ML, et al. (2006) High resolution structure of the HDGF PWWP domain: A potential DNA binding domain. *Protein Science* **15:** 314-323

Strahl BD, and Allis CD (2000) The language of covalent histone modifications. *Nature* **403:** 41-45

Suetake I, et al. (2003) Distinct Enzymatic Properties of Recombinant Mouse DNA Methyltransferases Dnmt3a and Dnmt3b. Vol. 133, pp. 737-744.

Suetake I, et al. (2004) DNMT3L Stimulates the DNA Methylation Activity of Dnmt3a and Dnmt3b through a Direct Interaction. *Journal of Biological Chemistry* **279:** 27816-27823

Suzuki MM, and Bird A (2008) DNA methylation landscapes: provocative insights from epigenomics. *Nat Rev Genet* **9:** 465-476

Svedruzic ZM, and Reich NO (2005) DNA Cytosine C5 Methyltransferase Dnmt1: Catalysis-Dependent Release of Allosteric Inhibition. *Biochemistry* **44:** 9472-9485

Swaffield JC, Melcher K, and Johnston SA (1995) A highly conserved ATPase protein as a mediator between acidic activation domains and the TATA-binding protein. *Nature* **374:** 88-91

Swaminathan J, Baxter EM, and Corces VG (2005) The role of histone H2Av variant replacement and histone H4 acetylation in the establishment of Drosophila heterochromatin. *Genes & Development* **19:** 65-76

Tachibana M, et al. (2008) G9a/GLP complexes independently mediate H3K9 and DNA methylation to silence transcription. *EMBO J* **27:** 2681-2690

Tachibana M, et al. (2005) Histone methyltransferases G9a and GLP form heteromeric complexes and are both crucial for methylation of euchromatin at H3-K9. *Genes & Development* **19:** 815-826

Takeshima H, et al. (2006) Distinct DNA Methylation Activity of Dnmt3a and Dnmt3b towards Naked and Nucleosomal DNA. *J Biochem* **139:** 503-515

Takeshima H, Suetake I, and Tajima S (2008) Mouse Dnmt3a Preferentially Methylates Linker DNA and Is Inhibited by Histone H1. *Journal of Molecular Biology* **383:** 810-821

Talbert PB, and Henikoff S (2006) Spreading of silent chromatin: inaction at a distance. *Nat Rev Genet* **7:** 793-803

Tamaru H, et al. (2003) Trimethylated lysine 9 of histone H3 is a mark for DNA methylation in Neurospora crassa. *Nat Genet* **34:** 75-79

Tang L-Y, et al. (2003) The Eukaryotic DNMT2 Genes Encode a New Class of Cytosine-5 DNA Methyltransferases. Vol. 278, pp. 33613-33616.

Tate CM, Lee J-H, and Skalnik DG (2009) CXXC Finger Protein 1 Contains Redundant Functional Domains That Support Embryonic Stem Cell Cytosine Methylation, Histone Methylation, and Differentiation. *Mol Cell Biol* **29:** 3817-3831

Terasaki M, et al. (2003) Localization and Dynamics of Cdc2-Cyclin B during Meiotic Reinitiation in Starfish Oocytes. *Mol Biol Cell* **14:** 4685-4694

Thambirajah AA, et al. (2009) New developments in post-translational modifications and functions of histone H2A variants. *Biochemistry and Cell Biology* **87:** 7-17

Tovy A, et al. (2010) A New Nuclear Function of the Entamoeba histolytica Glycolytic Enzyme Enolase: The Metabolic Regulation of Cytosine-5 Methyltransferase 2 (Dnmt2) Activity. *PLoS Pathog* **6:** e1000775

Tsukada Y-i, et al. (2006) Histone demethylation by a family of JmjC domain-containing proteins. *Nature* **439:** 811-816

Tudisca V, et al. (2010) Differential localization to cytoplasm, nucleus or P-bodies of yeast PKA subunits under different growth conditions. *European Journal of Cell Biology* **89:** 339-348

Vaissière T, Sawan C, and Herceg Z (2008) Epigenetic interplay between histone modifications and DNA methylation in gene silencing. *Mutation Research/Reviews in Mutation Research* **659:** 40-48

Vakoc CR, et al. (2005) Histone H3 Lysine 9 Methylation and HP1³ Are Associated with Transcription Elongation through Mammalian Chromatin. **19:** 381-391

Vasilescu J, and Figeys D (2006) Mapping protein-protein interactions by mass spectrometry. *Current Opinion in Biotechnology* **17:** 394-399

Versteeg R, et al. (2003) The Human Transcriptome Map Reveals Extremes in Gene Density, Intron Length, GC Content, and Repeat Pattern for Domains of Highly and Weakly Expressed Genes. *Genome Research* **13:** 1998-2004

Vilkaitis G, et al. (2000) Functional Roles of the Conserved Threonine 250 in the Target Recognition Domain of HhaI DNA Methyltransferase. *Journal of Biological Chemistry* **275:** 38722-38730

Waas WF, et al. (2007) Role of a tRNA Base Modification and Its Precursors in Frameshifting in Eukaryotes. *Journal of Biological Chemistry* **282:** 26026-26034

Wagschal A, et al. (2008) G9a Histone Methyltransferase Contributes to Imprinting in the Mouse Placenta. *Mol Cell Biol* **28:** 1104-1113

Wang AC, et al. (1977) Binding of E.coli lac repressor to non-operator DNA. *Nucl Acids Res* **4:** 1579-1594

Wang J, et al. (2009) The lysine demethylase LSD1 (KDM1) is required for maintenance of global DNA methylation. *Nat Genet* **41:** 125-129

Weber M, et al. (2007) Distribution, silencing potential and evolutionary impact of promoter DNA methylation in the human genome. *Nat Genet* **39:** 457-466

Wen B, et al. (2008) Overlapping euchromatin/heterochromatin- associated marks are enriched in imprinted gene regions and predict allele-specific modification. *Genome Research* **18:** 1806-1813

Wilkinson CRM, et al. (1995) The fission yeast gene pmt1+ encodes a DNA methyltransferase homologue. *Nucl Acids Res* **23:** 203-210

Williams KL, and Newell PC (1976) A genetic study of aggregation in the cellular slime mould Dictyostelium discoideum using complementation analysis. *Genetics* **82:** 287-307

Wion D, and Casadesus J (2006) N6-methyl-adenine: an epigenetic signal for DNA-protein interactions. *Nat Rev Micro* **4:** 183-192

Wu JC, and Santi DV (1987) Kinetic and catalytic mechanism of HhaI methyltransferase. *Journal of Biological Chemistry* **262:** 4778-4786

Wysocka J, et al. (2006) A PHD finger of NURF couples histone H3 lysine 4 trimethylation with chromatin remodelling. *Nature* **442:** 86-90

Yang X-J, and Seto E (2008) Lysine Acetylation: Codified Crosstalk with Other Posttranslational Modifications. *Molecular Cell* **31:** 449-461

Yoder JA, and Bestor TH (1998) A candidate mammalian DNA methyltransferase related to pmt1p of fission yeast. *Hum Mol Genet* **7:** 279-284

Zhang M, et al. (2010) DNA cytosine methylation in plant development. *Journal of Genetics and Genomics* **37:** 1-12

Zhao Q, et al. (2009) PRMT5-mediated methylation of histone H4R3 recruits DNMT3A, coupling histone and DNA methylation in gene silencing. *Nat Struct Mol Biol* **16:** 304-311

Zhou W, et al. (2008) Histone H2A Monoubiquitination Represses Transcription by Inhibiting RNA Polymerase II Transcriptional Elongation. **29:** 69-80

Zhu J-K (2009) Active DNA Demethylation Mediated by DNA Glycosylases. *Annual Review of Genetics* **43:** 143-166

Zilberman D (2008) The evolving functions of DNA methylation. *Current Opinion in Plant Biology* **11:** 554-559

Zilberman D, et al. (2008) Histone H2A.Z and DNA methylation are mutually antagonistic chromatin marks. *Nature* **456:** 125-129